伊犁哈萨克自治州科学技术局
伊犁哈萨克自治州财　政　局 文件

伊州科字〔2024〕9号

关于下达2024年自治州科技创新发展专项（第二批）及经费安排的通知

自治州直属各县市科技局、财政局，各项目承担单位:

2024年自治州科技创新发展专项（第二批）共安排3类专项、80个项目，财政科技专项资金支持总额度2400万元、本年度拨付1800万元。具体分配如下:

一、自治州重点研究与技术开发专项

安排项目22项，财政科技专项资金全周期支持总额度1500万元、本年度拨付900万元。

二、自治州科技成果转化示范专项

（一）乡村振兴产业发展科技行动计划。共安排项目12项，财政科技专项资金支持总额度270万元、本年度拨付270万元。

（二）科技特派员农村科技创业行动计划。共安排项目8项，财政科技专项资金支持总额度130万元、本年度拨付130万元。

（三）科技型中小企业发展科技行动计划。共安排项目13项，财政科技专项资金支持总额度200万元、本年度拨付200万元。

（四）科技援疆（江苏专项）计划。共安排项目4项，财政科技专项资金支持总额度150万元、本年度拨付150万元。

三、自治州基础研究、应用研究与公益性专项

（一）基础研究与社会发展科技计划。共安排项目21项，财政科技专项资金支持总额度150万元、本年度拨付150万元。

现将2024年自治州科技创新发展专项（第二批）及经费下达。请各项目承担单位认真做好项目的组织实施工作，同时加强项目绩效管理，按要求填报《项目支出绩效目标表》。

附件：2024年自治州科技创新发展专项（第二批）及经费安排表

附件：

2024年自治州科技创新发展专项（第二批）及经费安排表

自治州重点研究与技术开发专项

单位：万元

序号	项目编号	所属产业集群/领域	项目名称	实施年限	项目承担单位	项目资金			
						总额	自筹	自治州科技拨款	
								计划拨款	本次拨款
14	YZD2024A14	新能源新材料等战略性新兴产业集群	金属纳米材料在高端电子元器件涂层中的应用优化研究	2024.05—2026.03	新疆纳杨科技有限公司	700	580	120	72
22	YZD2024A22	现代商贸物流产业集群	霍尔果斯自贸区国际商品集采服务中心物流信息平台研发与应用	2024.05—2026.05	霍尔果斯陆港国际物流有限公司	460	360	100	60

2024年自治州科技创新发展专项（第二批）及经费安排表

自治州科技成果转化示范专项—乡村振兴产业发展科技行动计划

单位：万元

序号	项目编号	所属产业集群/领域	项目名称	实施年限	项目承担单位	项目资金			
						总额	自筹	自治州科技拨款	
								计划拨款	本次拨款
5	YXC2024A05	优质畜产品产业集群	伊犁马肉发酵肠深加工关键技术研发及产业化应用	2024.05—2025.12	伊犁西极马食品有限公司	60	45	15	15

2024年自治州科技创新发展专项（第二批）及经费安排表

自治州科技成果转化示范专项—科技型中小企业发展科技行动计划

单位：万元

序号	项目编号	所属产业集群/领域	项目名称	实施年限	项目承担单位	项目资金			
						总额	自筹	自治州科技拨款	
								计划拨款	本次拨款
1	YKX2024A01	新能源新材料等战略性新兴产业集群	临床级人诱导多能干细胞衍生的视网膜色素上皮细胞工艺和质量标准建立以及对年龄相关性黄斑变性治疗研究	2024.05—2026.03	霍尔果斯新生泉干细胞医疗有限公司	30	20	10	10
7	YKX2024A07	绿色有机果蔬产业集群	小浆果高效、绿色气囊压榨装备制造	2024.05—2025.04	伊犁唐古莱昆莫生物技术有限公司	140	115	25	25
8	YKX2024A08	新能源新材料等战略性新兴产业集群	中小微企业全链条智能孵化关键技术研究与开发	2024.05—2025.04	新疆禾丰汇通信息技术有限公司	60	45	15	15

2024年自治州科技创新发展专项（第二批）及经费安排表

自治州基础研究、应用研究与公益性专项—基础研究与社会发展科技计划

单位：万元

序号	项目编号	所属产业集群/领域	项目名称	实施年限	项目承担单位	项目资金			
						总额	自筹	自治州科技拨款	
								计划拨款	本次拨款
7	YJC2024A07	新能源新材料等战略性新兴产业集群	合成生物学生产角鲨烯的关键技术研究	2024.05—2026.04	伊犁川宁生物技术股份有限公司	20	15	5	5
15	YJC2024A15	医疗卫生领域	表观遗传药物在结直肠癌治疗中的作用与机制探究	2024.05—2026.05	霍尔果斯市人民医院	15	10	5	5

文件编号：伊州科字〔2024〕9 号
项目编号：YJC2024A15

伊犁哈萨克自治州科技计划项目合同书

项　目　名　称：表观遗传药物在结直肠癌治疗中的作用与机制探究

所　属　专　项：基础研究、社会发展类

起　止　时　间：2024-05-01 至 2026-05-01

管理单位(甲方)：伊犁哈萨克自治州科学技术局

承担单位(乙方)：霍尔果斯市人民医院

保证单位(丙方)：霍尔果斯市科技局

伊犁哈萨克自治州科学技术局 印制

填 写 说 明

一、本合同书为伊犁州科技计划（指令性）项目的合同书，请严格按要求填写各项内容。

二、甲方为自治州科技局，乙方为项目承担单位，丙方为项目承担单位的主管部门或所在县（市）科技局。各方名称须填写全称，并与所加盖公章信息保持一致。

三、计划类别、项目编号由自治州科技局统一编排。

四、项目分设课题的，本合同书可以课题为单位填写，“项目名称”栏填写格式为：“×××项目×××课题”。

五、本合同正文使用宋体小四号字，合同文本规格为A4纸双面印刷，封面纸质同内页纸质。

本合同书所称表观遗传药物在结直肠癌治疗中的作用与机制探究项目，由伊州科字〔2024〕9号文件批准立项。为规范项目实施和管理，项目管理单位伊犁哈萨克自治州科学技术局（甲方）和项目承担单位霍尔果斯市人民医院（乙方）及项目承担单位主管部门（保证单位）霍尔果斯市科技局（丙方）签署本合同书。

合同附表

伊犁哈萨克自治州科技计划项目合同信息表

<table>
<tr><td>项目名称</td><td colspan="3">表观遗传药物在结直肠癌治疗中的作用与机制探究</td><td>项目编号</td><td>YJC2024A15</td></tr>
<tr><td>所属专项</td><td colspan="5">基础研究、社会发展类</td></tr>
<tr><td>预期成果形式</td><td colspan="5">13.其他</td></tr>
<tr><td rowspan="4">项目负责人</td><td>姓　　名</td><td>张宝明</td><td>性　　别</td><td colspan="2">☑男□女</td></tr>
<tr><td>出生日期</td><td>1981-03-07</td><td>职　　称</td><td colspan="2">☑高级 □中级 □初级 □其他</td></tr>
<tr><td>最高学位</td><td>☑博士□硕士 □学士□其他</td><td>从事专业</td><td colspan="2">外科学</td></tr>
<tr><td>联系电话</td><td>18961325782</td><td>移动电话</td><td colspan="2">18961325782</td></tr>
<tr><td rowspan="5">项目承担单位</td><td>单位名称</td><td colspan="2">霍尔果斯市人民医院</td><td>机构代码</td><td>126540006934269436</td></tr>
<tr><td>单位性质</td><td colspan="4">其他事业单位</td></tr>
<tr><td>所在地区</td><td>新疆维吾尔自治区,伊犁哈萨克自治州,霍尔果斯市</td><td>主管部门</td><td colspan="2">霍尔果斯市科技局</td></tr>
<tr><td>联 系 人</td><td>张宝明</td><td>联系电话</td><td colspan="2">18961325782</td></tr>
<tr><td>单位账户信息</td><td colspan="4">账户名称：霍尔果斯市人民医院
开户银行：中国农业银行霍尔果斯支行
账号：30108101040004118</td></tr>
<tr><td rowspan="2">项目协作单位</td><td colspan="2">单位名称</td><td>单位性质</td><td>联系人</td><td>联系电话</td></tr>
<tr><td colspan="2">新疆大学</td><td>大专院校</td><td>责祎旦</td><td>18817871527</td></tr>
<tr><td>项目摘要（300字以内）</td><td colspan="5">全球最新癌症负担数据显示，结直肠癌（CRC）患者占全球新确诊癌症人数的9.7%，已发展成为仅次于乳腺癌、肺癌的第三大常见癌症。多项研究表明，表观遗传突变会导致表观修饰蛋白功能异常缺失或获得，从而参与了多种人类肿瘤和疾病的发生和发展。表观遗传药物因其抑癌效果确切、毒副作用少、适合长期使用等特点近来备受关注，然而在结直肠癌中的作用还未有报道。ITF2357 是一种安全且可耐受的 HDAC 抑制剂，其抗肿瘤活性已在一些血液系统肿瘤和实体瘤中被报道。本课题拟通过体外实验证明表观遗传药物对结直肠癌的抑制作用，并通过多组学测序探寻其可能的潜在靶点，为结直肠癌的深入研究和临床应用提供方向。</td></tr>
<tr><td>起始时间</td><td colspan="2">2024-05-01</td><td>终止时间</td><td colspan="2">2026-05-01</td></tr>
<tr><td>经费</td><td>总经费</td><td>15.0 万元</td><td colspan="2">其中：自治州拨款</td><td>5.0 万元</td></tr>
</table>

投入				

一、目标和主要研究开发内容（拟解决的主要技术问题及创新点）

全球最新癌症负担数据显示，结直肠癌（CRC）患者占全球新确诊癌症人数的9.7%，已发展成为仅次于乳腺癌、肺癌的第三大常见癌症。多项研究表明,表观遗传突变会导致表观修饰蛋白功能异常缺失或获得,从而参与了多种人类肿瘤和疾病的发生和发展。ITF2357 是一种具有广泛的抗炎活性的，安全且可耐受的 HDAC 抑制剂，其抗肿瘤活性已在一些血液系统肿瘤和实体瘤中被报道。虽然表观遗传药物因其抑癌效果确切、毒副作用少、适合长期使用等特点近来备受关注，然而在结直肠癌中的作用还未有报道。基于以上背景，本课题的研究内容如下：

第一部分 检测表观遗传药物对结直肠癌细胞的影响

由于结肠癌大多数患者来就诊时就已经处于疾病的中晚期,晚期肿瘤从定义上讲它更加异质性，积累了更多的表观遗传改变。因此，本课题以全球第三大癌症结肠癌为研究对象，在细胞水平上系统探讨表观遗传药物 ITF2357 对人结直肠癌细胞增殖、迁移、凋亡及周期的影响。

第二部分 检测表观遗传药物在体内对肿瘤生长的影响

通过建立结直肠癌小鼠模型，检测表观遗传药物 ITF2357 在体内对肿瘤生长的影响基于细胞水平所得实验结果，进一步探究表观遗传药物 ITF2357 在体内抗结肠癌的效果。通过将人结直肠癌细胞注入小鼠后建立结直肠癌小鼠模型，检测表观遗传药物 ITF2357 对小鼠体重、肿瘤大小及器官指数的影响。为寻找一种以表观遗传为基础的，抑癌效果确切、毒副作用少、适合长期使用的针对肿瘤表观遗传的潜在药物提供理论基础。

第三部分 探索表观遗传药物在结直肠癌治疗中的作用机制

为探讨表观遗传药物 ITF2357 抗结肠癌的作用机制，本课题通过综合分析转录组数据及小 RNA 测序的结果，再进一步与现有结肠癌与癌旁组织的转录组数据及小 RNA 表达谱芯片数据综合分析，寻找靶基因。并在临床样品中验证靶基因，最后通过在结肠癌细胞中敲降靶基因，验证其功能。

解决的技术难点

鉴于表观遗传修饰在结直肠癌发生发展过程中的重要作用,我们计划系统的在细胞水平上探索表观遗传药物 ITF2357 对结肠癌的作用和分子机制，并在动物层面进一步做深入探究，为基于表观遗传疗法治疗结肠癌打下坚实的理论基础。

可能的创新点

1. 本研究通过体内外实验验证表观遗传药物 ITF2357 对结直肠癌的作用，为结直肠癌的治疗提供候选策略。

2. 通过初步探索表观遗传药物 ITF2357 抗结肠癌的潜在的作用机制，有望拓展结肠癌发生发展中的分子机制，为结直肠癌的深入研究和临床治疗提供理论依据。

二、考核指标（主要技术指标 、主要经济指标 、其他考核指标）

1. 深入研究表观遗传药物抗结直肠癌的作用与分子机制。 2. 寻找一种抑癌效果确切、毒副作用少、适合长期使用的针对肿瘤表观遗传组学的表观遗传疗法，有望提高以表观遗传为基础的结直肠癌治疗效果。 3.在有国际影响力的期刊杂志发表 SCI 论文 1-2 篇。

三、项目实施年限、阶段计划及目标

（一）项目实施年限： 2024 年 5 月至 2026 年 5 月	
（二）阶段计划及阶段主要目标：	
2024 年 5 月至 2025 年 5 月	通过体内外实验检测表观遗传药物 ITF2357 的抗肿瘤效果。通过转录组测序和小 RNA 测序探讨 ITF2357 对结直肠癌生长的作用机制并进行验证。
2025 年 5 月至 2026 年 5 月	分析实验结果，撰写文章投稿，撰写结题报告。

四、主要研究开发人员

序号	姓　名	性别	职务/职称	工作分工	所在单位
（一）项目负责人：					
1	张宝明	男	院长 副高级	课题设计，论文撰写	霍尔果斯市人民医院
（二）主要研究开发人员：					
1	叶尔布拉提·道肯	男	副书记/副院长 正高级	样本收集	霍尔果斯市人民医院
2	责祎旦·加帕尔	女	副教授 副高级	课题设计，论文撰写	新疆大学
3	肖红兵	男	科主任 副高级	样本收集	霍尔果斯市人民医院
4	王治立	男	科主任 副高级	分析数据	霍尔果斯市人民医院
5	王楠	女	科副主任 中级	分析数据	霍尔果斯市人民医院
6	珠娜	女	研究生 其他	数据整理及分析	新疆大学
7	朱容欣	女	研究生 其他	体外试验	新疆大学
8	巴力根·赛力克拜	女	研究生 其他	结肠癌小鼠模型的建立及机制研究	新疆大学
9	梁通	男	研究生 其他	体内、体外机制研究	新疆大学
10	麦热帕提•马合木提	女	研究生 其他	结肠癌小鼠模型的建立及机制研究	新疆大学

五、经费预算

（一）经费预算　　单位：万元（保留两位小数）

预算科目	总预算数	其中:自治州财政拨款	备注
(1)	(2)	(3)	(4)
一、预算来源合计	15.0	5.0	
（一）自治州财政拨款	5.0	5.0	
（二）自筹经费	10.0		
1.其他财政拨款	0.0		
（1）国家部委拨款	0.0		
（2）自治区财政拨款	0.0		
（3）主管部门配套	0.0		
2.承担单位自有货币资金	10.0		
3.从银行获得的贷款	0.0		
4.其他资金	0.0		
二、支出预算合计	15.0	5.0	
（一）直接费用	13.0	5.0	
1.设备费	0.0	0.0	
其中：购置设备费	0.0	0.0	
2.业务费	10.0	4.0	
3.劳务费	3.0	1.0	
（二）间接费用	2.0	0.0	

（二）自治州科技拨款预算安排

自治州本级财政为本项目安排的科技拨款人民币5.0万元（￥5.0万元），根据项目进展情况和年度经费预算一次性拨付或分年度拨付。

六、项目承担单位和项目协作单位分工

项目承担单位：申请单位在项目中承担核心职责，涉及项目启动的各个关键环节，从立项申请到规划编制，再到资源整合与风险管理，以及全过程的进度、质量和成本控制，确保项目按照既定目标高效、有序地推进。结合临床，分析数据，撰写文章及结题报告，确保课题的顺利结题。
项目协作单位：随时了解课题进展情况并及时向项目负责人汇报；协助项目负责人完成项目年度汇报及结题评估工作。研究表观遗传药物抗结直肠癌的作用与分子机制，同时分析数据及参与论文的撰写与投稿。

七、共同条款

签约各方共同遵守《伊犁哈萨克自治州州直科技计划项目管理办法》（简称“办法”，下同）：

1.乙方必须按要求编报年度计划执行情况和有关统计报表，于规定时间报送甲方。逾期不报，甲方有权停止或追回拨款。

2.因乙方原因（如与合同内容有出入、挪用经费、技术措施或某些条件不落实等）致使计划无法继续执行或按期完成的，甲方根据情况有权中止合同，并根据具体情况，由乙方部分或全部退还甲方所拨经费。

3.乙方获得的自治州科技计划拨款按《伊犁州本级科技经费管理（暂行）办法》规定的使用范围开支。甲方根据相关规定监督乙方经费的使用情况，凡不符合规定的开支，甲方有权提出调整意见。

4.合同执行过程中，甲方无故解除或不履行合同时，所拨经费不得追回。

5.项目涉及的保密事项，按国家、自治区和自治州有关规定执行。

6.丙方应监督、检查和保证乙方执行合同，协调解决项目执行中出现的问题。

7.签约各方发生争议或纠纷时，按“办法”的有关条款处理。

8.合同正式文本一式 4 份，均具有同等法律效力。其中甲方 2 份、乙方 1 份、丙方 1 份。本合同自签订之日起生效，有效期至项目验收后一年内。

9.其它条款：

八、合同签约各方

甲方　伊犁哈萨克自治州科学技术局

（单位公章）

法人代表（或受委托人）（签章）：

项目管理人员（签字）：

乙方（承担单位）霍尔果斯市人民医院

（单位公章）

法人代表（或受委托人）（签章）：周美娟

项目负责人（签字）：

财务负责人（签章）：徐斐

丙方（乙方主管部门或所在县市科技局）霍尔果斯市科技局

（单位公章）

法人代表（或受委托人）（签章）：

签约日期：　　年　　月　　日

附件材料

序号	附件名称
1	项目自筹经费来源说明.pdf

项目自筹经费来源说明

霍尔果斯市人民医院张宝明申请的伊犁州科技局项目《表观遗传药物在结直肠癌治疗中的作用与机制探究》（项目编号：YJC2024A15），科研经费共计15万元，其中5万元由州财政拨款，其中10万元自筹经费由霍尔果斯市人民医院负责配套保障。

霍尔果斯市人民医院

2024年5月22日

文件编号：伊州科字〔2024〕9号
项目编号：YJC2024A15

伊犁哈萨克自治州科技计划项目合同书

项　目　名　称：表观遗传药物在结直肠癌治疗中的作用与机制探究

所　属　专　项：基础研究、社会发展类

起　止　时　间：2024-05-01至2026-05-01

管理单位（甲方）：伊犁哈萨克自治州科学技术局

承担单位（乙方）：霍尔果斯市人民医院

保证单位（丙方）：霍尔果斯市科技局

伊犁哈萨克自治州科学技术局　印制

八、合同签约各方

甲方　伊犁哈萨克自治州科学技术局

（单位公章）

法人代表（或受委托人）（签章）：叶尔波力·马高

项目管理人员（签字）：

乙方（承担单位）霍尔果斯市人民医院

（单位公章）

法人代表（或受委托人）（签章）：周美娟

项目负责人（签字）：

财务负责人（签章）：徐斐

丙方（乙方主管部门或所在县市科技局）霍尔果斯市科技局

（单位公章）

法人代表（或受委托人）（签章）：

签约日期：　　年　　月　　日

附件 1

伊犁哈萨克自治州科技计划项目
申　请　书

项目名称：表观遗传药物在结直肠癌治疗中的作用与机制探究

申请单位：霍尔果斯市人民医院

主管部门：霍尔果斯市科技局

联 系 人：张宝明 联系电话：18961325782

传　　真：0999-6580102 电子邮箱：zhbm202@163.com

地　　址：新疆省霍尔果斯市平安路 12 号

伊犁哈萨克自治州科学技术局印制

填 写 说 明

一、填写要求：

1、目标明确；

2、研究内容重点突出、项目设置合理；

3、所选技术路线可行；

4、经费预算合理，符合有关规定。

二、中外文专业名词首次出现时，要写清全称和缩写，再次出现时可使用缩写。

三、正文使用宋体小四号字，A4 纸双面印刷，封面纸质同内页纸质，骑马钉中缝装订，一式两份。

四、主管部门指：州直属各县（市）科技局、州直各项目申报单位的上级业务主管部门。

一、基本信息

<table>
<tr><td>项目名称</td><td colspan="5">表观遗传药物在结直肠癌治疗中的作用与机制探究</td></tr>
<tr><td>所属领域</td><td colspan="5">3.卫生健康领域</td></tr>
<tr><td>申请日期</td><td colspan="2">2024-05-01</td><td>实施年限</td><td colspan="2">2026-05-01</td></tr>
<tr><td colspan="2">经费预算总额</td><td>15.0 万元</td><td colspan="2">其中：申请自治州财政拨款</td><td>15.0 万元</td></tr>
<tr><td rowspan="3">申请单位</td><td>单位名称</td><td colspan="4">霍尔果斯市人民医院</td></tr>
<tr><td>单位性质</td><td colspan="4">其他事业单位</td></tr>
<tr><td>主管部门</td><td colspan="4">霍尔果斯市科技局</td></tr>
<tr><td rowspan="5">申请
负责人</td><td>姓名</td><td>张宝明</td><td>性别</td><td colspan="2">男</td></tr>
<tr><td>出生日期</td><td>1981-03-07</td><td>职称</td><td colspan="2">高级职称</td></tr>
<tr><td>最高学位</td><td>博士</td><td>从事专业</td><td colspan="2">外科学</td></tr>
<tr><td>联系电话</td><td>18961325782</td><td>移动电话</td><td colspan="2">18961325782</td></tr>
<tr><td>传真号码</td><td>0999-6580102</td><td>电子信箱</td><td colspan="2">zhbm202@163.com</td></tr>
<tr><td rowspan="2">协作单位</td><td colspan="2">单位名称</td><td>单位性质</td><td colspan="2">联系电话</td></tr>
<tr><td colspan="2">新疆大学</td><td>大专院校</td><td colspan="2">0991-8582232</td></tr>
<tr><td colspan="6">项目摘要（简要说明项目的主要内容、预期目标等，300 字以内）：
全球最新癌症负担数据显示，结直肠癌（CRC）患者占全球新确诊癌症人数的 9.7%，已发展成为仅次于乳腺癌、肺癌的第三大常见癌症。多项研究表明,表观遗传突变会导致表观修饰蛋白功能异常缺失或获得，从而参与了多种人类肿瘤和疾病的发生和发展。表观遗传药物因其抑癌效果确切、毒副作用少、适合长期使用等特点近来备受关注，然而在结直肠癌中的作用还未有报道。ITF2357 是一种安全且可耐受的 HDAC 抑制剂，其抗肿瘤活性已在一些血液系统肿瘤和实体瘤中被报道。本课题拟通过体外实验证明表观遗传药物对结直肠癌的抑制作用，并通过多组学测序探寻其可能的潜在靶点，为结直肠癌的深入研究和临床应用提供方向。</td></tr>
</table>

二、项目组主要研究开发人员

序号	姓　名	性别	出生年月	职务/职称	现从事专业	在项目中分担的任务	所在单位
1	张宝明	男	1981-03-07	院长 副高级	临床医学	课题设计、论文撰写	霍尔果斯市人民医院
2	叶尔布拉提·道肯	男	1972-12-31	副书记/副院长 正高级	临床医学	样本收集	霍尔果斯市人民医院
3	责祎旦·加帕尔	女	1989-11-17	副教授 副高级	生物学	课题设计、论文撰写	新疆大学
4	肖红兵	男	1967-01-25	科主任 副高级	临床医学	样本收集	霍尔果斯市人民医院
5	王治立	男	1975-12-08	科主任 副高级	临床医学	分析数据	霍尔果斯市人民医院
6	王楠	女	1990-01-20	无 中级	临床医学	分析数据	霍尔果斯市人民医院
7	珠娜	女	1998-06-01	研究生 其他	生物学	数据整理及分析	新疆大学
8	朱容欣	女	1999-11-13	研究生 其他	生物学	药物对肿瘤的作用	新疆大学
9	巴力根·赛力克拜	女	1999-03-15	研究生 其他	生物学	结肠癌小鼠模型的建立及治疗	新疆大学
10	麦热帕提•马合木提	女	2000-10-07	研究生 其他	生物学	结肠癌小鼠模型的建立及治疗	新疆大学

三、项目情况

（一）项目主要研究内容、拟解决的技术难点和可能的创新点，及技术风险分析（包括技术障碍、解决途径及风险因素）

主要研究内容

第一部分 检测表观遗传药物对结直肠癌细胞的影响

由于结肠癌大多数患者来就诊时就已经处于疾病的中晚期，晚期肿瘤从定义上讲它更加异质性，积累了更多的表观遗传改变。因此，本课题以全球第三大癌症结肠癌为研究对象，在细胞水平上系统探讨表观遗传药物 ITF2357 对人结直肠癌细胞增殖、迁移、凋亡及周期的影响。

第二部分 检测表观遗传药物在体内对肿瘤生长的影响

通过建立结直肠癌小鼠模型，检测表观遗传药物 ITF2357 在体内对肿瘤生长的影响基于细胞水平所得实验结果，进一步探究表观遗传药物 ITF2357 在体内抗结肠癌的效果。通过将人结直肠癌细胞注入小鼠后建立结直肠癌小鼠模型，检测表观遗传药物 ITF2357 对小鼠体重、肿瘤大小及器官指数的影响。为寻找一种以表观遗传为基础的，抑癌效果确切、毒副作用少、适合长期使用的针对肿瘤表观遗传的潜在药物提供理论基础。

第三部分 探索表观遗传药物在结直肠癌治疗中的作用机制

为探讨表观遗传药物 ITF2357 抗结肠癌的作用机制，本课题通过综合分析转录组数据及小 RNA 测序的结果，再进一步与现有结肠癌与癌旁组织的转录组数据及小 RNA 表达谱芯片数据综合分析，寻找靶基因。并在临床样品中验证靶基因，最后通过在结肠癌细胞中敲降靶基因，验证其功能。

解决的技术难点

鉴于表观遗传修饰在结直肠癌发生发展过程中的重要作用，我们计划系统的在细胞水平上探索表观遗传药物 ITF2357 对结肠癌的作用和分子机制，并在动物层面进一步做深入探究，为基于表观遗传疗法治疗结肠癌打下坚实的理论基础。

可能的创新点

1. 本研究通过体内外实验验证表观遗传药物 ITF2357 对结直肠癌的作用，为结直肠癌的治疗提供候选策略。

2. 通过初步探索表观遗传药物 ITF2357 抗结肠癌的潜在的作用机制，有望拓展结肠癌发生发展中的分子机制，为结直肠癌的深入研究和临床治疗提供理论依据。

技术风险分析

1. 技术障碍：机制研究风险：表观遗传调控机制复杂，研究具有难度。在研究过程中，可能会遇到实验误差、假阳性结果等问题，导致对药物作用机制的错误理解。

2. 解决途径：建立科学、严谨的研究体系，确保实验设计和数据分析的准确性和可靠性。积极与相关领域专家合作，共同开展研究，提高研究的科学性和可信度。 重视伦理和法律问题，遵守相关规定，确保研究对象的权益得到充分保障。

（二）项目主要研究技术的区内外发展现状与趋势

作为癌症相关死亡的第三大原因，结直肠癌相关研究是相当重要的。肿瘤的发生是一个多因素、多阶段、多基因协同作用的过程，遗传背景比较复杂。结直肠癌半数以上由腺瘤发展而来，其特征是遗传和表观紊乱的逐步累积，分子事件伴随组织学的紊乱，从正常结肠上皮发展到小腺瘤，再从小腺瘤的轻度隐窝结构异常发展到最终的浸润性癌症[1]。手术治疗、化疗、放疗、靶向药物治疗等均是目前临床上常用的治疗策略，但这些治疗手段难以对后期转移肿瘤进行有效治疗。早期检测以及抑制肿瘤的侵袭转移，早诊断和进行有效的治疗是有效控制肿瘤恶性发展的关键,对结直肠癌防治与治疗有重大意义。手术治疗是目前结直肠癌最主要的治疗方式，但大约 30%-50% 的患者术后会发生转移并严重影响患者的生存质量[2]。化疗也是治疗结直肠癌的重要策略，该方法利用不同的药物或药物组合来减少癌细胞分裂从而达到治疗目的，近几年临床大多选用奥沙利铂、伊立替康等药物进行联合治疗。传统的结直肠癌化疗会将药物输送到非药物靶点处，从而对患者容易产生不良副作用[3]。另外，长期使用传统化疗药物将增加耐药性产生的风险，迄今为止化疗手段对结直肠癌进行治疗尚未取得令人满意的

结果[3]。因此，筛选高效、副作用少且耐药性小的抗结直肠癌药物成为当前临床研究的热点和难点。

参与细胞生长和分化相关基因功能的基因组调控是癌症的主要原因。结直肠癌的发生涉及从遗传改变的积累到遗传和表观遗传学的调节和染色体异常的各种过程以及抑癌基因和致癌基因的突变[4]。表观遗传学的改变可以通过使用特定类别的药物来逆转，这些药物可以恢复基因的原始表达和功能[5]。组蛋白是真核生物染色体的基本组成蛋白。组蛋白的磷酸化、甲基化、乙酰化、泛素化和 ADP 核糖基化等修饰会改变染色体结构，从而调控 DNA 的复制、转录和修复等。组蛋白去乙酰化酶 (HDACs)通过调节组蛋白的乙酰化，调控细胞生长、分化、DNA 修复以及蛋白质稳定性等重要过程，而 HDACs 的基因突变、表达改变或者失调都与癌症的发生与发展密切相关。一些相关研究揭示了 HDACs 在不同类型肿瘤中的异常表达，在乳腺、肺、前列腺、结直肠、肝、宫颈和胃癌等肿瘤中作为生物标志物[6]，提示疾病的起始和进展。近年来，HDACi 在临床应用上取得了很多突破，Vorinostat（SAHA，MK0683）和 Romidepsin（FK-228，Depsipeptide）被 FDA 批准治疗皮肤 T 细胞淋巴瘤；Belinostat（PXD101）和西达本胺（Chidamide/epidaza，爱谱沙）被批准用于治疗外周 T 细胞淋巴瘤；Panobinostat（Farydak,LBH589）被批准治疗多发性骨髓瘤[7]。HDACi 通过影响组蛋白与非组蛋白的乙酰化来抑制癌症的发展，诱导癌细胞死亡。HDACi 抗肿瘤的主要作用机制包括改变基因表达和染色体结构、诱导 ROS 的产生、抑制血管生成、抑制癌细胞转移以及影响自噬、细胞代谢、免疫信号通路等[28]。Hyun-Jung Kim 等人提出正常细胞对 HDACi 具有抗性，而肿瘤细胞比较敏感，并发生生长阻滞或细胞死亡。P21 的上调和阻断细胞周期蛋白/CDK 复合物是 HDACi 抑制细胞周期阻滞和分化的主要原因[9]。

越来越多的证据表明，许多 miRNA 在包括癌症在内的各种疾病中异常表达并参与多种生物学过程，如细胞增殖、分化和迁移，并与肿瘤的发生和进展相关。多种 miRNA 已被证明在结直肠癌中的表达谱具有特异性。相关研究指出，miR-155 在结直肠癌组织中表达上调，其表达水平与患者的结直肠癌浸润、淋巴结转移和分期呈正相关，与肿瘤细胞分化呈负相关，这表明 miR-155 可能作为结直肠癌的分子标志物物，也是基因治疗的新靶点[10]。miR-671-5p 在结直肠癌

组织和细胞系中表达上调，并与结直肠癌患者的生存率相关。miR-671-5p 可能通过靶向 TRIM67 促进体外细胞增殖、迁移和侵袭，作为结直肠癌的致癌基因[11]。此外，miR-510 在结直肠癌的过表达促进了结直肠癌细胞的增殖、迁移和侵袭，而其敲降抑制了这些细胞过程，表明 miR-510 在结直肠癌的进展过程中起着启动肿瘤的作用[12]。miR-200 家族在上皮-间充质转化（EMT）中发挥重要作用，主要通过直接抑制 ZEB1/2 转录因子，影响许多与上皮和间充质表型相关的基因。而 Knudsen 等人表明 miR-200b 在侵袭前沿的表达下降，尤其是在出芽的细胞中，这一发现发现支持了结直肠癌出芽状细胞中的 EMT 样过程的假设[13]。miR-200b 的表达是否具有临床意义有待进一步研究。

此外，非编码 RNA 表达在 HDAC 抑制剂抗癌机制中发挥重要作用，例如奇达胺和放疗联合治疗肺鳞状细胞癌研究中发现 MiR-375-EIF4G3 轴协同诱导细胞凋亡并抑制肿瘤生长和癌症干性，抑制 MiR-375 的表达减弱了单用奇达胺或放疗治疗诱导细胞凋亡的促进作用，并恢复其癌症干细胞干性[14]。SAHA 诱导乳腺癌细胞中的 miR-200c 的过表达来抑制抑制乳腺癌细胞的增殖，侵袭和迁移，敲低 miR-200c 实验结果证明其在 SAHA 抑癌机制中发挥重要作用[15]。因此，寻找对结直肠癌发生发展起关键作用的 miRNA 对于结直肠癌早期诊断、治疗以及预后具有十分重要的作用。

ITF2357 是一种具有广泛的抗炎活性的，安全且可耐受的 HDACi，其抗肿瘤活性已在一些血液系统肿瘤和实体瘤中被报道[16]。Francesco Marampon 等人证明 ITF2357 处理胶质母细胞瘤能够显著抑制肿瘤细胞生长或诱导凋亡，且呈剂量依赖性并在异种移植小鼠模型中抑制了胶质母细胞瘤干细胞样细胞群和肿瘤的生长 。不同剂量的 ITF2357 能够诱导胶质母细胞瘤细胞 G1/S 细胞周期阻滞或激活程序性细胞凋亡，这主要通过上调 p21 和 p27 的表达，下调 CDK1、细胞周期蛋白 A 和细胞周期蛋白 B，并诱导视网膜母细胞瘤蛋白的低磷酸化或者抑制其磷酸化[17]。除此之外，ITF2357 在人角膜间质成纤维细胞中通过 TGF-β/BMP 7 信号通路抑制角膜纤维化，它通过 TGF-β/Smad/BMP 7 的下游靶点 Id3 发挥作用[18]。ITF2357 在结肠炎小鼠模型中的炎症中的研究显示，ITF 具有较好抗炎活性。先前研究表明，HDACi 可以直接靶向核转录因子 NF-kB,而 NF-kB 被指出为炎症诱导肿瘤生长发展的关键靶点因子[19]。此外，在几种类型

的实体肿瘤中都可以检测到 NF-kB 的激活增加。NF-kB 表达水平被减弱时，肿瘤细胞和炎症均显著减少[20]。在 ITF2357 存在的情况下，可以观察到 NF-kB 的活性减弱，然而还不能证明 ITF2357 对 NF-kB 具有特异性的调控作用，但已有研究证明 HDACi 能够直接调节 NF-kB 的激活[21]。因此，通过 HDACi 抑制 NF-kb 的转录可能有助于抑制炎症和肿瘤生长。目前，ITF2357 在结直肠癌中的作用以及可能的作用机理尚未报道。

参考文献：

[1] Kim Bum Jun, Jeong Jae Ho, Kim Jung Han, et al. The role of targeted agents in the adjuvant treatment of colon cancer: a meta-analysis of randomized phase III studies and review[J]. 2017, 8(19):31112-31118.

[2] Ades Steven. Adjuvant chemotherapy for colon cancer in the elderly: moving from evidence to practice[J]. 2009, 23(2):162-7.

[3] Son Hyun-Sook, Lee Woo Yong, Lee Won-Suk, et al. Compliance and effective management of the hand-foot syndrome in colon cancer patients receiving capecitabine as adjuvant chemotherapy[J]. 2009, 50(6):796-802.

[4] Bin Guo, Jingwen Liu, Lokesh Bhatt, et al. Target Genetic Abnormalities for the Treatment of Colon Cancer and Its Progression to Metastasis[J]. 2021, 22(7):722-733.

[5] Parizadeh Seyed Mostafa, Jafarzadeh-Esfehani Reza, Ghandehari Maryam, et al. Epigenetic Drug Therapy in the Treatment of Colorectal Cancer[J]. 2018, 24(23):2701-2709.

[6] Mohammed Manal, M.J.N. Chandrasekar, Jeyapal Gomathi Priya, et al. Inhibitors of histone deacetylase as antitumor agents: A critical review[J]. 2016, 67:18-42.

[7]王奕,吴晔明.近五年中国大陆神经母细胞瘤基础研究述评[J].中华小儿外科杂志,2017,38(04):241-246.

[8] Paul A. Marks, . Histone deacetylase inhibitors: A chemical genetics approach to understanding cellular functions[J]. 2010, 1799(10):717-725.

[9] Kim HJ, Bae SC. Histone deacetylase inhibitors: molecular mechanisms of action and clinical trials as anti-cancer drugs. Am J Transl Res. 2011;3(2):166-179.

[10] Cao Hongliang, Huang Shaojun, Liu Aihua, et al. Up-regulated expression of miR-155 in human colonic cancer[J]. 2018, 14(3):604-607.

[11] Jin Wei, Shi Jinsheng, Liu Meiqin, et al. Overexpression of miR-671-5p indicates a poor prognosis in colon cancer and accelerates proliferation, migration, and invasion of colon cancer cells[J]. 2019, 12:6865-6873.

[12] Hang J, Wei F, Yan Z, Zhang X, Xu K, Zhu Y. The value of miR-510 in the prognosis nd development of colon cancer. Open Med (Wars). 2021;16(1):795-804.

[13] Knudsen KN, Lindebjerg J, Nielsen BS, Hansen TF, Sørensen FB. MicroRNA-200b is downregulated in colon cancer budding cells. PLoS One. 2017;12(5):e0178564.

[14] Huang X, Bi N, Wang J, et al. Chidamide and Radiotherapy Synergistically Induce Cell Apoptosis and Suppress Tumor Growth and Cancer Stemness by Regulating the MiR-375-EIF4G3 Axis in Lung Squamous Cell Carcinomas. J Oncol. 2021;2021:4936207.

[15] Eckschlager T, Plch J, Stiborova M, Hrabeta J. Histone Deacetylase Inhibitors as Anticancer Drugs. Int J Mol Sci. 2017;18(7):1414. Published 2017 Jul 1.

[16] Del Bufalo D, Desideri M, De Luca T, et al. Histone deacetylase inhibition synergistically enhances pemetrexed cytotoxicity through induction of apoptosis and autophagy in non-small cell lung cancer. Mol Cancer. 2014;13:230.
[17] Marampon Francesco, Leoni Flavio, Mancini Andrea, et al. Correction to: Histone deacetylase inhibitor ITF2357 (givinostat) reverts transformed phenotype and counteracts stemness in in vitro and in vivo models of human glioblastoma[J]. 2019, 145(9):2411.
[18] Lim RR, Tan A, Liu YC, et al. ITF2357 transactivates Id3 and regulate TGFβ/BMP7 signaling pathways to attenuate corneal fibrosis. Sci Rep. 2016;6:20841.
[19] Michael Karin, Florian R. Greten . NF-κB: linking inflammation and immunity to cancer development and progression[J]. 2005, 5(1):749-759.
[20] Koliaraki V, Pasparakis M, Kollias G. IKKβ in intestinal mesenchymal cells promotes initiation of colitis-associated cancer. J Exp Med. 201;212(13):2235-2251.
[21] Takada Yasunari, Gillenwater Ann, Ichikawa Haruyo, et al. Suberoylanilide hydroxamic acid potentiates apoptosis, inhibits invasion, and abolishes osteoclastogenesis by suppressing nuclear factor-kappaB activation[J]. 2006, 281(9):5612-22.

（三）项目预期达到的目标、主要技术和经济指标，可获得的成果、知识产权和人才培养情况

1. 深入研究表观遗传药物抗结直肠癌的作用与分子机制。

2. 寻找一种抑癌效果确切、毒副作用少、适合长期使用的针对肿瘤表观遗传组学的表观遗传疗法，有望提高以表观遗传为基础的结直肠癌治疗效果。

3. 未来三年培养研究生 1-2 名，在有国际影响力的期刊杂志发表 SCI 论文 1-2 篇。

（四）项目拟采取的研究方法，项目技术路线及其可行性分析

研究方法

第一部分 检测表观遗传药物在体外对结直肠癌细胞的影响；

首先通过 MTT 法检测 ITF2357 对结直肠癌细胞的抑制活性。其次，通过 CCK8 实验检测 ITF2357 对结直肠癌细胞增殖的影响。划痕实验检测细胞迁移，并通过流式细胞术检测 ITF2357 对结直肠癌细胞周期和细胞凋亡的影响，此外通过 Western Blot 实验检测细胞周期相关蛋白的表达水平等功能实验验证表观遗传药物 ITF2357 在体外对结直肠癌细胞的作用。

第二部分 检测表观遗传药物在体内对肿瘤生长的影响

通过建立结直肠癌小鼠模型，分为对照组和治疗组。定期腹腔注射药物后，测量小鼠体重、肿瘤大小并检测器官指数。在体内验证表观遗传药物 ITF2357 抗结肠癌的作用，以期探寻治疗结直肠癌的新型表观遗传药物。

第三部分 探索表观遗传药物在结直肠癌中的潜在作用机制

为进一步探索表观遗传药物 ITF2357 抗结直肠癌的分子机制。进行转录组测序和小 RNA 测序，并通过与结直肠癌与癌旁组织转录组及小 RNA 测序的结果结合分析，寻找与结直肠癌预后相关性强的靶基因，并在临床样品中验证靶基因的表达。同时，通过在结直肠癌细胞中干扰靶基因验证其功能。

技术路线

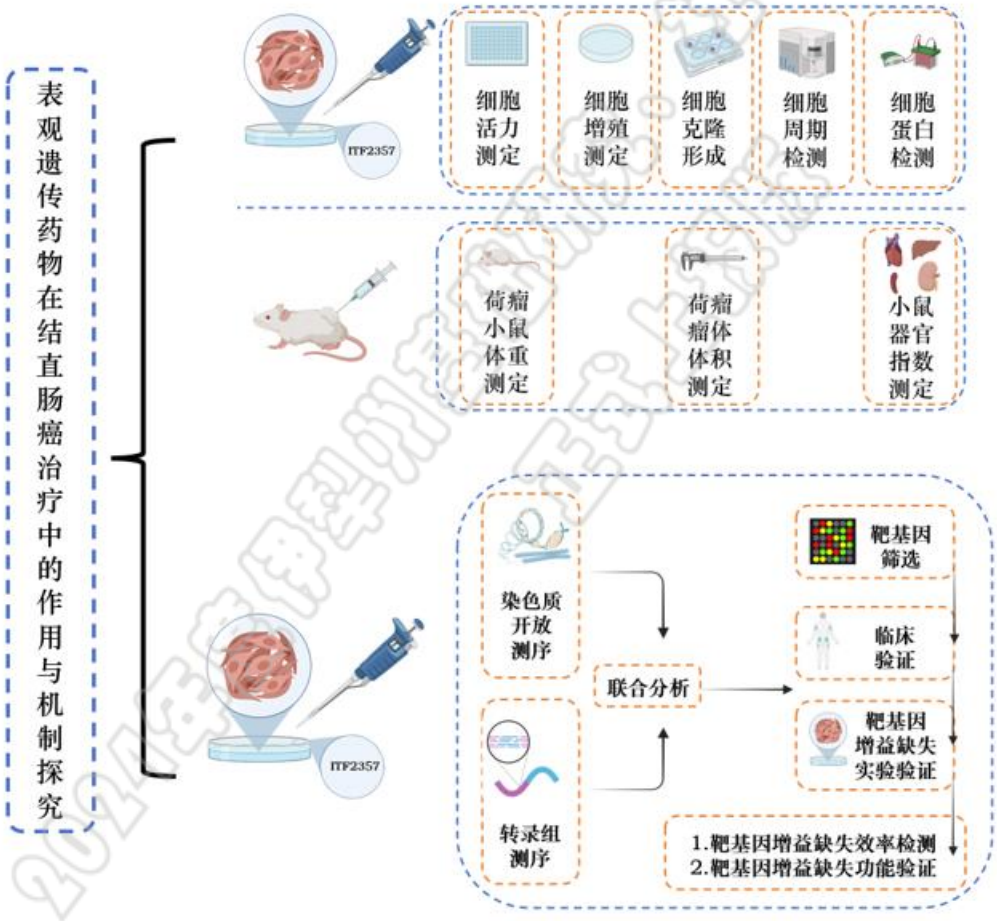

可行性分析

（1）申请人博士研究生学历，接受过严格的科研训练，作为霍尔果斯市人民医院院长（连一医援疆胃肠外科专家）、连一医援疆医疗队队长长期致力于胃肠道恶性肿瘤的临床与基础研究，擅长腹壁疝、腹股沟疝、胃食管反流性疾病、炎症

性肠道疾病的治疗。

（2）协作单位专家在博士期间接受了首席科学家的严格训练，对该领域具有深厚的研究基础，系统掌握了分子与细胞的各种关键技术，如基因敲除与过表达、构建质粒、RNA 抽提、定量 PCR、免疫荧光染色、蛋白质印迹法、RNA 免疫共沉淀、染色质免疫共沉淀、流式细胞术、动物实验等。新疆大学能够提供研究所需的各种仪器设备和动物研究平台。

（3）协作单位实验室具备相关实验基础，与熟练的技术支持。并且已经开展了部分实验例如表观遗传药物 ITF2357 在小鼠体内外抑制结直肠癌的实验，并且实验室有丰富的结肠癌小鼠模型的建立基础

（4）协作单位实验室现有硕士研究生 10 名，联合培养硕士研究生 2 名，以及本科生 6 名。本项目的研究内容是在前期工作基础上提出，研究目标明确，技术路线可靠，有前期数据作为依据，没有可预见性困难。

前期实验基础

在前期的实验结果中，我们已在发现表观遗传药物 ITF2357 在小鼠体内外均能抑制结直肠癌,这为 ITF2357 作为抗结直肠癌的候选药物提供了理论基础。

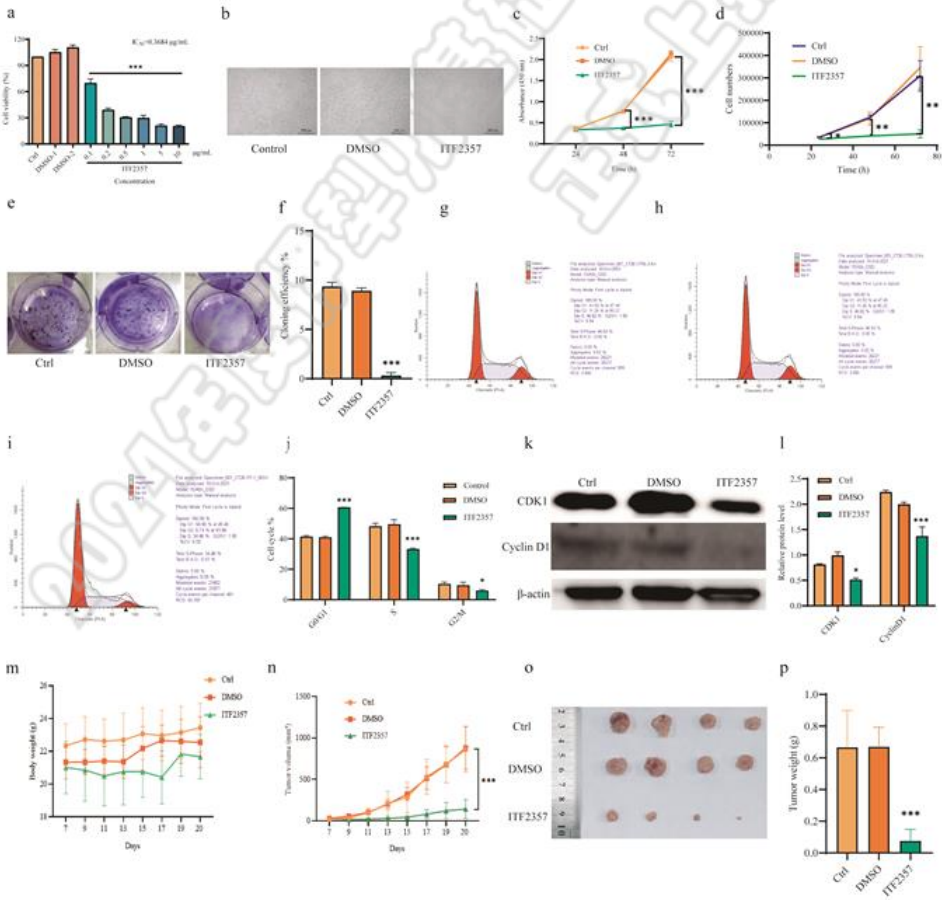

图 1 ITF2357 在结直肠癌中的作用研究

（a）MTT 法检测 ITF2357 对 CT26 细胞活性；（b）观察 ITF2357 对 CT26 细胞形态的影响;（c-d）CCK8 法检测 ITF2357 对 CT26 细胞增殖的影响;（e-f）克隆形成实验检测 ITF2357 对 CT26 细胞克隆形成能力的影响;（f-j）流式检测 ITF2357 对细胞周期分布的影响;（k-l）WB 检测细胞周期相关蛋白的表达;（m）药物治疗期间测量小鼠体重；（n）测量小鼠肿瘤体积;（o-p）小鼠处死后肿瘤拍照和称量肿瘤重量。

（五）项目研究的年度进度及年度考核指标

2024 年 5 月-2025 年 5 月

通过体内外实验检测表观遗传药物 ITF2357 的抗肿瘤效果。通过转录组测序和小 RNA 测序探讨 ITF2357 对结直肠癌生长的作用机制并进行验证。

2025 年 6 月至 2026 年 5 月

分析实验结果，撰写文章投稿，撰写结题报告。

（六）项目的组织和分工（包括申请单位和协作单位的任务分工，实施的组织措施及其与总体目标的关系等）

任务分工

申请单位在项目中承担核心职责，涉及项目启动的各个关键环节，从立项申请到规划编制，再到资源整合与风险管理，以及全过程的进度、质量和成本控制，确保项目按照既定目标高效、有序地推进。

协作单位在项目中扮演着执行和服务的角色，负责执行专家组和项目负责人的决议，管理项目资料和成果，保持与项目成员的密切联系，组织内部会议，编写项目简报和会议纪要，进行数据统计，并协助专家组完成年度汇报和结题评估，同时提供专业服务，实施质量控制和安全管理，确保信息沟通。

实施的组织措施

1. 成立项目专家组，由外聘专家组成，专家组对项目和课题研究提供技术指导和咨询，为项目和课题负责人做出决策提供建议，参与项目和课题实施过程中的监督检查、审核、评估与验收准备等工作。组织学术研讨与交流，对项目和

课题的关键技术问题、阶段研究成果及最终研究成果等进行技术咨询和把关。

2.协作单位主要职责为：执行专家组及项目负责人的各项决议；负责收集、整理和保管与本项目有关的资料、项目成果和数据等，保证项目成员的共享；负责保持经常性联系，随时了解课题进展情况并及时向项目负责人和项目专家组成员汇报；

保障措施及与总体目标的关系

1. 团队参与人获得过国家自然科学基金青年项目、天山英才、天池博士计划、天山青年等项目及荣誉称号。研究成果获得国内外同行专家的高度关注和广泛认可；在国内外知名期刊发表论文数几十余篇，为项目的成功提供了坚实的保障。

2. 项目的组织和分工是为了实现项目的总体目标而设计的。通过明确分工和有效组织，可以确保项目按照预计划和质量要求顺利进行，从而达到项目的总体目标。

（七）项目预期研究成果应用前景分析（包括国内外应用或市场现状、潜在用户、市场前景，相应效益分析等）

结直肠癌是最常见的消化道恶性肿瘤之一，其发病率和死亡率均比较高。CRC 发病率仅次于肺癌、前列腺癌（男性）和乳腺癌（女性），且死亡率仅次于肺癌（第二大癌症相关全因素死亡原因）。近年来，随着患病人群逐渐年轻化，引起了较大的关注。年轻结直肠癌患者的肿瘤往往有更具有侵袭性，因此年轻人的死亡率呈现逐年上升的趋势。研究表明，早期患者术后 5 年生存率可达到90%以上，早发现、早诊断、早治疗对于结直肠癌的预防和治疗具有重要意义。因此，寻找结直肠癌有效的治疗药物及靶点，改善其患者的生存率成为了主要研究目标。手术治疗、放疗、化疗以及靶向药物治疗等均是目前临床上常用的治疗策略。手术切除是最主要的治疗手段，但接受手术治疗的患者尤其是中晚期患者中，大约 30-50%仍然会出现术后复发和转移，因此放化疗联合手术治疗是一种重要的策略，然而，就常见的化疗药物而言，药物会非靶向运输并产生毒副作用。此外，长期服用化疗药物也会产生机体耐药性。。因此，选高效、具有靶向性且

安全的抗 CRC 药物是较为紧迫的临床研究任务。表观遗传学改变的可逆性是与经典遗传学不同的特点之一。研究表明，异常的表观遗传修饰通常发生于恶性肿瘤的早期阶段，因此表观遗传修饰变化可作为早期诊断的生物标志物且有助于提高诊疗效果。本项目预期研究成果将为结直肠癌的治疗提供新的用药方案，提高治疗效果，降低副作用。本项目将带来显著的社会和经济效益，包括减少患者的病痛、提高患者的生活质量、降低医疗费用等。同时，通过培养一批具有专业水平的研究人才，将产生深远的社会效益。

（八）项目申请单位承诺提供的支撑条件

本单位郑重承诺严格按照项目相关管理制度执行， 对申请项目组和负责人提供研发场地， 提供国内行业一流的实验设备及实验装置和自筹资金支持， 协助其顺利完成项目实施， 对获批经费进行专项管理。

（九）项目经费预算表

单位：万元

预算科目	总预算数	其中：自治州财政拨款	备注
(1)	(2)	(3)	(4)
一、预算来源合计	15.0	15.0	
（一）自治州财政拨款	15.0	15.0	
（二）自筹经费	0.0		
1.其他财政拨款	0.0		
（1）国家部委拨款	0.0		
（2）地州市财政拨款	0.0		
（3）主管部门配套	0.0		
2.承担单位自有货币资金	0.0		
3.从银行获得的贷款	0.0		
4.其他资金	0.0		
二、支出预算合计	15.0	15.0	
（一）直接费用	12.0	12.0	
1.设备费	0.0	0.0	
其中：购置设备费	0.0	0.0	
2.业务费	10.0	10.0	
3.劳务费	2.0	2.0	
（二）间接费用	3.0	3.0	

四、项目申请单位及协作单位情况

（一）项目申请单位基本情况（包括单位的经济技术实力、组织管理水平、相关研究开发基础，科研人员、科研投入、科研成果应用，以及承担国家、自治区和自治州科技计划项目等情况）

霍尔果斯市人民医院是一所集医疗、教学、急救、科研、预防保健和康复治疗为一体的，环境优美、功能齐全、设备先进、技术优良的二级综合医院。设有临床、医技、行政后勤等 29 个科室，拥有西门子 CT、奥林巴斯胃肠镜等高端设备 50 余台，可开展腹腔镜下胆囊切除术、腹腔黏连松解术、胃穿孔修补术、腹腔镜下阑尾切除术等多项手术，开展新项目新技术 62 项。2023 年霍尔果斯市人民医院正式获批“国门医院”，取得涉外医疗资质，成为全疆唯一一所县市级获批的医疗机构，已为 3000 余人次外籍患者提供健康咨询。

霍尔果斯市人民医院积极对接连云港市卫健委，连云港市第一人民医院医院及江苏省转化医学研究基地及中心实验室展开深入合作。同时与疆内外高校积极推进基础医学与临床转化研究，为推动科研进展提供了有利平台。

（二）协作单位基本情况（企业单位重点说明与项目相关的技术开发与应用水平、管理能力和经济实力，与本项目相关产品的开发、生产、经营情况等；非企业类单位重点说明在项目相关技术方面的研发能力、技术基础及管理能力等）

新疆生物资源基因工程重点实验室为国家科技部与新疆共建重点实验室，是新疆唯一具有长江特聘教授岗位、设备最先进、具博士授予点的研究基地。实验室用于项目研究的主要仪器设备有：常规 PCR 仪、定量 PCR 仪、高速离心机、超高速离心机、高速冷冻离心机，FACSCalibur 流式细胞仪、超低温冰箱、UV3100 紫外分光光度计、酶标仪、倒置荧光显微成像系统、激光共聚焦显微镜及其它分子生物学研究常规仪器，实验室还具有细胞房、动物饲养房。此外新疆大学理化分析中心拥有先进的液相色谱、扫描电镜、透射电镜、红外光谱仪、气相色谱-

质谱联用设备及其他高精度测试和分析大型仪器设备可供研究使用。协作单位负责人毕业于同济大学，获理学博士学位，现为新疆大学生命科学与技术学院副教授，硕士生导师，新疆生物物理理事会理事。主持国家自然科学基金青年项目 1 项，省部级科研项目 2 项，厅局级科研项目 1 项，横向项目 1 项，校级项目 1 项。2023 年获批自治区天山英才—青年拔尖人才项目，在 Aging Cell、Stem Cell Reports、Cell Stem Cell、Nature Communication、Stem Cell 等国际著名 SCI 杂志发表论文十余篇，累计影响因子大于 100 。已授权专利 2 项，其中国际授权专利 1 项。新申请专利 1 项。其实验室目前有硕士生 10 名，其中联合培养 2 名，本科生 6 名。且本项目的研究内容是在前期工作基础上提出的，研究假说明确，技术路线可靠。

五、申请单位意见

1．项目申请单位意见 签　章 年　月　日
2．协作单位意见 协作单位（一） 签　章 年　月　日
协作单位（二） 签　章 年　月　日
协作单位（三） 签　章 年　月　日
３．主管部门意见 签　章 年　月　日

六、其它需要说明的情况和附件

1	申请单位及协作单位意见.pdf
2	项目负责人承诺书.pdf

3	单位承诺书.pdf
4	连云港市委、市政府援疆委派文件.pdf
5	ITF2357 induces cell cycle arrest and apoptosis of meningioma cells__via the PI3K-Akt pathway.pdf
6	pharmaceutics-15-00155-1.pdf
7	Disulfiram loaded hollow copper sulfide nanoparticles show antitumor effects in preclinical models of colorectal cancer.pdf
8	Hollow Nanoporous Prussian Blue Nanocubes Enriched with Cu2+ and Loaded with Quercetin for Synergistic Tumor Therapy.pdf
9	Aging Cell - 2022 - Jiapaer - Regulation and roles of RNA modifications in aging-related diseases.pdf

五、申请单位意见

1. 项目申请单位意见

同意

签 章

年 月 日

2. 协作单位意见

协作单位（一）

同意

签 章

年 月 日

协作单位（二）

签 章

年 月 日

协作单位（三）

签 章

年 月 日

3. 主管部门意见

自治州科技计划项目诚信承诺书

项目负责人承诺:

本人作为申报2024年度自治州基础研究、社会发展类科技计划项目（表观遗传药物在结直肠癌治疗中的作用与机制探究）的负责人，在充分知晓并接受项目管理有关规定的前提下，郑重承诺如下:

本人保证项目申报材料的真实性和合法性；本项目申请没有出现违反法律及有关规定的内容，项目组成员身份均真实有效。如该项目立项，我将严格履行项目负责人职责，主动承担项目责任，严格遵守项目管理的有关规定，严格落实科技项目经费管理办法及项目经费预算书，建立专项账目，做到专款专用，切实保证研究工作时间，认真开展工作，按时报送有关材料，确保项目顺利完成。若填报失实或违反规定，本人将承担相关责任。

项目负责人(亲笔签字按手印):

2024年3月11日

自治州科技计划项目诚信承诺书

项目承担单位承诺：

按照项目管理有关规定，对申报项目的负责人和项目组成员资格及项目申报材料相关内容进行了审核，申请材料真实有效。如项目立项，在项目实施期间，我单位保证对项目实施所需要的人力、物力和工作时间等条件给予保障，严格遵守项目管理的有关规定，严格落实科技项目经费管理办法及项目经费预算书，建立专项账目，做到专款专用，督促项目负责人和项目组成员按照项目管理的有关规定执行。若申报材料内容信息失实、执行项目中违反规定，本单位将承担相关责任。

单位名称（加盖公章）：

2024年3月16日

№ 000001

中共连云港市委办公室

连 办〔2023〕15号

市委办公室　市政府办公室
关于调整市支援新疆霍尔果斯经济开发区（霍尔果斯市）前方工作组的通知

各县区委、人民政府，市委各部委，市各委办局，市各直属单位，驻连部省属单位：

根据省委、省政府选派第十一批援疆干部人才工作安排，经市委、市政府研究，决定调整市支援新疆霍尔果斯经济开发区（霍尔果斯市）前方工作组组成人员，名单如下：

组　长：许　峰　市国资委副主任、党委委员

副组长：李瑾伟　灌云县委常委、宣传部部长

成　员：张龙文　市委组织部综合考核处二级主任科员

王晓光　市重大项目办公室项目一处处长

李小华　市工信局节能与综合利用处处长、一级主任科员

岳洪波　市公安局海州分局副局长、党委委员，海防大队大队长，一级警长

张宝明　市第一人民医院胃肠外科副主任医师

徐行茹　市中医院影像科副主任医师

李文娟　市第二人民医院新生儿科主治医师

冯　鑫　市东方医院产科副主任医师

工作组在市委、市政府和省对口支援新疆伊犁州指挥部领导下开展工作，负责做好对口援助规划编制和具体工作的组织实施、与新疆霍尔果斯经济开发区（霍尔果斯市）及有关部门的沟通协调。

工作组人员在新疆工作期间与原单位工作脱钩，工资、奖金、福利由原单位负责；享受援疆干部各项待遇；休假探亲按国家有关规定执行；工作经费由市财政按规定核拨。

中共连云港市委办公室
连云港市人民政府办公室
2023年4月25日

中共连云港市委办公室　　2023年4月26日印发

Medical Oncology (2023) 40:21
https://doi.org/10.1007/s12032-022-01883-w

ORIGINAL PAPER

ITF2357 induces cell cycle arrest and apoptosis of meningioma cells via the PI3K-Akt pathway

Lingying Zhang[1] · Chengyu Li[1] · Marhaba·Aziz[1] · Rongxin Zhu[1] · Zeyidan Jiapaer[1]

Received: 19 August 2022 / Accepted: 2 November 2022

Abstract

As a type of central nervous system tumor, meningioma usually compresses the nerve center due to its local expansion, further causing neurological deficits. However, there are limited therapeutic approaches for meningiomas. ITF2357, a potent class I and II histone deacetylase inhibitor (HDACi), has been shown to inhibit cell proliferation, promote apoptosis, and block the cell cycle in various sarcoma cells, including glioblastoma and peripheral T-cell lymphoma. Here, we investigated the potential role of ITF2357 on meningioma cancer cells (IOMM-Lee cells). First, we demonstrated that the half-maximal inhibitory concentration (IC50) of ITF2357 was 1.842 μM by MTT assay. In addition, ITF2357 effectively inhibited the proliferation and colonization ability of IOMM-Lee cells. Flow cytometry analysis showed that ITF2357 induced G0/G1 and G2/M phase cell cycle arrest and cell apoptosis. Mechanically, the RNA sequencing data revealed that ITF2357 could affect the PI3K-Akt signaling pathway and the cell cycle progression. Furthermore, the expression levels of Akt, PI3K, p-Akt, and p-PI3K were determined by western blotting. Collectively, our data revealed that ITF2357 induces G0 G1 and G2/M phase arrest and apoptosis by inhibiting hyperactivation of the PI3K-Akt pathway, ultimately inhibiting cell viability and proliferation of meningioma cells, which developed a new approach to the treatment of meningioma.

Keywords Meningioma · ITF2357 · Cell cycle · Cell apoptosis · PI3K-Akt pathway

Introduction

Meningioma, which mainly originates from meningeal epithelial cells derived from the neural crest of the arachnoid dura layer, accounts for 20% of intracranial tumors and is one of the typical primary tumors in the central nervous system [1]. In the latest WHO 2021 classification of CNS tumors, meningiomas are classified into 3 grades, WHO grade I meningiomas account for about 81% and usually present as benign and do not exhibit invasive behavior. WHO grade II and III meningiomas account for about 17% and 2%, respectively, with high recurrence rates [2, 3]. The pathogenesis of meningiomas is complex and associated with many factors, including physicochemical, genetic, and estrogenic factors [4, 5]. Surgery is the most effective treatment modality, supplemented by radiation therapy [6]. However, although surgical treatment can remove the tumor, the infiltrative growth of meningioma results in a high likelihood of recurrence. Therefore, drug therapy is usually chosen after surgery. Some contemporary chemical drugs used to treat meningiomas include interferon and growth inhibitor (SST) [7, 8]. However, these chemical drugs can cause damage to other tissues and organs in the body while acting on tumor cells. Due to their high safety, therapeutic targeting and reversibility, epigenetic agents have become anti-tumor drugs [9].

Epigenetics refers to reversible and heritable alterations in gene function without altering the nucleotide sequence [10]. Numerous studies have shown that epigenetic modifications play an essential role in the development of meningioma, mainly including altered DNA methylation, abnormal microRNA expression, mutations in histone and chromatin modifications [11]. Among them, histone deacetylation as a critical element of epigenetic regulation, its inhibitors can bind to histones of DNA, wrap histones, and play a role in

Lingying Zhang and Chengyu Li have contributed equally to this work.

✉ Zeyidan Jiapaer
zeyidan@xju.edu.cn

[1] Xinjiang Key Laboratory of Biological Resources and Gentic Engineering, College of Life Science and Technology, Xinjiang University, Urumqi 830046, China

Published online: 29 November 2022

various tumors by regulating the tightness of DNA to histones. The HDAC inhibitors panobinostat, LAQ824 and HC have been found to reduce the viability of meningioma cells [12]. However, the mechanism in meningioma has not been elucidated. ITF2357 has been shown to inhibit both glioblastoma (GBM) and peripheral T-cell lymphoma (PTCL), but its study in meningioma has not been reported [13, 14].

In this study, we not only investigated that ITF2357 can inhibit the proliferation of meningioma cells, but also explored its potential mechanism, which laid the theoretical foundation for ITF2357 in treating meningioma.

Results

ITF2357 inhibits cell proliferation in IOMM-Lee cells

First, we evaluated the effect of ITF2357 on IOMM-Lee cell viability, we found that ITF2357 strongly reduced the cell viability in a dose-dependent manner with an IC50 value of 1.842 μM (Fig. 1a). The proliferation of IOMM-Lee cells after ITF2357 (1.842 μM) treatment was also significantly inhibited as evidenced by the cell morphology (Fig. 1b). Notably, the colony formation assay results showed that ITF2357 strongly inhibited colony growth, indicating that ITF2357 can affect the long-term survival of IOMM-Lee cells (Fig. 1c, d).

ITF2357 induces cell cycle arrest at the G0/G1 and G2/M phase in IOMM-Lee cells

To examine if the inhibitory effects of ITF2357 on proliferation were due to cell cycle arrest, we used flow cytometry to analyze the distribution of the cell cycle (Fig. 2a–c). After 48 h of ITF2357 treatment, compared to the CTRL group, the percentage of cells in G0/G1 and G2/M phases increased by 19.97% and 7.19%, respectively. By contrast, those in the S phase decreased by 33.89% (Fig. 2d). Similarly, the percentage of cells in the G0/G1 and G2/M phase gradually increased, whereas the number of cells in the S phase gradually decreased compared to the DMSO group (Fig. 2d). Cyclin D1 is a key protein in the G0 to G1 phase transition, and CDK1 and cyclin B1 activation is a major checkpoint of transition from the G2/M [15, 16]. We found that the expression levels of these proteins were inhibited by ITF2357 compared to the CTRL/DMSO groups (Fig. 2e).

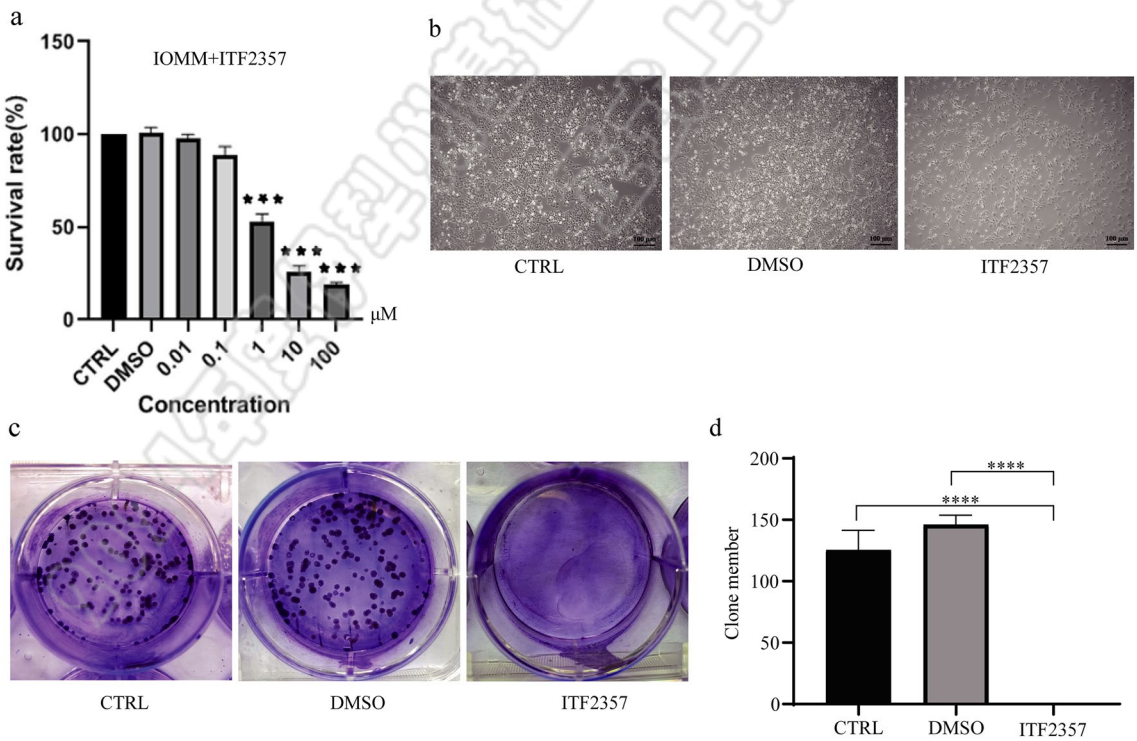

Fig. 1 ITF2357 inhibits cell proliferation in IOMM-Lee cells (**a**) MTT assay showed that the viability of IOMM-Lee cell was correlated with ITF2357 concentrations (0.01, 0.1, 1, 10, 100 μM) and calculate the IC50 values of IOMM-Lee cells to ITF2357. ***$P<0.001$ (**b**) representative phase contrast images of IOMM-Lee cells treated with DMSO/ITF2357 for 48 h. Data are representative of three independent experiments. Scale bar, 100 μm (**c**, **d**) colony forming assay. $n=4$ biologically independent samples per condition. Images are representative of two independent experiments. All scale bars 100 μm. ***$P<0.001$

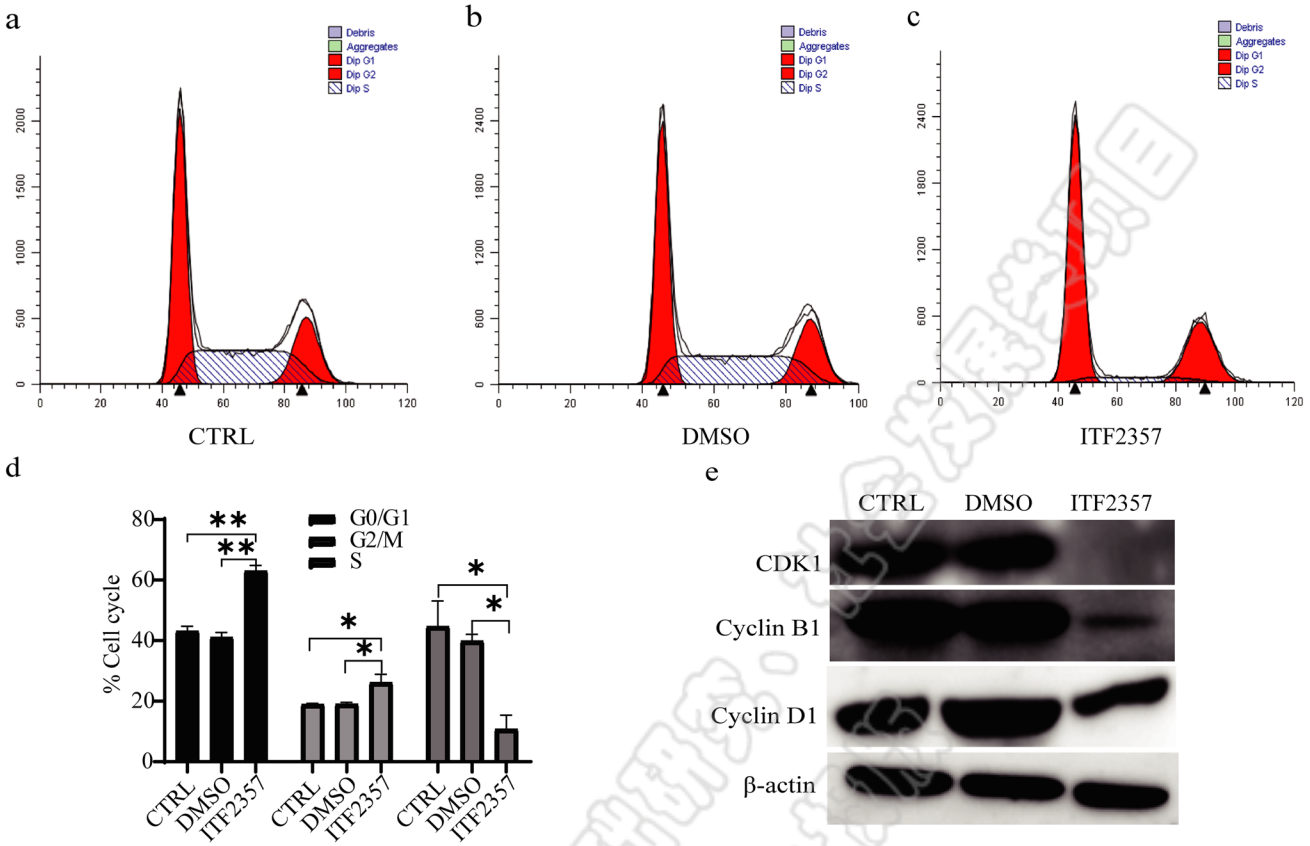

Fig. 2 ITF2357 induces cell cycle arrest at the G0/G1 G2/M and phase in IOMM-Lee cells (**a**–**d**) cell cycle arrest caused by ITF2357, and analyzed by flow cytometry. One of three repetitions with similar results is shown here. $^{*}P<0.05$, $^{**}P<0.01$ **e** Western blot analysis of the protein levels of cyclin D1, cyclin B1 and CDK1 in the ITF2357 -treated IOMM-Lee cells, β-actin was used as a loading control

These findings suggest that ITF2357 induces a G0/G1 and G2/M phase cell cycle arrest by inhibiting the expression levels of cyclin D1, cyclin B1, and CDK1, which leads to an inhibition of the viability in IOMM-Lee cells.

ITF2357 induces cell apoptotic in IOMM-Lee cells

Besides, we assessed the apoptotic effects of ITF2357 by cytofluorimetric analysis of AnnexinV/propidium iodide (PI) staining. We found that the number of apoptotic cells increased in the ITF2357-treated group compared to the control group especially the early apoptosis cells (Fig. 3a–d). In conclusion, ITF2357 inhibited the proliferation of IOMM-Lee cells by inducing cell cycle arrest and promoting apoptosis.

ITF2357 induces cell apoptotic in IOMM-Lee cells via PI3K-Akt signaling pathway

Next, to investigate the potential mechanisms by which ITF2357 affects IOMM-Lee cell cycle arrest and tumor cell apoptosis. Transcriptome changes were detected in IOMM-Lee cells treated with ITF2357 for 48 h. Heat map and cluster analysis showed that there were 6199 differentially expressed genes in ITF2357-treated IOMM-Lee cells compared to controls, of which 4318 genes were upregulated and 1881 genes were downregulated (Fig. 4a, b). GO enrichment analysis revealed that biological processes such as microtubule cytoskeleton organization ($P=2.96656080203397E-07$), regulation of chromosome ($P=2.63399218186944E-07$), organelle fission ($P=2.26447930877253E-07$) were dysregulated (Fig. 4c). KEGG pathway analysis highlighted that PI3K-Akt signaling pathway ($P=0.000372$) and cell cycle ($P=8.01E-07$) were dysregulated (Fig. 4d). Thus, ITF2357 may induce cell cycle arrest and apoptosis by affecting the PI3K-Akt signaling pathway.

ITF2357 induces cell cycle arrest through the PI3K-Akt pathway in IOMM-Lee cancer cells

RNA sequencing data showed that ITF2357 affected the PI3K-Akt signaling pathway in IOMM-Lee cells. Therefore,

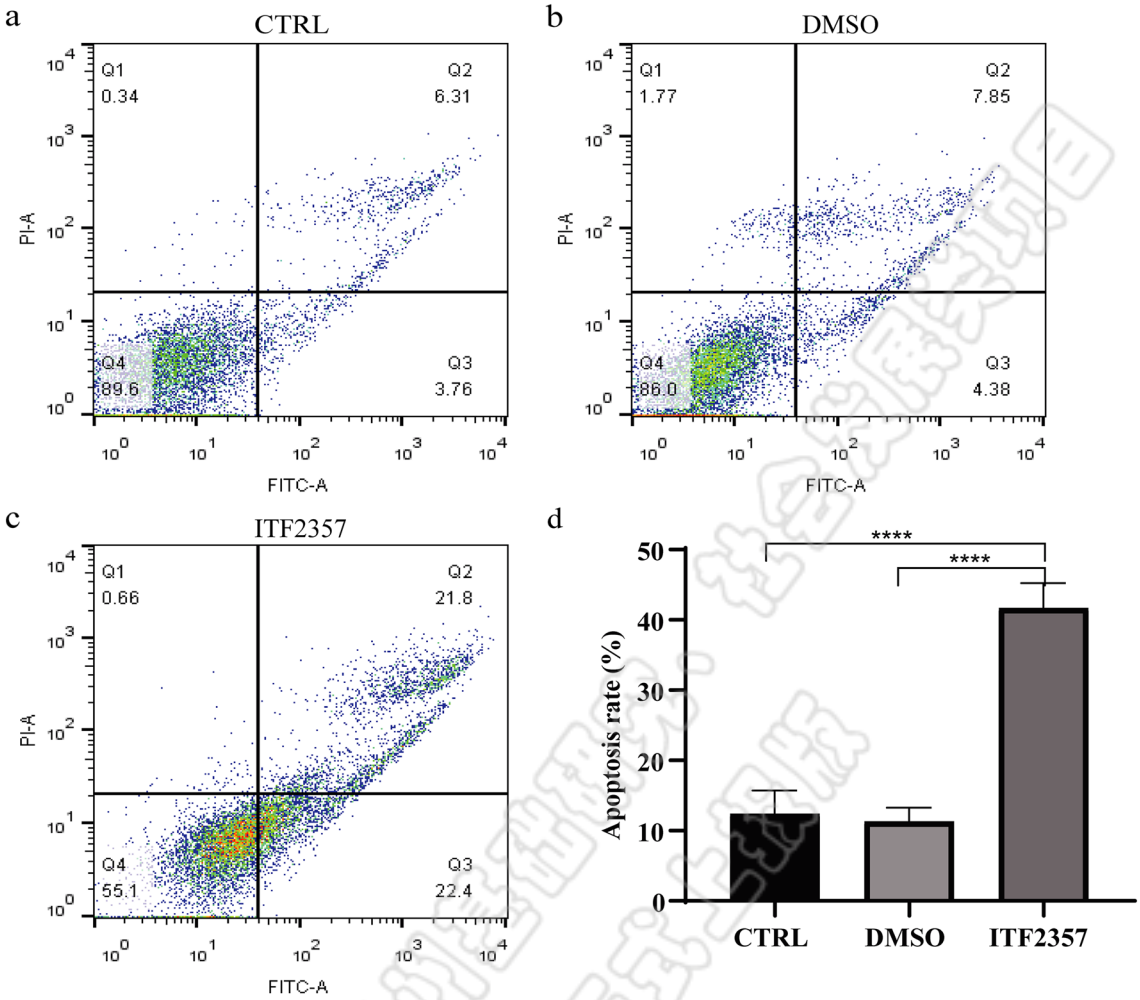

Fig. 3 ITF2357 induces apoptotic in IOMM-Lee cells (**a**–**d**) IOMM-Lee cells apoptosis induced by ITF2357, and analyzed with flow cytometry. One of three repetitions with similar results is shown here. ****$P < 0.0001$

we examined the expression levels of Akt, PI3K, p-AKT, and p-PI3K by western blotting and the results showed that the Akt and PI3K expression did not differ compared to the CTRL/DMSO groups, but p-AKT and p-PI3K were down-regulated in IOMM-Lee cells (Fig. 5), which is consistent with the KEGG dataset analysis. These results confirmed that ITF2357 affects the proliferation of IOMM-Lee cells by affecting the PI3K-Akt signaling pathway.

Discussion

Meningioma is a primary brain tumor of the central nervous system with various pathological variations. Its treatment includes surgical resection combined with radiotherapy and chemotherapy. However, its frequent recurrence can lead to a poor prognosis [17]. Therefore, research into new approaches to meningioma treatment has become urgent. It has been shown that meningioma development is associated with aberrant expression of various epigenetic modifications, including DNA methylation and acetylation [18, 19]. HDACi is a novel epigenetic antitumor agent, ITF2357, a class I and II HDACi, has been shown to effectively inhibit the proliferation of sarcoma, glioblastoma, and hepatocellular carcinoma [13, 20, 21]. However, its study in meningioma has not been reported. In this study, we found that ITF2357 inhibited the proliferation of IOMM-Lee cells in a dose-dependent manner via MTT. In addition, ITF2357 inhibited the colonization of IOMM-Lee cells in vitro, suggesting that ITF2357 plays a vital role in inhibiting meningiomas.

Cell cycle arrest is a potential way to treat tumors [22]. Previous studies have found that drug treatment can induce cell cycle arrest in breast, liver, and lung cancers [23–25]. ITF2357 (1.842 μM) induced cell cycle arrest in IOMM-Lee cells at G0/G1 and G2/M stages in this study. Besides, Cell cycle proteins play an essential role in tumorigenesis as

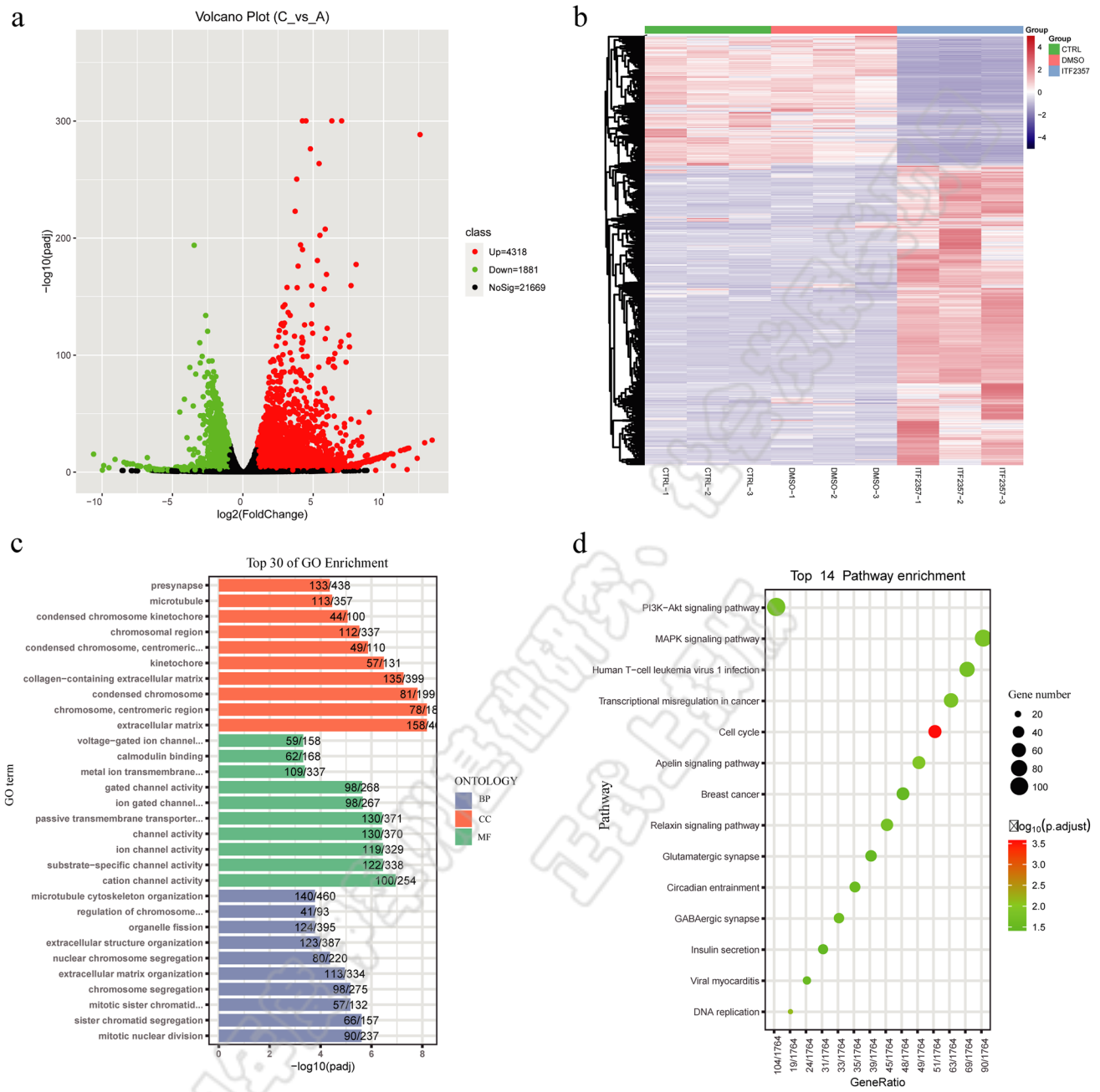

Fig. 4 ITF2357 induces cell apoptotic in IOMM-Lee cells via PI3K-Akt Signaling pathway (**a**) volcano plot of the gene expression profiles corresponding to RNA-seq. The fold changes and *P* values are estimated using the log2 and the log10-transformations, respectively. The green nodes represent the downregulated genes after the ITF2357 treatment. The red nodes stand for the upregulated genes after the ITF2357 treatment. **b** Heatmap showing the z-transformed expression values of library size-normalized read counts for each differentially expressed gene, colored from blue to red. RNA-Seq data from each independent sample are shown in the columns. **c** Gene Ontology (GO) term analysis of differentially regulated genes, as revealed using RNA-seq, in samples. The *x*-axis is the GO term, *y*-axis is the percentage of gene. The size of an orange, green, and blue represents the number of genes. **d** KEGG pathway annotation of differentially expressed genes. The color scale represented − log *P* adjust (Color figure online)

regulators of cell cycle progression [26]. Our study revealed that ITF2357 downregulated the expression of CyclinD1, CyclinB1, and CDK1. In addition, apoptosis, an important mechanism of tumor annihilation, has an essential role in tumor development [27]. Previous studies have found that raddeanin A can induce apoptosis and block the cell cycle by regulating the PI3K-Akt signaling pathway in colorectal cancer cells [28]. Interestingly, in our study we found that ITF2357 could not only block the cell cycle at G0/G1 and G2/M phases but also induce apoptosis.

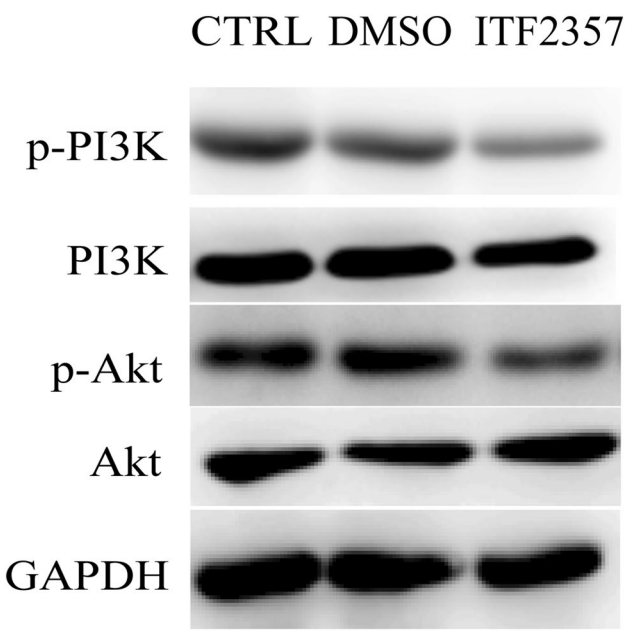

Fig. 5 ITF2357 induces cell cycle arrest through the PI3K-Akt pathway in IOMM-Lee cancer cells IOMM-Lee cells were treated with ITF2358 (1.842 μM) for 48 h. The expression levels of Akt, PI3K, p-Akt, and p-PI3K proteins were analyzed by western blot. GAPDH served as loading controls. Blots are representative of three independent experiments

Previous studies have shown that the PI3K-Akt signaling pathway is hyperactivated in many tumors, such as hepatocellular, colorectal, breast, and cervical cancer [29]. In addition, abnormalities in histone acetylation and lysine modifications also lead to excessive activation of Akt in tumor cells, which affects cancer cell proliferation, cycle arrest, and apoptosis [30, 31].In the present study, RNA-seq sequencing data showed that ITF2357 could significantly affect the PI3K-Akt signaling pathway, and the results of western blotting confirmed that ITF2357 inhibited the phosphorylation of AKT and PI3K. Therefore, ITF2357 is potentially valuable for the treatment of meningiomas, and the underlying mechanism is through affecting the PI3K-Akt signaling pathway.

Our data suggest that ITF2357 can induce apoptosis and cell cycle arrest by inhibiting cycle-related proteins in the PI3K-Akt signaling pathway. Our study provides a theoretical basis for the potential application of ITF2357 in the clinical treatment of meningioma.

Materials and methods

Drug

ITF2357 was purchased from Selleck.

Cell culture

IOMM-Lee cell line, purchased from the Procell, and cells cultured in Dulbecco's modified Eagle's medium (DMEM) supplemented with 10% (V/V) fetal bovine serum (FBS) and 1% penicillin/streptomycin, at 37℃ under an atmosphere of 5% CO_2. Absence of mycoplasma contamination which was routinely tested using PCR detection.

MTT viability assays

IOMM-Lee cells were plated at 5000 cells/well in 96-well plates in DMEM (six replica data point). IC50 values were determined by MTT after 48 h of treatment with doses of ITF2357 (from 1, 5, 10, 20, and 50 μM). Afterward, the supernatant was removed and supplemented with 100 μl (0.5 μM) MTT per well and incubated for 4 h at 37℃. The cells were centrifuged at 1200 rpm for 7 min at room temperature and the medium was removed. Furthermore, the medium was replaced with 150 μl DMSO and vortexed for 7 min. The absorbance was measured at 490 nm to obtain the OD value. The IC50 of ITF2357 was calculated using Prism v.8.0c software (GraphPad, San Diego, CA).

Colony formation assay

Cells were treated with DMSO/ITF2357 (1.842 μM) and seeded with 500 cells in each well of a 6-well plate in four replicates per treatment group. After 12 days of incubation, cells were washed once with phosphate buffer solution (PBS) and fixed with 4% paraformaldehyde for 15 min. Wash again with PBS for 5 min and repeat 3 times. After staining with 4 mg/mL crystal violet for 15 min, the cells were washed with PBS and the stained cells were counted.

Cell cycle analysis

IOMM-Lee cells (200,000 cells/well) were seeded in the six-well plate in 2 ml of growth medium by treating with DMSO/ITF2357 (1.842 μM) for 48 h. PBS was discarded after centrifugation at 1000 rpm for 4 min. cells were fixed in 70% ethanol at − 4 °C overnight, rinsed with ice cold PBS, then stained with propidium iodide (PI). Cell cycle distribution was determined by flow cytometry (CytoFLEX, Beckman Coulter, USA) and the data analysis using the software FlowJo V10. We analyzed only single cells in G0/G1, S, and G2/M that lay on the diagonal. Cell aggregates falling below the diagonal and cell debris with less PI fluorescence than the subG0 peak were excluded.

Cell apoptosis

Cells were seeded in 6-well plates at a density of 2×10^5 cells per well by treating with DMSO/ITF2357 (1.842 μM) for 48 h. Cells were collected and centrifuged at 1000 rpm for 4 min, then washed with PBS. The treated cells were resuspended in 100 μl binding buffer, then incubated with 10 μl PI and 5 μl Annexin V-FITC for 15 min at room temperature. Furthermore, 400 μl binding buffer was added. Apoptotic cells were detected using a flow cytometer (CytoFLEX, Beckman Coulter, USA).

RNA-seq

To obtain RNA for sequencing, 2×10^5 cells with DMSO/ITF2357 (1.842 μM) treatment or control were seeded onto 6-well plates in four replicates and cultured at 37 ℃ under an atmosphere of 5% CO_2 for 48 h. We extracted RNA using the TRIzol (Invitrogen). The mRNA was enriched by Oligo (dT), broken into 150–300nt fragments at 94 °C and inverted to cDNA. The double-stranded cDNA was synthesized by RNaseH (2.5U) and DNA polymerase (25U) enzymes and sequenced with sequencing junctions on both ends of the double-stranded cDNA, purified using AMPure XP bead and PCR amplified to obtain the final cDNA library. After library construction, the libraries were tested for insert size using an Agilent 2100, and passing the library test. The libraries were pooled and sequenced on the HiSeq platform according to the effective concentration and the target downstream data volume. Afterward, differential expression analysis was performed of mRNA.

Western blot

Cells were washed with cold PBS and lysed with WB and IP cell lysis solution (KeyGEN BioTECH) and protease inhibitor cocktail (CWBIO). Cell lysates were placed on ice for 30 min, followed by centrifugation at 12,000 rpm for 15 min at 4 °C. Proteins were standardized using the BCA protein assay kit (Thermo Fisher Scientific). Then equal amounts of protein were subjected to SDS-PAGE and transferred to 0.45 μm PVDF membranes (Sigma Aldrich). The membranes were blocked with 5% defatted milk (1 h at room temperature), washed with TBST (PBS, 0.1% Tween 20), then incubated with primary antibody overnight at 4 °C. Washed 3 times with TBST, incubated with secondary antibodies (1:1000) at room temperature for 1 h and washed again with PBST. Finally, the membranes were detected with ECL reagents (biosharp) using Image Lab software. The primary antibodies used were CDK1 (AF1516, Beyotime), Anti-β-Actin (Lot#M21205, TRAN), Cyclin B1 (AF1606, Beyotime), p-Akt (4060, Cell signaling Technology), p-PI3K (ab182651, Abcam), PI3K (4292, Cell signaling Technology), Akt (9272, Cell signaling Technology), GAPDH (#SC-47724, Santa Cruz), Goat Anti-Mouse (Lot#M21015, TRAN), Goat Anti-Rabbit IgG (Lot 01334/34721, CWBIO).

Statistical analysis

Statistical analysis and plotting of the data were performed using GraphPad Prism v.8.0. All data are presented as mean ± standard deviation. The statistical significance of differences between two groups was analyzed by one-way analysis or two-tailed student's *t*-test. $^*P < 0.05$ was considered statistically significant.

Author contributions LZ and CL: contributed equally to this work, including study conception and design, performing the experiments, data analysis, and manuscript writing. MA and RZ: were involved in manuscript preparation. RZ: contributed to the microarray data analysis. ZJ: designed and supervised the project and provided financial support and manuscript writing.

Funding This work was supported by the National Natural Science Foundation of China (Grant No. 81900287), Tianshan Youth Foundation of Xinjiang (Grant No. 2019Q066).

Data availability All relevant data and materials are within the paper.

Declarations

Conflict of interest The author reports no conflicts of interest in this work.

References

1. Lee DH, Sim HS, Hwang JH, Kim KS, Lee SY. Extracranial meningioma presenting as an eyebrow mass. J Craniofac Surg. 2017;28:e305–7. https://doi.org/10.1097/scs.0000000000003555.
2. Louis DN, et al. The 2021 WHO classification of tumors of the central nervous system: a summary. Neuro Oncol. 2021;23:1231–51. https://doi.org/10.1093/neuonc/noab106.
3. Piper K, et al. Radiation of meningioma dural tail may not improve tumor control rates. Front Surg. 2022;9:908745. https://doi.org/10.3389/fsurg.2022.908745.
4. Gupte TP, et al. Clinical and genomic factors associated with seizures in meningiomas. J Neurosurg. 2020. https://doi.org/10.3171/2020.7.Jns201042.
5. Muskens IS, et al. Body mass index, comorbidities, and hormonal factors in relation to meningioma in an ethnically diverse population: the Multiethnic Cohort. Neuro Oncol. 2019;21:498–507. https://doi.org/10.1093/neuonc/noz005.
6. Patel B, et al. Identification and management of aggressive meningiomas. Front Oncol. 2022;12: 851758. https://doi.org/10.3389/fonc.2022.851758.

7. Kunert-Radek J, Stepien H, Radek A, Pawlikowski M. Somatostatin suppression of meningioma cell proliferation in vitro. Acta Neurol Scand. 1987;75:434–6. https://doi.org/10.1111/j.1600-0404.1987.tb05474.x.
8. Nigim F, Wakimoto H, Kasper EM, Ackermans L, Temel Y. Emerging medical treatments for meningioma in the molecular era. Biomedicines. 2018;6(3):86. https://doi.org/10.3390/biomedicines6030086.
9. Murnyák B, Bognár L, Klekner Á, Hortobágyi T. Epigenetics of meningiomas. Biomed Res Int. 2015. https://doi.org/10.1155/2015/532451.
10. Sánchez-Romero MA, Casadesús J. The bacterial epigenome. Nat Rev Microbiol. 2020;18:7–20. https://doi.org/10.1038/s41579-019-0286-2.
11. Galani V, et al. Genetic and epigenetic alterations in meningiomas. Clin Neurol Neurosurg. 2017;158:119–25. https://doi.org/10.1016/j.clineuro.2017.05.002.
12. Tatman PD, et al. High-throughput mechanistic screening of epigenetic compounds for the potential treatment of meningiomas. J Clin Med. 2021;10(14):3150. https://doi.org/10.3390/jcm10143150.
13. Marampon F, et al. Histone deacetylase inhibitor ITF2357 (givinostat) reverts transformed phenotype and counteracts stemness in in vitro and in vivo models of human glioblastoma. J Cancer Res Clin Oncol. 2019;145:393–409. https://doi.org/10.1007/s00432-018-2800-8.
14. Piekarz RL, et al. Inhibitor of histone deacetylation, depsipeptide (FR901228), in the treatment of peripheral and cutaneous T-cell lymphoma: a case report. Blood. 2001;98:2865–8. https://doi.org/10.1182/blood.v98.9.2865.
15. Samukawa E, et al. Angiotensin receptor blocker telmisartan inhibits cell proliferation and tumor growth of cholangiocarcinoma through cell cycle arrest. Int J Oncol. 2017. https://doi.org/10.3892/ijo.2017.4177.
16. Yang Y, et al. c-Myc regulates the CDK1/cyclin B1 dependent-G2/M cell cycle progression by histone H4 acetylation in Raji cells. Int J Mol Med. 2018. https://doi.org/10.3892/ijmm.2018.3519.
17. Liu J, Xia C, Wang G. Multi-omics analysis in initiation and progression of Meningiomas: from pathogenesis to diagnosis. Front Oncol. 2020;10:1491. https://doi.org/10.3389/fonc.2020.01491.
18. Burns SS, et al. Histone deacetylase inhibitor AR-42 differentially affects cell-cycle transit in meningeal and meningioma cells, potently inhibiting NF2-deficient meningioma growth. Cancer Res. 2013;73:792–803. https://doi.org/10.1158/0008-5472.Can-12-1888.
19. Paramasivam N, et al. Mutational patterns and regulatory networks in epigenetic subgroups of meningioma. Acta Neuropathol. 2019;138:295–308. https://doi.org/10.1007/s00401-019-02008-w.
20. Armeanu S, et al. Apoptosis on hepatoma cells but not on primary hepatocytes by histone deacetylase inhibitors valproate and ITF2357. J Hepatol. 2005;42:210–7. https://doi.org/10.1016/j.jhep.2004.10.020.
21. Di Martile M, et al. Histone deacetylase inhibitor ITF2357 leads to apoptosis and enhances doxorubicin cytotoxicity in preclinical models of human sarcoma. Oncogenesis. 2018;7:20. https://doi.org/10.1038/s41389-018-0026-x.
22. Pereira BJA, et al. Cyclin E1 expression and malignancy in meningiomas. Clin Neurol Neurosurg. 2020;190:105647. https://doi.org/10.1016/j.clineuro.2019.105647.
23. Mun B, Park YJ, Sung GH, Lee Y, Kim KH. Synthesis and antitumor activity of (-)-bassianolide in MDA-MB 231 breast cancer cells through cell cycle arrest. Bioorg Chem. 2016;69:64–70. https://doi.org/10.1016/j.bioorg.2016.09.008.
24. Liu Q, et al. Anti-tumor effect of ginkgetin on human hepatocellular carcinoma cell lines by inducing cell cycle arrest and promoting cell apoptosis. Cell Cycle. 2022;21:74–85. https://doi.org/10.1080/15384101.2021.1995684.
25. Abdik H. Antineoplastic effects of erufosine on small cell and non-small cell lung cancer cells through induction of apoptosis and cell cycle arrest. Mol Biol Rep. 2022;49:2963–71. https://doi.org/10.1007/s11033-022-07117-6.
26. Liu SL, et al. GSK3β-dependent cyclin D1 and cyclin E1 degradation is indispensable for NVP-BEZ235 induced G0/G1 arrest in neuroblastoma cells. Cell Cycle. 2017;16:2386–95. https://doi.org/10.1080/15384101.2017.1383577.
27. Wang M, et al. Microglia-mediated neuroinflammation: a potential target for the treatment of cardiovascular diseases. J Inflamm Res. 2022;15:3083–94. https://doi.org/10.2147/jir.S350109.
28. Meng C, Teng Y, Jiang X. Raddeanin A induces apoptosis and cycle arrest in human HCT116 cells through PI3K/AKT pathway regulation in vitro and in vivo. Evid Based Complement Alternat Med. 2019. https://doi.org/10.1155/2019/7457105.
29. Amirani E, Hallajzadeh J, Asemi Z, Mansournia MA, Yousefi B. Effects of chitosan and oligochitosans on the phosphatidylinositol 3-kinase-AKT pathway in cancer therapy. Int J Biol Macromol. 2020. https://doi.org/10.1016/j.ijbiomac.2020.07.137.
30. Miller SA, et al. Lysine-specific demethylase 1 mediates AKT activity and promotes epithelial-mesenchymal transition in PIK3CA mutant colorectal cancer. Mol Cancer Res. 2019. https://doi.org/10.1158/1541-7786.mcr-19-0748.
31. Song Y, et al. The Wnt/β-catenin and PI3K/Akt signaling pathways promote EMT in gastric cancer by epigenetic regulation via H3 lysine 27 acetylation. Tumor Biology. 2017. https://doi.org/10.1177/1010428317712617.

pharmaceutics

MDPI

Review

Extracellular Non-Coding RNAs in Cardiovascular Diseases

Zeyidan Jiapaer [1,2,†], Chengyu Li [1,2,†], Xinyu Yang [3,†], Lingfei Sun [4], Emeli Chatterjee [4], Lingying Zhang [1,2], Ji Lei [5,*] and Guoping Li [4,*]

1 College of Life Science & Technology, Xinjiang University, Urumqi 830046, China
2 Xinjiang Key Laboratory of Biological Resources and Genetic Engineering, Urumqi 830046, China
3 Fangshan Hospital Beijing University of Chinese Medicine, Beijing 102400, China
4 Cardiovascular Research Center, Massachusetts General Hospital, Harvard Medical School, Boston, MA 02114, USA
5 Center for Transplantation Science, Massachusetts General Hospital, Harvard Medical School, Boston, MA 02114, USA
* Correspondence: jlei2@mgh.harvard.edu (J.L.); gli21@mgh.harvard.edu (G.L.)
† These authors contributed equally to this work.

Abstract: Cardiovascular diseases (CVDs) remain the world's leading cause of death despite the best available healthcare and therapy. Emerging as a key mediator of intercellular and inter-organ communication in CVD pathogenesis, extracellular vesicles (EVs) are a heterogeneous group of membrane-enclosed nano-sized vesicles released by virtually all cells, of which their RNA cargo, especially non-coding RNAs (ncRNA), has been increasingly recognized as a promising diagnostic and therapeutic target. Recent evidence shows that ncRNAs, such as small ncRNAs, circular RNAs, and long ncRNAs, can be selectively sorted into EVs or other non-vesicular carriers and modulate various biological processes in recipient cells. In this review, we summarize recent advances in the literature regarding the origin, extracellular carrier, and functional mechanisms of extracellular ncRNAs with a focus on small ncRNAs, circular RNAs, and long ncRNAs. The pathophysiological roles of extracellular ncRNAs in various CVDs, including atherosclerosis, ischemic heart diseases, hypertension, cardiac hypertrophy, and heart failure, are extensively discussed. We also provide an update on recent developments and challenges in using extracellular ncRNAs as biomarkers or therapeutical targets in these CVDs.

Keywords: extracellular RNAs; non-coding RNAs; cardiovascular diseases; biomarkers; therapeutical targets

Citation: Jiapaer, Z.; Li, C.; Yang, X.; Sun, L.; Chatterjee, E.; Zhang, L.; Lei, J.; Li, G. Extracellular Non-Coding RNAs in Cardiovascular Diseases. *Pharmaceutics* **2023**, *15*, 155. https://doi.org/10.3390/pharmaceutics15010155

Academic Editor: Lucio Barile

Received: 20 November 2022
Revised: 22 December 2022
Accepted: 27 December 2022
Published: 3 January 2023

1. Introduction

Cardiovascular diseases (CVDs) are widely recognized as the leading cause of death worldwide. Despite the considerable advances in both healthcare and therapies over the past decades, CVD has contributed to 17.9 million deaths in 2019 and is estimated to result in 22.2 million deaths in 2030 [1,2]. There is, therefore, an unmet medical need to develop novel diagnostics and therapeutics targeting CVDs. Emerging evidence suggests that extracellular non-coding RNAs (Ex-ncRNAs), particularly non-coding RNAs (ncRNAs) encapsulated in extracellular vesicles (EVs), function as key mediators of intercellular and inter-organ communication and play versatile roles in both homeostasis and disease [3]. EVs are continuously secreted by cells into circulation and are found in all biological fluids. The encapsulated molecular cargo inside EVs, especially RNAs, are increasingly recognized as promising biomarkers and therapeutic targets for various diseases, including CVDs [4–6].

Ex-ncRNAs are a heterogeneous group of RNAs, including small ncRNAs, long ncRNAs (lncRNAs), and circular RNAs (circRNAs), which encompass the majority of the extracellular transcriptome [7,8]. Ex-ncRNAs can be translocated into receipt cells after being secreted into the extracellular space through a variety of methods, thereby regulating various biological processes in targeted cells under both physiological and

pathological conditions [9] (Figure 1). This review summarizes the recent updates of Ex-ncRNAs and discusses the diagnosis and therapeutic aspects of Ex-ncRNAs in CVDs, including atherosclerosis, ischemic heart diseases, hypertension, cardiac hypertrophy, and heart failure.

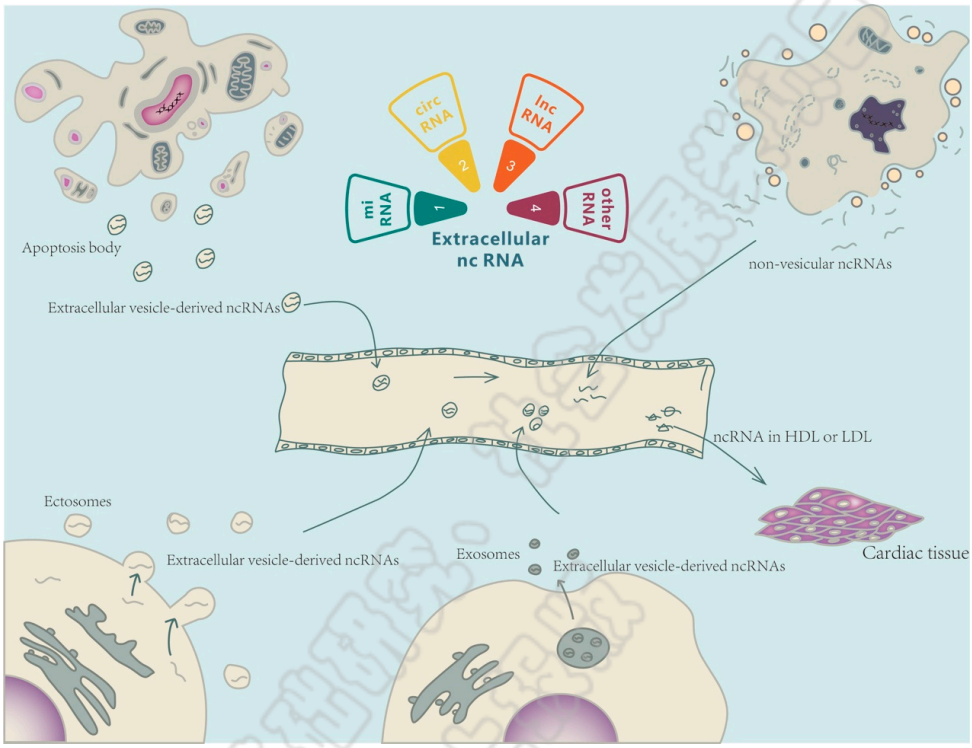

Figure 1. Extracellular non-coding RNA-mediated intercellular crosstalk. Extracellular non-coding RNAs (Ex-ncRNAs) are a heterogeneous group of RNAs and mainly include small ncRNAs, lncRNAs, and circRNAs. Ex-ncRNAs can be translocated into receipt cells and modulate the cellular functions of targeted cells (heart or other cardiovascular systems). Ex-ncRNAs can be secreted into the extracellular space through a variety of pathways, including embedded into exosomes, ectosomes, and apoptotic bodies, or partnered with ribonucleoproteins and lipoproteins.

2. Ex-ncRNAs

2.1. Extracellular Small ncRNAs

The main classes of small ncRNAs are miRNAs, small interfering RNAs (siRNAs), piwi-interacting RNAs (piRNAs), Y-RNAs, and tRNA-derived small RNAs (tDRs) [10,11]. Most small ncRNAs are capable of regulating gene expression either transcriptionally or epitranscriptionally [10,12]. Recent evidence suggests that small ncRNAs are encapsulated into EVs and modulate the transcriptome of recipient cells following release through cellular autocrine or paracrine pathways. In addition, small ncRNAs, embedded in ribonucleoproteins and lipoproteins, are found to be secreted into extracellular spaces [13]. An increasing number of studies have detected extracellular small ncRNAs in a variety of biological fluids, such as serum or plasma, and indicated that extracellular small ncRNA profiles in various body fluids could serve as novel biomarkers for different pathological conditions [14–17]. As one of the most abundant RNA species in circulation, extracellular small ncRNAs are actively involved in a variety of pathological and physiological processes. Therefore, the detection of specific circulating small ncRNAs, based on the small ncRNA profiles, could be a promising approach to diagnosing diseases.

2.2. Extracellular LncRNAs

LncRNAs are a class of transcripts with a length of more than 200 nucleotides and lack protein-coding potential [18]. There are many categories and sub-categories of lncRNAs,

with major classifications including antisense, bi-directional, enhancer-associated, intergenic lncRNAs (lincRNAs), and pseudogenes [19]. They function primarily in two fashions: (1) regulating the expression of miRNA target genes by mimicking miRNA sponges via competitive endogenous RNA (ceRNA) inhibition, and (2) regulating the post-translational modification of specific proteins, thereby affecting the activity of downstream signaling pathways [20]. Recent studies have noted that EVs are the primary means through which lncRNAs are transferred outside cells [21]. Extracellular lncRNAs can affect a broad range of downstream effects. In general, lncRNAs act as heterologous RNAs that can be transferred to target cells by EVs and regulate the cellular functions of receipt cells [22]. The membrane-bound nature of EVs shields ncRNA cargos from degradation. Due to the lack of evolutionary conservation and high specificity in different cells/organs, lncRNAs continue to be investigated as potential mediators of intercellular communication, exemplifying a valuable class of therapeutic targets for disorders as well as potential biomarkers [23].

2.3. Extracellular CircRNAs

CircRNAs are single-stranded RNAs that are linked end-to-end by a back-splicing mechanism. According to their splicing sequence, circRNAs can be categorized into the following groups: exonic circular RNAs (ecircRNAs), circular intronic RNAs (ciRNAs), exon-intron circular RNAs (EIciRNAs), intergenic circRNAs, anti-sense circRNAs, and tRNA intronic circRNAs (tricRNAs). Until now, the functionalities of circRNAs have been mainly classified into four categories: (1) acting as ceRNAs or sponges; (2) regulation of pre-RNA cleavage; (3) regulation of gene expression; and (4) as a potential source for translation of proteins and peptides [24]. Similar to the aforementioned ncRNAs, circRNAs can also be loaded into EVs to mediate cell-cell communication [13]. CircRNAs demonstrate a notable advantage over other ncRNAs. Without a linear terminal, circRNAs have a longer half-life, allowing for accumulation in tissues with a low proliferation rate. Additionally, the lack of a linear terminal impedes RNase degradation and improves stability and integrity in the extracellular environment, thus elevating their utility as biomarkers of disease [25]. Recent evidence has identified a crucial role of several extracellular circRNAs in alleviating damage due to cardiomyocyte hypertrophy, heart failure (HF), myocardial infarction (MI), and dysfunction caused by ischemia-reperfusion (I/R) [26]. Furthermore, several studies have also reported their association with proliferation, apoptosis, and inflammatory responses, thus influencing physiological and pathological phenomena in various tissues [7,27]. Investigation of circRNAs continues to elucidate their role in the pathogenesis of CVDs and provides a potential avenue for therapeutic development.

3. Ex-ncRNAs as Biomarkers in CVDs

In recent decades, several molecular mechanisms have been identified to be associated with the induction and progression of CVDs, especially in coronary atherosclerosis and HF [28]. Although clinical management of HF is improving, incidence rates remain above 20% in the adult population, with mortality rates hovering at 50% within 5 years of diagnosis, which makes HF a leading cause of morbidity and mortality in developed countries [29]. Consequently, it is necessary to delve into the disease's underlying mechanisms and subsequent release of ncRNAs to develop more effective diagnostic and prognostic tools to reduce mortality (Table 1).

3.1. Atherosclerosis

Atherosclerosis is a chronic inflammatory artery disease characterized by the deposition of atherosclerotic plaque in the arteries, which leads to the hardening and narrowing of the artery lumen and subsequent obstruction of blood flow [30]. Atherosclerotic plaque results from the accumulation of circulating low-density lipoprotein (LDL) cholesterol alongside fibrous materials and inflammatory cells on the inner layers of arteries [31]. On the contrary, other cholesterol classes, namely high-density lipoproteins (HDLs), hold a

significant anti-atherosclerotic role, transporting cholesterol from peripheral tissues to the liver for metabolism [32].

3.1.1. Extracellular Small ncRNAs

In 2011, a study found that circulating HDLs and LDLs can transport miRNAs, such as HDL-transported miR-223, to regulate different intercellular signaling pathways in atherosclerosis [33,34]. In addition to cholesterol-driven miRNA transport, circulating miRNAs have also been identified as potential biomarkers of atherosclerosis in hypertensive patients. By comparing the expression levels of miR-92a in plasma of different levels of carotid intima-media thickness (CIMT) and hypertensive patients, a recent study found that the increased level of miR-92a expression was positively correlated with the measured value of CIMT, ambulatory blood pressure monitoring results and carotid-femoral pulse wave velocity, all symptoms of atherosclerosis [35]. Given that lipoproteins play an important role in the progression of atherosclerosis, differential expression of HDL-miRNAs, in addition to circulating miRNAs, can help track disease progression and enable more accurate diagnosis and treatment.

3.1.2. Extracellular LncRNAs

Extracellular lncRNAs such as lncRNA Sox2 Overlapping Transcript (SOX2-OT) have also been shown to be potentially involved in the development of vascular disease [36]. Serum SOX2-OT levels were found to be significantly elevated in atherosclerotic patients. The results revealed that it could be used as a diagnostic biomarker and an excellent modality to assess patient prognosis [37].

3.1.3. Extracellular CircRNAs

Another study quantified circRNA in the plasma of patients with coronary artery disease. It was reported that the plasma level of hsa_circ_0001445 was reduced in patients with coronary artery sclerosis, and the condition remained stable in patients with reduced expression of hsa_circ_0001445. The expression level of hsa_circ_0001445 was inversely correlated with the degree of coronary atherosclerosis. Combined with coronary computed tomography, its quantification significantly improved the diagnosis of the degree of disease [38].

3.2. Ischemic Heart Disease

Ischemic cardiomyopathy is caused by an imbalance in the myocardial oxygen demand and available oxygen supply, most often induced by coronary artery stenosis. Based on the pathophysiology, ischemic cardiomyopathy includes coronary heart disease and myocardial infarction (MI) [39].

Although stenting is a crucial method to relieve myocardial ischemia, it may result in long-term cardiac damage when blood flow is suddenly restored, also known as ischemia-reperfusion (I/R) injury [40,41]. I/R injury after reperfusion often occurs due to cardiomyocytes undergoing anaerobic metabolism, sodium-potassium pump dysfunction, and ribosome shedding. Various intracellular ATP-dependent ion pumps become inactive, leading to ion accumulation, pH down-regulation, and up-regulation of intracellular osmolarity. Ultimately, ischemic cardiomyocytes experience cell swelling, impaired enzyme activities, and clumped nuclear chromatin. Due to the low concentration of antioxidants in ischemic cardiomyocytes, the increased reactive oxygen species after reperfusion causes oxidative stress, which further causes cellular dysfunction, DNA damage, and local inflammatory responses in cardiomyocytes. Thus, the persistence of inflammation and oxidative stress may trigger a cytokine storm that exposes cells to severe damage [42].

3.2.1. Extracellular Small ncRNAs

Currently, the primary diagnosis of MI is mainly based on the detection of MI markers like cardiac troponin [43,44]. However, there is evidence showing that elevated cardiac

troponins are present outside cardiac injury and can compromise the diagnosis of MI [45]. This opens an avenue to pursue Ex-ncRNA levels as a circulating biomarker for acute myocardial infarction (AMI) [46]. A previous study observed a 1600-fold elevated expression of miR-208b in AMI compared to the control group. Further, miR-208b identified earlier detection than troponin T regarding MI progression. In addition, another study found that miR-204 was down-regulated, and lncRNA-NEAT1 and matrix metalloproteinase-9 (MMP-9) were upregulated in serum EVs from patients with acute ST-segment elevation MI [47]. Serum-derived miRNA signatures have been used to distinguish healthy volunteers from patients with coronary atherosclerosis through the expression levels of miR-370-3p and miR-409-3p, which can serve as a fingerprint for coronary heart disease [48]. By exploring the expression levels of EV-derived miRNAs in the plasma and serum of CS and AMI patients, EV miRNA landscapes facilitated disease differentiation [49].

Novel miRNAs have been found to identify the evolution of cardiac I/R injury [50]. MiRNAs with diagnostic or therapeutic potential have been identified in the context of early cardiac I/R injury with miRNA arrays conducted to screen for differential expression in a mouse model of cardiac I/R injury. A total of 1882 miRNAs were screened, among which 11 were observably down-regulated and 41 were markedly up-regulated 3 h after reperfusion. miR-3113-5P and miR-223-3p were among the most differentially expressed miRNAs and have been confirmed to be up-regulated in the early stage of cardiac tissue I/R injury [51,52]. This data confirms that cardiac miRNAs, such as miRNA-3113-5p, might be a valuable target for therapeutic purposes, and circulating miRNAs such as miRNA-3113-5p might serve as a stable marker for the early diagnosis of cardiac I/R injury.

Extracellular tDR is a newly identified small regulatory RNA species. A recent study has demonstrated that extracellular tDRs are much more dynamically regulated than intracellular tDRs and extracellular miRNAs in both cardiomyocytes and cardiac fibroblasts upon the treatments of ischemia/reperfusion-related stressors [11]. Notably, more than 3000 extracellular tDRs are significantly regulated by nutritional deprivation or ischemia, and approximately 2000 extracellular tDRs are differentially expressed upon ischemia/reoxygenation treatment mimicking ischemia/reperfusion injury in both cardiomyocytes and cardiac fibroblasts [11]. Detailedly, extracellular tDR-1:32-His-GTG-1, tDR-37:72-Val-TAC-1, tDR-1:32-Pro-AGG-1-M4, tDR-2:30-Glu-CTC-1, tDR-2:30-Glu-CTC-1-D4G, tDR-1:31-Glu-TTC-4, tDR-3:31-Gly-GCC-2-M2, and tDR-40:72-Asn-GTT-1-M2 were significantly induced by ischemia/reoxygenation from both cardiomyocytes and cardiac fibroblasts, and extracellular tDR-1:36-Glu-CTC-1, tDR-1:36-Glu-CTC-1-D5G, tDR-1:36-Asp-GTC-2-M2, and tDR-42:75-Ser-GCT-3 were downregulated considerably upon cardiac ischemia/reoxygenation [11]. Although this study is a preliminary cell culture model, the findings clearly suggest that the extracellular tDR may be a promising biomarker for diagnostic and prognostic assessments of ischemic heart diseases.

3.2.2. Extracellular LncRNAs

A previous study has shown that lncRNAs can also serve as potential biomarkers for AMI [53]. It was found that the level of circulating lncRNA ENST000005566899.1 and lncRNA ENST00000575985.1 were significantly elevated in the plasma-derived EVs of AMI patients compared to healthy individuals. Further study of these lncRNAs in combination with mature biomarkers will enhance the understanding of disease progression which is fundamental for developing lncRNA therapeutics treating MI. Owing to the similarities of disease presentation and the vast differences in management, it becomes imperative to pursue avenues that allow for identifying the types and stages of diseases using noninvasive biomarkers.

3.2.3. Extracellular CircRNAs

Previous studies have shown that the downregulation of circRNA MICRA in peripheral blood is associated with the risk of left ventricular remodeling and dysfunction after MI. Additionally, the upregulation of hsa-circ-0098964 and circRNA-284 in the serum has been found to be associated with an increased risk of hypertension and acute ischemia [54].

3.3. Hypertension

Hypertension is a significant cause of heart disease and death worldwide [55]. As the heart pumps blood, the blood applies outward pressure on the arterial wall. The maximum pressure exerted while beating is defined as systolic pressure. Conversely, blood pressure on the arterial wall during relaxation and dilatation of the heart muscles is known as diastolic pressure. Hypertension is diagnosed when systolic pressure exceeds 140 mmHg, or diastolic pressure exceeds 90 mmHg [56]. One of the leading causes of hypertension is vascular dysfunction which manifests as endothelial dysfunction, vascular inflammation, arterial remodeling, and lowered vascular elasticity [57].

Extracellular Small ncRNAs

Extracellular miR-133a, miR-21, and miR-27a have previously been reported to play an essential role in the development of hypertension [58–60]. Based on these findings, a study was conducted on a general population over five years, measuring the serum levels of miR-133a, miR-21, and miR-27a using RT-qPCR. It was found that the serum expression levels of miR-133a and miR-27a were negatively correlated with the incidence of hypertension and, as a result, could be used as diagnostic biomarkers and preventive and predictive biomarkers of hypertension [61]. Recently, a study using serum from hypertensive patients quantified miR-92a and found that its expression was significantly increased in the serum of hypertensive patients, verifying its potential as a biomarker [62]. An in vitro study further supports the potential of extracellular miR-92a as a biomarker of hypertension as it targets vascular smooth muscle cells to regulate vascular SMC phenotype, thereby causing arterial stiffness and participating in the occurrence and development of hypertension [62].

Hypertensive disorder during pregnancy is a common type of hypertension [63,64]. Commonly, severe pregnancy-induced hypertension causes irreversible damage to the mother and offspring. Previous studies have revealed that miR-200a-3p can coordinate the function of trophoblast [65]. Based on this conclusion, one study quantified miR-200a-3p in the serum of hypertensive patients during pregnancy by RT-qPCR and found that the expression level of miR-200a-3p in the serum of hypertensive patients during pregnancy was up-regulated. Moreover, its expression level was positively correlated with the development of the disease. As a result, the level of miR-200a-3p bears prognostic potential for gestational hypertension [66].

3.4. Heart Failure

HF is a clinical syndrome of structural or functional abnormalities of the heart [67]. As HF may not have symptoms at its early stage, early screening using biomarkers can significantly reduce the risk of HF. The current standard for diagnosis utilizes the N-terminal-proB-type Natriuretic Peptide (NT-proBNP) test. However, increased concentrations of BNPs are not always associated with the onset of HF and may impede accurate and earlier diagnosis of HF.

3.4.1. Extracellular Small ncRNAs

A previous study has examined the expression of Ex-ncRNAs in plasma in relation to the progression of HF [68], and found altered expression of miR-192, miR-194, and miR-134a in the plasma from patients with HF, implying the capacity of small ncRNAs to identify cardiomyocyte death and HF [68]. Similarly, another study showed that paracrine signaling via cardiomyocyte-derived EVs containing miR-30d could improve cardiac function by reducing myocardial fibrosis and cardiomyocyte apoptosis [69]. Small ncRNAs have also been assessed in the serum of acute HF patients following dilated cardiomyopathy. In this cohort, miR-92b-5p expression was up-regulated in the EVs of the patients, suggesting its use as a potential biomarker in diagnosing acute AHF caused by dilated cardiomyopathy [70].

3.4.2. Extracellular LncRNAs

Ischemic cardiomyopathy (ICM) caused by MI is a major cause of HF. In the context of circulating biomarkers, lncRNAs in ICM have been widely explored. Genome-wide transcriptome analysis has verified that a number of protein-coding genes previously reported to be associated with HF demonstrated altered expression following ICM [71,72]. Among 145 differentially expressed lncRNAs screened in ICM, 35 lncRNAs showed strong positive correlations. Expression correlation coefficient analysis of differentially expressed lncRNAs and the protein-coding genes yielded a strong correlation between lncRNAs and ECM protein-coding genes. The overexpression or knockdown of selected lncRNAs in the cardiac fibroblasts indicated that lncRNAs were significant regulators of fibrosis and ECM synthesis gene expression [73,74]. In addition, lncRNAs were found to be involved in the TGF-β pathway to regulate ECM gene expression and myofibroblast differentiation [75]. This data suggests that lncRNAs might be novel modulators of heart function and HF.

Table 1. Ex-ncRNAs as biomarkers in CVDs.

Reference	Ex-ncRNA	Carriers	Expression (↑)	Expression (↓)	Type of CVDs
Kasey et al. [33]	miR-223	HDL	↑	-	Atherosclerosis
Huang et al. [35]	miR-92a	-	↑	-	Atherosclerosis
Tao et al. [37]	LncRNA SOX2-OT	-	↑	-	Atherosclerosis
Vilades et al. [38]	hsa_circ_0001445	-	-	↓	Atherosclerosis
Corsten et al. [46]	miR-208b	-	↑	-	Acute myocardial infarction
Li et al. [11]	tDR-1:32-His-GTG-1, tDR-37:72-Val-TAC-1, tDR-1:32-Pro-AGG-1-M4, etc.	-	↑		Cardiac ischemia/reperfusion
	tDR-1:36-Glu-CTC-1, tDR-1:36-Glu-CTC-1-D5G, tDR-1:36-Asp-GTC-2-M2, etc.	-		↓	
Chen et al. [47]	LncRNA-NEAT1, miR-204	EV	↑	↓	Acute ST-segment elevation myocardial infarction
Hildebrandt et al. [48]	miR-370-3p, miR-409-3p	EV	↑	-	Coronary heart disease
Chen et al. [50]	microRNA 3113-5P	-	↑	-	Cardiac ischemia/Reperfusion injury
Zheng et al. [53]	lncRNA ENST00000556899.1, lncRNA ENST00000575985.1	EV	↑	-	Acute myocardial infarction
Kishore et al. [54]	circRNA MICRA, circRNA-284, hsa-circ-0098964	-	↑	↓	Myocardial infarction, Ischemic heart disease, Hypertension
Suzuki et al. [61]	miR-133a, miR-27a	-	-	↓	Hypertension
Wang et al. [62]	miR-92a	-	↑	-	Hypertension
He et al. [66]	miR-200a-3p	-	↑	-	Hypertension
Janjusevic et al. [68]	lncRNA LIPCAR, miR-192, miR-134a, miR-194, miR-30d	EV	↑	↓	Heart failure
Li et al. [69]	miR-30d	EV	-	↓	Heart failure
Wu et al. [70]	miR-92b-5p	EV	↑	-	Heart failure

4. Ex-ncRNAs as Therapeutic Targets in CVDs

Over the past decade, substantial effort has been made toward better understanding the functional roles of Ex-ncRNAs in CVDs and the clinical applications of novel therapies targeting Ex-ncRNAs, based on the approaches modulating their expression or their interactions with targets. The therapeutic functions of most of the small ncRNAs can be induced by synthesized RNA oligos, known as mimics, with multiple chemical modifications that improve pharmacokinetics and pharmacodynamics [76]. With the recent success of two COVID-19 mRNA vaccines [77], long RNA mimics have been emerging as promising therapeutics to induce functional effects of lncRNAs in patients. Besides the synthetic circRNA mimics, circRNAs are usually overexpressed by gene-expressing viral or non-viral vectors [78], which can also be used to express some small and long ncRNAs. The tools exploiting the exquisite sensitivity of base-pair complementarity have been used extensively to inhibit the functions of disease-causing Ex-ncRNAs [76,78,79], which include antisense oligonucleotides (ASOs), small interfering RNAs (siRNAs), short hairpin RNAs (shRNAs), antisense, miRNA sponges, CRISPR/Cas9-based DNA editing

tools, and CRISPR/Cas13-based RNA editing tools. Here, we describe recent studies that targeted Ex-ncRNAs in various CVDs (Table 2).

4.1. Atherosclerosis

4.1.1. Extracellular Small ncRNA

It is well-known that inflammation plays a vital role in the development of coronary atherosclerotic diseases (CAD) [80,81]. Evidence suggests that intercellular crosstalk of Ex-ncRNAs can influence the development of inflammation and subsequent CAD progression. EV-encapsulated miRNA-146a-5p treatment resulted in production of proinflammatory cytokines, injury of the coronary endothelial cell barrier, and cardiomyocyte dysfunction, by targeting inflammation-triggering Toll-like receptor 7 (TLR7) [82]. Other avenues facilitating atherosclerosis progression include Ex-ncRNAs acting as danger-associated molecular patterns (DAMPs) through stimulation of the vascular endothelial growth factor (VEGF) receptor-2 system to increase vascular permeability and inflammatory cell aggregation [83].

4.1.2. Extracellular LncRNAs

A previous study has shown that lncRNA-RNCR3 is significantly upregulated during atherosclerosis. RNCR3 acts as a ceRNA for miR-185-5p, leading to the upregulation of its target gene KLF2, a critical transcription factor for endothelial vasoprotection. Targeting RNCR3 may thereby protect from atherosclerosis-related injury [84].

4.1.3. Extracellular CircRNAs

The studies focusing on circRNAs for therapeutic application have identified a wide range of potential targets against atherosclerosis development and progression. A recent study reported the specific mechanism of hsa_circ_0001445 on endothelial injury following treatment with oxidized LDL (ox-LDL) [85]. hsa_circ_0001445 was found to directly target miR-208b-5p and lead to the upregulation of ABCG1, the direct target of miR-208b-5p [85]. The study concludes that targeting hsa_circ_0001445 promotes aortic endothelial cell proliferation and migration through the mir-208b-5p/ABCG1 axis and inhibits inflammation and extracellular matrix (ECM) to reduce the damage of ox-LDL to endothelial cells (ECs) [85].

As most Ex-ncRNAs, except circRNAs, contain linear terminals, targeting ncRNAs using RNases presents a route for therapeutic inhibition. RNases are capable of hydrolyzing Ex-ncRNAs. In linear ncRNAs, such as small and lncNRAs, RNase digestion can inhibit the development of arterial inflammation and suppress atherosclerosis [86]. Investigations on RNase-based therapies targeting Ex-ncRNAs have begun to reveal yet another critical avenue of ncRNA therapeutics [87].

4.2. Ischemic Heart Disease

4.2.1. Extracellular Small ncRNAs

In the immune microenvironment, EVs produced by immune cells can selectively carry Ex-ncRNAs that affect the development of MI [88]. Among the highly expressed pro-inflammatory miRNAs, miR-155 was found to inhibit angiogenesis and promote cardiac dysfunction by downregulating Rac family small GTPase 1 (RAC1), p21-activated kinase 2 (PAK2), Sirtuin 1 (Sirt1), and protein kinase AMP-activated catalytic subunit alpha 2 (AMPKα2) [89]. These proteins subsequently reduce the ability of ECs to induce angiogenesis and advance inflammation, leading to the exacerbation of MI [89]. In another vein, miR-1271-5p, carried by M2-like macrophage-derived EVs, plays a protective role in AMI [90]. It directly affects the expression of SRY-Box transcription factor 6, which prevents cardiomyocyte damage and promotes cardiac repair and cardiomyocyte viability [90]. Additionally, miR-30d, the HF biomarker mentioned above, may potentially target integrin 5 and mitogen-activated protein kinase 4 (MAPK4) in cardiac fibroblasts in response to acute cardiac damage [69].

In addition to macrophages, dendritic cells (DCs) also play an essential role in the immune microenvironment after MI. This study has found that miR-494-3p could be loaded

into DC-derived EVs and promote post-MI angiogenesis by inducing VEGF expression in mice [91]. Mesenchymal stem cells (MSCs) derived Ex-ncRNAs also have been found to play a crucial role in intercellular communication. Overexpression of miR-486-5p, derived from MSCs, silences MMP19 and promotes the activity of ECs to induce angiogenesis [92]. As such, MSC EVs may be potentially used to promote angiogenesis by delivering miR-486-5p-loaded EVs. This modality may be a critical therapeutic approach in myocardial ischemic compensation [92]. MSC-derived EV transfer of miR-210 has also been found to protect cardiomyocytes from apoptotic cell death, with miR-210 downregulating the expression level of apoptosis-inducing factor mitochondria associated 3 (AIFM3) and affecting PI3K/AKT and p53 signaling pathways to reduce apoptosis in cardiomyocytes and improve cardiac function [93]. To a certain extent, MSCs under hypoxic conditions offer significant protection against I/R injury. Upregulated miR-224-5p in mouse adipose, MSC EVs were found to target thioredoxin-interacting protein (TXNIP), thereby inhibiting the degradation of GATA binding protein 4 (GATA4) and maintaining the expression of Bcl-2 [94]. TXNIP was also identified as a target for miR-150-5p [95]. Therefore, as expected, overexpression of miR-150-5p protected rat hearts during I/R by inhibiting the expression of TXNIP.

The persistence of inflammation and oxidative stress may trigger a cytokine storm that exposes cells to severe damage [42]. Bone marrow mesenchymal stem cells (BMSC) EVs exert protective effects at different levels of oxidation [96]. It is worth noting that the miR-29c was upregulated in BMCS EVs and protected against hypoxia/reoxygenation (H/R) injury by inhibiting the PTEN/Akt/mTOR axis. Additionally, two extracellular miRNAs: miR-149 and let-7c, were significantly upregulated in EVs from normal BMSCs compared to H/R BMSCs [97]. These two upregulated miRNAs downregulate the expression of the Faslg gene by promoting the miR-149/Let-7c/FASLG axis [97]. Another study using BMSC-derived EVs has shown that miR-338 is highly enriched in BMSC EVs [98]. Upregulation of miR-338 inhibits MAP3K2 gene expression by suppressing the MAP3K2/JNK axis, thus inhibiting apoptosis in cardiomyocytes. As such, it can be concluded that BMSC EVs have the potential to ameliorate cardiac conditions during MI.

Cardiac cell-derived EVs encapsulate many miRNAs like miR-146a, miR-181b, and miR-26a, and have exhibited improved cardio-protective and therapeutic effects than MSC EVs under MI conditions [99–102]. Using single RNA tracing, cardiac endothelial cells and cardiac fibroblasts have shown increased intake of cardiosphere cell-derived EVs following injury [103]. Several cardiomyocyte EC-derived miRNAs such as miR-23a-3p, miR-424, let-7f, miR-378, and miR-214 might be one of the crucial cardio protecting factors [104]. Moreover, evidence suggests that miR-19a-3p can downregulate hypoxia-inducing factor-1α (HIF-1α), leading to the inhibition of cardiomyocyte proliferation and angiogenesis. Administration of the miR-19a-3p antagomir has downregulated miR-19a-3p expression, accelerated angiogenesis, and exerted a protective effect after MI [105]. Another study has shown that the downregulated expression of miR-143 in cardiomyocyte-derived EVs leads to the induction of angiogenesis and reduces cardiac ischemic pressure through the IGF-IR/NO signaling pathway [106]. Through a small RNA sequencing study, cardiac telomeric cell-derived EVs have demonstrated the transport of miR-21-5p to ECs, where it silences Cdip1 gene expression. Silencing of Cdip1 downregulates caspase-3 protein expression and promotes angiogenesis, subsequently suppressing ischemic cardiomyopathy [107].

4.2.2. Extracellular LncRNAs

It is reported that human BMSC EVs containing lncRNA HCP5 could protect cardiomyocytes from I/R injury by inhibiting the IGF1/PI3K/AKT axis [108]. In detail, it functions as a sponge for endogenous miR-497, which targets the expression of IGF-1 [108]. Another study using human umbilical cord mesenchymal stem cell (ucMSC)-derived EVs to treat H/R cardiac microvascular ECs and I/R rats has found that human ucMSC-derived EVs containing the lncRNA UCA1 reduces the injury of cardiac microvascular ECs in vivo [109]. UCA1 sponges miR-143 and subsequently inhibits Bcl-2 via the miR-143/Bcl-2/Beclin-1 axis [109].

4.2.3. Extracellular CircRNAs

Researchers have found that circRNAs also have protective effects against MI. For example, circ-HIPK3-rich EVs were released from cardiomyocytes under hypoxic conditions and protected the heart from oxidative stress injury [110]. Circ-HIPK3 sponges miR-29a and promotes the expression of vascular endothelial growth factor A (VEGFA), accelerating the proliferation, migration, and angiogenesis of ECs. Upregulation of VEGFA thereby reduces the effects of MI and protects against MI [110]. Another study used microarray analysis to establish the circRNA expression profile of EVs derived from M2-like macrophages. This was followed by the identification, and functional characterization of M2-like macrophage-derived EVs in MI mice models [111]. From this, it was found that highly expressed circRNA-UB3A can enter cardiac fibroblasts to sponge the expression of miR-138-5p. This results in the inhibition of Rho C expression, which exacerbates myocardial fibrosis after MI [111]. In summary, Ex-ncRNAs (miRNAs, lncRNAs, and circRNAs) derived from various resources (cardiomyocytes, stem cells, immune cells) mediate crosstalk between cell-to-cell through a variety of modalities, affecting the proliferation and apoptosis of cardiomyocytes alongside promoting angiogenesis. At the same time, they can counteract the generation of ischemic injury of cardiomyocytes.

4.3. Hypertension

Extracellular Small ncRNAs

Endothelial dysfunction is a significant manifestation of hypertension. It was shown that miR-483 could target transforming growth factor-β (TGF-β), TGF-β receptor 2 (TGFBR2), β-catenin, connective tissue growth factor (CTGF), interleukin-1β (IL-1β), and endothelin-1 (ET-1) to obtain anti-hypertensive effects [112]. The protective mechanisms mediated by extracellular miR-483-3p derived from ECs in hypertension were also elucidated [113]. This study showed that miR-483-3p was associated with the progression of hypertension and that the expression level of miR-483-3p in serum was proportional to vascular function. Overexpression of miR-483-3p reduced the expression of TGF-β, CTGF, angiotensin-converting enzyme 1 (ACE1), and ET-1 genes both in ECs and smooth muscle cells (SMCs). Therefore, extracellular miR-483-3p may become one of the promising therapeutic targets for the treatment of various types of endothelial dysfunction represented by hypertension [113].

MiR-634, as a circulating biomarker, has been implicated in playing a role in pulmonary hypertension as well as systemic hypertension [114,115]. It was found that the expression level of miR-634 was reduced in the plasma of hypertensive patients, and miR-634 could target HASMCs through the Wnt/β-catenin signaling pathway and downregulate the expression of Wnt4, thereby inhibiting the proliferation and migration of HASMCs and influencing the course of hypertension by affecting vascular remodeling [116].

4.4. Cardiac Hypertrophy

Cardiac hypertrophy is mainly caused by changes in the mechanical stress of the heart. It is a compensatory mechanism of the heart to resist the increased hemodynamic pressure. The process of myocardial hypertrophy is primarily characterized by the enlargement of cardiomyocytes along with myocardial fibrosis and inflammation, resulting in myocardial dysfunction [117,118].

Extracellular Small ncRNAs

The process of myocardial hypertrophy is primarily characterized by the enlargement of cardiomyocytes along with myocardial fibrosis and inflammation, resulting in myocardial dysfunction [117,118]. It has been reported that miR-217 expression was increased in the hearts of thoracic aortic constriction (TAC) mice and CHF patients. In cases of stress overload and miR-217 overexpression in cardiac hypertrophy, fibrosis, and dysfunction, effects were reversed via miR-217-TUD-mediated miR-217 downregulation. It has been established that miR-217 directly targets PTEN, a protein involved in cell cycle regulation and proliferation. Importantly, exosomes produced from cardiomyocytes containing miR-

217 promoted fibroblast growth in vitro. Following its implications in cardiac fibrosis and hypertrophy through control of PTEN, miR-217 is undoubtedly highlighted as a potential therapeutic target for chronic HF [119].

MiR-21-3p has been identified as upregulated in cardiac fibroblast-derived EVs by miRNA profiling assay and qRT-PCR. Exploration of the crosstalk between cardiac fibroblasts and cardiomyocytes in a co-culture system further validated the paracrine function of cardiac fibroblast-derived miR-21-3p on cardiomyocytes. Co-incubation of fibroblast-derived miR-21-3p and cardiomyocytes further confirmed the capacity of miR-21-3p to mediate cardiomyocyte hypertrophy. This study further demonstrates that miR-21-3p produced by cardiac fibroblasts silenced the expression of SH3 domain-containing protein 2 (SH3P2) and the PDZ and LIM domains in cardiomyocytes, encouraging hypertrophy and fibrosis. As a result, miR-21-3p may be a crucial therapeutic target for preventing cardiac hypertrophy [120]. On the other hand, miR-21-5p is known to regulate the ERK-MAP kinase signaling pathway in cardiac fibroblasts and influence the cardiac structure and function [121–123]. Interestingly, miR-21-5p levels are selectively increased in the fibroblasts of failing hearts and have enhanced ERK-MAP kinase activity by inhibiting sprouting homolog 1 (Spry1) [121]. In a murine model of pressure overload-induced cardiac hypertrophy, silencing of miR-21-5p by miRNA inhibitors suppressed the cardiac ERK-MAP kinase activity, attenuated interstitial fibrosis, and alleviated cardiac dysfunction [121]. Therefore, miR-21 served as the disease target for myocardial fibrosis and cardiac hypertrophy and defined the therapeutic efficacy of microRNA therapeutic interventions in CVDs.

The inflammatory immune microenvironment plays an important role in the development of myocardial hypertrophy. In parallel to the micro-immune microenvironment, immune-derived exosomes have become effective regulators of inflammatory response [124]. A study confirmed that exosomes derived from angiotensin II (Ang II)-induced hypertrophic cardiomyocytes (HCs) disturbed inflammatory signaling pathways in the macrophages [125]. The incubation of mouse macrophage cell line RAW264.7 in the presence of exosomes derived from HC medium activated the secretion of inflammatory cytokines interleukin (IL)-6 and IL-8 when compared with the exosomes derived from normal cardiomyocytes (NCs). The cytokine release triggered by exosomes derived from HCs was prevented by Argonaute2 (AGO2) down-regulation, suggesting that ncRNAs were involved in the exosome-induced inflammation in the RAW 264.7 macrophages. RNA sequencing further revealed that a total of seven microRNAs were differentially expressed between NCs-derived and HCs-derived exosomes, of which miR-155 plays a crucial role in the initiation of macrophage inflammation [126]. Further analysis showed that the HC-derived exosomes abducted the phosphorylation of ERK, c-Jun N-terminal kinase (JNK), and p38 through miR-155 [126]. These findings support that exosomal microRNA has become an important inflammatory response regulator in adjusting cardiac hypertrophy.

Cardiac hypertrophy, specifically myocardial hypertrophy, is often exacerbated by valvular calcification, a progressive disease prevalent in elderly individuals. Early intervention in the development of valvular calcification is a crucial measure to prevent myocardial hypertrophy [127,128]. In the cardiac interstitium, telocytes establish a complex association between cardiac stem cells and cardiomyocytes. When valvular calcification occurs, telocytes-derived EVs modulate myocardial regeneration, reduce myocardial fibrosis, and restore some functions [129]. Extraction of T telocytes EVs and knockdown of miR-30b expression revealed that inhibition of miR-30b could reduce calcium deposition in the valve, protecting the aortic valve and mitigating cardiac hypertrophy [129].

4.5. Heart Failure

4.5.1. Extracellular Small ncRNAs

HF is a complex and progressive disease that may be caused by a variety of pathological conditions. Previous studies have indicated that Ex-ncRNAs also participate in the progression of HF. For example, a recent study demonstrated that the expression level of miR-21-5p was dysregulated in cardiac stromal cell-derived EVs from HF patients using

microRNA arrays and qPCR analysis [130]. When the miR-21-5p level is downregulated, the repair effect in HF patients diminishes as it inhibits phosphatase and Tensin homologs to enhance AKT activity, thus causing the promotion of angiogenesis and protection of cardiomyocytes. This offers a promising therapeutical target for treating HF.

4.5.2. Extracellular LncRNAs

LncRNAs are significant in heart development and disease. One study verified exercise-regulated cardiac lncRNA, called lncExACT, that was evolutionarily conserved and reduced in the exercising heart but augmented in the human and experimental HF [131]. The cardiac lncExACT1 overexpression led to pathological hypertrophy and HF. LncExACT1 suppressed physiological hypertrophy and cardiomyogenesis, preventing cardiac fibrosis and dysfunction. Further, lncExACT1 regulated microRNA-222, calcineurin signaling, and Hippo/Yap1 signaling vis DCHS2 [132,133]. Overexpression of DCHS2 in the zebrafish cardiomyocytes led to pathological hypertrophy and impaired cardiac regeneration, thereby promoting scar formation after injury [134]. On the contrary, DCHS2 depletion caused physiological hypertrophy and accelerated cardiomyogenesis in mice. These data demonstrated that lncExACT1-DCHS2 was identified as a new pathway for regulating HF.

Table 2. Ex-ncRNAs as therapeutic targets in CVDs.

Reference	Donor Cells	Ex-ncRNAs	Carriers	Expression Quantity (↑)	Expression Quantity (↓)	Target/Pathway	Type of CVDs
Shimada et al. [82]	-	miR-146a-5p	EV	↑	-	TLR7	Atherosclerosis
Shan et al. [84]	Human umbilical vein endothelial cells	lncRNA-RNCR3	EV	↑	-	miR-185-5p/KLF2	Atherosclerosis
Yang et al. [85]	-	hsa_circ_0001445	-	-	↓	mir-208b-5p/ABCG1	Atherosclerosis
Liu et al. [89]	M1-like macrophage	miR-155	EV	↑	-	Sirt1/AMPKα2 and RAC1-PAK2	Acute myocardial infarction
Long et al. [90]	M2-like macrophage	miR-1271-5p	EV	↑	-	SOX6	Acute myocardial infarction
Li et al. [69]	Cardiomyocytes	miR-30d	EV	↑	-	MAP4K4 and integrin α5	Ischemic HF
Liu et al. [91]	Dendritic cell	miR-494-3p	EV	↑	-	VEGF	Myocardial infarction
Li et al. [92]	MSC	miR-486-5p	EV	↑	-	MMP 19/VEGF	Myocardial infarction
Cheng et al. [93]	MSC	miR-210	EV	↑	-	AIFM3/PI3K/AKT and p53	Myocardial infarction
Mao et al. [94]	MSC	miR-224-5p	EV	↑	-	TXNIP/GATA4/Bcl-2	Ischemia-reperfusion injury
He et al. [95]	MSC	miR-150-5p	EV	↑	-	TXNIP	Ischemia-reperfusion injury
Li et al. [96]	BMSC	miR-29c	EV	↑	-	PTEN/Akt/mTOR	Ischemia-reperfusion injury
Zou et al. [97]	-	miR-149, let-7c	EV	↑	-	miR-149/Let-7c/FASLG	Ischemia-reperfusion injury
Fu et al. [98]	BMSC	miR-338	EV	↑	-	MAP3K2/JNK axis	Myocardial infarction
Walravens et al. [99–102]	CDC	miR-26a, miR-146a, miR-181b	EV	↑	-	Adam17, TLR-NFkB, PKCδ	Myocardial infarction
Moghiman et al. [104]	MSC, Cardiomyocyte, EC	miR-23a-3p, miR-424, let-7f, miR-378, miR-214	EV	↑	-	HOXA5, GAX, p38 MAPK, Smad2/3, ATM	Myocardial infarction
Gou et al. [105]	Cardiomyocyte	miR-19a-3p	EV	↑	-	HIF-1α	Myocardial infarction
Geng et al. [106]	Cardiomyocyte	miR-143	EV	-	↓	IGF-IR/NO	Myocardial infarction
Liao et al. [107]	CT	miR-21-5p	EV	↑	-	Cdip1/caspase-3	Myocardial infarction
Li et al. [108]	BMSC	lncRNA HCP5	EV	↑	-	miR-497/IGF1/PI3K/AKT	Ischemia-reperfusion injury

Table 2. *Cont.*

Reference	Donor Cells	Ex-ncRNAs	Carriers	Expression Quantity (↑) (↓)		Target/Pathway	Type of CVDs
Diao et al. [109]	hUCMSC	lncRNA UCA1	EV	↑	-	miR-143/Bcl-2/Beclin-1	Ischemia-reperfusion injury
Wang et al. [110]	Cardiomyocyte	circ-HIPK3	EV	↑	-	miR-29a/VEGFA	Myocardial infarction
Wang et al. [111]	M2-like macrophage	circRNA-UB3A	EV	↑	-	miR-138-5p/RhoC	Myocardial fibrosis after myocardial infarction
Zhang et al. [112]	-	miR-483	-	-	↓	TGF-β, TGFBR2, β-catenin, CTGF, IL-1β, ET-1	Hypertension
Shang et al. [113]	-	miR-483-3p	EV	↑	-	TGF-β, CTGF, ACE1, ET-1	Hypertension
Niu et al. [116]	-	miR-634	-	-	↓	Wnt/β-catenin	Hypertension
Xiang et al. [119]	Cardiomyocyte	miR-217	EV	↑	-	PTEN	Cardiac hypertrophy
Claudia et al. [120]	Cardiac fibroblast	miR-21-3p	EV	↑	-	SH3 domain-containing protein 2 and PDZ and LIM domain 5	Cardiac hypertrophy
Thum et al. [121]	-	miR-21	-	↑	-	ERK-MAPK and Spry1	Cardiac hypertrophy
Yu et al. [125]	Macrophage	miR-155	EV	↑	-	Son of Sevenless 1 and Suppressor of Cytokine Signaling 1	Cardiac hypertrophy
Yang et al. [129]	Telocyte	miR-30b	EV	↑	-	Runx2/Wnt/β-catenin	Cardiac hypertrophy
Li et al. [130]	Cardiac stromal cell	miR-21-5p	EV	↑	-	phosphatase and tensin homolog/Akt	HF
Li et al. [131–133]	-	lncExACT1	-	↑	-	DCHS2	HF

5. Clinical Developments and Applications of Ex-ncRNAs in CVDs

Recently, significant progress has been made in understanding the regulation and roles of Ex-ncRNAs in CVDs and in translating these findings into clinical applications as biomarkers or therapeutic targets [9]. Ex-ncRNAs have been identified as critical regulators in the pathogenesis of CVDs and are thus important candidates for improved diagnosis or prognosis assessment and advanced therapeutics.

5.1. Ex-ncRNAs as Biomarkers

Despite the increasing interest in searching for Ex-ncRNA as reliable biomarkers, this field still faces many significant scientific and technical hurdles, including preanalytical and analytical factors that influence data quality and reliability. These factors include sample types, Ex-ncRNA isolation, detection and processing techniques, normalization strategies, and the influence of other cofounders such as drug usage and other CVDs [9,135]. Therefore, the clinical use of Ex-ncRNAs as biomarkers for CVDs is still in its infancy, despite the promising efficacy and feasibility in animal models and a small number of patients as mentioned above. Of note, hsa-Chr8:96, a human homolog of mmu-miR-721, was identified as a novel extracellular small ncRNA for the detection of acute myocarditis in four independent cohorts of patients with myocarditis [136], which demonstrates both the unmet medical need and the enormous promise for developing Ex-ncRNAs as novel biomarkers for CVDs. Currently, more than 10 clinical trials on identifying Ex-ncRNA as novel CVD biomarkers have been initiated or are ongoing, such as ischemic heart diseases (NCT02691286, NCT01875484), atherosclerosis (NCT03279770, NCT03855891), hypertension (NCT04193046), and HF (NCT03345446). A better understanding of the biology of Ex-ncRNAs and the advances in methods for Ex-ncRNA isolation, detection, and analysis, will undoubtedly pave the way for the translation of Ex-ncRNA biomarker research to clinical routine.

5.2. Ex-ncRNAs as Therapeutics Targets

Therapeutic targeting of Ex-ncRNAs, including small ncRNAs, lncRNAs, and circRNAs either inside or outside the cells, represents an attractive strategy for treating CVDs. The RNA-targeting approaches include ASOs, siRNAs, shRNAs, antisense, miRNA sponges, CRISPR/Cas9-based DNA editing tools, and CRISPR/Cas13-based RNA editing

tools. Notably, siRNAs and ASO have been approved by the United States of America Food and Drug Administration (FDA) and/or the European Medicines Agency (EMA) for clinical use. siRNA is a single- or double-stranded RNA oligo, which exploits the endogenous miRNA pathway to silence mRNAs by loading them into RNA-induced silencing complexes (RISC) for degradation [137]. The successful clinical use of siRNAs targeting proprotein convertase subtilisin/kexin type 9 (PCSK9) mRNAs for lowering circulating LDL cholesterol and then decreasing the CVD risks in human patients has proved the tremendous promise of using siRNAs targeting CVD-causing Ex-ncRNAs, in particular lncRNAs. ASO is a single-stranded DNA oligo with entire or partial complementarity to the target RNAs and may act either by inducing the degradation of target RNAs or by sequestering the interaction of target RNAs with their partner compounds [138]. ASO was first approved by FDA for silencing mRNA in 1998 and has now been widely used to target other ncRNAs, including small ncRNAs [139], lncRNAs [140], and circRNAs [78]. Over the past decades, extensive efforts have been made to clinically utilize siRNAs or ASO to target mRNAs, such as ApoA, PCSK9, Angiotensinogen, FOXO3, and SERCA2A, and only recently target ncRNAs for treating CVDs (Table 3) [141]. CDR132L, a synthetic ASO blocking the functions of miR-132, has entered the Phase II clinical trial for treating patients with reduced left ventricular ejection fraction after MI (NCT05350969). Other strategies, such as antisense, miRNA sponges, and CRISPR/Cas9-based gene editing tools, have also demonstrated promising preclinical effects and are being translated into the clinical routine.

Table 3. RNA Therapies Approved or in Clinical Trials for CVDs.

Stage	Drug	Modification and Delivery	Target Gene	Disease	Comments
Clinical trials	AZD8601	naked mRNA	VEGF-A	HF	Phase 2
	CDR132L	ASO	miR-321	HF	Phase 2
	IONIS-AGT-LRx	Antisense	Angiotensinogen	HF	Phase 2
	Olezarsen	Antisense	ApoC-III	Lipid disorders	Phase 3
	Olpasiran	siRNA	Lp(a)	Lipid disorders	Phase 2
	Pelacarsen	Antisense	Lp(a)	Lipid disorders	Phase 3
	Vupanorsen	Antisense	ANGPTL3	Lipid disorders	Phase 2
FDA/EMA approved	Inclisiran	siRNA	PCSK9	Lipid disorders	FDA approved
	Volanesorsen	ASO	APO-C3	Triglycerides	EMA approved

There are also many challenges to be overcome to further the clinical application of RNA-based therapeutics, mainly the specificity and delivery. Virtually all RNA-targeting approaches exploiting the exquisite sensitivity of base-pair complementarity have off-target effects [142]. The quality of RNA therapy is determined by both the efficacy of its on-target effects as well as the minimized off-target side effects, namely specificity. These can be achieved by the development of algorithms for improved RNAi therapeutic design and by chemical modifications. In the past 60 years, hundreds of nucleic acid chemical modifications have been characterized and synthesized, and a number of them have been successfully utilized in RNA therapeutics improving the potency and specificity [143], including the first generation of 2′-deoxy-2′-fluoro (2′-F), 2′-O-methylation (2′-OMe), and the phosphorothioates (PS) backbones, the second generation of 2′-O-(2-methoxyethylation) (2-O-MOE), and the third generation of LNA modification. Efficient and specific delivery of RNA therapeutics to organs/cells still remain the top two greatest challenges in this field [143], owing to their instability, negative charge, hydrophilic nature which prevents diffusion through cell membranes, and rapid cleaning by the liver after systematic administration. The first and second generations of chemical modifications greatly improve the stability and enhance cellular uptake [144]. Specific delivery to targeted cells/tissues can be achieved using modified lipid- and polymer-based nanoparticles, conjugation with different homing ligands, or engineering into specific EVs, among which the endosomal escape of the RNA therapeutics, also termed functional delivery, should be considered. A

vast number of other strategies, such as viral vectors with cell type-specific promoters or different envelop proteins, can also be employed for specific and efficient delivery [145].

6. Conclusions and Perspectives

The poor recovery of cardiac function following heart tissue injury and the lack of effective strategies facilitating this recovery in clinical settings emphasize the importance of preventative monitoring and diagnosis [146]. Ex-ncRNAs, selectively released by different cells, play versatile roles in numerous biological processes and diseases [147]. Recently, studies elucidating the Ex-ncRNAs-mediated intercellular crosstalk in the pathogenesis of various CVDs are emerging [148], and Ex-ncRNAs are increasingly recognized as promising diagnostic biomarkers and druggable targets [149,150]. In this review, we have systematically summarized the regulation and roles of Ex-ncRNAs, including small ncRNAs, circRNAs, and lncRNAs, involved in major cardiovascular events, such as atherosclerosis, ischemic heart diseases, hypertension, cardiac hypertrophy, and HF (Figure 2). We also discussed the strategies and challenges for utilizing Ex-ncRNAs as biomarkers or therapeutical targets.

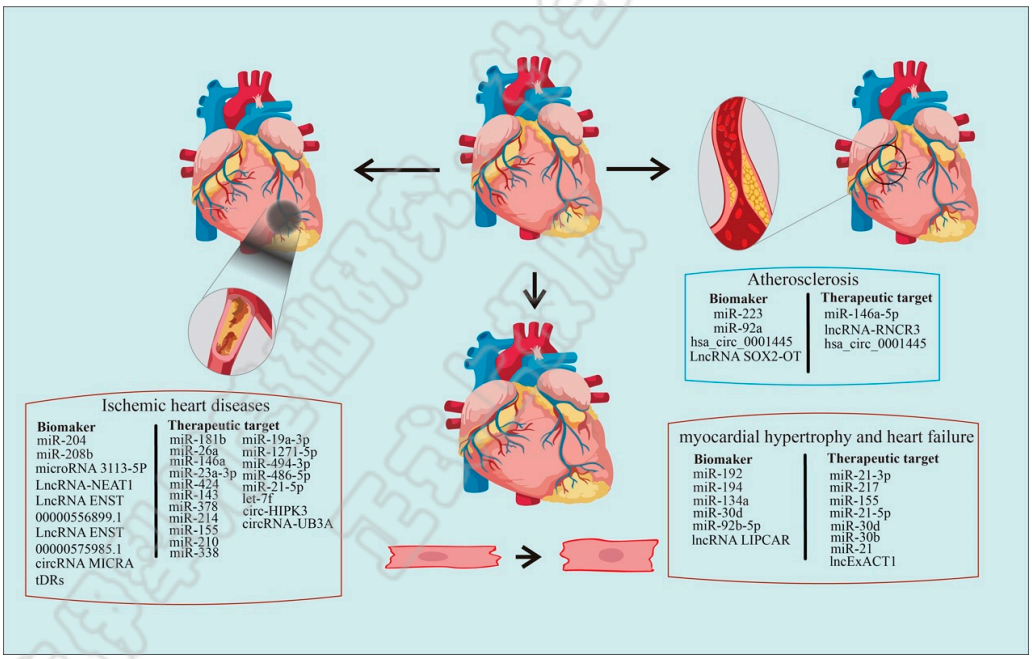

Figure 2. Extracellular non-coding RNAs as biomarkers or therapeutic targets for cardiovascular diseases. The summary of Ex-ncRNAs being identified as potential biomarkers or therapeutical targets for cardiovascular diseases.

Although increasing research interests have been attracted to the roles of Ex-ncRNAs during the onset, progression, and prognosis of CVDs [151,152], the utilization of Ex-ncRNAs as biomarkers and therapeutics is still in its infancy in its clinical routine. Due to the heterogeneity of Ex-ncRNAs in different biofluids or even in plasma samples from the same patient at different time points, a robust, reliable, and reproducible readout of specific Ex-ncRNA is indispensable for developing it as a clinical CVD biomarker, which may be achieved by a better understanding of the biology of Ex-ncRNAs and the advances in methods for Ex-ncRNA isolation, detection, and analysis. Similarly, although the specificity of RNA targeting is significantly improved, the specific delivery of RNA therapeutics to desired organs/cells still remains the leading challenge for furthering RNA therapeutics, among which EV-mediated delivery of RNA therapeutics holds the greatest potential. Further understanding of Ex-ncRNA biology and advances in related techniques will eventually establish well-defined diagnostic and therapeutic approaches using Ex-ncRNAs to alleviate the current medical burdens associated with CVDs.

Author Contributions: Conceptualization, Z.J., C.L., X.Y. and G.L.; methodology, formal analysis, investigation, resources, and data curation, Z.J., C.L., X.Y., L.S., L.Z. and G.L.; writing—original draft preparation, Z.J., C.L., X.Y., L.S., E.C. and L.Z.; writing—review and editing, X.Y., L.S., E.C., J.L. and G.L.; supervision and project administration, J.L. and G.L.; funding acquisition, Z.J., X.Y. and J.L. All authors have read and agreed to the published version of the manuscript.

Funding: This work was supported by the National Natural Science Foundation of China to Z.J (No. 81900287) and X.Y. (No. 82205088), the Tianshan Youth Foundation of Xinjiang (No. 2019Q066) to Z.J., and the Massachusetts General Hospital Institutional fund (No. 219863) to J.L.

Institutional Review Board Statement: Not applicable.

Informed Consent Statement: Not applicable.

Data Availability Statement: Not applicable.

Acknowledgments: We thank Tiffaney Hisa from the Department of Neurosurgery, Massachusetts General Hospital and Harvard Medical School, for her help with the language editing.

Conflicts of Interest: The authors declare no conflict of interest.

References

1. Campbell, N.R.C.; Ordunez, P.; Giraldo, G.; Rodriguez Morales, Y.A.; Lombardi, C.; Khan, T.; Padwal, R.; Tsuyuki, R.T.; Varghese, C. WHO HEARTS: A Global Program to Reduce Cardiovascular Disease Burden: Experience Implementing in the Americas and Opportunities in Canada. *Can. J. Cardiol.* **2021**, *37*, 744–755. [CrossRef] [PubMed]
2. Şahin, B.; İlgün, G. Risk factors of deaths related to cardiovascular diseases in World Health Organization (WHO) member countries. *Health Soc. Care Community* **2022**, *30*, 73–80. [CrossRef] [PubMed]
3. Fang, Y.; Dai, X. Emerging Roles of Extracellular Non-Coding RNAs in Vascular Diseases. *J. Cardiovasc. Transl. Res.* **2022**, *15*, 492–499. [CrossRef] [PubMed]
4. Thompson, A.G.; Gray, E.; Heman-Ackah, S.M.; Mäger, I.; Talbot, K.; Andaloussi, S.E.; Wood, M.J.; Turner, M.R. Extracellular vesicles in neurodegenerative disease—Pathogenesis to biomarkers. *Nat. Rev. Neurol.* **2016**, *12*, 346–357. [CrossRef]
5. Zijlstra, C.; Stoorvogel, W. Prostasomes as a source of diagnostic biomarkers for prostate cancer. *J. Clin. Investig.* **2016**, *126*, 1144–1151. [CrossRef]
6. Gruner, H.N.; McManus, M.T. Examining the evidence for extracellular RNA function in mammals. *Nat. Rev. Genet.* **2021**, *22*, 448–458. [CrossRef]
7. Lin, Z.; Lu, F.; Ma, X.; Xia, X.; Zou, F.; Jiang, J. Roles of circular RNAs in the pathogenesis of intervertebral disc degeneration (Review). *Exp. Ther. Med.* **2021**, *22*, 1221. [CrossRef]
8. Sato-Kuwabara, Y.; Melo, S.A.; Soares, F.A.; Calin, G.A. The fusion of two worlds: Non-coding RNAs and extracellular vesicles–diagnostic and therapeutic implications (Review). *Int. J. Oncol.* **2015**, *46*, 17–27. [CrossRef]
9. Poller, W.; Dimmeler, S.; Heymans, S.; Zeller, T.; Haas, J.; Karakas, M.; Leistner, D.M.; Jakob, P.; Nakagawa, S.; Blankenberg, S.; et al. Non-coding RNAs in cardiovascular diseases: Diagnostic and therapeutic perspectives. *Eur. Heart J.* **2018**, *39*, 2704–2716. [CrossRef]
10. Hu, Y.Y.; Cheng, X.M.; Wu, N.; Tao, Y.; Wang, X.N. Non-coding RNAs Regulate the Pathogenesis of Aortic Dissection. *Front. Cardiovasc. Med.* **2022**, *9*, 890607. [CrossRef]
11. Li, G.; Manning, A.C.; Bagi, A.; Yang, X.; Gokulnath, P.; Spanos, M.; Howard, J.; Chan, P.P.; Sweeney, T.; Kitchen, R.; et al. Distinct Stress-Dependent Signatures of Cellular and Extracellular tRNA-Derived Small RNAs. *Adv. Sci.* **2022**, *9*, e2200829. [CrossRef] [PubMed]
12. Brandão, B.B.; Guerra, B.A.; Mori, M.A. Shortcuts to a functional adipose tissue: The role of small non-coding RNAs. *Redox Biol.* **2017**, *12*, 82–102. [CrossRef] [PubMed]
13. Videira, R.F.; da Costa Martins, P.A. Non-coding RNAs in Cardiac Intercellular Communication. *Front. Physiol.* **2020**, *11*, 738. [CrossRef] [PubMed]
14. Kondkar, A.A.; Abu-Amero, K.K. Utility of circulating microRNAs as clinical biomarkers for cardiovascular diseases. *Biomed. Res. Int.* **2015**, *2015*, 821823. [CrossRef] [PubMed]
15. Peters, L.J.F.; Biessen, E.A.L.; Hohl, M.; Weber, C.; van der Vorst, E.P.C.; Santovito, D. Small Things Matter: Relevance of MicroRNAs in Cardiovascular Disease. *Front. Physiol.* **2020**, *11*, 793. [CrossRef]
16. Shang, X.; Fang, Y.; Xin, W.; You, H. The Application of Extracellular Vesicles Mediated miRNAs in Osteoarthritis: Current Knowledge and Perspective. *J. Inflamm. Res.* **2022**, *15*, 2583–2599. [CrossRef]
17. Wahid, F.; Shehzad, A.; Khan, T.; Kim, Y.Y. MicroRNAs: Synthesis, mechanism, function, and recent clinical trials. *Biochim. Biophys. Acta* **2010**, *1803*, 1231–1243. [CrossRef]
18. Xia, W.; Zhu, X.-W.; Mo, X.-B.; Wu, L.-F.; Wu, J.; Guo, Y.-F.; Zeng, K.-Q.; Wang, M.-J.; Lin, X.; Qiu, Y.-H.; et al. Integrative multi-omics analysis revealed SNP-lncRNA-mRNA (SLM) networks in human peripheral blood mononuclear cells. *Human Genet.* **2017**, *136*, 451–462. [CrossRef]

19. Robinson, E.K.; Covarrubias, S.; Carpenter, S. The how and why of lncRNA function: An innate immune perspective. *Biochim. Biophys. Acta Gene Regul. Mech.* **2020**, *1863*, 194419. [CrossRef]
20. Sun, R.; He, X.Y.; Mei, C.; Ou, C.L. Role of exosomal long non-coding RNAs in colorectal cancer. *World J. Gastrointest. Oncol.* **2021**, *13*, 867–878. [CrossRef]
21. Dragomir, M.; Chen, B.; Calin, G.A. Exosomal lncRNAs as new players in cell-to-cell communication. *Transl. Cancer Res.* **2018**, *7*, S243–S252. [CrossRef] [PubMed]
22. Xue, M.; Chen, W.; Li, X. Extracellular vesicle-transferred long noncoding RNAs in bladder cancer. *Clin. Chim. Acta* **2021**, *516*, 34–45. [CrossRef] [PubMed]
23. Ye, M.; Wang, J.; Pan, S.; Zheng, L.; Wang, Z.-W.; Zhu, X. Nucleic acids and proteins carried by exosomes of different origins as potential biomarkers for gynecologic cancers. *Mol. Ther.-Oncolytics* **2021**, *24*, 101–113. [CrossRef] [PubMed]
24. Zhang, Y.; Zhang, X.; Xu, Y.; Fang, S.; Ji, Y.; Lu, L.; Xu, W.; Qian, H.; Liang, Z.F. Circular RNA and Its Roles in the Occurrence, Development, Diagnosis of Cancer. *Front. Oncol.* **2022**, *12*, 845703. [CrossRef]
25. Tang, X.; Ren, H.; Guo, M.; Qian, J.; Yang, Y.; Gu, C. Review on circular RNAs and new insights into their roles in cancer. *Comput. Struct. Biotechnol. J.* **2021**, *19*, 910–928. [CrossRef]
26. Jiang, L.; Wang, X.; Zhan, X.; Kang, S.; Liu, H.; Luo, Y.; Lin, L. Advance in circular RNA modulation effects of heart failure. *Gene X* **2020**, *5*, 100036. [CrossRef]
27. Yan, F.; Xie, X.; Huo, Q.; Zhang, W.; Wu, T.; Daniyaer, D.; Shi, L. circ-CCND1 regulates the CCND1/P53/P21 pathway through sponging miR-138-5p in valve interstitial cells to aggravate aortic valve calcification. *J. Physiol. Biochem.* **2022**, *78*, 845–854. [CrossRef]
28. E, S.; Costa, M.C.; Kurc, S.; Drożdż, A.; Cortez-Dias, N.; Enguita, F.J. The circulating non-coding RNA landscape for biomarker research: Lessons and prospects from cardiovascular diseases. *Acta Pharmacol. Sin.* **2018**, *39*, 1085–1099. [CrossRef]
29. Shen, S.; Jiang, H.; Bei, Y.; Xiao, J.; Li, X. Long Non-Coding RNAs in Cardiac Remodeling. *Cell. Physiol. Biochem.* **2017**, *41*, 1830–1837. [CrossRef]
30. Zhang, Y.; Ying, F.; Tian, X.; Lei, Z.; Li, X.; Lo, C.-Y.; Li, J.; Jiang, L.; Yao, X. TRPM2 Promotes Atherosclerotic Progression in a Mouse Model of Atherosclerosis. *Cells* **2022**, *11*, 1423. [CrossRef]
31. Aryal, B.; Suárez, Y. Non-coding RNA regulation of endothelial and macrophage functions during atherosclerosis. *Vascul. Pharmacol.* **2019**, *114*, 64–75. [CrossRef] [PubMed]
32. Lund-Katz, S.; Phillips, M.C. High density lipoprotein structure-function and role in reverse cholesterol transport. *Subcell. Biochem.* **2010**, *51*, 183–227. [CrossRef] [PubMed]
33. Vickers, K.C.; Palmisano, B.T.; Shoucri, B.M.; Shamburek, R.D.; Remaley, A.T. MicroRNAs are transported in plasma and delivered to recipient cells by high-density lipoproteins. *Nat. Cell Biol.* **2011**, *13*, 423–433. [CrossRef] [PubMed]
34. Lu, H.; Buchan, R.J.; Cook, S.A. MicroRNA-223 regulates Glut4 expression and cardiomyocyte glucose metabolism. *Cardiovasc. Res.* **2010**, *86*, 410–420. [CrossRef]
35. Huang, Y.; Tang, S.; Ji-Yan, C.; Huang, C.; Li, J.; Cai, A.P.; Feng, Y.Q. Circulating miR-92a expression level in patients with essential hypertension: A potential marker of atherosclerosis. *J. Hum. Hypertens.* **2017**, *31*, 200–205. [CrossRef]
36. Yang, G.; Lin, C. Long Noncoding RNA SOX2-OT Exacerbates Hypoxia-Induced Cardiomyocytes Injury by Regulating miR-27a-3p/TGFβR1 Axis. *Cardiovasc. Ther.* **2020**, *2020*, 2016259. [CrossRef]
37. Tao, J.; Hu, Y. Diagnostic and prognostic significance of lncRNA SOX2-OT in patients with carotid atherosclerosis. *BMC Cardiovasc. Disord.* **2022**, *22*, 211. [CrossRef]
38. Vilades, D.; Martinez-Camblor, P.; Ferrero-Gregori, A.; Bar, C.; Lu, D.; Xiao, K.; Vea, A.; Nasarre, L.; Sanchez Vega, J.; Leta, R.; et al. Plasma circular RNA hsa_circ_0001445 and coronary artery disease: Performance as a biomarker. *FASEB J.* **2020**, *34*, 4403–4414. [CrossRef]
39. Moroni, F.; Gertz, Z.; Azzalini, L. Relief of Ischemia in Ischemic Cardiomyopathy. *Curr. Cardiol. Rep.* **2021**, *23*, 80. [CrossRef]
40. Han, D.; Kang, S.-H.; Yoon, C.-H.; Youn, T.-J.; Chae, I.-H. Attenuation of ischemia–reperfusion injury by intracoronary chelating agent administration. *Sci. Rep.* **2022**, *12*, 2050. [CrossRef]
41. Rios-Navarro, C.; Daghbouche-Rubio, N.; Gavara, J.; de Dios, E.; Perez, N.; Vila, J.M.; Chorro, F.J.; Ruiz-Sauri, A.; Bodi, V. Ischemia-reperfusion injury to coronary arteries: Comprehensive microscopic study after reperfused myocardial infarction. *Ann. Anat.* **2021**, *238*, 151785. [CrossRef] [PubMed]
42. Wu, M.Y.; Yiang, G.T.; Liao, W.T.; Tsai, A.P.; Cheng, Y.L.; Cheng, P.W.; Li, C.Y.; Li, C.J. Current Mechanistic Concepts in Ischemia and Reperfusion Injury. *Cell. Physiol. Biochem.* **2018**, *46*, 1650–1667. [CrossRef] [PubMed]
43. Kuster, D.W.; Cardenas-Ospina, A.; Miller, L.; Liebetrau, C.; Troidl, C.; Nef, H.M.; Möllmann, H.; Hamm, C.W.; Pieper, K.S.; Mahaffey, K.W.; et al. Release kinetics of circulating cardiac myosin binding protein-C following cardiac injury. *Am. J. Physiol. Heart Circ. Physiol.* **2014**, *306*, H547–H556. [CrossRef] [PubMed]
44. Okamoto, R.; Hirashiki, A.; Cheng, X.W.; Yamada, T.; Shimazu, S.; Shinoda, N.; Okumura, T.; Takeshita, K.; Bando, Y.; Kondo, T.; et al. Usefulness of serum cardiac troponins T and I to predict cardiac molecular changes and cardiac damage in patients with hypertrophic cardiomyopathy. *Int. Heart J.* **2013**, *54*, 202–206. [CrossRef] [PubMed]
45. Mannu, G.S. The non-cardiac use and significance of cardiac troponins. *Scott. Med. J.* **2014**, *59*, 172–178. [CrossRef]

46. Corsten, M.F.; Dennert, R.; Jochems, S.; Kuznetsova, T.; Devaux, Y.; Hofstra, L.; Wagner, D.R.; Staessen, J.A.; Heymans, S.; Schroen, B. Circulating MicroRNA-208b and MicroRNA-499 reflect myocardial damage in cardiovascular disease. *Circ. Cardiovasc. Genet.* **2010**, *3*, 499–506. [CrossRef]
47. Chen, Z.; Yan, Y.; Wu, J.; Qi, C.; Liu, J.; Wang, J. Expression level and diagnostic value of exosomal NEAT1/miR-204/MMP-9 in acute ST-segment elevation myocardial infarction. *IUBMB Life* **2020**, *72*, 2499–2507. [CrossRef]
48. Hildebrandt, A.; Kirchner, B.; Meidert, A.S.; Brandes, F.; Lindemann, A.; Doose, G.; Doege, A.; Weidenhagen, R.; Reithmair, M.; Schelling, G.; et al. Detection of Atherosclerosis by Small RNA-Sequencing Analysis of Extracellular Vesicle Enriched Serum Samples. *Front. Cell. Dev. Biol.* **2021**, *9*, 729061. [CrossRef]
49. Crouser, E.D.; Julian, M.W.; Bicer, S.; Ghai, V.; Kim, T.K.; Maier, L.A.; Gillespie, M.; Hamzeh, N.Y.; Wang, K. Circulating exosomal microRNA expression patterns distinguish cardiac sarcoidosis from myocardial ischemia. *PLoS ONE* **2021**, *16*, e0246083. [CrossRef]
50. Chen, Y.; Ye, X.; Yan, F. MicroRNA 3113-5p is a novel marker for early cardiac ischemia/reperfusion injury. *Diagn. Pathol.* **2019**, *14*, 121. [CrossRef]
51. Liu, X.; Xu, Y.; Deng, Y.; Li, H. MicroRNA-223 Regulates Cardiac Fibrosis After Myocardial Infarction by Targeting RASA1. *Cell. Physiol. Biochem. Int. J. Exp. Cell. Physiol. Biochem. Pharmacol.* **2018**, *46*, 1439–1454. [CrossRef] [PubMed]
52. Yang, F.; You, X.; Xu, T.; Liu, Y.; Ren, Y.; Liu, S.; Wu, F.; Xu, Z.; Zou, L.; Wang, G. Screening and Function Analysis of MicroRNAs Involved in Exercise Preconditioning-Attenuating Pathological Cardiac Hypertrophy. *Int. Heart J.* **2018**, *59*, 1069–1076. [CrossRef] [PubMed]
53. Zheng, M.L.; Liu, X.Y.; Han, R.J.; Yuan, W.; Sun, K.; Zhong, J.C.; Yang, X.C. Circulating exosomal long non-coding RNAs in patients with acute myocardial infarction. *J. Cell. Mol. Med.* **2020**, *24*, 9388–9396. [CrossRef]
54. Kishore, R.; Garikipati, V.N.S.; Gonzalez, C. Role of Circular RNAs in Cardiovascular Disease. *J. Cardiovasc. Pharmacol.* **2020**, *76*, 128–137. [CrossRef] [PubMed]
55. DeGuire, J.; Clarke, J.; Rouleau, K.; Roy, J.; Bushnik, T. Blood pressure and hypertension. *Health Rep.* **2019**, *30*, 14–21. [CrossRef] [PubMed]
56. Desai, A.N. High Blood Pressure. *JAMA* **2020**, *324*, 1254–1255. [CrossRef] [PubMed]
57. Cameron, A.C.; Lang, N.N.; Touyz, R.M. Drug Treatment of Hypertension: Focus on Vascular Health. *Drugs* **2016**, *76*, 1529–1550. [CrossRef]
58. Besler, C.; Urban, D.; Watzka, S.; Lang, D.; Rommel, K.P.; Kandolf, R.; Klingel, K.; Thiele, H.; Linke, A.; Schuler, G.; et al. Endomyocardial miR-133a levels correlate with myocardial inflammation, improved left ventricular function, and clinical outcome in patients with inflammatory cardiomyopathy. *Eur. J. Heart Fail.* **2016**, *18*, 1442–1451. [CrossRef]
59. Cengiz, M.; Yavuzer, S.; Kılıçkıran Avcı, B.; Yürüyen, M.; Yavuzer, H.; Dikici, S.A.; Karataş, Ö.F.; Özen, M.; Özen, M.; Uzun, H.; et al. Circulating miR-21 and eNOS in subclinical atherosclerosis in patients with hypertension. *Clin. Exp. Hypertens.* **2015**, *37*, 643–649. [CrossRef]
60. Zou, X.; Wang, J.; Chen, C.; Tan, X.; Huang, Y.; Jose, P.A.; Yang, J.; Zeng, C. Secreted Monocyte miR-27a, via Mesenteric Arterial Mas Receptor-eNOS Pathway, Causes Hypertension. *Am. J. Hypertens.* **2020**, *33*, 31–42. [CrossRef]
61. Suzuki, K.; Yamada, H.; Fujii, R.; Munetsuna, E.; Yamazaki, M.; Ando, Y.; Ohashi, K.; Ishikawa, H.; Mizuno, G.; Tsuboi, Y.; et al. Circulating microRNA-27a and -133a are negatively associated with incident hypertension: A five-year longitudinal population-based study. *Biomarkers* **2022**, *27*, 496–502. [CrossRef] [PubMed]
62. Wang, C.; Wu, H.; Xing, Y.; Ye, Y.; He, F.; Yin, Q.; Li, Y.; Shang, F.; Shyy, J.Y.; Yuan, Z.Y. Endothelial-derived extracellular microRNA-92a promotes arterial stiffness by regulating phenotype changes of vascular smooth muscle cells. *Sci. Rep.* **2022**, *12*, 344. [CrossRef]
63. Corsello, S.M.; Paragliola, R.M. Evaluation and Management of Endocrine Hypertension During Pregnancy. *Endocrinol. Metab. Clin. N. Am.* **2019**, *48*, 829–842. [CrossRef]
64. Shah, S.; Gupta, A. Hypertensive Disorders of Pregnancy. *Cardiol. Clin.* **2019**, *37*, 345–354. [CrossRef] [PubMed]
65. Cao, G.; Cui, R.; Liu, C.; Zhang, Z. MicroRNA regulation of transthyretin in trophoblast biofunction and preeclampsia. *Arch. Biochem. Biophys.* **2019**, *676*, 108129. [CrossRef] [PubMed]
66. He, X.; Ding, D. High miR-200a-3p expression has high diagnostic values for hypertensive disorders complicating pregnancy and predicts adverse pregnancy outcomes. *BMC Pregnancy Childbirth* **2022**, *22*, 490. [CrossRef] [PubMed]
67. Bozkurt, B.; Coats, A.J.S.; Tsutsui, H.; Abdelhamid, C.M.; Adamopoulos, S.; Albert, N.; Anker, S.D.; Atherton, J.; Böhm, M.; Butler, J.; et al. Universal definition and classification of heart failure: A report of the Heart Failure Society of America, Heart Failure Association of the European Society of Cardiology, Japanese Heart Failure Society and Writing Committee of the Universal Definition of Heart Failure. *Eur. J. Heart Fail.* **2021**, *23*, 352–380. [CrossRef]
68. Janjusevic, M.; Fluca, A.L.; Ferro, F.; Gagno, G.; D'Alessandra, Y.; Beltrami, A.P.; Sinagra, G.; Aleksova, A. Traditional and Emerging Biomarkers in Asymptomatic Left Ventricular Dysfunction-Promising Non-Coding RNAs and Exosomes as Biomarkers in Early Phases of Cardiac Damage. *Int. J. Mol. Sci.* **2021**, *22*, 4937. [CrossRef]
69. Li, J.; Salvador, A.M.; Li, G.; Valkov, N.; Ziegler, O.; Yeri, A.; Yang Xiao, C.; Meechoovet, B.; Alsop, E.; Rodosthenous, R.S.; et al. Mir-30d Regulates Cardiac Remodeling by Intracellular and Paracrine Signaling. *Circ. Res.* **2021**, *128*, e1–e23. [CrossRef]
70. Wu, T.; Chen, Y.; Du, Y.; Tao, J.; Zhou, Z.; Yang, Z. Serum Exosomal MiR-92b-5p as a Potential Biomarker for Acute Heart Failure Caused by Dilated Cardiomyopathy. *Cell. Physiol. Biochem.* **2018**, *46*, 1939–1950. [CrossRef]

71. Huang, Z.P.; Ding, Y.; Chen, J.; Wu, G.; Kataoka, M.; Hu, Y.; Yang, J.H.; Liu, J.; Drakos, S.G.; Selzman, C.H.; et al. Long non-coding RNAs link extracellular matrix gene expression to ischemic cardiomyopathy. *Cardiovasc. Res.* **2016**, *112*, 543–554. [CrossRef] [PubMed]
72. Ounzain, S.; Micheletti, R.; Beckmann, T.; Schroen, B.; Alexanian, M.; Pezzuto, I.; Crippa, S.; Nemir, M.; Sarre, A.; Johnson, R.; et al. Genome-wide profiling of the cardiac transcriptome after myocardial infarction identifies novel heart-specific long non-coding RNAs. *Eur. Heart J.* **2015**, *36*, 353–368. [CrossRef] [PubMed]
73. Kumarswamy, R.; Bauters, C.; Volkmann, I.; Maury, F.; Fetisch, J.; Holzmann, A.; Lemesle, G.; de Groote, P.; Pinet, F.; Thum, T. Circulating long noncoding RNA, LIPCAR, predicts survival in patients with heart failure. *Circ. Res.* **2014**, *114*, 1569–1575. [CrossRef]
74. Han, P.; Li, W.; Lin, C.H.; Yang, J.; Shang, C.; Nuernberg, S.T.; Jin, K.K.; Xu, W.; Lin, C.Y.; Lin, C.J.; et al. A long noncoding RNA protects the heart from pathological hypertrophy. *Nature* **2014**, *514*, 102–106. [CrossRef]
75. Piersma, B.; Bank, R.A.; Boersema, M. Signaling in Fibrosis: TGF-β, WNT, and YAP/TAZ Converge. *Front. Med.* **2015**, *2*, 59. [CrossRef]
76. Winkle, M.; El-Daly, S.M.; Fabbri, M.; Calin, G.A. Noncoding RNA therapeutics-challenges and potential solutions. *Nat. Rev. Drug Discov.* **2021**, *20*, 629–651. [CrossRef]
77. Rohner, E.; Yang, R.; Foo, K.S.; Goedel, A.; Chien, K.R. Unlocking the promise of mRNA therapeutics. *Nat. Biotechnol.* **2022**, *40*, 1586–1600. [CrossRef]
78. He, A.T.; Liu, J.; Li, F.; Yang, B.B. Targeting circular RNAs as a therapeutic approach: Current strategies and challenges. *Signal Transduct. Target. Ther.* **2021**, *6*, 185. [CrossRef]
79. Das, S.; Shah, R.; Dimmeler, S.; Freedman, J.E.; Holley, C.; Lee, J.M.; Moore, K.; Musunuru, K.; Wang, D.Z.; Xiao, J.; et al. Noncoding RNAs in Cardiovascular Disease: Current Knowledge, Tools and Technologies for Investigation, and Future Directions: A Scientific Statement from the American Heart Association. *Circ. Genom. Precis. Med.* **2020**, *13*, e000062. [CrossRef]
80. Burger, F.; Baptista, D.; Roth, A.; da Silva, R.F.; Montecucco, F.; Mach, F.; Brandt, K.J.; Miteva, K. NLRP3 Inflammasome Activation Controls Vascular Smooth Muscle Cells Phenotypic Switch in Atherosclerosis. *Int. J. Mol. Sci.* **2021**, *23*, 340. [CrossRef]
81. Cao, R.Y.; Zhang, Y.; Feng, Z.; Liu, S.; Liu, Y.; Zheng, H.; Yang, J. The Effective Role of Natural Product Berberine in Modulating Oxidative Stress and Inflammation Related Atherosclerosis: Novel Insights Into the Gut-Heart Axis Evidenced by Genetic Sequencing Analysis. *Front. Pharmacol.* **2021**, *12*, 764994. [CrossRef]
82. Shimada, B.K.; Yang, Y.; Zhu, J.; Wang, S.; Suen, A.; Kronstadt, S.M.; Jeyaram, A.; Jay, S.M.; Zou, L.; Chao, W. Extracellular miR-146a-5p Induces Cardiac Innate Immune Response and Cardiomyocyte Dysfunction. *Immunohorizons* **2020**, *4*, 561–572. [CrossRef]
83. Preissner, K.T.; Fischer, S.; Deindl, E. Extracellular RNA as a Versatile DAMP and Alarm Signal That Influences Leukocyte Recruitment in Inflammation and Infection. *Front. Cell. Dev. Biol.* **2020**, *8*, 619221. [CrossRef]
84. Shan, K.; Jiang, Q.; Wang, X.Q.; Wang, Y.N.; Yang, H.; Yao, M.D.; Liu, C.; Li, X.M.; Yao, J.; Liu, B.; et al. Role of long non-coding RNA-RNCR3 in atherosclerosis-related vascular dysfunction. *Cell Death Dis.* **2016**, *7*, e2248. [CrossRef]
85. Yang, Z.; Liang, X.; Yang, L. Circular RNA circ_0001445 alleviates the ox-LDL-induced endothelial injury in human primary aortic endothelial cells through regulating ABCG1 via acting as a sponge of miR-208b-5p. *Gen. Thorac. Cardiovasc. Surg.* **2022**, *70*, 779–792. [CrossRef]
86. Gao, X.F.; Wang, Z.M.; Chen, A.Q.; Wang, F.; Luo, S.; Gu, Y.; Kong, X.Q.; Zuo, G.F.; Jiang, X.M.; Ding, G.W.; et al. Plasma Small Extracellular Vesicle-Carried miRNA-501-5p Promotes Vascular Smooth Muscle Cell Phenotypic Modulation-Mediated In-Stent Restenosis. *Oxidative Med. Cell. Longev.* **2021**, *2021*, 6644970. [CrossRef]
87. Simsekyilmaz, S.; Cabrera-Fuentes, H.A.; Meiler, S.; Kostin, S.; Baumer, Y.; Liehn, E.A.; Weber, C.; Boisvert, W.A.; Preissner, K.T.; Zernecke, A. Role of extracellular RNA in atherosclerotic plaque formation in mice. *Circulation* **2014**, *129*, 598–606. [CrossRef]
88. Chiou, N.T.; Kageyama, R.; Ansel, K.M. Selective Export into Extracellular Vesicles and Function of tRNA Fragments during T Cell Activation. *Cell Rep.* **2018**, *25*, 3356–3370.e4. [CrossRef]
89. Liu, S.; Chen, J.; Shi, J.; Zhou, W.; Wang, L.; Fang, W.; Zhong, Y.; Chen, X.; Chen, Y.; Sabri, A.; et al. M1-like macrophage-derived exosomes suppress angiogenesis and exacerbate cardiac dysfunction in a myocardial infarction microenvironment. *Basic Res. Cardiol.* **2020**, *115*, 22. [CrossRef]
90. Long, R.; Gao, L.; Li, Y.; Li, G.; Qin, P.; Wei, Z.; Li, D.; Qian, C.; Li, J.; Yang, G. M2 macrophage-derived exosomes carry miR-1271-5p to alleviate cardiac injury in acute myocardial infarction through down-regulating SOX6. *Mol. Immunol.* **2021**, *136*, 26–35. [CrossRef]
91. Liu, H.; Zhang, Y.; Yuan, J.; Gao, W.; Zhong, X.; Yao, K.; Lin, L.; Ge, J. Dendritic cell-derived exosomal miR-494-3p promotes angiogenesis following myocardial infarction. *Int. J. Mol. Med.* **2021**, *47*, 315–325, Corrigendum in *Int. J. Mol. Med.* **2022**, *49*, 5096. [CrossRef]
92. Li, Q.; Xu, Y.; Lv, K.; Wang, Y.; Zhong, Z.; Xiao, C.; Zhu, K.; Ni, C.; Wang, K.; Kong, M.; et al. Small extracellular vesicles containing miR-486-5p promote angiogenesis after myocardial infarction in mice and nonhuman primates. *Sci. Transl. Med.* **2021**, *13*, eabb0202. [CrossRef]
93. Cheng, H.; Chang, S.; Xu, R.; Chen, L.; Song, X.; Wu, J.; Qian, J.; Zou, Y.; Ma, J. Hypoxia-challenged MSC-derived exosomes deliver miR-210 to attenuate post-infarction cardiac apoptosis. *Stem Cell Res. Ther.* **2020**, *11*, 224. [CrossRef]

94. Mao, C.; Li, D.; Zhou, E.; Gao, E.; Zhang, T.; Sun, S.; Gao, L.; Fan, Y.; Wang, C. Extracellular vesicles from anoxia preconditioned mesenchymal stem cells alleviate myocardial ischemia/reperfusion injury. *Aging* **2021**, *13*, 6156–6170. [CrossRef]
95. Ou, H.; Teng, H.; Qin, Y.; Luo, X.; Yang, P.; Zhang, W.; Chen, W.; Lv, D.; Tang, H. Extracellular vesicles derived from microRNA-150-5p-overexpressing mesenchymal stem cells protect rat hearts against ischemia/reperfusion. *Aging* **2020**, *12*, 12669–12683. [CrossRef]
96. Li, T.; Gu, J.; Yang, O.; Wang, J.; Wang, Y.; Kong, J. Bone Marrow Mesenchymal Stem Cell-Derived Exosomal miRNA-29c Decreases Cardiac Ischemia/Reperfusion Injury Through Inhibition of Excessive Autophagy via the PTEN/Akt/mTOR Signaling Pathway. *Circ. J.* **2020**, *84*, 1304–1311. [CrossRef]
97. Zou, L.; Ma, X.; Wu, B.; Chen, Y.; Xie, D.; Peng, C. Protective effect of bone marrow mesenchymal stem cell-derived exosomes on cardiomyoblast hypoxia-reperfusion injury through the miR-149/let-7c/Faslg axis. *Free Radic. Res.* **2020**, *54*, 722–731. [CrossRef]
98. Fu, D.L.; Jiang, H.; Li, C.Y.; Gao, T.; Liu, M.R.; Li, H.W. MicroRNA-338 in MSCs-derived exosomes inhibits cardiomyocyte apoptosis in myocardial infarction. *Eur. Rev. Med. Pharmacol. Sci.* **2020**, *24*, 10107–10117. [CrossRef]
99. Walravens, A.S.; Smolgovsky, S.; Li, L.; Kelly, L.; Antes, T.; Peck, K.; Quon, T.; Ibrahim, A.; Marbán, E.; Berman, B.; et al. Mechanistic and therapeutic distinctions between cardiosphere-derived cell and mesenchymal stem cell extracellular vesicle non-coding RNA. *Sci. Rep.* **2021**, *11*, 8666. [CrossRef]
100. de Couto, G.; Gallet, R.; Cambier, L.; Jaghatspanyan, E.; Makkar, N.; Dawkins, J.F.; Berman, B.P.; Marbán, E. Exosomal MicroRNA Transfer Into Macrophages Mediates Cellular Postconditioning. *Circulation* **2017**, *136*, 200–214. [CrossRef]
101. de Couto, G.; Jaghatspanyan, E.; DeBerge, M.; Liu, W.; Luther, K.; Wang, Y.; Tang, J.; Thorp, E.B.; Marbán, E. Mechanism of Enhanced MerTK-Dependent Macrophage Efferocytosis by Extracellular Vesicles. *Arterioscler. Thromb. Vasc. Biol.* **2019**, *39*, 2082–2096. [CrossRef]
102. Ibrahim, A.G.; Cheng, K.; Marbán, E. Exosomes as critical agents of cardiac regeneration triggered by cell therapy. *Stem Cell Rep.* **2014**, *2*, 606–619. [CrossRef]
103. Ciullo, A.; Li, C.; Li, L.; Ungerleider, K.C.; Peck, K.; Marbán, E.; Ibrahim, A.G.E. Biodistribution of unmodified cardiosphere-derived cell extracellular vesicles using single RNA tracing. *J. Extracell. Vesicles* **2022**, *11*, e12178. [CrossRef]
104. Moghiman, T.; Barghchi, B.; Esmaeili, S.A.; Shabestari, M.M.; Tabaee, S.S.; Momtazi-Borojeni, A.A. Therapeutic angiogenesis with exosomal microRNAs: An effectual approach for the treatment of myocardial ischemia. *Heart Fail. Rev.* **2021**, *26*, 205–213. [CrossRef]
105. Gou, L.; Xue, C.; Tang, X.; Fang, Z. Inhibition of Exo-miR-19a-3p derived from cardiomyocytes promotes angiogenesis and improves heart function in mice with myocardial infarction via targeting HIF-1α. *Aging* **2020**, *12*, 23609–23618. [CrossRef]
106. Geng, T.; Song, Z.Y.; Xing, J.X.; Wang, B.X.; Dai, S.P.; Xu, Z.S. Exosome Derived from Coronary Serum of Patients with Myocardial Infarction Promotes Angiogenesis through the miRNA-143/IGF-IR Pathway. *Int. J. Nanomed.* **2020**, *15*, 2647–2658. [CrossRef]
107. Liao, Z.; Chen, Y.; Duan, C.; Zhu, K.; Huang, R.; Zhao, H.; Hintze, M.; Pu, Q.; Yuan, Z.; Lv, L.; et al. Cardiac telocytes inhibit cardiac microvascular endothelial cell apoptosis through exosomal miRNA-21-5p-targeted cdip1 silencing to improve angiogenesis following myocardial infarction. *Theranostics* **2021**, *11*, 268–291. [CrossRef]
108. Li, K.S.; Bai, Y.; Li, J.; Li, S.L.; Pan, J.; Cheng, Y.Q.; Li, K.; Wang, Z.G.; Ji, W.J.; Zhou, Q.; et al. LncRNA HCP5 in hBMSC-derived exosomes alleviates myocardial ischemia reperfusion injury by sponging miR-497 to activate IGF1/PI3K/AKT pathway. *Int. J. Cardiol.* **2021**, *342*, 72–81. [CrossRef]
109. Diao, L.; Zhang, Q. Transfer of lncRNA UCA1 by hUCMSCs-derived exosomes protects against hypoxia/reoxygenation injury through impairing miR-143-targeted degradation of Bcl-2. *Aging* **2021**, *13*, 5967–5985. [CrossRef]
110. Wang, Y.; Zhao, R.; Shen, C.; Liu, W.; Yuan, J.; Li, C.; Deng, W.; Wang, Z.; Zhang, W.; Ge, J.; et al. Exosomal CircHIPK3 Released from Hypoxia-Induced Cardiomyocytes Regulates Cardiac Angiogenesis after Myocardial Infarction. *Oxidative Med. Cell. Longev.* **2020**, *2020*, 8418407. [CrossRef]
111. Wang, Y.; Li, C.; Zhao, R.; Qiu, Z.; Shen, C.; Wang, Z.; Liu, W.; Zhang, W.; Ge, J.; Shi, B. CircUbe3a from M2 macrophage-derived small extracellular vesicles mediates myocardial fibrosis after acute myocardial infarction. *Theranostics* **2021**, *11*, 6315–6333. [CrossRef] [PubMed]
112. Zhang, J.; He, Y.; Yan, X.; Chen, S.; He, M.; Lei, Y.; Zhang, J.; Gongol, B.; Gu, M.; Miao, Y.; et al. MicroRNA-483 amelioration of experimental pulmonary hypertension. *EMBO Mol. Med.* **2020**, *12*, e11303. [CrossRef] [PubMed]
113. Shang, F.; Guo, X.; Chen, Y.; Wang, C.; Gao, J.; Wen, E.; Lai, B.; Bai, L. Endothelial MicroRNA-483-3p Is Hypertension-Protective. *Oxidative Med. Cell. Longev.* **2022**, *2022*, 3698219. [CrossRef] [PubMed]
114. Li, S.; Zhu, J.; Zhang, W.; Chen, Y.; Zhang, K.; Popescu, L.M.; Ma, X.; Lau, W.B.; Rong, R.; Yu, X.; et al. Signature microRNA expression profile of essential hypertension and its novel link to human cytomegalovirus infection. *Circulation* **2011**, *124*, 175–184. [CrossRef] [PubMed]
115. Sarrion, I.; Milian, L.; Juan, G.; Ramon, M.; Furest, I.; Carda, C.; Cortijo Gimeno, J.; Mata Roig, M. Role of circulating miRNAs as biomarkers in idiopathic pulmonary arterial hypertension: Possible relevance of miR-23a. *Oxidative Med. Cell. Longev.* **2015**, *2015*, 792846. [CrossRef] [PubMed]
116. Niu, L.; Sun, N.; Kong, L.; Xu, Y.; Kang, Y. miR-634 inhibits human vascular smooth muscle cell proliferation and migration in hypertension through Wnt4/β-catenin pathway. *Front. Biosci. (Landmark. Ed.)* **2021**, *26*, 395–404. [CrossRef] [PubMed]
117. Shah, A.K.; Bhullar, S.K.; Elimban, V.; Dhalla, N.S. Oxidative Stress as A Mechanism for Functional Alterations in Cardiac Hypertrophy and Heart Failure. *Antioxidants* **2021**, *10*, 931. [CrossRef] [PubMed]

118. Yang, F.; Dong, A.; Mueller, P.; Caicedo, J.; Sutton, A.M.; Odetunde, J.; Barrick, C.J.; Klyachkin, Y.M.; Abdel-Latif, A.; Smyth, S.S. Coronary artery remodeling in a model of left ventricular pressure overload is influenced by platelets and inflammatory cells. *PLoS ONE* **2012**, *7*, e40196. [CrossRef]
119. Nie, X.; Fan, J.; Li, H.; Yin, Z.; Zhao, Y.; Dai, B.; Dong, N.; Chen, C.; Wang, D.W. miR-217 Promotes Cardiac Hypertrophy and Dysfunction by Targeting PTEN. *Mol. Ther. Nucleic Acids* **2018**, *12*, 254–266. [CrossRef]
120. Bang, C.; Batkai, S.; Dangwal, S.; Gupta, S.K.; Foinquinos, A.; Holzmann, A.; Just, A.; Remke, J.; Zimmer, K.; Zeug, A.; et al. Cardiac fibroblast-derived microRNA passenger strand-enriched exosomes mediate cardiomyocyte hypertrophy. *J. Clin. Investig.* **2014**, *124*, 2136–2146. [CrossRef]
121. Thum, T.; Gross, C.; Fiedler, J.; Fischer, T.; Kissler, S.; Bussen, M.; Galuppo, P.; Just, S.; Rottbauer, W.; Frantz, S.; et al. MicroRNA-21 contributes to myocardial disease by stimulating MAP kinase signalling in fibroblasts. *Nature* **2008**, *456*, 980–984. [CrossRef] [PubMed]
122. Sayed, D.; Rane, S.; Lypowy, J.; He, M.; Chen, I.Y.; Vashistha, H.; Yan, L.; Malhotra, A.; Vatner, D.; Abdellatif, M. MicroRNA-21 targets Sprouty2 and promotes cellular outgrowths. *Mol. Biol. Cell.* **2008**, *19*, 3272–3282. [CrossRef] [PubMed]
123. Tatsuguchi, M.; Seok, H.Y.; Callis, T.E.; Thomson, J.M.; Chen, J.F.; Newman, M.; Rojas, M.; Hammond, S.M.; Wang, D.Z. Expression of microRNAs is dynamically regulated during cardiomyocyte hypertrophy. *J. Mol. Cell. Cardiol.* **2007**, *42*, 1137–1141. [CrossRef] [PubMed]
124. Wu, R.; Gao, W.; Yao, K.; Ge, J. Roles of Exosomes Derived from Immune Cells in Cardiovascular Diseases. *Front. Immunol.* **2019**, *10*, 648. [CrossRef]
125. Yu, H.; Qin, L.; Peng, Y.; Bai, W.; Wang, Z. Exosomes Derived from Hypertrophic Cardiomyocytes Induce Inflammation in Macrophages via miR-155 Mediated MAPK Pathway. *Front. Immunol.* **2020**, *11*, 606045. [CrossRef]
126. Wang, C.; Zhang, C.; Liu, L.; A, X.; Chen, B.; Li, Y.; Du, J. Macrophage-Derived mir-155-Containing Exosomes Suppress Fibroblast Proliferation and Promote Fibroblast Inflammation during Cardiac Injury. *Mol. Ther. J. Am. Soc. Gene Ther.* **2017**, *25*, 192–204. [CrossRef]
127. Summerhill, V.I.; Moschetta, D.; Orekhov, A.N.; Poggio, P.; Myasoedova, V.A. Sex-Specific Features of Calcific Aortic Valve Disease. *Int. J. Mol. Sci.* **2020**, *21*, 5620. [CrossRef]
128. Duan, C.; Cao, Z.; Tang, F.; Jian, Z.; Liang, C.; Liu, H.; Xiao, Y.; Liu, L.; Ma, R. miRNA-mRNA crosstalk in myocardial ischemia induced by calcified aortic valve stenosis. *Aging* **2019**, *11*, 448–466. [CrossRef]
129. Yang, R.; Tang, Y.; Chen, X.; Yang, Y. Telocytes-derived extracellular vesicles alleviate aortic valve calcification by carrying miR-30b. *ESC Heart Fail.* **2021**, *8*, 3935–3946. [CrossRef]
130. Qiao, L.; Hu, S.; Liu, S.; Zhang, H.; Ma, H.; Huang, K.; Li, Z.; Su, T.; Vandergriff, A.; Tang, J.; et al. microRNA-21-5p dysregulation in exosomes derived from heart failure patients impairs regenerative potential. *J. Clin. Investig.* **2019**, *129*, 2237–2250. [CrossRef]
131. Li, H.; Trager, L.E.; Liu, X.; Hastings, M.H.; Xiao, C.; Guerra, J.; To, S.; Li, G.; Yeri, A.; Rodosthenous, R.; et al. lncExACT1 and DCHS2 Regulate Physiological and Pathological Cardiac Growth. *Circulation* **2022**, *145*, 1218–1233. [CrossRef] [PubMed]
132. Guo, H.; Lu, Y.W.; Lin, Z.; Huang, Z.P.; Liu, J.; Wang, Y.; Seok, H.Y.; Hu, X.; Ma, Q.; Li, K.; et al. Intercalated disc protein Xinβ is required for Hippo-YAP signaling in the heart. *Nat. Commun.* **2020**, *11*, 4666. [CrossRef] [PubMed]
133. Moya, I.M.; Halder, G. Hippo-YAP/TAZ signalling in organ regeneration and regenerative medicine. *Nat. Rev. Mol. Cell. Biol.* **2019**, *20*, 211–226. [CrossRef] [PubMed]
134. Bezzerides, V.J.; Platt, C.; Lerchenmüller, C.; Paruchuri, K.; Oh, N.L.; Xiao, C.; Cao, Y.; Mann, N.; Spiegelman, B.M.; Rosenzweig, A. CITED4 induces physiologic hypertrophy and promotes functional recovery after ischemic injury. *JCI Insight* **2016**, *1*, 5620. [CrossRef]
135. Li, K.; Rodosthenous, R.S.; Kashanchi, F.; Gingeras, T.; Gould, S.J.; Kuo, L.S.; Kurre, P.; Lee, H.; Leonard, J.N.; Liu, H.; et al. Advances, challenges, and opportunities in extracellular RNA biology: Insights from the NIH exRNA Strategic Workshop. *JCI Insight* **2018**, *3*, e98942. [CrossRef]
136. Blanco-Dominguez, R.; Sanchez-Diaz, R.; de la Fuente, H.; Jimenez-Borreguero, L.J.; Matesanz-Marin, A.; Relano, M.; Jimenez-Alejandre, R.; Linillos-Pradillo, B.; Tsilingiri, K.; Martin-Mariscal, M.L.; et al. A Novel Circulating MicroRNA for the Detection of Acute Myocarditis. *N. Engl. J. Med.* **2021**, *384*, 2014–2027. [CrossRef]
137. Elbashir, S.M.; Harborth, J.; Lendeckel, W.; Yalcin, A.; Weber, K.; Tuschl, T. Duplexes of 21-nucleotide RNAs mediate RNA interference in cultured mammalian cells. *Nature* **2001**, *411*, 494–498. [CrossRef]
138. Crooke, S.T. Molecular Mechanisms of Antisense Oligonucleotides. *Nucleic Acid Ther.* **2017**, *27*, 70–77. [CrossRef]
139. Shah, A.M.; Giacca, M. Small non-coding RNA therapeutics for cardiovascular disease. *Eur. Heart J.* **2022**, *43*, 4548–4561. [CrossRef]
140. Haemmig, S.; Feinberg, M.W. Targeting LncRNAs in Cardiovascular Disease: Options and Expeditions. *Circ. Res.* **2017**, *120*, 620–623. [CrossRef]
141. Robinson, E.L.; Port, J.D. Utilization and Potential of RNA-Based Therapies in Cardiovascular Disease. *JACC Basic Transl. Sci.* **2022**, *7*, 956–969. [CrossRef]
142. Lieberman, J. Tapping the RNA world for therapeutics. *Nat. Struct. Mol. Biol.* **2018**, *25*, 357–364. [CrossRef]
143. Egli, M.; Manoharan, M. Re-Engineering RNA Molecules into Therapeutic Agents. *Acc. Chem. Res.* **2019**, *52*, 1036–1047. [CrossRef]
144. Baumann, V.; Winkler, J. miRNA-based therapies: Strategies and delivery platforms for oligonucleotide and non-oligonucleotide agents. *Future Med. Chem.* **2014**, *6*, 1967–1984. [CrossRef]

145. Johannes, L.; Lucchino, M. Current Challenges in Delivery and Cytosolic Translocation of Therapeutic RNAs. *Nucleic Acid Ther.* **2018**, *28*, 178–193. [CrossRef]
146. Borden, A.; Kurian, J.; Nickoloff, E.; Yang, Y.; Troupes, C.D.; Ibetti, J.; Lucchese, A.M.; Gao, E.; Mohsin, S.; Koch, W.J.; et al. Transient Introduction of miR-294 in the Heart Promotes Cardiomyocyte Cell Cycle Reentry After Injury. *Circ. Res.* **2019**, *125*, 14–25. [CrossRef]
147. Žarković, M.; Hufsky, F.; Markert, U.R.; Marz, M. The Role of Non-Coding RNAs in the Human Placenta. *Cells* **2022**, *11*, 1588. [CrossRef]
148. Palazzo, C.; D'Alessio, A.; Tamagnone, L. Message in a Bottle: Endothelial Cell Regulation by Extracellular Vesicles. *Cancers* **2022**, *14*, 1969. [CrossRef]
149. Sykaras, A.G.; Christofidis, K.; Politi, E.; Theocharis, S. Exosomes on Endometrial Cancer: A Biomarkers Treasure Trove? *Cancers* **2022**, *14*, 1733. [CrossRef]
150. Samra, M.; Srivastava, K. Non-coding RNA and their potential role in cardiovascular diseases. *Gene* **2023**, *851*, 147011. [CrossRef]
151. Davidson, S.M.; Padró, T.; Bollini, S.; Vilahur, G.; Duncker, D.J.; Evans, P.C.; Guzik, T.; Hoefer, I.E.; Waltenberger, J.; Wojta, J.; et al. Progress in cardiac research: From rebooting cardiac regeneration to a complete cell atlas of the heart. *Cardiovasc. Res.* **2021**, *117*, 2161–2174. [CrossRef] [PubMed]
152. Bansal, P.; Arora, M. RNA Binding Proteins and Non-coding RNA's in Cardiovascular Diseases. *Adv. Exp. Med. Biol.* **2020**, *1229*, 105–118. [CrossRef]

Biochemical and Biophysical Research Communications 635 (2022) 291–298

Contents lists available at ScienceDirect

Biochemical and Biophysical Research Communications

journal homepage: www.elsevier.com/locate/ybbrc

Disulfiram-loaded hollow copper sulfide nanoparticles show anti-tumor effects in preclinical models of colorectal cancer

Zeyidan Jiapaer [a, b, *], Lingying Zhang [a, b, 1], Wanli Ma [c, d], Haoqiang Liu [a, b], Chengyu Li [a, b], Weidong Huang [e], Shuxuan Shao [f, **]

[a] College of Life Science & Technology, Xinjiang University, Xinjiang, 830046, China
[b] Xinjiang Key Laboratory of Biological Resources and Genetic Engineering, Xinjiang, 830046, China
[c] 100049 State Key Laboratory of Respiratory Disease, Guangzhou Institutes of Biomedicine and Health, Chinese Academy of Sciences, Guangzhou, 510530, China
[d] University of Chinese Academy of Sciences, Beijing, 100049, China
[e] Xinjiang Jiayin Hospital, Xinjiang, 830046, China
[f] College of Biology, Hunan University, Changsha, 410082, China

ARTICLE INFO

Article history:
Received 4 October 2022
Accepted 5 October 2022
Available online 7 October 2022

Keywords:
Colorectal cancer
CuS NPs
Disulfiram
Photothermal therapy

ABSTRACT

Colorectal cancer is one of the most common malignancies causing the majority of cancer-related deaths. There is an urgent need to develop new anticancer modalities. Recently, efforts have been made to turn clinically approved drugs into anticancer agents in specific tumor microenvironments via NPs. Disulfiram (DSF) as an effective copper (Cu^{2+})-dependent anti-tumour drug, which has been more widely used in antitumor research. Here, we constructed a novel therapeutic nanoplatforms, DSF@CuS, by encapsulating DSF in hollow CuS NPs to enable in situ chemoselective activation of DSF and hyperthermal amplified chemotherapy. The anticancer effect of DSF was enhanced by the thermal energy generated under NIR irradiation through the intrinsic photothermal conversion of CuS. As a result, significant apoptosis was induced in vitro, and tumor elimination was achieved in vivo. Collectively, DSF@CuS combined with photothermal therapy can significantly promote the apoptosis of CT26 colorectal cancer cells both in vitro and in vivo, providing a potential theoretical agent for the treatment of colorectal cancer.

1. Introduction

Colorectal cancer is one of the most common human cancers, and its mortality rate, up to 50% of localized diseases, eventually metastasizes [1,2]. Therefore, early treatment of colorectal cancer can help improve the therapeutic effect, slow down the metastasis of cancer cells and increase the survival time of patients [3]. Despite decades of development in colorectal cancer treatment, unfortunately, there is still a lack of proven strategies for the efficient treatment of colorectal cancer. Currently, the majority of monotherapy strategies are unable to cure colorectal cancer. At the same time, the use of chemotherapy drugs causes strong side effects and brings a heavy economic burden to patients [4–6]. In recent years, nanomedicine-based cancer treatment strategies have received much attention. Compared with traditional chemical drugs, the unique physical and chemical properties of NPs endow them with great application potential in cancer therapy [7–10]. Hence, introducing nanomaterials can significantly reduce the usage of drugs while achieving efficient cancer therapy. As a non-invasive treatment strategy, photothermal therapy, with superior depth of tissue penetration and minor side effects, has gradually become one of the most critical cancer therapy methods in the last decade [11–13]. Owing to the unique laser surface plasmon resonance (LSPR) effect, nanomaterials are increasingly used as photothermal agents to mediate photothermal therapy of tumor [14,15]. Especially, CuS NPs are preferred for photothermal therapy as the advantages of lower cost, superior photothermal performance, and easy synthesis [16,17]. Numerous studies have demonstrated the potential of CuS NPs in photothermal and chemodynamic therapy, promising emerging nanoplatforms for therapeutic integration [18–20]. Recently, pH-sensitive CuS@Cu_2S@Au NPs have been successfully constructed, and the time-dependent release of drugs from the NPs

* Corresponding author. College of Life Science & Technology, Xinjiang University, Xinjiang, 830046, China.
** Corresponding author.
E-mail addresses: zeyidan@xju.edu.cn (Z. Jiapaer), Shaoshux@126.com (S. Shao).
[1] These authors contributed equally to this work.

https://doi.org/10.1016/j.bbrc.2022.10.027

is more suitable for the long-time and lasting treatment of colorectal cancer [21]. However, CuS-induced photothermal therapy is difficult to cure tumors completely, and it is easy to cause cancer recurrence and metastasis during the treatment process [22].

As an FDA-approved drug, DSF is used clinically to combat alcoholism. It can effectively inhibit the activity of acetaldehyde dehydrogenase, which causes acetaldehyde to accumulate in the body, thus covalently binding to some proteins and phospholipids in the body and inactivating them, resulting in abstinence from alcohol [23]. Concurrently, DSF exhibits potent anti-tumor activity against various tumors, including nasopharyngeal carcinoma, medulloblastoma, breast cancer, and colorectal cancer [24–28]. In the tumor milieu, DSF reacts with Cu^{2+} to generate the complex Cu $(DTC)_2$ in situ, which inhibits the molecular target of tumor action, NPL4, thus achieving superior anti-tumor effects [29]. Moreover, DSF has the advantages of being relatively inexpensive and having relatively low cytotoxic side effects [30]. However, although DSF shows intense anticancer activity upon transformation into Cu $(DTC)_2$, the difficulty of in situ conversion of Cu^{2+} in the tumor milieu to generate sufficient Cu $(DTC)_2$ limits its clinical application [31,32].

Based on the above considerations, we delicately designed DSF-loaded hollow CuS NPs for efficient cancer therapy. Hollow CuS NPs were obtained by the one-pot method. As expected, hollow CuS NPs exhibit excellent photothermal conversion efficiency (23.88%), which is attributed to a large specific surface area. More importantly, the hollow structure endows NPs with an ultra-high drug loading rate (94.2%). In the tumor milieu, the collapse of the hollow structure contributes to the pH-responsive drug release behavior of CuS NPs. These properties make DSF@CuS promising as an ideal nanomedicine for efficient colorectal cancer therapy. As expected, both in vitro and in vivo experiments confirmed that DSF@CuS nanomedicine provides outstanding treatment effect, achieving complete tumor clearance. In summary, our work designs an intriguing strategy to construct intelligent nanoplatforms for cancer synergistic photothermal/chemo therapy with negligible side effects, providing a new paradigm for cancer therapy.

2. Materials and methods

2.1. Materials

Female BALB/c mice (16–18 g, five weeks) were purchased from the Animal Research Center of Xinjiang Medical University and kept at Xinjiang University. All animal studies complied with relevant ethical regulations for animal testing and research (Follow the ethics of Xinjiang University, number: XJ2022009). DSF, Phosphate buffered saline (PBS), fetal bovine serum (FBS), penicillin/streptomycin (PS), and Dulbecco's Modified Eagle's Medium (DMEM) were bought from Thermo Fisher Technology Co., Ltd (Shanghai, China). Polyvinylpyrrolidone (PVP–K30, 40 kDa) was purchased from Yuanye Bio-Technology Co., Ltd (Shanghai, China). $CuCl_2$ was provided by Shanpu Chemical Co., Ltd (Shanghai, China). CT26 cells were purchased from Procell CO., Ltd (Wuhan, China). 3-(4,5-Dimethylthiazol-2-yl)-2,5-diphenyltetrazolium bromide (MTT) was obtained from Beyotime Biotechnology Co., Ltd (Haimen, China). Annexin V-FITC/propidium iodide (PI) apoptosis detection kit was supplied by Yeasen Biotech Co., Ltd (Shanghai, China).

2.2. Preparation of hollow CuS

In a typical Hollow CuS NPs synthesis procedure, 1 ml of 0.5 M $CuCl_2 \bullet 2H_2O$ and 2.4g of PVP-K30 were added to 250 ml of deionized water under continuous stirring for 2 min at room temperature. Then, 250 ml of 0.01 mM NaOH (pH = 9) was added with stirring, followed by 40 μl of 80% $N_2H_4 \cdot H_2O$ to form a bright yellow Cu_2O pellet suspension. Then, 2 mL of 1.33 M Na_2S was added to the solution, stirring (400 rpm) the mixture solution at 60 °C and continued for 12h. Finally, allowed to cool naturally to room temperature and centrifuged (11000 rpm, 15 min). The supernatant was removed and washed using ethanol and deionized water three times to remove free CuS, then freeze-drying and stored at room temperature for later use.

2.3. Characterization

The morphologies of the Hollow CuS NPs were characterized by a Representative transmission electron microscopy (TEM, JEM-200 CX). A UV–vis (Mapada, UV-1200) spectrophotometer measured the UV–vis spectra. The photothermal performance of Hollow CuS NPs was measured by an 808 nm NIR laser (MDL-H-808-5W, Changchun New Industry Optoelectronics Technology Co., Ltd., China).

2.4. Photothermal effect of hollow CuS NPs

To evaluate the photothermal performance and stability of CuS NPs, the CuS NPs of solutions with different concentrations (0, 50, 100, 200, 800 μg/mL) were exposed to 808 nm laser at 1 W/cm^2 for 10 min. The temperature changes of CuS NPs were recorded in 10s intervals by a digital thermometer. Furthermore, CuS NPs (800 μg/mL) were exposed to 808 nm laser at different power (0, 0.5, 0.75, 1, 1.25, 1.5 W/cm^2) for 10 min. Finally, in the solutions of hollow CuS NPs (800 μg/mL), five cycles of NIR laser on/off tests were performed to test photothermal stability.

2.5. Loading of DSF and releasing of DSF in hollow CuS NPs

DSF was dissolved in absolute ethanol with different concentrations (5, 10, 15, 20, and 25 μg/mL) and determined by a UV–visible spectrophotometer. The 2.5 mg CuS NPs were added into 5 ml (1 mg/ml) DSF solution while stirring. After 24h, the solution was centrifugation at 11000 rpm for 15min and collected supernatant. The absorbance value of the supernatant solution was measured. DSF loading capacity was measured using the following equation:

$$\text{Laoding capacity} = \frac{(\text{total DSF} - \text{unbounded DSF})}{\text{total CuS}}$$

The dialysis bag method was used to test the release capacity of DSF from CuS NPs. 0.5 mg hollow CuS NPs were dispersed in 25 ml PBS (pH = 7.2 or pH = 5.0) in a dialysis bag (MWCO = 3500) with continuous stirring at 37 °C. 1 ml of the release medium was taken out with a supplement of 1 ml of fresh medium. A UV–visible spectrophotometer measured the absorption spectrum of sampled solution at specified periods.

2.6. Cell culture

Murine colorectal cancer (CT26) cells were purchased from Procell CO., Ltd, (Wuhan, China), which were maintained in DMEM (Gibco) containing 10% FBS (BI) and 1% PS (Gibco) at 37 °C with 5% CO_2 and cultured for fewer than ten passages.

2.7. In vitro anti-tumor activity

The cells were seeded in 96-well plates (5×10^3 cells per dish) with five replicate wells per group and cultured for 24h. The cells were treated with CuS NPs at different concentrations (0, 6.25, 12.5,

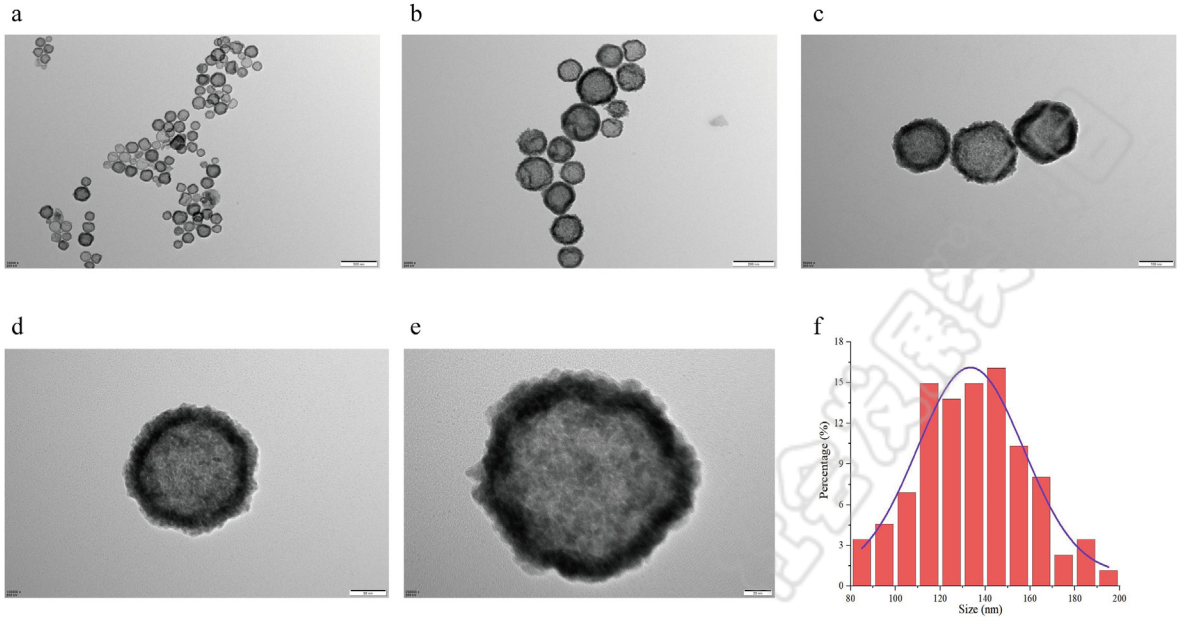

Fig. 1. Synthesis and characterization of CuS NPs
(a-e) The SEM images of CuS NPs. Scale bars are 500 nm, 200 nm, 100 nm, 50 nm and 20 nm, respectively. (f) Diameters of CuS NPs.

25, 50 μg/ml). After 24h incubation, the cells were washed three times with PBS. In another independent experiment, after the cells were incubated with different concentrations of CuS NPs, exposing the 808 nm NIR laser at 1 W/cm^2 for 5 min. All the relative cell viability was assessed by the MTT method. To obtain the effect of DSF or NIR laser irradiation on CT26 cell viability. CT26 cells cultured with different powers (0, 0.5, 0.75, 1, 1.25, 1.5 W/cm^2) or concentrations of DSF (0, 5, 10, 20, 50, 75, 100 μg/ml) as mentioned, and the relative cell viability were also detected by MTT method.

2.8. Apoptosis assay

The CT26 cells were seeded in 6-well plates (1×10^4 cells per dish). After 24h, the cells were treated with fresh complete DMEM medium, CuS NPs (5 μg/ml), and DSF@CuS + NIR (5 μg/ml). For the NIR treatment group, cells were exposed to an 808 nm NIR laser (1 W/cm^2, 5 min) and incubated for 24 h. After that, the cells were washed with PBS and collected by centrifugation. Apoptosis was measured by flow cytometry.

2.9. Animal experiments

First, 1×10^6 CT26 cells were subcutaneously injected into the right notum of BALB/c mice. After 7 days of modeling, the tumor volume reached approximately 100 mm^3. Then, the mice were randomly divided into three groups (n = 3): control, CuS, and DSF@CuS + NIR. The mice were injected 100 μL (10 mg/kg) of DMSO, CuS, or DSF@CuS orthotopic in each group. After 12h, the mice tumor in the DSF@CuS + NIR group were irradiated with 808 nm laser at 1 W/cm^2 for 5 min. Moreover, tumor weights and volumes were measured every two days. After two weeks, the mice were sacrificed, and tumor tissues were collected, photographed, and weighed.

$$\text{Tumor volume} = \text{Tumor length} \times \text{Tumor width}^2/2$$

2.10. Statistical analysis

Statistical analysis was performed by prism 8.0.1 software. All data were expressed as the mean ± standard deviation (SD), and the two-tailed Student's t-test was conducted. $p < 0.05$ was supposed to be statistically significant (*$p < 0.05$, **$p < 0.01$, ***$p < 0.001$, ****$p < 0.0001$)

3. Results and discussion

3.1. Synthesis and characterization of CuS NPs

The synthesis of CuS NPs follows the method of the previous study [33], with slight modifications. Initially, $CuCl_2$ and PVP-K30 were stirred and mixed at room temperature, and then a bright yellow Cu_2O suspension was obtained by adding $N_2H_4 \cdot H_2O$. Finally, CuS NPs were synthesised by adding Na_2S and reacting at 60 °C for 12 h in an aqueous solution. Representative TEM images showed that the synthesised CuS NPs had a well-defined spherical morphology (Fig. 1a–e). In addition, the average diameter of CuS NPs approximately 150 nm. (Fig. 1f)

3.2. Photothermal performance of CuS NPs

UV–Vis spectrum showed that CuS NPs exhibit a broad and strong near-infrared absorption band in the 700–1000 nm range (Fig. 2a). Therefore, CuS NPs have the potential to be used as a phototherapeutic agent for the photothermal ablation of cancer cells with NIR laser. To verify the potential of CuS NPs as an ideal photothermal agent, different concentrations of CuS NPs (0, 50, 100, 200 and 800 μg/mL) were irradiated under an 808 nm NIR laser (1 W/cm^2) for 10min (Fig. 2b). The results showed that the solution temperature gradually increased with increasing CuS NPs concentration, indicating that CuS NPs have good photothermal properties. Furthermore, the heating ability of the CuS NPs solution under different power of NIR laser irradiation were also explored (Fig. 2c). The heating capacity of the CuS NPs solution became stronger with increasing power, which showed that the heating capacity of the

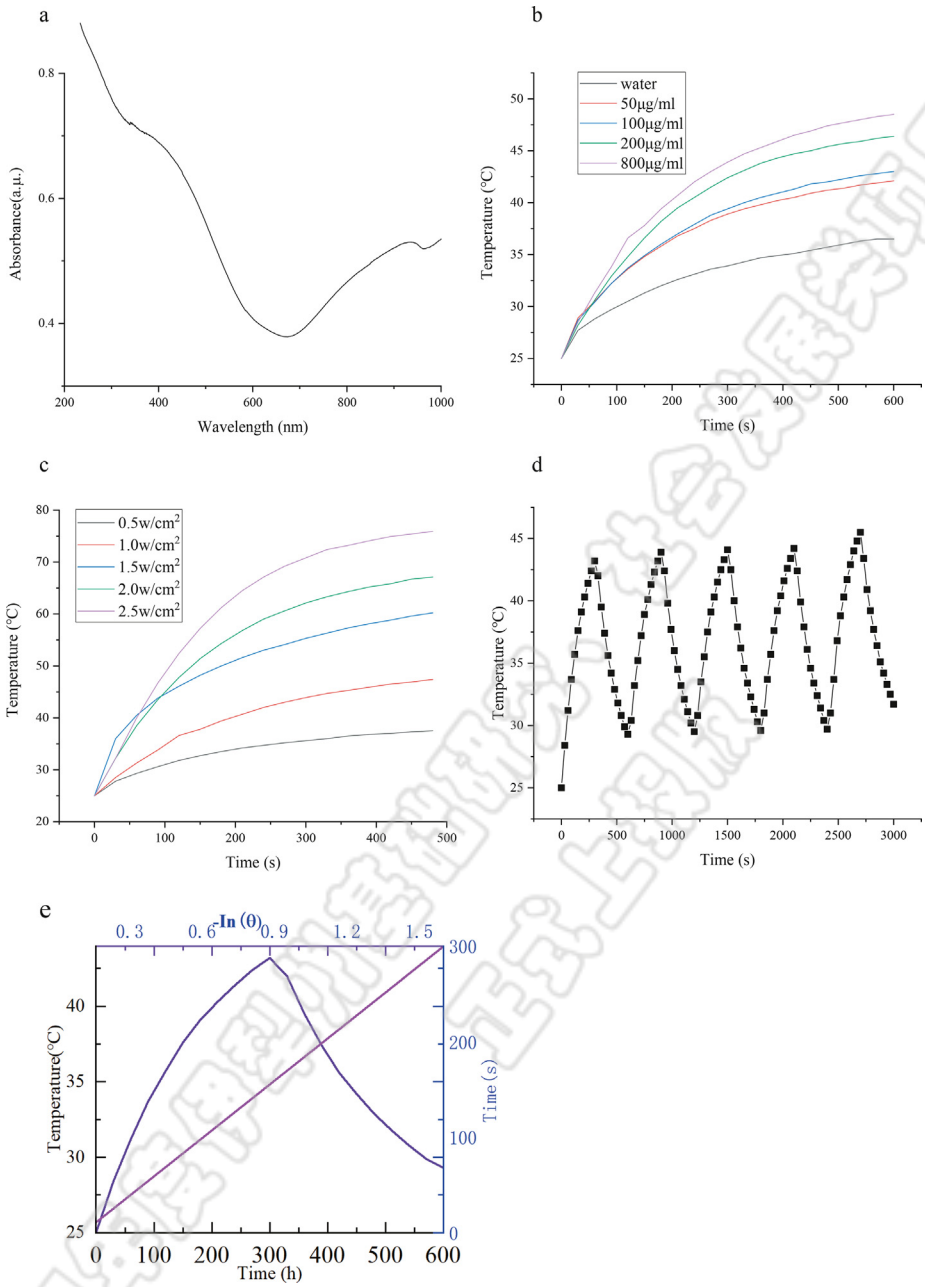

Fig. 2. Photothermal Performance of CuS NPs
(a) UV–vis spectrum of CuS NPs. (b) Temperature-rise curves of solutions containing different concentrations of CuS NPs within 10 min under irradiation of 808 nm NIR laser. (c) Temperature-rise curves of varied power densities of CuS NPs within 10 min under 808 nm NIR laser irradiation. (d) Recycling heating curves of the solution containing CuS NPs for five on/off cycles of the 808 nm NIR laser irradiation (1 W/cm^2). (e) Calculated photothermal-conversion efficiency of CuS NPs at 808 nm.

CuS NPs solution depended on the laser power density. In addition, the photothermal stability of CuS NPs was examined from the perspective of practical applications (Fig. 2d). We found no significant decay in the heating capacity of CuS NPs over five cycles, indicating that they can generate sufficient heat efficiently and consistently in near-infrared radiation. Finally, based on the heat transfer time constant and the maximum temperature, the photothermal conversion efficiency (η) of CuS NPs at 808 nm was calculated to be 23.88% (Fig. 2e), which indicated that CuS NPs have excellent photothermal conversion efficiency. These results suggest that CuS NPs can be used as an effective NIR-mediated photothermal therapy compound for tumor therapy.

3.3. Loading and Release Behavior of DSF in CuS NPs

Encouraged by the unique structure and high specific surface area of CuS NPs, its drug loading capacity was further investigated. Herein, we chose DSF as a tumor treatment agent and loaded it into the CuS NPs. As shown in Fig. 3a, the UV–Vis absorption spectrum shows that DSF has a robust characteristic absorption peak at 217 nm. According to the calculation (Fig. 3b), the loading of DSF was 94.2%, indicating that CuS NPs have excellent loading capacity. In addition, the cumulative release of DSF at different pH values (pH = 5.0 or 7.2) was investigated (Fig. 3c). At pH 7.2, the cumulative release of DSF was the only release rate. When the pH was reduced to 5.0, it increased rapidly to release rate within 48 h,

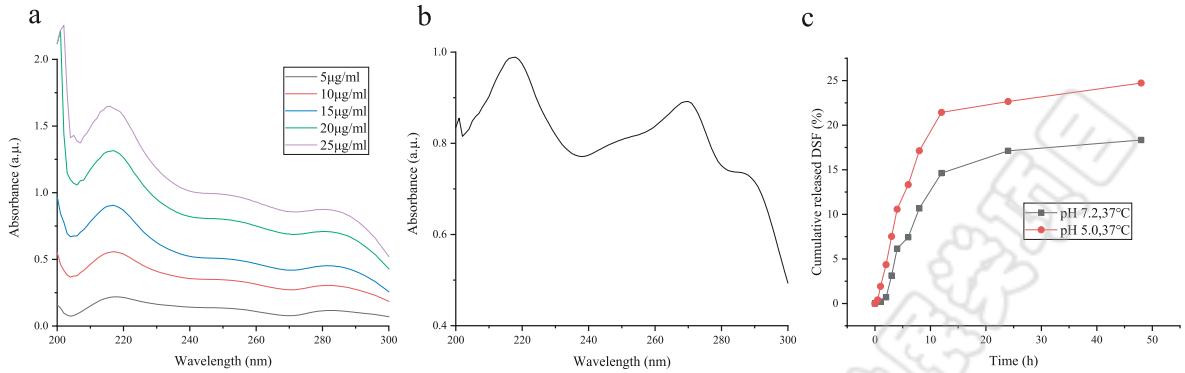

Fig. 3. Loading and Release Behavior of DSF in CuS NPs
(a) UV–vis spectrum of DSF at different concentrations. (b) UV–vis spectrum of the supernatant of a mixture of DSF solution and CuS NPs after centrifugation. (c) In vitro release of DSF in DSF@CuS at different pH values (5.0 or 7.2).

indicating that the release rate of DSF was higher in a weakly acidic environment. These results suggest that DSF@CuS NPs have ultra-high loading capacity for drugs and pH-responsive release behavior, which makes them a promising and excellent therapeutic agent.

3.4. The efficient therapeutic efficacy in vitro

Next, we analyzed the anticancer activity of DSF@CuS with photothermal therapy in vitro. Previous studies have shown that CuS NPs were not cytotoxicity to normal cells. mouse fibroblast cell line L929 (512 μg/ml (8000 cells/per cell)) [34]. Therefore, we evaluated the cell cytotoxicity of CuS NPs to CT26 cells by MTT assay. As shown in Fig. 4a, low concentrations (0–25 μg/mL) of CuS NPs were negligible toxicity to CT26 cells. Only the concentration of 50 μg/mL shows specific cytotoxicity, which initially indicated good biocompatibility of CuS NPs. In addition, we explored the changes in relative cell viability with increasing laser power (0–1.5 W/cm^2) using 808 nm NIR laser irradiation. The result showed that it had no significant effect on the viability of CT26 cells, which indicated the extreme tolerance of CT26 cells to laser irradiation (Fig. 4b).

Furthermore, we investigated the effect of CuS NPs on CT26 cell viability under NIR laser at 808 nm. CT26 cells were treated with CuS and then irradiated with NIR laser. Cell viability decreased as the CuS concentration increased. Cell viability decreased to 50% at a concentration of 25 μg/mL, which showed negligible effect on CT26 cell viability in the absence of NIR laser (Fig. 4c). This is due to the CuS NPs can convert laser energy to heat under laser irradiation, further causing a decrease in the viability of CT26 cells. DSF, a member of binding copper and an inhibitor of aldehyde dehydrogenase, is a promising anti-tumor drug [35]. Previous studies have found that NIR irradiation could amplify to release of both Cu^{2+} and DSF under an acidic tumor microenvironment, further inducing an anti-tumor effect [23]. In this study, CT26 cells were treated with different concentrations of DSF, as shown in Fig. 4d. DSF significantly inhibited the activity of CT26 cells, which was positively correlated with DSF concentration. In addition, the concentration of DSF (10 μg/ml) inhibited CT26 cells by about 50%. This result indicated that DSF could effectively inhibit the activity of CT26 cells in vitro. Next, flow cytometry assays were performed to quantify apoptosis of CT26 cells in each treatment group. The results showed that the DSF@CuS + NIR group has a 65.8% apoptosis rate (Fig. 4e). However, the CuS groups have a lower tumor apoptosis rate. Together, this finding demonstrated that DSF@CuS synergistic anticancer effect with photothermal therapy.

3.5. In vivo anti-tumor effect

Encouraged by the excellent therapeutic efficacy of DSF@CuS mediated photothermal therapy in vitro, the anticancer efficiency in vivo was investigated in CT26 tumor-bearing models in BALB/c mice (Fig. 5a). To evaluate the synergistic effect, the tumor volumes of all mice were recorded every other day during the whole treatment. Surprisingly, the DSF@CuS + NIR group tumor growth was significantly inhibited and had no recurrence within 14 days (Fig. 5b). By contrast, there was no significant change in tumor volumes in CuS groups compared to the control group. This robust tumor-inhibiting response of DSF@CuS + NIR could be attributed to the synergistic effect of chemotherapy and phototherapy.

Moreover, the change in tumor weights again demonstrated the excellent synergistic therapeutic efficacy of DSF@CuS, as the tumors in the mice completely disappeared after laser treatment. However, the other groups displayed only weak tumor suppression compared to the control group (Fig. 5c and d). In summary, the constructed DSF@CuS NPs showed promising synergistic anticancer effects under irradiation of a NIR laser, which has important implications for cancer treatment.

4. Conclusion

In summary, we successfully constructed CuS NPs loaded with DSF. Moreover, the cooperative treatment model of in-situ toxification and photothermal chemotherapeutics has been realized both in vivo and in vitro. Photothermal chemotherapeutics were attributed to the CuS NPs prepared by the chemical etching method, and the photothermal conversion efficiency of CuS NPs was determined to be 23.88% by an 808 nm laser. At the same time, the therapeutic benefit of in-situ toxification was derived from the chelation reaction of DSF with Cu^{2+} in the tumor microenvironment to generate cytotoxic bis (N, N-diethyl dithiocarbamato) copper (II) complexes $Cu(DTC)_2$ [36]. In vitro, our results showed that the apoptosis rate of cells treated with DSF@CuS + NIR Laser reached 72%, indicating that DSF@CuS + NIR Laser had a significant pro-apoptotic effect on CT26. At the same time, we injected DSF@CuS in situ into subcutaneous tumor-bearing BALB/c mice. We stimulated CuS nanospheres by an 808 nm laser to attain photothermal conversion, which showed that the tumor growth inhibition value reached 100%. Therefore, our results indicate that DSF@CuS + NIR Laser is a new anticancer treatment model with significant therapeutic benefit and is expected to achieve translation in clinical application.

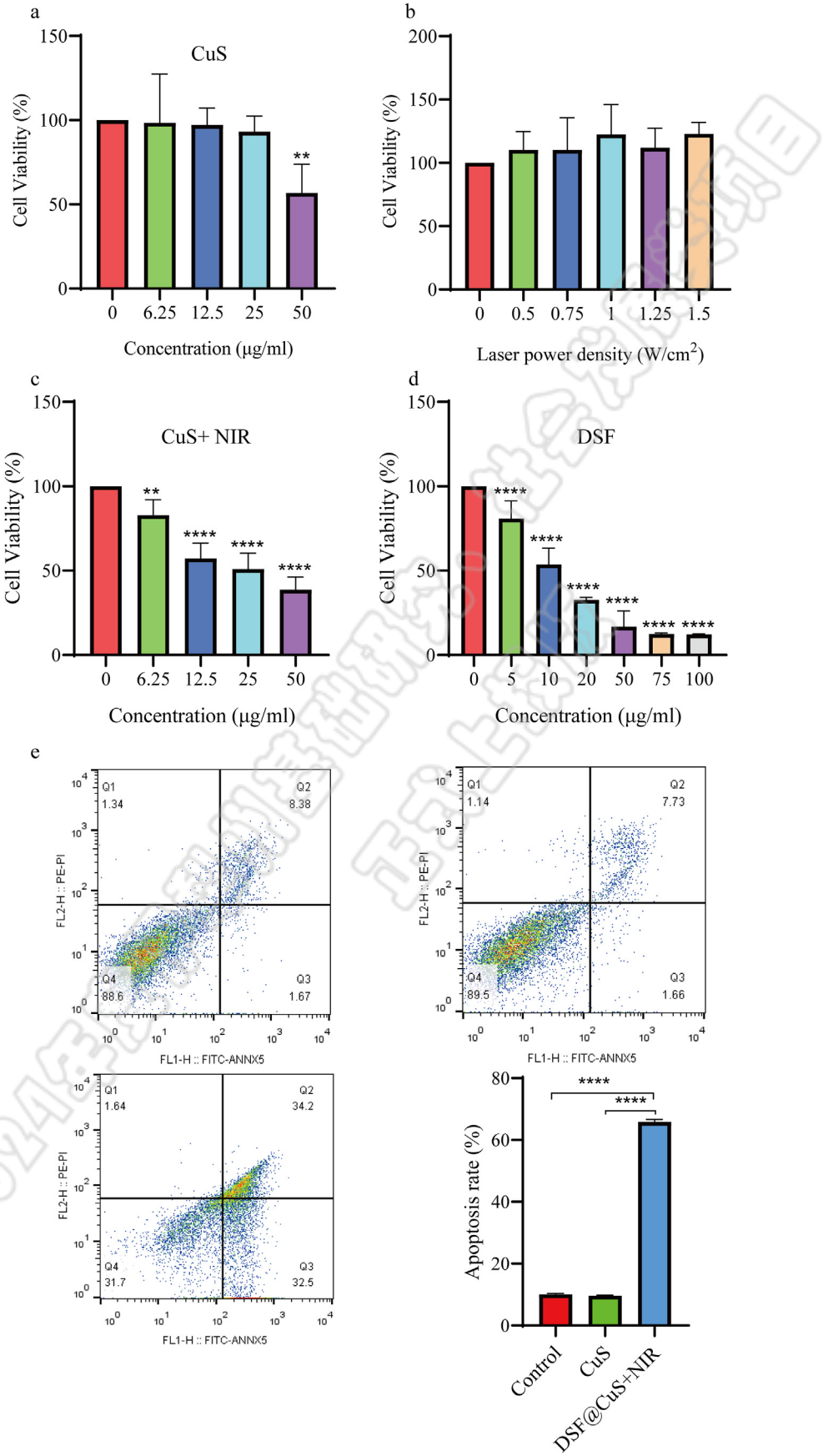

Fig. 4. The in vitro synergistic therapeutic efficacy
(a-d) Cell viability of CT26 cells with different treatment groups: only CuS (0, 6.25, 12.5, 25, 50 μg/ml); only NIR laser (0, 0.5, 0.75, 1, 1.25, 1.5W/cm^2); CuS + NIR (0, 6.25, 12.5, 25, 50 μg/ml); only DSF (0, 5, 10, 20, 50, 75, 100 μg/ml). (N = 6, *p < 0.5, **p < 0.01, ***p < 0.001; ****p < 0.0001). (e) Flow cytometric analysis of cell apoptosis of NIR laser treatment groups. (n = 3, ****p < 0.0001).

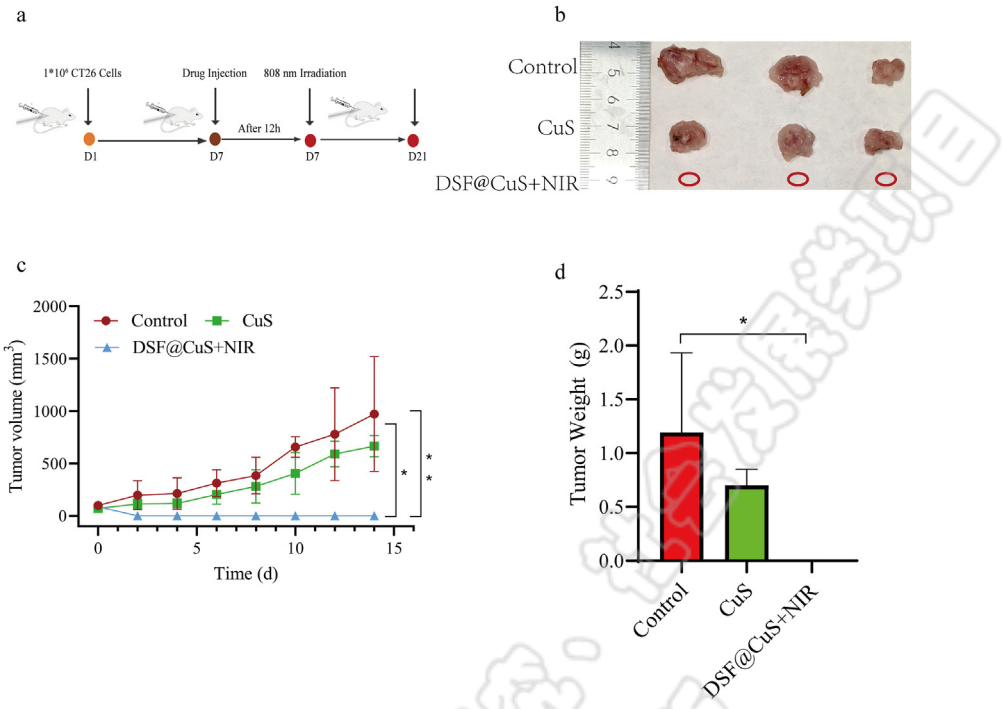

Fig. 5. In vivo therapeutic efficacy of DSF@CuS on tumor-bearing mice model
(a) Schematic diagram of CT26 subcutaneous tumor BALB/c mice model development and treatment process. (b) The representative photographs of dissected tumors after different treatments (control, CuS, DSF@CuS + NIR groups). (c) The body weights change of mice. (n = 3). (d) The tumor volumes and weights change during the treatment process. (n = 3, *p < 0.05, **p < 0.01).

Author contributions

Zeyidan Jiapaer and Lingying Zhang contributed equally to this work, including study conception and design, experiments, data analysis, and manuscript writing. Wanli Ma and Shuxuan Shao are involved in constructing the CuS@DSF nanoplatforms. Haoqiang Liu, Chengyu Li, and Weidong Huang were involved in manuscript preparation. Zeyidan Jiapaer, Shuxuan Shao, and Weidong Huang designed and supervised the project, and Zeyidan Jiapaer and Weidong Huang provided financial support and manuscript writing.

Declaration of competing interest

The author reports no conflicts of interest in this work.

Acknowledgments

This work was supported by the National Natural Science Foundation of China (No: 81900287), the Natural Science Foundation of Xinjiang (No. 2019D01A35), and the Tianshan Youth Foundation of Xinjiang (No. 2019Q066).

References

[1] H. Zhu, Y. Li, Z. Ming, W. Liu, Glucose oxidase-mediated tumor starvation therapy combined with photothermal therapy for colon cancer, Biomater. Sci. 9 (2021) 5577–5587, https://doi.org/10.1039/d1bm00869b.
[2] R. Tiwari, et al., Correction: SPINK1 promotes colorectal cancer progression by downregulating Metallothioneins expression, Oncogenesis 10 (2021) 16, https://doi.org/10.1038/s41389-021-00305-2.
[3] Y. Ma, J. Huang, S. Song, H. Chen, Z. Zhang, Cancer-Targeted nanotheranostics: recent advances and perspectives, Small 12 (2016) 4936–4954, https://doi.org/10.1002/smll.201600635.
[4] D.J. Robertson, U. Ladabaum, Opportunities and challenges in moving from current guidelines to personalized colorectal cancer screening, Gastroenterology 156 (2019) 904–917, https://doi.org/10.1053/j.gastro.2018.12.012.
[5] D. Ciardiello, et al., Immunotherapy of colorectal cancer: challenges for therapeutic efficacy, Cancer Treat Rev. 76 (2019) 22–32, https://doi.org/10.1016/j.ctrv.2019.04.003.
[6] S. Piawah, A.P. Venook, Targeted therapy for colorectal cancer metastases: a review of current methods of molecularly targeted therapy and the use of tumor biomarkers in the treatment of metastatic colorectal cancer, Cancer 125 (2019) 4139–4147, https://doi.org/10.1002/cncr.32163.
[7] J. Shi, P.W. Kantoff, R. Wooster, O.C. Farokhzad, Cancer nanomedicine: progress, challenges and opportunities, Nat. Rev. Cancer 17 (2017) 20–37, https://doi.org/10.1038/nrc.2016.108.
[8] S. Yu, Z. Chen, X. Zeng, X. Chen, Z. Gu, Advances in nanomedicine for cancer starvation therapy, Theranostics 9 (2019) 8026–8047, https://doi.org/10.7150/thno.38261.
[9] Z. Xie, et al., Emerging combination strategies with phototherapy in cancer nanomedicine, Chem. Soc. Rev. 49 (2020) 8065–8087, https://doi.org/10.1039/d0cs00215a.
[10] D.J. Irvine, E.L. Dane, Enhancing cancer immunotherapy with nanomedicine, Nat. Rev. Immunol. 20 (2020) 321–334, https://doi.org/10.1038/s41577-019-0269-6.
[11] Y. Liu, P. Bhattarai, Z. Dai, X. Chen, Photothermal therapy and photoacoustic imaging via nanotheranostics in fighting cancer, Chem. Soc. Rev. 48 (2019) 2053–2108, https://doi.org/10.1039/c8cs00618k.
[12] X. Li, J.F. Lovell, J. Yoon, X. Chen, Clinical development and potential of photothermal and photodynamic therapies for cancer, Nat. Rev. Clin. Oncol. 17 (2020) 657–674, https://doi.org/10.1038/s41571-020-0410-2.
[13] C. Xu, K. Pu, Second near-infrared photothermal materials for combinational nanotheranostics, Chem. Soc. Rev. 50 (2021) 1111–1137, https://doi.org/10.1039/d0cs00664e.
[14] L.A. Austin, M.A. Mackey, E.C. Dreaden, M.A. El-Sayed, The optical, photothermal, and facile surface chemical properties of gold and silver nanoparticles in biodiagnostics, therapy, and drug delivery, Arch. Toxicol. 88 (2014) 1391–1417, https://doi.org/10.1007/s00204-014-1245-3.
[15] L. Wei, et al., Silver nanoparticles: synthesis, properties, and therapeutic applications, Drug Discov. Today 20 (2015) 595–601, https://doi.org/10.1016/j.drudis.2014.11.014.
[16] L. Cui, et al., Integrin αvβ3-targeted [(64)Cu]CuS nanoparticles for PET/CT imaging and photothermal ablation therapy, Bioconjugate Chem. 29 (2018) 4062–4071, https://doi.org/10.1021/acs.bioconjchem.8b00690.
[17] Y. Li, et al., Copper sulfide nanoparticles for photothermal ablation of tumor cells, Nanomedicine 5 (2010) 1161–1171, https://doi.org/10.2217/nnm.10.85.
[18] X. Deng, et al., A hollow-structured CuS@Cu(2) S@Au nanohybrid: synergistically enhanced photothermal efficiency and photoswitchable targeting

effect for cancer theranostics, Adv. Mater. 29 (2017), https://doi.org/10.1002/adma.201701266.
[19] W. Liu, et al., Nanomedicine enables drug-potency activation with tumor sensitivity and hyperthermia synergy in the second near-infrared biowindow, ACS Nano 15 (2021) 6457–6470, https://doi.org/10.1021/acsnano.0c08848.
[20] Z. Qin, et al., Development of copper vacancy defects in a silver-doped CuS nanoplatform for high-efficiency photothermal-chemodynamic synergistic antitumor therapy, J. Mater. Chem. B 9 (2021) 8882–8896, https://doi.org/10.1039/d1tb01629f.
[21] E. Yan, Z. Zhang, pH-sensitive CuS@Cu(2)S@Au nanoparticles as a drug delivery system for the chemotherapy against colon cancer, Biochem. Biophys. Res. Commun. (2020), https://doi.org/10.1016/j.bbrc.2020.01.097.
[22] E.K. Lim, et al., Nanomaterials for theranostics: recent advances and future challenges, Chem. Rev. 115 (2015) 327–394, https://doi.org/10.1021/cr300213b.
[23] W. Wu, et al., Copper-enriched prussian blue nanomedicine for in situ disulfiram toxification and photothermal antitumor amplification, Adv. Mater. 32 (2020), e2000542, https://doi.org/10.1002/adma.202000542.
[24] Y. Li, et al., Disulfiram/copper induces antitumor activity against both nasopharyngeal cancer cells and cancer-associated fibroblasts through ROS/MAPK and ferroptosis pathways, Cancers 12 (2020), https://doi.org/10.3390/cancers12010138.
[25] R. Serra, et al., Disulfiram and copper combination therapy targets NPL4, cancer stem cells and extends survival in a medulloblastoma model, PLoS One 16 (2021), e0251957, https://doi.org/10.1371/journal.pone.0251957.
[26] W. Yao, et al., Disulfiram acts as a potent radio-chemo sensitizer in head and neck squamous cell carcinoma cell lines and transplanted xenografts, Cells (2021), https://doi.org/10.3390/cells10030517, 10.
[27] L. Hou, et al., In situ triggering antitumor efficacy of alcohol-abuse drug disulfiram through Cu-based metal-organic framework nanoparticles, Acta Pharm. Sin. B 11 (2021) 2016–2030, https://doi.org/10.1016/j.apsb.2021.01.013.
[28] Y. Hu, et al., The disulfiram/copper complex induces autophagic cell death in colorectal cancer by targeting ULK1, Front. Pharmacol. 12 (2021), 752825, https://doi.org/10.3389/fphar.2021.752825.
[29] Z. Skrott, et al., Alcohol-abuse drug disulfiram targets cancer via p97 segregase adaptor NPL4, Nature 552 (2017) 194–199, https://doi.org/10.1038/nature25016.
[30] H. Zhang, et al., Co-delivery of nanoparticle and molecular drug by hollow mesoporous organosilica for tumor-activated and photothermal-augmented chemotherapy of breast cancer, J. Nanobiotechnol. 19 (2021) 290, https://doi.org/10.1186/s12951-021-01025-w.
[31] W. Chen, W. Yang, P. Chen, Y. Huang, F. Li, Disulfiram copper nanoparticles prepared with a stabilized metal ion ligand complex method for treating drug-resistant prostate cancers, ACS Appl. Mater. Interfaces 10 (2018) 41118–41128, https://doi.org/10.1021/acsami.8b14940.
[32] L. Zhang, et al., A copper-mediated disulfiram-loaded pH-triggered PEG-shedding TAT peptide-modified lipid nanocapsules for use in tumor therapy, ACS Appl. Mater. Interfaces 7 (2015) 25147–25161, https://doi.org/10.1021/acsami.5b06488.
[33] B. Ji, et al., Hybrid membrane camouflaged copper sulfide nanoparticles for photothermal-chemotherapy of hepatocellular carcinoma, Acta Biomater. 111 (2020) 363–372, https://doi.org/10.1016/j.actbio.2020.04.046.
[34] S. Roy, J.-W. Rhim, L. Jaiswal, Bioactive agar-based functional composite film incorporated with copper sulfide nanoparticles, Food Hydrocolloids (2019), https://doi.org/10.1016/j.foodhyd.2019.02.034.
[35] D. Chen, Q.C. Cui, H. Yang, Q.P. Dou, Disulfiram, a clinically used anti-alcoholism drug and copper-binding agent, induces apoptotic cell death in breast cancer cultures and xenografts via inhibition of the proteasome activity, Cancer Res. 66 (2006) 10425–10433, https://doi.org/10.1158/0008-5472.Can-06-2126.
[36] W. Liu, et al., Nanomedicine enables drug-potency activation with tumor sensitivity and hyperthermia synergy in the second near-infrared biowindow, ACS Nano (2021), https://doi.org/10.1021/acsnano.0c08848.

ACS APPLIED NANO MATERIALS

www.acsanm.org Article

Hollow Nanoporous Prussian Blue Nanocubes Enriched with Cu^{2+} and Loaded with Quercetin for Synergistic Tumor Therapy

Shuxuan Shao, Haoqiang Liu, Fanxing Meng, Wanfeng Wu, Xinbo Li, Mengjiao Duan, and Zeyidan Jiapaer*

Cite This: *ACS Appl. Nano Mater.* 2023, 6, 4969−4977 Read Online

ACCESS | Metrics & More | Article Recommendations | Supporting Information

ABSTRACT: Combination therapy based on Prussian blue nanoparticles (PB NPs) is particularly effective in cancer because of their outstanding photothermal properties and excellent biocompatibility. However, the application of PB in tumor therapy is hindered by their poor reactive oxygen species (ROS) production capacity, and low drug loading rate. More importantly, PB NPs could activate heat shock proteins (HSPs) in photothermal therapy, which induces the self-protection of tumor cells. Structural and functional modulation improved antitumor efficacy by enhancing reactive oxygen species (ROS) production and inhibiting heat shock protein expression. In this work, we synthesized Cu^{2+}-enriched hollow nanoporous PB nanocubes (Cu-HNPB NCs) that enhanced the •OH generating capability of PB as Cu hybridization increases the oxidation potential of PB. Moreover, in the tumor milieu, Cu^{2+} release depletes glutathione (GSH) and converts to Cu^{+}, further improving ROS levels. Excess ROS amplifies cellular oxidative stress and destroys the heat-induced formation of HSPs, thus breaking the self-protection mechanism of tumor cells. To enhance the therapeutic efficiency, quercetin (QUE) was loaded in Cu-HNPB NCs (Cu-HNPB@QUE NCs). Surprisingly, the large specific surface area (127.79 m^2 g^{-1}) endowed Cu-HNPB NCs with ultrahigh loading capacity (57.25%). As the nanoplatform enhances synergistic therapeutic effects, this study provides a new approach for designing multimodal combination nanomedicine.

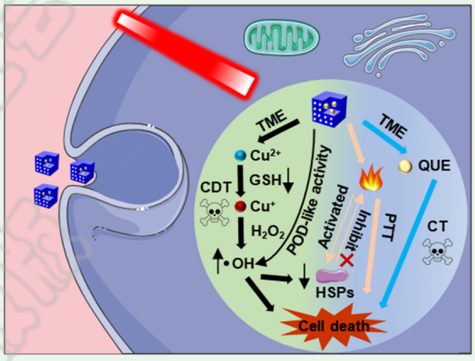

KEYWORDS: *copper hybridization, in situ conversion, synergistic therapy, ultrahigh load capacity, tumor theranostics*

1. INTRODUCTION

A major challenge of cancer therapy is unsatisfactory therapeutic efficiency and severe side effects.[1−3] In recent years, several nanocarriers have been developed to mitigate the toxicity of anticancer drugs to normal cells.[4−6] Still, the metabolism of these drugs can cause unavoidable damage to normal tissues. Meanwhile, several of the most frequently utilized advanced tumor therapies, including chemodynamic therapy (CDT),[7] immunotherapy (IMT),[8] and photothermal therapy (PTT),[9] fail to eradicate tumor cells completely, resulting in tumor recurrence and spread.[10,11] Prussian blue (PB) emerged as a promising candidate for effective multimodal combination therapy attributed to its superior biocompatibility, availability of surface functionalization, and excellent photothermal conversion efficiency.[12−15] However, the weak •OH radical generation capacity, poor drug loading capacity of PB NPs, and the activation of heat shock proteins during PTT attenuated their therapeutic efficiency.[16−18]

Herein, a series of strategies have been employed to overcome these shortcomings. First, a hollow nanoporous PB nanocubes (HNPB NCs) was constructed to improve the drug loading. What is more, the inherent redox property of PB could be modulated via element doping.[19] Copper (Cu) is an ideal hybridizer, which can functionalize PB and activate its chemodynamic properties by generating reactive oxygen species (ROS).[20,21] In tumor milieu, Cu^{2+} depletes GSH and converts in situ to Cu^{+}, which reacts with endogenous H_2O_2 to generate the highly toxic •OH radical.[22,23] The intracellular accumulation of •OH radical can downgrade the expression of HSPs and break the thermal protection mechanism of tumor cells, thereby amplifying the effect of combined therapy.[24−27]

These remarkable properties motivated us to use the "three birds with one stone" strategy and constructed pH-responsive Cu-HNPB@QUE NCs. In brief, hollow nanoporous structure was obtained to enhance the drug loading capacity. Furthermore, the ion exchange method was adopted to obtain Cu-enriched hollow nanoporous PB nanocubes (Cu-HNPB NCs), which significantly enhanced the chemodynamic properties of PB. Meanwhile, as a flavonoid, quercetin (QUE) has strong antioxidant activity and significantly inhibits the proliferation of various cancer cells via regulating the expression

Received: February 19, 2023
Accepted: March 3, 2023
Published: March 15, 2023

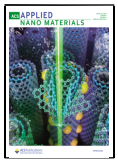

https://doi.org/10.1021/acsanm.3c00764
ACS Appl. Nano Mater. 2023, 6, 4969−4977

Scheme 1. (A) Construction of Cu-HNPB@QUE NCs[a]

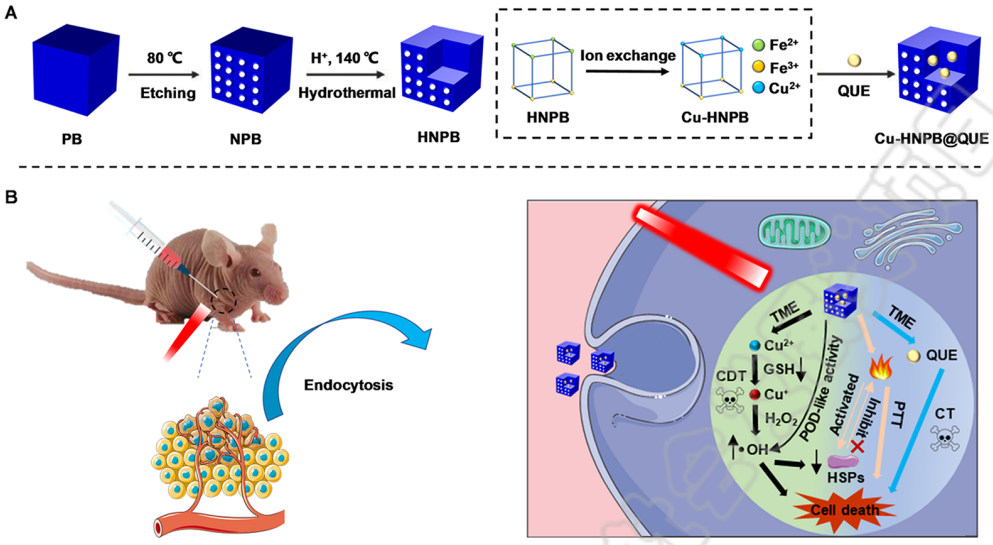

[a](B) Illustration of the combined therapy by in situ conversion of Cu^{2+} and photothermal effect under NIR laser irradiation.

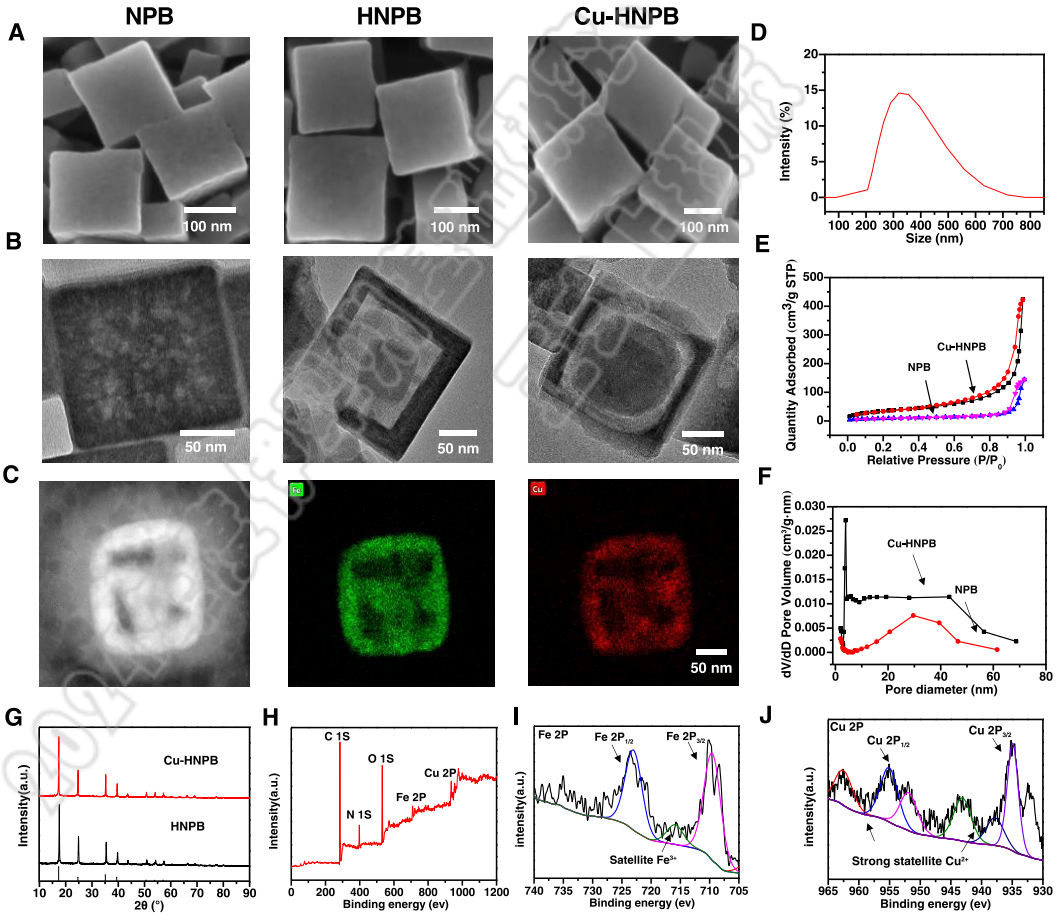

Figure 1. Characterization of NPB NCs, HNPB NCs, and Cu-HNPB NCs. (A, B). Scanning electron microscopy (SEM) and transmission electron microscopy (TEM) images of NPB NCs, HNPB NCs, and Cu-HNPB NCs. (C) HADDF image of Cu-HNPB NCs and corresponding elemental mapping. (D) DLS-measured hydrodynamic sizes based on the intensity distribution for Cu-HNPB NCs incubated in water. (E). N_2 adsorption−desorption isotherms of NPB NCs and Cu-HNPB NCs. (F) Corresponding pore size distribution of NPB NCs and Cu-HNPB NCs. (G) XRD spectra of HNPB NCs and Cu-HNPB NCs. (H−J) High-resolution Fe 2P and Cu 2P XPS data of Cu-HNPB NCs in different binding-energy ranges.

of tumor suppressor gene transfer and related signaling pathways.[28−30] However, poor stability and low utilization limit their application *in vivo*.[31] To address these problems, QUE was selected as the model drug to be loaded into Cu-HNPB

https://doi.org/10.1021/acsanm.3c00764
ACS Appl. Nano Mater. 2023, 6, 4969−4977

NCs. The Cu-HNPB@QUE NCs were synthesized as shown in Scheme 1A. Cu-HNPB NCs exhibited outstanding photothermal conversion efficiency (41.23%), ultrahigh biocompatibility, and stability. As expected, Cu-HNPB NCs also enabled a high QUE loading rate (56%) and pH-responsive drug release behavior. Under near-infrared (NIR) laser irradiation (one stone), natural active substances were released for chemotherapy (CT) (one bird). At the same time, degraded Cu^{2+} was converted to Cu^{+} in situ, and then, Cu^{+} reacted with H_2O_2 in the enriched tumor microenvironment (TME) to generate the •OH radical, enhancing the CDT efficiency (two birds). Meanwhile, Cu-HNPB NCs downregulated HSP70 and HSP90 expression and destroyed the self-protection of tumor cells (another bird) (Scheme 1B). *In vitro* and *in vivo* experiments confirmed that the Cu-HNPB@QUE NCs provide excellent synergistic therapeutic efficiency due to their unique properties. This work expands the application of bioactive substances in tumor therapy and provides a new strategy for constructing a multimodal combination therapy nanoplatform.

2. RESULTS AND DISCUSSION

2.1. Structural Functionalization and Performance Characterization of the Cu-HNPB NCs. HNPB NCs were synthesized using a stepwise hydrothermal method as described in Scheme 1A.[32] Poly(vinylpyrrolidone) (PVP) is used as a protective agent, while HCl serves as an etching agent. The concentration of HCl and reaction time are critical factors during the etching step. The morphology and structure of PB dramatically change with increasing the concentration of HCl and prolonging the reaction time. A bumpy surface appears on the surface of PB in the presence of HCl, and the interior hollow cavity gradually diffuses from the inside out (Figures 1A,B, and S1). Moreover, to achieve the regulation of HNPB NC functions, Cu^{2+} was doped into the HNPB NCs via ion exchange. The obtained Cu-HNPB NCs (320 nm) show distinct hollow nanoporous structure, large specific surface area (127.79 $m^2\ g^{-1}$), and broad pore size distribution (1.9−68.7 nm) (Figure 1D,E and F). The corresponding element mapping and energy-dispersive spectroscopy (EDS) analyses indicated that Cu^{2+} was successfully doped into metal−organic frameworks (Figure 1C). X-ray diffraction (XRD) and X-ray photoelectron spectroscopy (XPS) analyses suggested that the generation of a hollow nanoporous structure and doping of Cu^{2+} have not affected the original PB phase (Figure 1G−J).[33] More importantly, these nanoparticles can be effectively internalized by cells (Figure S15).

Cu-HNPB NCs exhibited a robust and broad concentration-dependent absorption band with a characteristic peak at about 600−900 nm (Figures 2A and S3). Based on the Lambert−Beer law, the mass extinction coefficient of Cu-HNPB NCs is 19.53 L $g^{-1}\ cm^{-1}$ at 808 nm (Figure S4), much higher than Au nanorods (13.9 L $g^{-1}\ cm^{-1}$) and nanoporous carbon nanospheres (6.35 L $g^{-1}\ cm^{-1}$).[34,35] Cu-HNPB NCs exhibited outstanding photothermal performance. The 50 $\mu g\ mL^{-1}$ Cu-HNPB NC solution temperature increased to 59.8 °C after 5 min of 808 nm laser (2 W cm^{-2}) irradiation (Figure 2B,C, and D). The photothermal conversion efficiency of Cu-HNPB NCs reached 41.23%, which is 1.4 times that of HNPB NCs (Figures 2E and S5). Meanwhile, no significant attenuation was observed for each cycle (Figure 2F).

Encouraged by the unique hollow nanoporous structure, the drug loading capacity of Cu-HNPB NCs was further evaluated. It is noteworthy that there were negligible changes in the

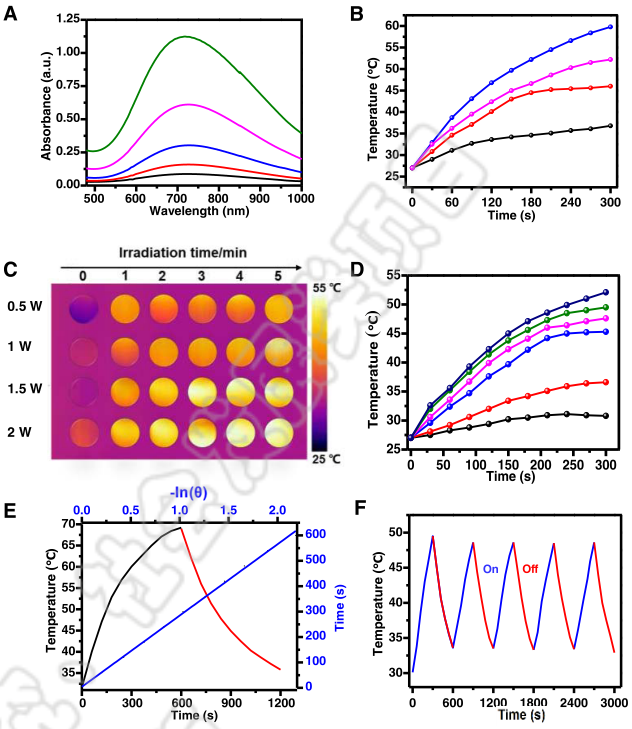

Figure 2. *In vitro* photothermal performance of Cu-HNPB NCs. (A) UV−vis absorbance spectra of Cu-HNPB NCs at different concentrations (from bottom to top: 3.125, 6.25, 12.5, 25, 50 $\mu g\ mL^{-1}$). (B) Cu-HNPB NCs within 5 min under irradiation of 808 nm laser at different power densities (from bottom to top: 0.5, 1, 1.5, 2 W cm^{-2}). (C) Photothermal images of Cu-HNPB NCs (100 $\mu g\ mL^{-1}$) with laser irradiation (1 W cm^{-2}) at different times. (D) Cu-HNPB NCs within 5 min under irradiation of 808 nm laser (1 W cm^{-2}) at different concentrations (from bottom to top: PBS, 3.125, 6.25, 12.5, 25, 50 $\mu g\ mL^{-1}$). (E) Calculated photothermal conversion efficiency of Cu-HNPB NCs at 808 nm (50 $\mu g\ mL^{-1}$, 1.5 W cm^{-2}). Black line: Temperature change curves of the solution under 808 nm laser irradiation for 5 min, and then, the laser was turned off. Red line: Cooling curve after turning off the laser. Blue line: Time constant (τs) for the heat transfer from the system obtained by applying the linear time data from the cooling period. (F) Recycling heating curves of the solution containing Cu-HNPB NCs for five on/off cycles of the 808 nm laser irradiation (1 W cm^{-2}).

diameters of the Cu-HNPB NCs after storage in neutral medium (pH 7.4) for at least 12 h, while the diameter decreased under acidic medium (pH 5.0), implying their excellent colloidal stability and biodegradability (Figure S2). The Cu−C≡N−Fe bond in Cu-HNPB NCs breaks rapidly in an acidic environment, leading to the structural collapse of Cu-HNPB NCs and rapid biodegradation (Figure 3A−C, Figures S6 and S7). This lays a solid foundation for the QUE loading. Meanwhile, QUE has excellent stability in aqueous solution (Figure 3D). A remarkable decrease in the absorbance of the supernatant of the loaded QUE at the characteristic peak (Figure 3E). The solution of Cu-HNPB @QUE NCs showed distinct absorption peaks at 378 nm (Figures S8 and S9), indicating that QUE was successfully loaded into Cu-HNPB NCs.[36] Notably, the loading rate of QUE was as high as 560 $\mu g\ mg^{-1}$ via circulation. Then, the QUE release behavior under different physiological conditions (37 °C, pH 7.4, and 5.0) is shown in Figure 3F. In detail, after 72 h, the cumulative release of QUE was up to 41.5% at pH 5.0 but only 25.4% at pH 7.4. This pH-responsive release

https://doi.org/10.1021/acsanm.3c00764
ACS Appl. Nano Mater. 2023, 6, 4969−4977

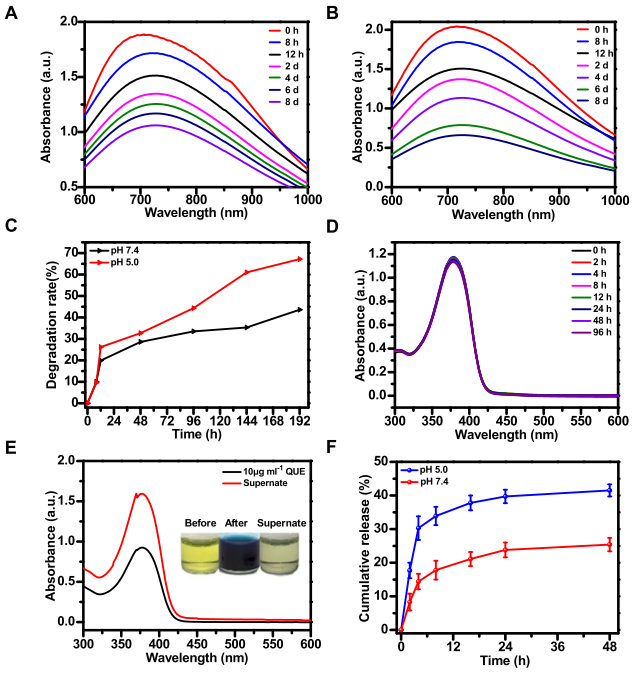

Figure 3. Estimating the behavior of Cu-HNPB NC loading and releasing QUE. (A, B). UV−vis absorbance spectra of Cu-HNPB NCs at the range of 600−1000 nm after immersing at pH 7.4 and 5.0 different times seperately. (C) Biodegradation curve of Cu-HNPB NC solutions with varied pH values after being placed different times. (D) Stability of QUE solutions after different store times. (E) UV−vis absorbance spectra of QUE solutions before and after loading (inset: the representative photos of QUE solution before (left) and after interaction with Cu-HNPB NCs (middle: before centrifugation, right: after centrifugation)). (F) Cumulative release curve of QUE at pH 7.4 and pH 5.0.

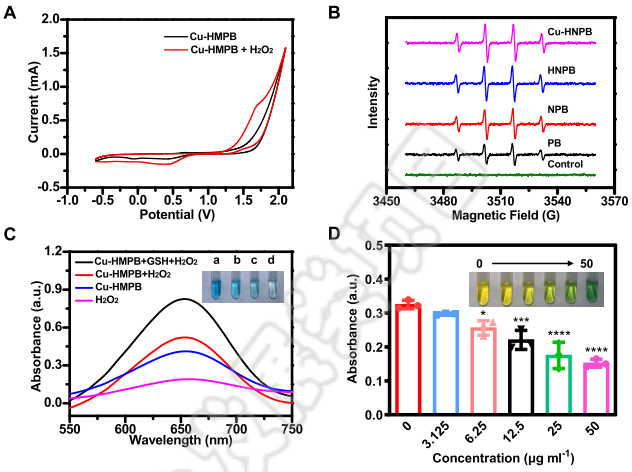

Figure 4. POD-like activity and GSH depletion of Cu-HNPB NCs. (A) Comparison CVs of Cu-HNPB NCs (black line) and Cu-HNPB NCs + H_2O_2 (red line) in the 0.1 M KCl solution, scan rate 50 mV s^{-1}. (B) Capacity of different nanomaterials on the formation of •OH radical from H_2O_2 (pH 3.5). (C) UV−vis absorption spectra and photographs (inset) of TMB aqueous solutions with (a) H_2O_2, (b) Cu-HNPB NCs, (c) Cu-HNPB NCs + H_2O_2, and (d) Cu-HNPB NCs + GSH + H_2O_2 ([TMB] = 40 mM, [H_2O_2] = 10 mM, [Cu-HNPB NCs] = 50 μg mL^{-1}, [GSH] = 2 mM). (D) UV−vis absorption spectra and photographs (inset) of DTNB aqueous solutions with GSH ([DTNB] = 10 mM, [GSH] = 2 mM) in the presence of different concentrations (3.125, 6.125, 12.5, 25, 50 μg mL^{-1}) of Cu-HNPB NCs ($p < 0.05$; $^{**}p < 0.01$; $^{***}p < 0.001$, $^{****}p < 0.0001$).

may be due to the disruption of the Cu-HNPB NC structure in a weakly acidic environment, accelerating the rate of drug release and diffusion. The slow-release behavior could improve the utilization of QUE at tumor tissue.

2.2. Enhanced Chemodynamic Properties and *In Vitro* Antitumor Efficacy. Cu-HNPB NCs enhance the •OH radical-producing capacity of catalytic H_2O_2. No apparent difference was found between the cyclic voltammetric curves of the three nanomaterials (NPB NCs, HNPB NCs, and Cu-HNPB NCs). (Figure S10). However, Cu hybridization significantly improved the H_2O_2 catalyzing ability of PB. The cyclic voltammetric (CV) curve of Cu-HNPB NCs is depicted in Figure 4A, where the addition of H_2O_2 resulted in a new oxidation peak (1.702 V, SCE). This proved that Cu-HNPB NCs with strong peroxidase-like (POD-like) activity and could catalyze H_2O_2 to generate •OH radical. On the contrary, no distinct oxidation peaks were found for NPB NCs and HNPB NCs (Figure S11). The electrochemical oxidation illustrates that Cu-HNPB NCs specifically and efficiently catalyze H_2O_2 decomposition to form •OH radical. The results imply that Cu hybridization enhances the capability of •OH radical production. To further verify this point, electron spin resonance (ESR) was used to detect the signals of •OH radical in solution dynamically. Similarly, the ESR signal was significantly enhanced in the Cu-HNPB NC solution than in PB NCs, NPB NCs, and HNPB NCs under an acidic environment (pH 3.5) (Figure 4B). At the same time, the significant signal intensity of DMPO/•OH was observed in the Cu-HNPB NC solution in a neutral environment (pH 7.4), suggesting that Cu-HNPB NCs exhibit POD-like activity in a wide pH range (Figure S12).

Cu-HNPB NCs reacted with GSH in the TME, converting Cu^{2+} to Cu^{+} in situ and promoting •OH radical production. As shown in Figure 4C, TMB coincubation with a H_2O_2 solution for 10 min exhibited a very low absorbance (0.19) at 652 nm. However, when TMB was incubated with H_2O_2 and solutions containing Cu-HNPB NCs, the absorbance remarkably increased to 0.52, implying the successful production of •OH radicals. Additionally, in the presence of GSH, a higher absorbance (0.82) at 652 nm was detected, meaning more •OH production, which can be attributed to GSH, promoting the Cu^{2+} conversion to Cu^{+} in situ. Subsequently, GSH depletion was systematically assessed. As shown in Figure 4D, the absorbance of TNB^{2-} at 412 nm decreased with increasing concentrations of Cu-HNPB NCs, demonstrating that Cu-HNPB NCs can effectively deplete high levels of GSH. A similar phenomenon was not observed in the aqueous solution of PB NCs and HNPB NCs (Figure S13). These findings suggest that Cu-HNPB NCs amplify oxidative stress levels by depleting GSH and enhancing ROS generation. Reduced GSH levels may lead to a greater vulnerability of tumor tissue to destruction. To understand the underlying mechanism of synergistic therapy, we further evaluated HSP family levels in Hela cells by western blotting (WB) assay. Here, HSP70 and HSP90 were used to assess the expression levels of HSPs under different treatments. Considering the interaction of HNPB NCs or Cu-HNPB NCs with QUE to affect the expression of HSP70, procyanidin B2 (OPC B2) was selected as another natural bioactive substance to exclude interference. When cells are exposed to high temperatures, HSPs are synthesized by thermal excitation to protect the cells.[37,38] As a result, compared with the control group, the expression of HSPs in the NIR group was significantly improved.

https://doi.org/10.1021/acsanm.3c00764
ACS Appl. Nano Mater. 2023, 6, 4969−4977

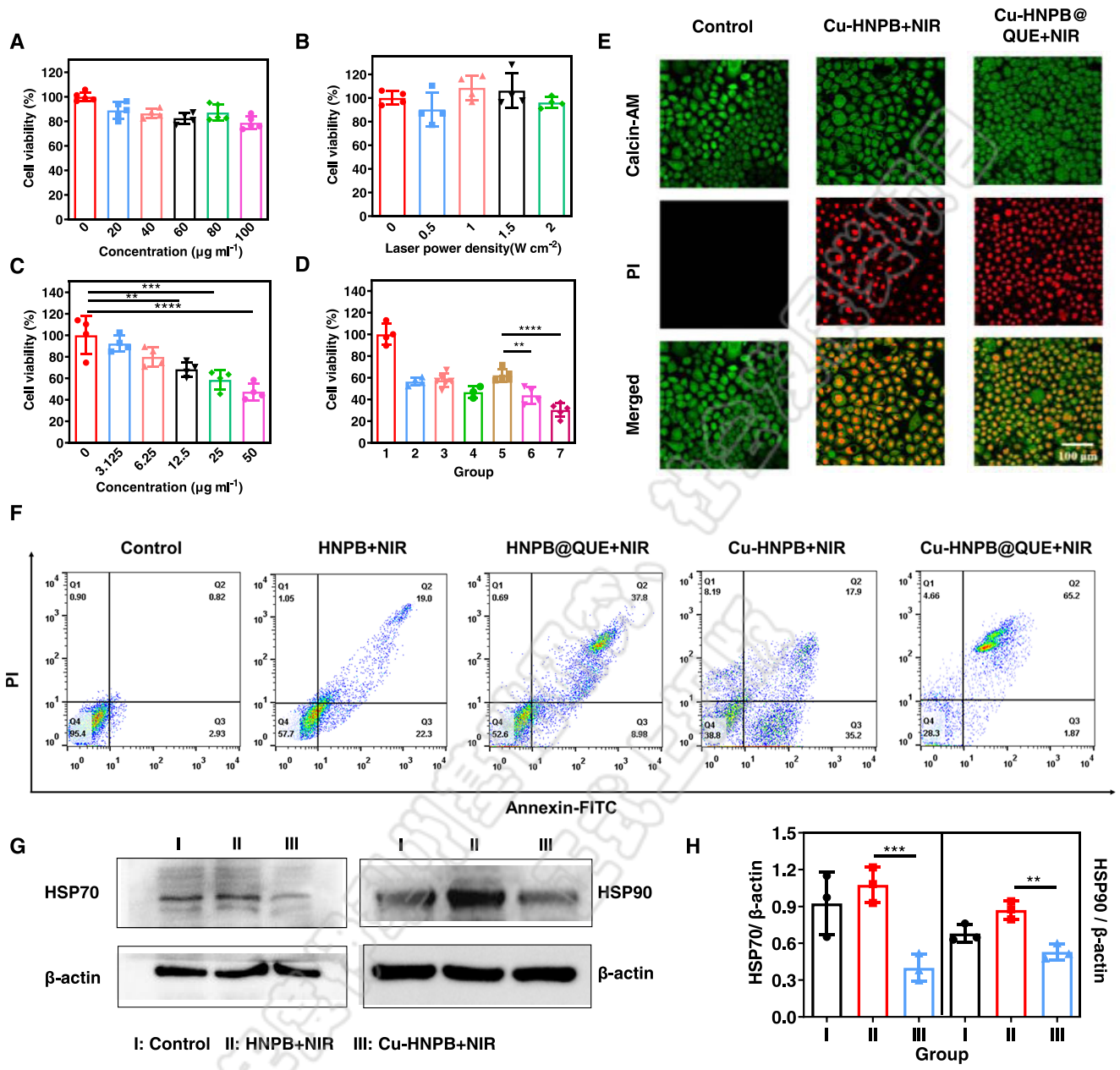

Figure 5. *In vitro* cytotoxicity of Hela. (A–C) Relative cell viabilities of Hela cells in different treatment groups: only Cu-HNPB; only NIR laser; and Cu-HNPB + NIR laser. (D) Relative cell viabilities of Hela cells after being under different treatments at a concentration of 50 μg mL^{-1}. Groups 1–7 represent control, QUE, HNPB + laser, HNPB@QUE + laser, Cu-HNPB@QUE, Cu-HNPB + laser, and Cu-HNPB@QUE + laser, respectively. (E) CLSM images of Hela cells in Cu-HNPB nanoplatform treatment groups. (F) Flow cytometric analysis of NIR laser treatment groups. (G, H) HSP70 and HSP90 expression levels by western blot analysis (n = 3) (p < 0.05; **p < 0.01; ***p < 0.001, ****p < 0.0001).

Conversely, Cu-HNPB + NIR laser-treated cells could obviously downregulate the HSP70 and HSP90 expression compared with other groups, which was consistent with the Cu-HNPB @QUE + NIR laser (Figures 5G,H and S14). These results suggest that the strong Fenton-like reaction induced by Cu-HNPB NCs significantly upregulated ROS levels and disrupted the expression of HSP family in Hela cells, thereby blocking the self-thermal protection mechanism of tumor cells.

Due to enhanced chemodynamic properties, the Cu-HNPB@QUE exhibit strong synergistic therapeutic efficiency (Figure S16). And the results of cytotoxicity assays showed that Cu-HNPB exhibits good biocompatibility (Figure 5A). Additionally, only NIR laser irradiation promoted cell growth to some extent, probably due to the increased temperature of the culture medium (Figure 5B). Comparatively, Cu-HNPB showed obvious cytotoxicity under the NIR laser (Figure 5C). The cell viability of the Cu-HNPB + NIR group (39.5%) was apparently lower than that of the HNPB + NIR group (57.7%) (Figure 5D). Ascribed to the outstanding synergistic therapeutic effect, the strongest PI fluorescence intensity was observed in the Cu-HNPB@QUE group (Figures 5E and S17). In the treatment group, red fluorescence overlaps with green fluorescence. It is likely that calcein staining is so strong in Hela cells that it picks it up in the "red" detector, resulting in a partial overlapping of signals in the images. This phenomenon has no effect on the results of the experiment. Flow cytometry results were

https://doi.org/10.1021/acsanm.3c00764
ACS Appl. Nano Mater. 2023, 6, 4969–4977

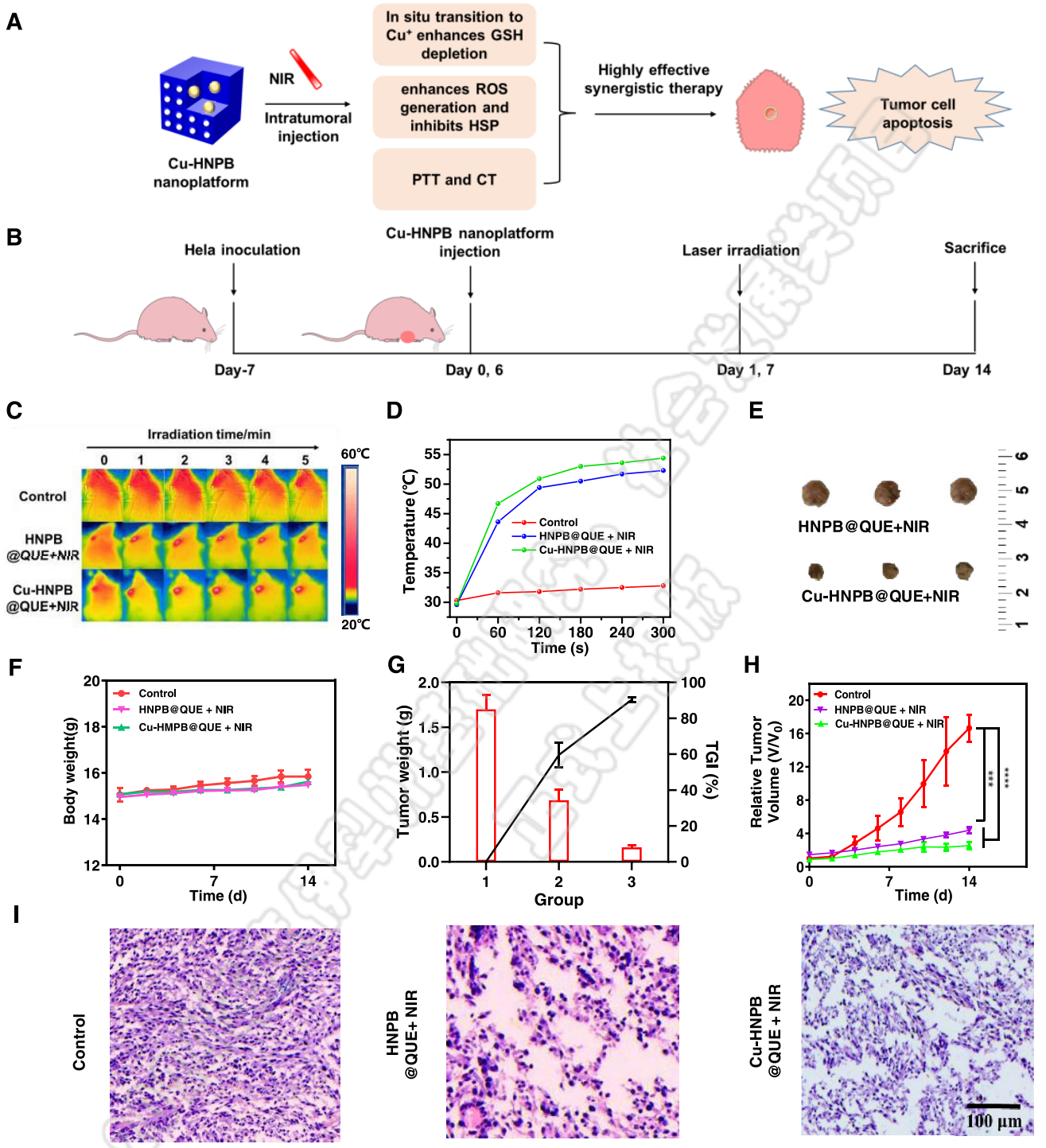

Figure 6. *In vivo* synergistic therapy of Cu-HNPB NCs on the Hela tumor-bearing mice model. (A) Schematic of the synergistic effect of Cu-HNPB nanoplatform. (B). Timeframe of tumor inoculaiton and treatment. (C) Infrared thermography of Hela tumor-bearing mice with an irradiation of 808 nm laser (1 W cm^{-2}) at 12 h after injection with PBS, HNPB@QUE, or Cu-HNPB@QUE. (D) Temperature changes of tumor sites with an irradiation of 808 nm laser (1 W cm^{-2}). (E) Photos of the tumors dissected from each group at the end of treatments (control group not given due to the tumor volume reaching over 2000 mm^3). (F) Changes in body weight of mice with various treatments within 14 days. (G) Final tumor weights of nude mice and tumor growth inhibition in various treatment groups. Groups 1−3 represent control, HNPB@QUE + laser, and Cu-HNPB@QUE + laser. (H) Relative tumor volume changes in various treatment groups during 14 days of treatment. (I) H&E-stained images of tumors with various groups (*p < 0.05; **p < 0.01; ***p < 0.001; ****p < 0.0001).

consistent with the MTT results described above. The Cu-HNPB NC nanoplatform showed excellent tumor cell killing efficiency, of which Cu-HNPB were 53.3% and even higher 70.6% for Cu-HNPB@QUE + NIR (Figure 5F). These findings indicate that Cu hybridization further strengthens the synergistic therapeutic impacts via •OH radical production and GSH depletion.

https://doi.org/10.1021/acsanm.3c00764
ACS Appl. Nano Mater. 2023, 6, 4969−4977

2.3. *In Vivo* Antitumor Efficacy Assay. Inspired by the excellent photothermal performance and chemodynamic properties of Cu-HNPB NCs, we further investigated the combination therapeutic efficiency *in vivo* in Hela tumor-bearing nude mice. The mechanism of synergistic tumor therapy in vivo and the Hela tumor model's establishment and treatment are illustrated in Figure 6A,B. Because of the superior biocompatibility of PB and PB analogues, the negligible effect on tumor growth was produced by NIR laser irradiation alone.[33,39−41] Herein, we only discuss the *in vivo* antitumour efficacy of the combination treatment group. Under NIR laser, HNPB@QUE NCs and Cu-HNPB @QUE NCs show excellent photothermal performance *in vivo* (Figure 6C,D). Figure 6E shows representative treatments and tumor photos of Hela-bearing mice in different groups at the end of the treatment. As expected, tumor growth was faster in mice injected with PBS solution only, while all treatment groups showed remarkable tumor suppression (Figure 6G,H). The tumor growth inhibition (TGI) rate of Cu-HNPB @QUE+NIR groups was 90.3%, which was significantly higher than the HNPB@QUE + NIR group (59.6%) (Figure 6G). Furthermore, hematoxylin and eosin (H&E) staining (Figure 6I) showed the obvious tumor necrosis in all treatment groups. Moreover, the most serious was observed in the Cu-HNPB@QUE+NIR groups, indicating the prominent antitumor effects of Cu-HNPB NCs.

To assess the safety and biocompatibility of the nanoplatform, we comprehensively evaluated their toxicity in mice. First, no significant red color was observed with Cu-HNPB NCs (800 μg mL^{-1}) (Figure S18). The phenomenon suggests that Cu-HNPB NCs do not cause significant hemolysis in the biological environment. Subsequently, we assessed the *in vivo* toxicity of the nanoplatform. There were no apparent differences in blood indexes, implying that the nanoplatform has ignorable toxicity *in vivo* (Figures S19 and S20). The H&E staining of the main organs of mice after different treatments displayed that there were no marked physiological abnormalities compared with the control group (Figure S21). In addition, no noticeable difference in body weight change was observed in the treated mice compared to the control group (Figure 6F), indicating that these synergistic treatment strategies have negligible side effects. Collectively, the Cu-HNPB nanoplatform shows satisfactory safety and excellent synergistic antitumor efficacy.

3. CONCLUSIONS

We precisely constructed Cu-HNPB@QUE NCs for synergistic cancer therapy by utilizing the POD-like activity and Fenton-like reaction mechanism. The outstanding synergistic antitumor efficiency may be attributed to the following aspects: (1) In high levels of GSH, Cu^{2+} conversion to Cu^{+} in situ significantly enhances the Fenton-like reaction, promoting the generation of more •OH radicals, thereby improving CDT efficiency; (2) •OH radical inhibits HSP70 and HSP90 expression and disrupts the thermal protection mechanism of tumor cells, amplifying oxidative stress damage in tumor cells; and (3) in the TME, NIR laser irradiation accelerates the release of QUE, resulting in enhanced synergistic therapeutic effects.

As a result, this mutually beneficial strategy achieved excellent anticancer effects *in vitro* and *in vivo*. In conclusion, this study designs a promising multifunctional nanoplatform, providing novel insights for safe and efficient tumor combination therapy.

■ ASSOCIATED CONTENT

Data Availability Statement

The raw/processed data required to reproduce these findings cannot be shared at this time as the data also forms part of an ongoing study.

Supporting Information

The Supporting Information is available free of charge at https://pubs.acs.org/doi/10.1021/acsanm.3c00764.

Supplementary methods; Supplementary figures (PDF)

■ AUTHOR INFORMATION

Corresponding Author

Zeyidan Jiapaer − *College of Life Science & Technol ogy, Xinjiang University, Xinjiang 830046, China; Xinjiang Key laboratory of Biological Resources and Gentic Engineering, Xinjiang 830046, China*; Email: zeyidan@xju.edu.cn

Authors

Shuxuan Shao − *College of Life Science & Technol ogy, Xinjiang University, Xinjiang 830046, China; Xinjiang Key laboratory of Biological Resources and Gentic Engineering, Xinjiang 830046, China; Molecular Science and Biomedicine Laboratory (MBL), State Key Laboratory of Chemo/Bio-Sensing and Chemometrics, College of Biology, Hunan University Changsha, Hunan 410082, China*

Haoqiang Liu − *College of Life Science & Technol ogy, Xinjiang University, Xinjiang 830046, China; Xinjiang Key laboratory of Biological Resources and Gentic Engineering, Xinjiang 830046, China*

Fanxing Meng − *College of Life Science & Technol ogy, Xinjiang University, Xinjiang 830046, China; Xinjiang Key laboratory of Biological Resources and Gentic Engineering, Xinjiang 830046, China*

Wanfeng Wu − *College of Life Science & Technol ogy, Xinjiang University, Xinjiang 830046, China; Xinjiang Key laboratory of Biological Resources and Gentic Engineering, Xinjiang 830046, China*

Xinbo Li − *College of Life Science & Technol ogy, Xinjiang University, Xinjiang 830046, China; Xinjiang Key laboratory of Biological Resources and Gentic Engineering, Xinjiang 830046, China*

Mengjiao Duan − *College of Life Science & Technol ogy, Xinjiang University, Xinjiang 830046, China; Xinjiang Key laboratory of Biological Resources and Gentic Engineering, Xinjiang 830046, China*

Complete contact information is available at: https://pubs.acs.org/10.1021/acsanm.3c00764

Notes

The authors declare no competing financial interest.

■ ACKNOWLEDGMENTS

This work was supported by the Tianshan Youth Foundation of Xinjiang (2019Q066).

■ REFERENCES

(1) Holohan, C.; Van Schaeybroeck, S.; Longley, D. B.; Johnston, P. G. Cancer Drug Resistance: An Evolving Paradigm. *Nat. Rev. Cancer* **2013**, *13*, 714−726.

(2) Peer, D.; Karp, J. M.; Hong, S.; Farokhzad, O. C.; Margalit, R.; Langer, R. Nanocarriers as an Emerging Platform for Cancer Therapy. *Nat. Nanotechnol.* **2007**, *2*, 751−760.

(3) Schirrmacher, V. From Chemotherapy to Biological Therapy: A Review of Novel Concepts to Reduce the Side Effects of Systemic Cancer Treatment (Review). *Int. J. Oncol.* **2019**, *54*, 407−419.
(4) Vega-Villa, K. R.; Takemoto, J. K.; Yáñez, J. A.; Remsberg, C. M.; Forrest, M. L.; Davies, N. M. Clinical Toxicities of Nanocarrier Systems. *Adv. Drug Delivery Rev.* **2008**, *60*, 929−938.
(5) Hossen, S.; Hossain, M. K.; Basher, M. K.; Mia, M. N. H.; Rahman, M. T.; Uddin, M. J. Smart Nanocarrier-Based Drug Delivery Systems for Cancer Therapy and Toxicity Studies: A Review. *J. Adv. Res.* **2019**, *15*, 1−18.
(6) Mitchell, M. J.; Billingsley, M. M.; Haley, R. M.; Wechsler, M. E.; Peppas, N. A.; Langer, R. Engineering Precision Nanoparticles for Drug Delivery. *Nat. Rev. Drug Discovery* **2021**, *20*, 101−124.
(7) Liu, G.; Zhu, J.; Guo, H.; Sun, A.; Chen, P.; Xi, L.; Huang, W.; Song, X.; Dong, X. Mo_2C-Derived Polyoxometalate for NIR-II Photoacoustic Imaging-Guided Chemodynamic/Photothermal Synergistic Therapy. *Angew. Chem., Int. Ed.* **2019**, *58*, 18641−18646.
(8) Gao, S.; Li, T.; Guo, Y.; Sun, C.; Xianyu, B.; Xu, H. Selenium-Containing Nanoparticles Combine the NK Cells Mediated Immunotherapy with Radiotherapy and Chemotherapy. *Adv. Mater.* **2020**, *32*, No. 1907568.
(9) Yu, Y.; Tang, D.; Liu, C.; Zhang, Q.; Tang, L.; Lu, Y.; Xiao, H. Biodegradable Polymer with Effective Near-Infrared-II Absorption as a Photothermal Agent for Deep Tumor Therapy. *Adv. Mater.* **2022**, *34*, No. 2105976.
(10) Nam, J.; Son, S.; Park, K. S.; Zou, W.; Shea, L. D.; Moon, J. J. Cancer Nanomedicine for Combination Cancer Immunotherapy. *Nat. Rev. Mater.* **2019**, *4*, 398−414.
(11) Sang, W.; Zhang, Z.; Dai, Y.; Chen, X. Recent Advances in Nanomaterial-Based Synergistic Combination Cancer Immunotherapy. *Chem. Soc. Rev.* **2019**, *48*, 3771−3810.
(12) Shokouhimehr, M.; Soehnlen, E. S.; Khitrin, A.; Basu, S.; Huang, S. D. Biocompatible Prussian Blue Nanoparticles: Preparation, Stability, Cytotoxicity, and Potential Use as an MRI Contrast Agent. *Inorg. Chem. Commun.* **2010**, *13*, 58−61.
(13) Liu, B.; Wang, W.; Fan, J.; Long, Y.; Xiao, F.; Daniyal, M.; Tong, C.; Xie, Q.; Jian, Y.; Li, B.; Ma, X.; Wang, W. RBC Membrane Camouflaged Prussian Blue Nanoparticles for Gamabutolin Loading and Combined Chemo/Photothermal Therapy of Breast Cancer. *Biomaterials* **2019**, *217*, No. 119301.
(14) Schultz, A. M.; Salvador, P. A.; Rohrer, G. S. Enhanced Photochemical Activity of α-Fe_2O_3 Films Supported on $SrTiO_3$ Substrates under Visible Light Illumination. *Chem. Commun.* **2012**, *48*, 2012−2014.
(15) Qin, Z.; Li, Y.; Gu, N. Progress in Applications of Prussian Blue Nanoparticles in Biomedicine. *Adv. Healthcare Mater.* **2018**, *7*, No. 1800347.
(16) Zhang, X.-Q.; Gong, S.; Zhang, Y.; Yang, T.; Wang, C.; Gu, N. Prussian Blue Modified Iron Oxide Magnetic Nanoparticles and Their High Peroxidase-like Activity. *J. Mater. Chem.* **2010**, *20*, 5110−5116.
(17) Chen, W.; Zeng, K.; Liu, H.; Ouyang, J.; Wang, L.; Liu, Y.; Wang, H.; Deng, L.; Liu, Y. N. Cell Membrane Camouflaged Hollow Prussian Blue Nanoparticles for Synergistic Photothermal-/Chemotherapy of Cancer. *Adv. Funct. Mater.* **2017**, *27*, No. 1605795.
(18) Nayebi, B.; Niavol, K. P.; Nayebi, B.; Kim, S. Y.; Nam, K. T.; Jang, H. W.; Varma, R. S.; Shokouhimehr, M. Prussian Blue-Based Nanostructured Materials: Catalytic Applications for Environmental Remediation and Energy Conversion. *Mol. Catal.* **2021**, *514*, No. 111835.
(19) Chen, J.; Wang, Q.; Huang, L.; Zhang, H.; Rong, K.; Zhang, H.; Dong, S. Prussian Blue with Intrinsic Heme-like Structure as Peroxidase Mimic. *Nano Res.* **2018**, *11*, 4905−4913.
(20) Kim, H.-E.; Nguyen, T. T. M.; Lee, H.; Lee, C. Enhanced Inactivation of Escherichia Coli and MS2 Coliphage by Cupric Ion in the Presence of Hydroxylamine: Dual Microbicidal Effects. *Environ. Sci. Technol.* **2015**, *49*, 14416−14423.
(21) Lee, H.; Seong, J.; Lee, K.-M.; Kim, H.-H.; Choi, J.; Kim, J.-H.; Lee, C. Chloride-Enhanced Oxidation of Organic Contaminants by Cu(II)-Catalyzed Fenton-like Reaction at Neutral PH. *J. Hazard. Mater.* **2018**, *344*, 1174−1180.
(22) Xiong, Y.; Xiao, C.; Li, Z.; Yang, X. Engineering Nanomedicine for Glutathione Depletion-Augmented Cancer Therapy. *Chem. Soc. Rev.* **2021**, *50*, 6013−6041.
(23) Lu, J.; Jiang, Z.; Ren, J.; Zhang, W.; Li, P.; Chen, Z.; Zhang, W.; Wang, H.; Tang, B. One-Pot Synthesis of Multifunctional Carbon-Based Nanoparticle-Supported Dispersed Cu^{2+} Disrupts Redox Homeostasis to Enhance CDT. *Angew. Chem., Int. Ed.* **2022**, *61*, No. e202114373.
(24) Sun, S.; Chen, Q.; Tang, Z.; Liu, C.; Li, Z.; Wu, A.; Lin, H. Tumor Microenvironment Stimuli-Responsive Fluorescence Imaging and Synergistic Cancer Therapy by Carbon-Dot−Cu^{2+} Nanoassemblies. *Angew. Chem., Int. Ed.* **2020**, *59*, 21041−21048.
(25) Zeng, F.; Tang, L.; Zhang, Q.; Shi, C.; Huang, Z.; Nijiati, S.; Chen, X.; Zhou, Z. Coordinating the Mechanisms of Action of Ferroptosis and the Photothermal Effect for Cancer Theranostics. *Angew. Chem., Int. Ed.* **2022**, *61*, No. e202112925.
(26) Wang, P.; Kankala, R. K.; Chen, B.; Zhang, Y.; Zhu, M.; Li, X.; Long, R.; Yang, D.; Krastev, R.; Wang, S.; Xiong, X.; Liu, Y. Cancer Cytomembrane-Cloaked Prussian Blue Nanoparticles Enhance the Efficacy of Mild-Temperature Photothermal Therapy by Disrupting Mitochondrial Functions of Cancer Cells. *ACS Appl. Mater. Interfaces* **2021**, *13*, 37563−37577.
(27) Wu, C.; Liu, Z.; Chen, Z.; Xu, D.; Chen, L.; Lin, H.; Shi, J. A Nonferrous Ferroptosis-like Strategy for Antioxidant Inhibition−Synergized Nanocatalytic Tumor Therapeutics. *Sci. Adv.* **2022**, *7*, No. eabj8833.
(28) Wang, W.; Sun, C.; Mao, L.; Ma, P.; Liu, F.; Yang, J.; Gao, Y. The Biological Activities, Chemical Stability, Metabolism and Delivery Systems of Quercetin: A Review. *Trends Food Sci. Technol.* **2016**, *56*, 21−38.
(29) Srivastava, S.; Somasagara, R. R.; Hegde, M.; Nishana, M.; Tadi, S. K.; Srivastava, M.; Choudhary, B.; Raghavan, S. C. Quercetin, a Natural Flavonoid Interacts with DNA, Arrests Cell Cycle and Causes Tumor Regression by Activating Mitochondrial Pathway of Apoptosis. *Sci. Rep.* **2016**, *6*, No. 24049.
(30) Hong, Y.; Lee, J.; Moon, H.; Ryu, C. H.; Seok, J.; Jung, Y.-S.; Ryu, J.; Baek, S. J. Quercetin Induces Anticancer Activity by Upregulating Pro-NAG-1/GDF15 in Differentiated Thyroid Cancer Cells. *Cancers* **2021**, *13*, 3022.
(31) Kandemir, K.; Tomas, M.; McClements, D. J.; Capanoglu, E. Recent Advances on the Improvement of Quercetin Bioavailability. *Trends Food Sci. Technol.* **2022**, *119*, 192−200.
(32) Hu, M.; Furukawa, S.; Ohtani, R.; Sukegawa, H.; Nemoto, Y.; Reboul, J.; Kitagawa, S.; Yamauchi, Y. Synthesis of Prussian Blue Nanoparticles with a Hollow Interior by Controlled Chemical Etching. *Angew. Chem., Int. Ed.* **2012**, *51*, 984−988.
(33) Wu, W.; Yu, L.; Pu, Y.; Yao, H.; Chen, Y.; Shi, J. Copper-Enriched Prussian Blue Nanomedicine for In Situ Disulfiram Toxification and Photothermal Antitumor Amplification. *Adv. Mater.* **2020**, *32*, No. 2000542.
(34) Song, G.; Hao, J.; Liang, C.; Liu, T.; Gao, M.; Cheng, L.; Hu, J.; Liu, Z. Degradable Molybdenum Oxide Nanosheets with Rapid Clearance and Efficient Tumor Homing Capabilities as a Therapeutic Nanoplatform. *Angew. Chem., Int. Ed.* **2016**, *55*, 2122−2126.
(35) Feng, L.; Li, K.; Shi, X.; Gao, M.; Liu, J.; Liu, Z. Smart PH-Responsive Nanocarriers Based on Nano-Graphene Oxide for Combined Chemo- and Photothermal Therapy Overcoming Drug Resistance. *Adv. Healthcare Mater.* **2014**, *3*, 1261−1271.
(36) Jiang, W.; Zhang, H.; Wu, J.; Zhai, G.; Li, Z.; Luan, Y.; Garg, S. CuS@MOF-Based Well-Designed Quercetin Delivery System for Chemo−Photothermal Therapy. *ACS Appl. Mater. Interfaces* **2018**, *10*, 34513−34523.
(37) Wu, J.; Liu, T.; Rios, Z.; Mei, Q.; Lin, X.; Cao, S. Heat Shock Proteins and Cancer. *Trends Pharmacol. Sci.* **2017**, *38*, 226−256.
(38) Shan, Q.; Ma, F.; Wei, J.; Li, H.; Ma, H.; Sun, P. Physiological Functions of Heat Shock Proteins. *Curr. Protein Pept. Sci.* **2020**, *21*, 751−760.

https://doi.org/10.1021/acsanm.3c00764
ACS Appl. Nano Mater. 2023, 6, 4969−4977

(39) Lu, L.; Zhang, C.; Zou, B.; Wang, Y. Hollow Prussian Blue Nanospheres for Photothermal/Chemo-Synergistic Therapy. *Int. J. Nanomed.* **2020**, *15*, 5165−5177.
(40) Mukherjee, S.; Rao, B. R.; Sreedhar, B.; Paik, P.; Patra, C. R. Copper Prussian Blue Analogue: Investigation into Multifunctional Activities for Biomedical Applications. *Chem. Commun.* **2015**, *51*, 7325−7328.
(41) Chen, W.; Ouyang, J.; Liu, H.; Chen, M.; Zeng, K.; Sheng, J.; Liu, Z.; Han, Y.; Wang, L.; Li, J.; Deng, L.; Liu, Y.-N.; Guo, S. Black Phosphorus Nanosheet-Based Drug Delivery System for Synergistic Photodynamic/Photothermal/Chemotherapy of Cancer. *Adv. Mater.* **2017**, *29*, No. 1603864.

Received: 18 February 2022 | Revised: 3 May 2022 | Accepted: 2 June 2022

DOI: 10.1111/acel.13657

Aging Cell WILEY

REVIEW ARTICLE

Regulation and roles of RNA modifications in aging-related diseases

Zeyidan Jiapaer[1,2] | Dingwen Su[3] | Lingyang Hua[4] | Helge Immo Lehmann[5] | Priyanka Gokulnath[5] | Gururaja Vulugundam[6] | Shannan Song[1,2] | Lingying Zhang[1,2] | Ye Gong[4] | Guoping Li[5]

[1]College of Life Science & Technology, Xinjiang University, Urumqi, China

[2]Xinjiang Key laboratory of Biological Resources and Genetic Engineering, Urumqi, China

[3]Friedrich Miescher Laboratory of the Max Planck Society, Tübingen, Germany

[4]Department of Neurosurgery, Huashan Hospital, Shanghai Medical College, Fudan University, Shanghai, China

[5]Cardiovascular Research Center, Massachusetts General Hospital and Harvard Medical School, Boston, MA, USA

[6]Institute of Biochemistry and Cellular Biology, National Research Council of Italy, Naples, Italy

Correspondence
Ye Gong, Department of Neurosurgery, Huashan Hospital, Shanghai Medical College, Fudan University, Shanghai, China.
Email: gong_ye@fudan.edu.cn

Guoping Li, Cardiovascular Research Center, Massachusetts General Hospital and Harvard Medical School, Boston, Massachusetts, USA.
Email: gli21@mgh.harvard.edu

Funding information
National Natural Science Foundation of China, Grant/Award Number: 81900287 and 82072788

Abstract

With the aging of the global population, accumulating interest is focused on manipulating the fundamental aging-related signaling pathways to delay the physiological aging process and eventually slow or prevent the appearance or severity of multiple aging-related diseases. Recently, emerging evidence has shown that RNA modifications, which were historically considered infrastructural features of cellular RNAs, are dynamically regulated across most of the RNA species in cells and thereby critically involved in major biological processes, including cellular senescence and aging. In this review, we summarize the current knowledge about RNA modifications and provide a catalog of RNA modifications on different RNA species, including mRNAs, miRNAs, lncRNA, tRNAs, and rRNAs. Most importantly, we focus on the regulation and roles of these RNA modifications in aging-related diseases, including neurodegenerative diseases, cardiovascular diseases, cataracts, osteoporosis, and fertility decline. This would be an important step toward a better understanding of fundamental aging mechanisms and thereby facilitating the development of novel diagnostics and therapeutics for aging-related diseases.

Abbreviations: 2′-OMe, 2′-O-methylation; 3′UTR, 3′ untranslated regions; AD, Alzheimer's disease; ADAR, adenosine deaminases acting on the RNA; ALS, amyotrophic lateral sclerosis; A-to-I editing, adenosine to inosine RNA editing; BS-seq, bisulfite sequencing; CHAPIR, cardiac-hypertrophy-associated piRNA; Cm, 2′-O-methylcytidine; CTSS, Cathepsin S; DART-seq, deamination adjacent to RNA modification targets sequencing; DKC1, dyskerin; Ψ, pseudouridine; FTO, alpha-ketoglutarate-dependent dioxygenase FTO; LECs, lens epithelium cells; LC, liquid chromatography; m1A, N1-methyladenosine; m1G, 1-methyl-guanosine; m2,2,7G, N2, N2, 7-trimethylguanosine; m5C, 5-Methylcytosine; m6A, N6 methylation of adenosine; m6A-SAC-seq, m6A selective allyl chemical labeling and sequencing; m6A-SNPs, m6A-associated single-nucleotide polymorphisms; m7G, 7-methylguanosine; m7G-MaP-seq, m7G mutational profiling sequencing; METTL3, methyltransferase-like 3; MS, mass spectrum; pri-miRNAs, primary microRNAs; PD, Parkinson's disease; PUS, pseudouridine synthases; Q/R, glutamine/arginine; snoRNAs, small nucleolar RNAs; SNPs, single nucleotide polymorphisms; TAC, transverse aortic constriction; UPR, unfolded protein response; YTHDF1, YTH domain-containing family protein 1.

Zeyidan Jiapaer, Dingwen Su and Lingyang Hua authors contribute equally to this work.

KEYWORDS
aging, aging-related disease, epitranscriptome, RNA modification

1 | INTRODUCTION

Aging is a natural gradually occurring process of progressive decline in an organism's physiological and psychological adaptability to the environment, culminating in its death. Molecular hallmarks of aging include genomic instability, telomere attrition, epigenetic alterations, loss of proteostasis, deregulated nutrient sensing, mitochondrial dysfunction, cellular senescence, stem cell exhaustion, and altered intercellular communication. In humans, aging can be correlated to increased risks of multiple diseases such as neurodegenerative diseases, cardiovascular diseases, osteoporosis, metabolic dysfunction, defective tissue repair and regeneration, decreased regulation of gut microbes, and cataracts (Cui et al., 2017; Lopez-Otin et al., 2013). Accumulating studies on aging have revealed that aging phenotypes and aging-related diseases usually result from the complicated interaction between an external environmental stimulus and internal gene expression regulation. Concerning epigenetically regulated gene expression in aging, though most attention has been given to transcriptional alterations, such as DNA methylation patterns, histone modifications, and chromatin remodeling, post-transcriptional regulators, in particular RNA modifications, have been previously underestimated due to the lack of relevant tools to investigate them (Saul & Kosinsky, 2021). One of the first hints in this direction was speculated by a study analyzing the transcriptomes of young and aging mouse livers, which showed that differentially expressed genes in the aging mice liver were significantly enriched in RNA modification-related pathways (White et al., 2015).

RNA modifications play a critical role in nearly every aspect of the biological process, ranging from early embryo development until aging (Mendel et al., 2018). The existence of modified RNA bases was firstly discovered via enzymatic digestion and electrophoresis in the early 1960s and 1970s (Lavi et al., 1977). Thin-layer chromatography, high-performance liquid chromatography (LC), and mass spectrum (MS) were then utilized to determine and detect RNA nucleobase modification based on the differences in the biophysical and biochemical properties between the modified and unmodified bases such as molecular mass, net charge, polarity, and hydrophobicity (Delatte et al., 2016; Jia et al., 2011; Shen et al., 2019). Although these methods are less quantitative, not high-throughput, and may miss the specific RNA context for a modification in some cases, they have expanded the world of RNA modifications. Recently, the next-generation sequencing-based methods with or without using RNA modification specific antibodies, such as m6A-seq, m6A-selective allyl chemical labeling and sequencing (m6A-SAC-seq), deamination adjacent to RNA modification targets (DART-seq), 7-methylguanosine mutational profiling sequencing (m7G-MaP-seq), bisulfite sequencing (BS-seq), and comparative Nanopore direct RNA sequencing, have been developed to probe the specific RNA modification in the whole transcriptome at single-base resolutions (Enroth et al., 2019; Helm & Motorin, 2017; Hu et al., 2022; Leger et al., 2021; Li et al., 2017; Meyer, 2019). Owing to the great advent of methods to detect them qualitatively and quantitatively, hundreds of RNA modifications have now been identified in mammalian cells and all known RNA species, including mRNA, miRNA, tRNA, rRNA, lncRNA, and other non-coding RNAs (Frye et al., 2016), further boosting the epitranscritome studies and suggesting their exigent biological functions. RNA modifications have been reported to critically contribute to nuclear export, translation initiation, transcript stability, splicing, folding, and localization (Roundtree et al., 2017). Along with the discoveries of RNA modifications, some enzymes that are responsible for writing, reading, and erasing these RNA modifications have also been identified (Kumar & Mohapatra, 2021). RNA modifications and corresponding modifying enzymes are gaining increasing attention due to their pivotal roles in numerous human diseases, such as obesity, diabetes, neurodegenerative diseases, multiple types of cancer, and even viral infections (Chatterjee et al., 2021; Zhang et al., 2021; Zhou et al., 2020). Many of these linkages arise from mutations and/or single nucleotide polymorphisms (SNPs) in RNA modification-related genes and pathways.

The biochemical aspects of RNA modifications have been extensively reviewed elsewhere (Harcourt et al., 2017). Here, we will introduce the biogenesis and molecular functions of the relatively well-studied RNA modifications in different RNA species. Further, we will focus on the regulation and roles of RNA modifications in aging-related diseases, including neurodegenerative diseases, cardiovascular diseases, cataracts, osteoporosis, and fertility decline.

2 | RNA MODIFICATIONS

2.1 | Modifications on mRNA

The recent discovery of reversible mRNA chemical modifications has opened a new era of post-transcriptional gene regulation in living organisms. Apart from the 5′ cap and 3'poly(A) tail in mature eukaryotic mRNAs, more than 100 distinct chemical modifications have been found to actively regulate mRNA behaviors, including differentially processing, splicing, translation, and decay (Boccaletto et al., 2022). Here, we will only focus on the main modifications that are reported to be critically involved in the regulation of mRNA functions (Figure 1).

2.1.1 | N6 methylation of adenosine (m6A)

The modification of m6A was first identified in 1970s (Dubin & Taylor, 1975). With the advances in identifying and quantifying

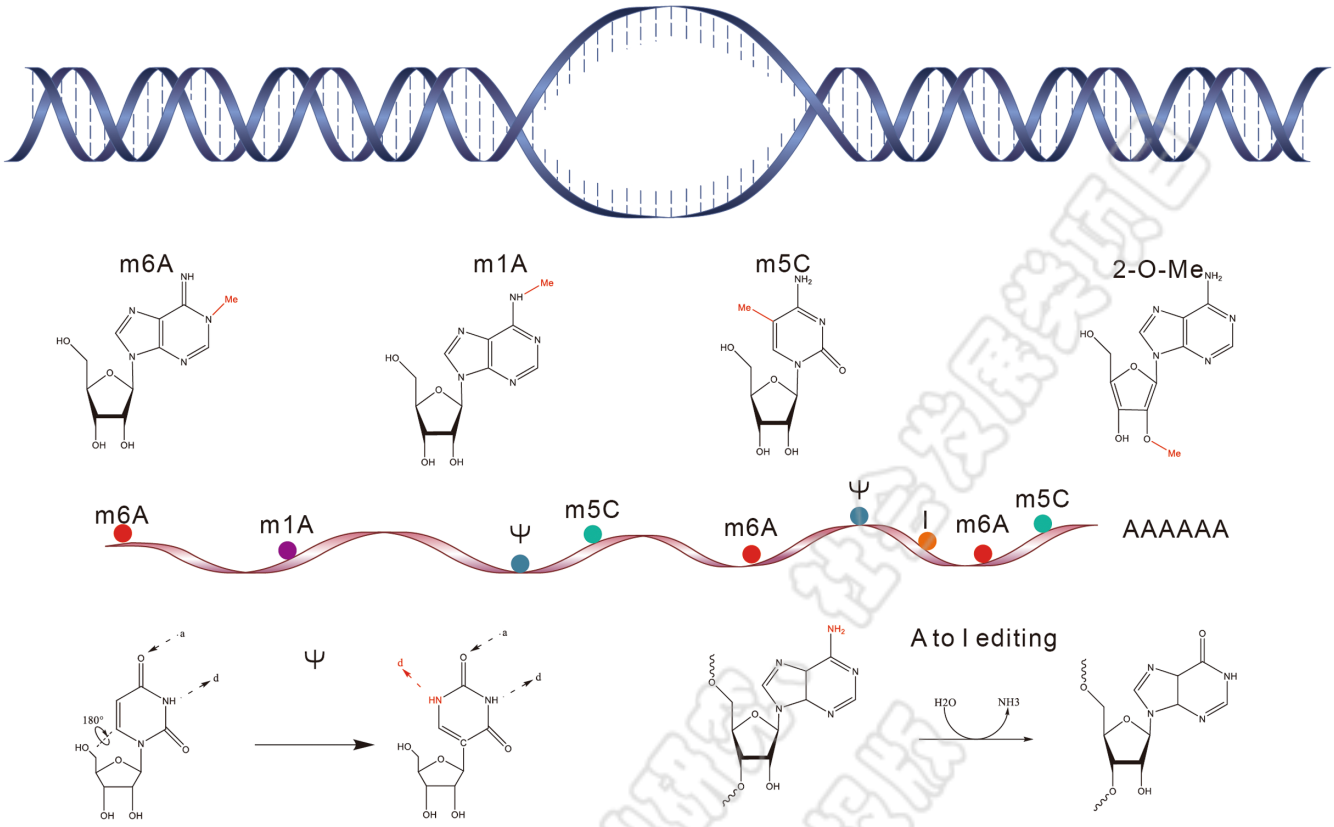

FIGURE 1 Chemical modifications in mRNA

m6A in the transcriptome at single-base resolution (Hu et al., 2022; Linder et al., 2015), m6A becomes the best-characterized and most abundant internal RNA modification with about 0.2%–0.6% of adenosines having m6A in mammalian mRNAs (Molinie et al., 2016). The transcriptome-wide m6A distribution in mice and humans revealed that m6A is enriched in the coding region and 3′ untranslated regions (3' UTR), with a significant enrichment near the stop codon (Dominissini et al., 2012; Meyer et al., 2012). m6A modification is catalyzed by METTL3-METTL14 complex and their cofactors, such as METTL16, ZCCHC4, RBM15, ZC3H13, VIRMA, CBLL1, and WTAP (Knuckles & Buhler, 2018; Liu et al., 2014; Warda et al., 2017; Wen et al., 2018; Yue et al., 2018). YTHDF1, YTHDF2, IGF2BP1, IGF2BP2, and IGF2BP3 are characterized as reader proteins that recognize the m6A methylation. Two prominent demethylation enzymes are FTO and ALKBH5. Functionally, m6A is involved in almost every step in the mRNA life cycle, from splicing and processing in the nucleus to translation and decay in the cytoplasm (Zhao et al., 2017). At the cellular level, m6A plays a critical role in cellular identity transition between distinct states during differentiation or stress response via influencing the transcriptome output (Zhao et al., 2017).

2.1.2 | N1 methylation of adenosine (m1A)

m1A is the methylation of the N1 position of adenosine which was identified in 1961 in tRNA and rRNA (Dunn, 1961). Recently, its presence in eukaryotic mRNA has been demonstrated and its transcriptome-wide distribution has also been mapped via high-throughput methods (Dominissini et al., 2016; Li et al., 2016). m1A is highly enriched around the start codon within the 5'UTR and is preferentially located in highly structured areas (Dominissini et al., 2016; Li et al., 2016). A recent study showed that the presence of m1A blocks reduces RNA base-pairing and induces local RNA duplex melting (Zhou et al., 2016). m1A has been shown to promote translation (Dominissini et al., 2016; Li et al., 2016), although the detailed molecular mechanism is not clear. The only known methyltransferase catalyzing m1A on mRNA is the TRMT6–TRMT61 complex (Safra et al., 2017). It has been reported that YTHDF2 is not only the reader of m6A but also can bind with low affinity to m1A, which suggests its potential role as an m1A reader in cells (Dai et al., 2018). Moreover, the known erasers of m1A in mRNA are ALKBH1 and ALKBH3 (Aas et al., 2003; Liu et al., 2016).

2.1.3 | 7-Methylguanosine (m7G)

m7G is a positively charged RNA modification that is modified by the addition of the 7-methylguanosine "cap" added to the first transcribed nucleotide, which is necessary for the translation of the majority of mRNAs (Cowling, 2009). RNMT is the first identified cap methyltransferase catalyse (Trotman et al., 2017). The reader and eraser proteins are yet to be identified.

2.1.4 | 2'O-methylation (2'-OMe)

2'-OMe is one of the classical RNA modifications wherein 2′ hydroxyl (–OH) groups have been added to the ribose. The 2'-OMe modification was first demonstrated in bacterial mRNA to affect translation efficiency (Hoernes et al., 2016). 2'-OMe can be added on the N1 (first transcribed nucleotide, m7GpppNmN-) and also on the N2 (second transcribed nucleotide, m7GpppNmNm-), respectively. CMTR1 may act as 2'-O-methyltransferase that modifies the N1 of the mRNA cap (Belanger et al., 2010). There is a need to develop highly sensitive and quantitative methods to gather more information regarding this modification.

2.1.5 | 5-Methylcytosine (m5C)

m5C is the most common modification of mRNA where methylation occurs at the 5th position of cytosine and was first reported in 1975. This modification is similar to DNA methylation m5C except for the ribose. NSUN2 is associated with this mRNA modification. The m5C modification could also be recognized by the mRNA export adaptor protein ALYREFRNA (Bohnsack et al., 2019; Yang et al., 2017), while the exact methyltransferase(s) responsible for m5C modifications in mRNAs is yet to be identified.

2.1.6 | Pseudouridine

Pseudouridine, or isomerization of uridine, also known as 5-ribosyl uracil and Ψ, was first discovered in 1957. This was initially identified as the fifth base in RNA due to its high abundance in cellular RNA. This modification in mRNA is partially attributed to several tRNA and rRNA pseudouridine synthases (PUS) conserved across eukaryotes (Eyler et al., 2019). Further biochemical research and understanding of Ψ in mRNAs are required. Due to its low abundance in mRNA, this modification has not been studied properly until recent technological advances such as the establishment of PseudoU-seq. This results from the post-transcriptional isomerization reaction of uridine (1-ribosyl uracil), which makes pseudouridine carry distinct chemical and biophysical properties compared with uridine. This rigidifies both single-stranded and duplex RNA locally, and thus restricts their flexibility. Expectedly, pseudouridine can affect the secondary structure of mRNA. This modification can have a substantial impact on the translation process and the outcome of translation especially when it occurs in the stop codons or nonsense codons, given that all stop codons start with U at the first base. Ψ-containing codons have been shown to be able to modestly affect the ribosomes, incorporating certain amino acids and Ψ-containing stop codons that have been observed to direct the nonsense suppression of translation termination (Eyler et al., 2019; Fernandez et al., 2013; Karijolich & Yu, 2011).

2.1.7 | Adenosine to inosine RNA editing (A-to-I editing)

Like RNA modification, A-to-I editing is a common event in the transcriptome. This conversion is catalyzed by adenosine deaminases acting on the RNA (ADAR) family of enzymes on both intermolecular and intramolecular double-stranded RNAs longer than 20 bp. Mammals have 3 ADAR enzymes, ADAR1 and ADAR2 being catalytically active while ADAR3 lacks catalytic activity. Considering both coding and non-coding transcripts, tens of thousands of A-to-I editing sites have been identified in mice and millions have been identified in humans. A-to-I editing levels vary across transcripts, tissues, and throughout development ranging from 1 to 100 percent at any given site (Porath et al., 2017; Tan et al., 2017).

Compared with adenosine, inosine has distinct thermodynamic base-pairing properties that could lead to possible alterations in the secondary structure and encoded information. Inosine can base pair with any natural bases with a preference toward C. Thus, A-to-I editing may directly change the amino acid sequence of the translated protein, which could have a global impact on the cells, depending upon the function of the protein. This editing can affect RNA splicing in eukaryotes if the A to I conversion happens at RNA splicing sites. Moreover, editing can affect the miRNA binding sites that regulate mRNA degradation and modulate mRNA abundance (Brummer et al., 2017; Nishikura, 2016). This modification is shown to have a significant contribution and relevance to neural development and neural diseases. For instance, protein-coding sequences of glutamate receptor GRIA2 and serotonin receptor HTR2C, are edited leading to striking alterations of protein functions (Chalk et al., 2019).

2.2 | RNA modifications on non-coding RNAs

In the last decades, after the discovery of the first noninfrastructural non-coding RNA molecules lin-4 in 1993 (Lee et al., 1993), an explosion of studies has suggested the critical functions of non-coding RNAs in various biological processes and human diseases. Although the regulatory modifications that control non-coding RNA transcription at the genomic level were well established, the chemical modifications at the RNA level that control the function of non-coding RNAs, have only recently begun to emerge (Figure 2).

2.2.1 | Modifications on miRNAs

miRNAs are small single-stranded non-coding RNAs (20 nt ~ 22 nt) that suppress gene expression post-transcriptionally. Emerging evidence shows that they harbor multiple RNA modifications, which are catalyzed by the same enzymes as other RNA species. These modifications regulate their biogenesis, stability, and base-pairing

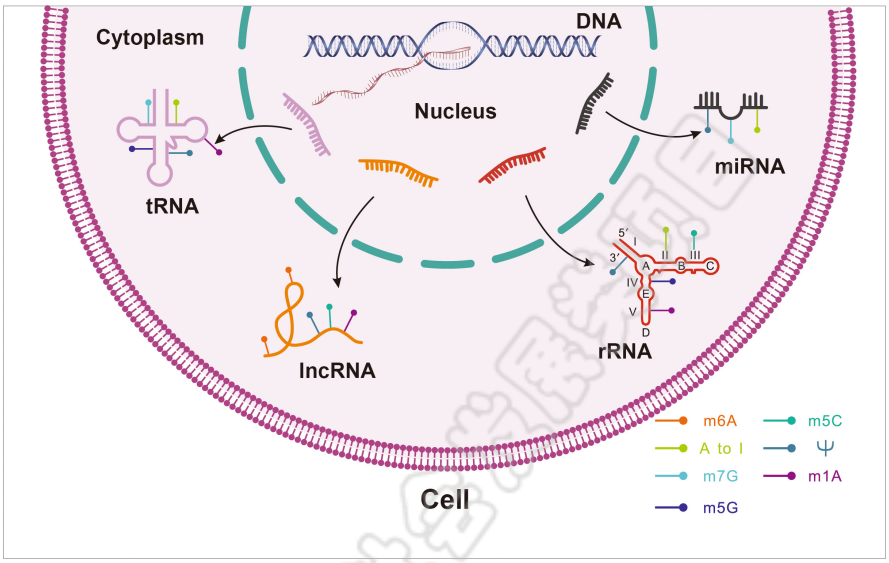

FIGURE 2 Classical RNA modification types in non-coding RNAs

with targets. After transcription, the biogenesis of microRNAs starts with the processing of primary microRNAs (pri-miRNAs) by the microprocessor complex formed by RNA-binding protein DGCR8 and the type III RNase DROSHA. In 2015, Alarcon et al. discovered that in mammalian cells, METTL3 methylates pri-miRNAs and marks them for recognition and processing by DGCR8, promoting miRNA maturation. Another methylation modification, "internal m7G," catalyzed by METTL1, has been found to occur on pri-miRNA and affects precursor-miRNA processing. Notably, precursor-miRNA is a double-stranded RNA specie, making them potential substrates for adenosine deaminases acting on RNA (ADAR) enzymes. As miRNA's function is dependent on their base pairing with the target mRNA, A-to-I editing in miRNAs may modulate their target specificity, resulting in decreased suppressing efficiency of one or more downstream target genes. Other modifications such as m5C and pseudouridine can also affect the binding of miRNAs to targets (De Paolis et al., 2021; Han et al., 2021; Zhang et al., 2016).

2.2.2 | Modifications on lncRNAs

Long non-coding RNAs or lncRNA are defined as transcripts longer than 200 nucleotides and not translated into functional proteins. Various functions and the importance of lncRNAs are getting recognized with the advancement of techniques such as next generation sequencing and exponential growth in our understanding of the genome. Depending upon the cellular localization and specific interactions with DNA, RNA, and proteins, lncRNAs can change the stability and translation of cytoplasmic mRNAs, modulate chromatin function, regulate and/or be involved in the assembly of certain complexes, interfere with signaling pathways (Statello et al., 2021). In contrast, their chemical modifications have not been well explored. MALAT-1, XIST, and HOX are some of the relatively well-studied examples of RNA modifications in lncRNAs. High-throughput methods revealed that in humans both m6A and m5C were mapped to lncRNAs (Squires et al., 2012). WTAP and METTL16, components of the m6A "writer" complexes can interact with certain lncRNAs whereas methyltransferases of the m5C modification in lncRNAs are not very clear (Dinescu et al., 2019). The tRNA m5C methyltransferase NSUN2 has been identified as the writer responsible for m5C methylation in several lncRNAs (Hussain et al., 2013; Khoddami & Cairns, 2013). Another methylation modification is the m1A, despite its proof of existence in lncRNAs, the specific writers are yet to be identified. Apart from methylation, ψ also occurs in lncRNA and is also catalyzed by PUS.

2.2.3 | Modifications on tRNAs

Transfer RNA species have a typical and distinctive cloverleaf secondary structure (Holley et al., 1965). Unlike mRNAs, tRNAs do not encode proteins but are the direct decoder of codons in mRNAs. They are the connecting link between coding information in nucleotides and amino acids in translated proteins. They are the most heavily modified RNA molecules in terms of quantity and diversity. About 1 out of 5 nucleotides are modified in mammalian tRNAs. Recent studies have shown the importance of RNA modifications at certain positions for tRNA function in key developmental processes. Notably, in animal cells, there are two sets of tRNAs, cytoplasmic tRNAs transcribed from the nuclear genome and the mitochondrial tRNAs transcribed from the mitochondrial genome. In some cases, modifications on different sets of tRNAs are carried out by different enzymes. On the contrary, the same type of modifications on different tRNA species will have different downstream targets and biological effects. A huge variety of RNA modifications have been found on tRNAs, such as N2-methylguanosine (m2G), N2,N2-dimethylguanosine (m22G), 1-methyl-guanosine (m1G), N4-acetylcytidine (ac4C), m1A, dihydrouridine, 3-(3-amino-3-carboxypropyl)uridine (acp3U), 3-methylcytidine (m3C), inosine, 1-methyl-inosine, 5-methoxycarbonylmethyluridine (mcm5U), 5-methoxycarb

onylmethyl-2-thiouridine (mcm5s2U), queuosine, galactosyl-queuosine (gal Q), mannosyl-queuosine (manQ), 5-formyl-20 -O-methylcytidine (f5Cm), N6-threonylcarbamoyladenosine (t6A), 2-methylthio- N6-threonylcarbamoyladenosine (ms2t6A), N6-methyl-N6-threonylcarbamoyladenosine (m6t6A), N6-isopentenyladenosine(i6A), peroxywybutosine (o2yW), wybutosine (yW), 1-methylpseudouridine (m1J), 20-O-methylpseudouridine (Jm), m7G, m5C, 2-methyladenosine (2 mA), and 5-methyluridine (5 mU) (de Crecy-Lagard et al., 2019; Juhling et al., 2009). All these modifications can be grouped based on their location, into 2 major types—modifications in the anti-codon loop, especially at the wobble position, and modifications outside the anticodon loop. For modifications within the anti-codon loop, RNA modifications can directly affect the decoding of the codons into amino acids by affecting the base pairing of the codon in mRNAs and tRNA-carrying amino acids (Suzuki, 2021). For modifications outside of the loop, they are most likely to influence the secondary structure of tRNAs.

2.2.4 | Modifications on rRNAs

Like tRNAs, rRNAs are non-coding but are directly involved in the process of translation. rRNA modifications are dense but lack diversity. Only about 2% of the nucleotides in rRNAs are modified, with most of them being 2'-OMe on the ribose sugar and isomerization of uridine. Modifications on the base, such as methylation, also exist. As the 2′ hydrophilic hydroxyl group on the ribose is what discriminates RNA bases from DNA bases, the 2'-OMe modification of RNA can have fundamentally altering effects on the structure and stability of RNA and even in the biogenesis of ribosomes. Yildirim et al. showed that 2'-OMe enhances duplex stability of RNA–RNA hybrids (Yildirim et al., 2014).

Despite the conservation of rRNA and ribosomal structure, composition, and function in both prokaryotes and eukaryotes, there are dichotomies in rRNA modifying machinery. In E. coli, modifications are carried out by pure protein enzymes that are site or region-specific whereas 2'-O-methylation and pseudouridylation in eukaryotes are done via site-specific small nucleolar RNA–protein complexes. Site specificity is determined by the small nucleolar RNAs (snoRNAs) through base pairing and it guides the modifying enzymes to the modification sites; Box C/D snoRNAs guide 2'-OMe and Box H/ACA snoRNAs guide pseudouridylation (Watkins & Bohnsack, 2012). RNA modifications in rRNA are not randomly distributed. Instead, they are mostly hidden inside the ribosome and occur in conserved sites and functional sites, such as the A, P, and E sites for tRNA binding, mRNA binding, and the peptidyl transfer center, respectively. The former feature suggests that most modifications happen before the ribosome assembly and once assembled, they are not easily accessible to the demodifying or remodifying enzymes if any. It is well appreciated that demodifying enzymes unlikely exist and change rRNA modifications in mature ribosomes. The latter feature implies that these modifications may have a global impact within the cell (Decatur & Fournier, 2002; Roundtree et al., 2017). Nonetheless, inducible modifications do exist. In yeast, it has been observed that post-diauxic growth and heat-shock induce pseudouridylation in two rRNAs which supports the idea that these modifications are dynamic and could serve to alter ribosome function (Carlile et al., 2014; Schwartz et al., 2014).

3 | RNA MODIFICATIONS IN AGING-RELATED NEURODEGENERATIVE DISEASES

Aging-related neurodegenerative diseases include Alzheimer's disease (AD), Parkinson's disease (PD), amyotrophic lateral sclerosis (ALS), stroke, and frontotemporal degeneration. Accumulating evidence has indicated that age-related neurodegenerative diseases result from various reasons. Among them, epigenetic changes especially RNA modification that could have serious implications in this aspect should be further explored.

3.1 | AD and RNA modification

AD was first described by Alois Alzheimer in 1906. It is one of the most damaging aging-related neurodegenerative diseases, the prevalence of which increases as the global population ages (Cummings et al., 2014). Despite its clinical importance, effective therapy against AD is yet to be identified. The core clinical manifestation of AD is the loss of synaptic plasticity, which is closely related to the decline in cognitive ability. Some of the initial clinical features of AD are defects in the capability of creating and storing new memories (Soria Lopez et al., 2019). Although AD was first described almost a century ago, the pathogenesis of AD though understood better than before, requires further investigation.

m6A is an abundant RNA modification in the brain, and recent studies have demonstrated that the m6A methylation of RNA could promote the development of AD. By using m6A-sequencing together with high-throughput liquid chromatography–tandem mass spectrometry (LC–MS/MS), it is found that the expression level of METTL3 was significantly reduced along with m6A levels in 5xFAD mice when compared with control mice (Shafik et al., 2021). Consistently, the significantly decreased neuronal m6A levels and METTL3 expression were also observed by immunoblot analysis in human AD brains compared with the age-matched control cases (Zhao et al., 2021). Knockdown of METTL3 in the mouse hippocampus caused memory loss, neurodegeneration, spine loss, and gliosis (Zhao et al., 2021). Mechanistically, METTL3 deficiency delays the mRNA degradation of m6A-modified cell cycle genes, including Cyclin D1 and Cyclin D2, in the hippocampus and in primary neuron cultures, which causes dysregulated cell cycle and oxidative stress (Zhao et al., 2021). In addition, a recent study examining the expression profiles of m6A-regulated genes in human AD post-mortem brains has reported the aberrant expression of METTL3 and RBM15B in the AD hippocampus and indicated that the accumulation of METTL3 in the insoluble fractions positively correlated with that of Tau in hippocampal lysates, suggesting that potential

perturbations in m6A signaling may contribute towards neuronal dysfunction in AD (Huang et al., 2020). Diabetes and obesity are thought to be closely related to AD. It is found that FTO activates mTOR signaling and reduces the mRNA level of TSC1, therefore activating the phosphorylation of Tau in insulin defects-associated AD, and conditional knockout of FTO in the neurons reduces the cognitive deficits in 3xTg AD mice (Li et al., 2018). Besides, the NIA-LOAD study identified a genetic variant in the FTO gene loci significantly associated with AD, and FTO expression was significantly lower in the cortex and amygdala tissues of AD patients compared with controls, suggesting the functional role of FTO in Alzheimer's Disease (Reitz et al., 2012). This is further confirmed by a prospective study showing FTO AA-genotype posed a higher risk for AD and dementia (Keller et al., 2011). These findings suggest that m6A modification may play a pivotal role in the pathogenesis and progression of AD.

LC–MS/MS revealed that small RNA modifications of AD patients changed compared with normal controls, including 2'-O-methylcytidine (Cm), m7G, and 2'-O-methylguanosine, were increased while N2, N2,7-trimethylguanosine (m2,2,7G), and N2,N2-dimethylguanosine were dramatically decreased in the 15-25 nt RNA fraction from the cortex of AD brains. RNA-seq analysis revealed that most of these fractions are miRNAs. Interestingly, in the 30–40-nt small RNA fraction, Cm, 2'-O-methyluridine (Um), and m7G modifications showed higher levels compared with controls whereas m1G, m2,2,7G, and pseudouridine modifications were reduced (Figure 1). Among them, tRNA-derived small RNAs, rRNA-derived small RNAs, Y RNA-derived small RNAs, and other unannotated RNAs were part of the major fractions in RNA-seq analysis (Zhang, Trebak, et al., 2020). By using microfluidic-based high-throughput PCR along with next-generation sequencing, it was found that A-to-I RNA editing levels were reduced in Alzheimer's disease samples when compared with controls (Khermesh et al., 2016). Similarly, the A-to-I RNA editing events of AD were systematically annotated (Wu et al., 2021). 1,676,363 editing sites were detected in 1524 samples across 9 brain regions from ROSMAP, MayoRNAseq, and MSBB studies, within which 108,010 and 26,168 editing events were identified to promote or inhibit AD progression, respectively (Wu et al., 2021). 5582 brain region-specific editing events with potentially dual roles in AD across different brain regions were also noticed (Wu et al., 2021).

3.2 | ALS and RNA modification

ALS is one of the most common age-related neurodegenerative diseases characterized by progressive weakness and muscle atrophy, causing damage to upper and lower motor neurons (Oskarsson et al., 2018). The pathogenesis of amyotrophic lateral sclerosis involves several mechanisms, among which RNA modifications deserve a more thorough investigation.

ADAR2 specifically catalyzes A-to-I RNA editing at the glutamine/arginine (Q/R) site of GluA2, a subunit in the majority of AMPA receptors in the adult brain, and changes the glutamine (position 607; encoded by CAG) to an arginine (edited to CIG and translated as CGG) within the ion pore of GluA2, which is indispensable for normal AMPA receptor function (Sommer et al., 1991). In conditional ADAR2 knockout mice, the Q/R site of GluA2 cannot be edited by ADAR2, which results in the slow death of the motor neurons (Hideyama et al., 2010; Hideyama & Kwak, 2011). Recent evidence demonstrated that the efficiency of RNA editing at the GluA2 Q/R site was significantly lower in all ALS cases compared with that of the control subjects. Interestingly, of the three members of the ADAR family, only the enzymatic activity of ADAR2 was downregulated in ALS motor neurons, which suggests that once ADAR2 expression levels decreased below the required threshold to edit all GluA2 Q/R sites, motor neurons enter a death cascade. It is also suggested that the progressive downregulation of ADAR2 may be closely related to the pathogenesis of ALS, wherein the failure of A-to-I transition at the GluA2 Q/R locus is critical (Hideyama et al., 2012). Furthermore, the CYFIP2 mRNA K/E site was predominantly edited by ADAR2 and has been newly identified as ADAR-mediated A-to-I editing positions, which could provide a clue to the pathogenesis of ALS (Kwak et al., 2008). Notably, a deeper understanding of the various RNA modifications may shine light on the mechanism-based therapeutic approach to treating age-related neurodegenerative diseases. Similarly, glutamate receptor GRIA2 editing is significantly reduced in the motor neurons of ALS patients as well as in patients with schizophrenia and bipolar disorder. Reduced editing is accompanied by reduced ADAR2 expression in these patients, with RNA editing deficiency contributing to motor neuron toxicity in ALS (Maas et al., 2006). Moreover, TDP-43, a pathological hallmark of ALS, is exclusively expressed in motor neurons lacking ADAR2 in patients with sporadic ALS (Aizawa et al., 2010), demonstrating the pathogenic role of unedited GluA2 at the Q/R locus in ALS.

4 | RNA MODIFICATIONS IN AGING-RELATED CARDIOVASCULAR DISEASES (CVDS)

CVDs remain the leading cause of death globally (Mortality, & Causes of Death, C, 2013), and biological aging is a major risk factor in CVDs, such as atherosclerosis, coronary heart disease, myocardial infarction, hypertension, stroke, cardiac hypertrophy, and heart failure (HF) (North & Sinclair, 2012). By 2030, approximately 20% of the population will be 65 years of age or older. By that time, CVDs will be responsible for 40% of deaths and the cost of treating CVDs will have tripled (Fleg et al., 2011; Heidenreich et al., 2011). Therefore, it is critical to understand the underlying mechanism by which aging acts as an important determinant of the etiology of CVDs. Here, we discuss some of the associations between RNA modifications and age-related CVDs.

4.1 | Atherosclerosis

Atherosclerosis is a chronic inflammatory disease that progresses slowly with the accumulation of cholesterol, lipids, and cellular debris in blood vessels, which in turn greatly increases the risk of restricting blood flow and rupture of blood vessels, contributing to

the development of heart attack (myocardial infarction) and stroke (Gistera & Hansson, 2017). Aging-related obesity is the predominant risk factor for atherosclerosis. New evidence revealed that zinc-finger protein 217 (ZFP217) can reduce the expression of m6A by activating the expression of FTO, which ultimately leads to increased adipogenesis and obesity (Song et al., 2019). Recent studies have also demonstrated that METTL3 plays a crucial role in atherogenesis induced by oxidative stress and disturbed blood flow. METTL3-mediated RNA hypermethylation stabilized NLRP1 mRNA and degraded KLF4 mRNA through YTHDF1 and YTHDF2 m6A reader proteins, respectively (Chien et al., 2021). Knockdown of METTL3 restored the mRNA levels of NLRP1 and KLF4 and prevented the atherogenic process (Chien et al., 2021). In addition, METTL14 was demonstrated to directly bind to FOXO1 mRNA and enhance FOXO1 mRNA translation by increasing its m6A modification, which thereby increases adhesion molecule expression, aggravating endothelial inflammation, and contributes to atherosclerosis development (Jian et al., 2020). Silencing METTL14 also inhibited the proliferation and invasion of atherosclerotic vascular endothelial cells (ASVECs) by inhibiting the expression of miR-19a which promotes the proliferation and invasion of ASVECs (Zhang et al., 2020).

ADAR1 is known to bind to a vast majority of the double-stranded RNAs and catalyzes the deamination of adenosine to inosine (A-to-I) (Stellos et al., 2016). Notably, ADAR1, the main RNA editor in endothelial cells, could enhance the stability of Cathepsin S (CTSS) and its expression by inducing A-to-I RNA editing in Alu elements in the 3'UTR of CTSS transcripts and recruiting HuR to the 3'UTR (Stellos et al., 2016). Moreover, analysis of microarray-based data and results of immunohistochemistry revealed that the expression levels of both CTSS and ADAR1 were upregulated in atherosclerotic carotid plaques. Besides, ADAR1-induced A-to-I RNA editing could stabilize the atherosclerosis-associated NEAT1 lncRNA expression (Vlachogiannis et al., 2021).

4.2 | Cardiac hypertrophy

While hypertrophy initially develops as an adaptive response to physiological and pathological stimuli, both physiological and pathological hypertrophy involves the enlargement of individual cardiomyocytes. Nearly a quarter of the transcripts in both mouse and human hearts showed m6A RNA methylation, and an increasing number of studies provide clear evidence that RNA modifications play important roles in cardiac hypertrophy (Kumari et al., 2021). Thus, a better understanding of the underlying molecular mechanisms that regulate cardiac hypertrophy would give better insight into novel therapeutic approaches.

With m6A sequencing, several studies have demonstrated that m6A methylation levels are markedly increased in cardiac hypertrophy. METTL3 could catalyze m6A methylation on specific mRNA subpopulations that drive cardiomyocyte hypertrophy. Both knockdown and overexpression of METTL3 in vitro and in vivo affect cell size and cell remodeling and the inhibition of METTL3 has been shown to be sufficient to prevent hypertrophy *in vitro* (Dorn et al., 2019; Kmietczyk et al., 2019). These findings underscore the significance of this novel mechanism of cardiac hypertrophy. It is well known that leptin directly induces cardiomyocyte hypertrophy. Recently, Gan et al. demonstrated that the expression levels of FTO were upregulated after leptin treatment in cultured myocytes, suggesting its potential role in mediating the hypertrophic response to leptin (Gan et al., 2013). Similarly, FTO knockdown can blunt the hypertrophy of neonatal rat cardiomyocytes induced by α-adrenergic stimulation with phenylephrine (Kmietczyk et al., 2019). These findings suggest that the effects of FTO on cardiac hypertrophy may be stimulation-dependent, in addition, the detailed molecular mechanism needs to be further clarified. Moreover, whether the demethylase activity of FTO is necessary for this function or not, requires further investigation.

Meanwhile, non-coding RNAs specifically expressed in the heart could participate in molecular networks associated with myocardial hypertrophy, including piRNAs. A recent study found that the expression level of DQ726659, an uncharacterized piRNA named cardiac-hypertrophy-associated piRNA (CHAPIR), was significantly increased in TAC-induced hypertrophic mouse hearts. CHAPIR directly interacted with METTL3 which suppresses the m6A modification of Parp10 mRNAs thereby increasing Parp10 protein levels and promoting NFATC4-induced pathological cardiac hypertrophy (Gao et al., 2020). Similarly, cardiac-specific targets of miR-133a were enriched in m6A modifications. IGF2BP2, a key m6A reader, was observed to promote the assembly of the m6A-modified miR-133a-AGO2-RISC complex on the mRNA targets of miR-133a, thereby enhancing the inhibitory effect of miR-133a and protecting from cardiac hypertrophy (Qian et al., 2021).

4.3 | RNA modification and other CVDs

Hypertension, one of the most important risk factors for CVDs, is usually defined as a prolonged increase in systemic arterial pressure above a certain threshold (Giles et al., 2009). The incidence of hypertension rises dramatically with age and 70% of older adults have hypertension in 2015 (Mozaffarian et al., 2015). Interestingly, 33 (2.67%) m6A-associated single-nucleotide polymorphisms (m6A-SNPs) were found to be significantly associated with blood pressure in three genome-wide association studies from East Asian populations, within which rs56001051 (C1orf167) and rs197922 (GOSR2) were significantly associated with hypertension (Mo et al., 2019a). Another study genotyped 217 individuals (86 men and 131 women) with hypertension and found FTO rs9939609 had a negative association with blood pressure in male hypertensive patients (Marcadenti et al., 2013).

The prevalence of HF, characterized as reduced cardiac function and left ventricular dilatation, is predicted to increase remarkably by 46% in the United States from 2012 to 2030 due to the aging population (Heidenreich et al., 2013). Recently, emerging studies have revealed the regulatory mechanisms of RNA methylation in

the pathogenesis of HF (Komal et al., 2021). m6A-sequencing and transcriptome analysis of the heart tissues from human HF patients and mouse transverse aortic constriction (TAC) models revealed that m6A modification profiles were changed more dramatically than gene expression and RNAs with altered m6A modification were mainly enriched in metabolic and regulatory pathways (Berulava et al., 2020). Furthermore, cardiomyocyte-specific deletion of FTO accelerated the progression of HF after TAC surgery (Berulava et al., 2020). Cardiomyocyte-specific deletion of ADAR1 leads to an excessive amount of cardiomyocyte loss, resulting in cardiac dysfunction and eventual lethality. Lack of ADAR1 leads to a global reduction in miRNA production, in particular of miR-199a-5p, and the activation of unfolded protein response (UPR)-driven apoptotic response, which hampers ER stress handling in cardiomyocytes. Inhibition of the UPR in ADAR1-knockout hearts significantly reduced cardiomyocyte loss and restored survival of the animals due to improved cardiac function, which pointed to an essential role for ADAR1 in cardiomyocyte survival and maintenance of cardiac function (El Azzouzi et al., 2020). Interestingly, it is also found that HF patients with reduced ejection fraction had higher concentrations of pseudouridine in plasma compared with healthy controls (Alexander et al., 2011). These studies suggest that RNA modification may serve as therapeutical target against HF.

Stroke is the second most common cause of CVD-related mortality and the number of strokes and deaths due to stroke increases substantially each year (Collaborators, 2021). Stroke was found to significantly increase the global m6A methylation levels in mouse cortex after reperfusion of transient focal ischemia and the genome-wide analysis of the methylated RNAs showed that 147 transcripts (127 mRNAs and 20 lncRNAs) have altered m6A levels, among which 95% (122 mRNAs and 17 lncRNAs) were significantly hypermethylated after stroke, which may due to the downregulation of FTO (Chokkalla et al., 2019). The integrative analysis of the association between m6A-SNPs and ischemic stroke found that 310 (7.39%) m6A-SNPs were nominally associated with ischemic stroke (Mo et al., 2019b). In addition, another study revealed that YTHDC1 expression was upregulated in the early phase of ischemic stroke, and overexpression of YTHDC1 significantly decreased brain infarct volume (Zhang, Wang, et al., 2020). Mechanistically, YTHDC1 activated Akt phosphorylation via promoting the degradation of m6A-modified PTEN mRNA (Zhang, Wang, et al., 2020).

Taken together, these studies suggested that epigenetic modifications of mRNAs have a great impact on aging-related CVDs which could provide critical clues to developing future therapies against age-related CVDs.

5 | RNA MODIFICATIONS IN AGING-RELATED CATARACTS

Aging-related cataracts are the main disease of visual impairment and blindness in the world, which commonly occur in people over 50 years old. Cataracts are formed due to the decrease in transparency of the lens (Yang et al., 2019), and so far, the only available treatment for cataracts is surgery (Dubois & Bastawrous, 2017). Therefore, research into the mechanism of cataracts is urgently required to find potential targets for novel therapeutics. A recent study investigated the involvement of m6A circRNAs and methyltransferases in the lens epithelium cells(LECs). By performing genome-wide profiling of m6A-modified circRNAs in lens epithelium cells, they found 2472 m6A peak distributions on 1248 circRNAs with the up-methylation degree and 2174 m6A peaks distribution on 1148 circRNAs with the down-methylation degree. Moreover, the expression of m6A-modified circRNAs in the age-related cataract LECs was lower than that of the controls, which strengthened the dynamic relationship between the m6A modifications at the circRNAs and expression of m6A circRNAs in age-related cataract LECs. They also examined the expression levels of a key methyltransferase, ALKBH5, and two major methyltransferases, METTL3 and WTAP. It was found that the mRNA expression levels of ALKBH5 were significantly upregulated when compared with the control groups, suggesting that ALKBH5 decreases the m6A modifications of circRNAs (Li, Yu, et al., 2020). Interestingly, METTL3 could modulate the proliferation and apoptosis of LECs in diabetic cataracts by targeting the 3'UTR of ICAM-1 and stabilizing its mRNA stability (Yang et al., 2020).

Isomerization of uridine to pseudouridine is one of the most abundant RNA modifications and is catalyzed by the H/ACA small ribonucleoprotein complex that is composed of four core proteins, dyskerin (DKC1), NOP10, NHP2, and GAR1. Histological analysis has revealed that in $Dkc1^{elu1/elu1}$ mutant larvae show microphthalmia and cataracts with abnormal eyes and retinas, accompanied by a large number of cells with neuroepithelial properties (Balogh et al., 2020). Using MeRIP-seq and RNA-seq, one recent study comprehensively analyzed the transcriptome-wide m6A methylome and gene expressions of the anterior capsule of the lens in highly myopic patients with nuclear cataract anterior. They found that METTL14 was upregulated whereas METTL3, FTO, ALKBH5, YTHDF1, and YTHDF2 were downregulated, which suggests that m6A methylation was strongly associated with the pathogenic mechanism of high myopia (Wen et al., 2021). Overall, these studies have uncovered the regulatory roles of m6A modifications in aging-related cataracts.

6 | RNA MODIFICATIONS IN AGING-RELATED OSTEOPOROSIS

Aging-related osteoporosis is characterized by low bone mass and over-accumulation of fatty tissue in the bone marrow environment that increases the risk of fracture (Duque et al., 2009). With aging, the composition of the bone marrow shifts to favor the presence of adipocytes, osteoclast activity increases and osteoblast function declines, leading to osteoporosis (Coughlan & Dockery, 2014). METTL3, the key methyltransferase of m6A, was observed to regulate the

fate of osteoporosis. Firstly, the expression levels of METTL3 and m6A methylation are significantly decreased in both osteoporosis patients and mouse models (Yan et al., 2020). Downregulation of METTL3 caused the decline in bone formation and overexpressed METTL3 could partially rescue the feature of osteoporosis such as reduction in bone formation. Molecularly, METTL3 mediates m6A methylation of RUNX2, a key factor involved in osteogenesis, and enhances its cellular stability (Yan et al., 2020). METTL3 knockout reduced the translation efficiency of MSCs lineage allocator Pth1r and then led to a reduction of the global methylation level of m6A and disruption of the PTH-induced osteogenic and adipogenic responses, which eventually affects the osteogenic and adipogenic differentiation of mesenchymal stem cells (Wu et al., 2018). Apart from this, a recent study revealed different molecular mechanisms of METTL3-dependent m6A modification in osteoclast differentiation. Here, the depletion of either METTL3 or YTHDF2 promoted the stability and the expression of Atp6v0d2 mRNA (Li, Cai, et al., 2020). Besides, knockdown of METTL3 reduces the expression level of VEGFA and its splice variants, VEGFA-164 and VEGFA-188 thereby regulating osteogenic differentiation (Tian et al., 2019). More interestingly, METTL3 can also regulate osteogenic differentiation by promoting m6A methylation modifications of the critical upstream regulator of NF-κB signaling: MYD88-RNA, which in turn triggers the activation of NF-κB, thereby inhibiting osteogenic progression (Yu et al., 2020). m6A methylation is also catalyzed by METTL14 which serves as the RNAbinding scaffold that recognizes the substrate. Recent studies demonstrated the critical roles of the miR-103-3p/METTL14/m6A signaling axis in osteoblast activity. Here, miR-103-3p inhibits osteoblast activity by directly targeting METTL14 while METTL14-dependent m6A methylation enhances the recognition of pri-miR-103-3p by DGCR8 and the subsequent processing into mature miR-103-3p, thereby modulating osteoblast activity (Sun, Wang, et al., 2021).

FTO is a key regulator associated with adipogenesis, and the complete depletion of FTO in mice results in postnatal growth retardation. FTO knockout mice have not only a significantly shorter body length over the lifetime but also a much lower bone mineral density (Gao et al., 2010). To evaluate the effect of FTO on bone mass and to prevent the potential confounding effect of FTO on global metabolism and body composition, mice lacking FTO selectively in osteoblasts ($FTO^{Oc\ KO}$) were generated. These mice showed a significant decrease in bone volume and trabecular number at 30 weeks of age. Furthermore, the results of static and dynamic histomorphometric analyses showed that the bone formation rate in mutant mice was decreased by 66% with bone marrow adipocyte number per bone marrow area being increased when compared with controls. FTO functioned through demethylating and then enhancing the stability of the mRNAs of Hspa1a and other genes that can protect cells from genotoxic damage (Zhang et al., 2019). The above results implied that FTO is required for the maintenance of bone mass and $FTO^{Oc\ KO}$ mice manifest the phenotype consistent with age-related bone loss. miR-149-3p was found to directly target FTO mRNA and modulate the adipogenic differentiation of bone marrow-derived mesenchymal stem cells (Li et al., 2019). Besides, during aging and osteoporosis, FTO was upregulated by GDF11 in both humans and mice, and then stabilized the Pparg mRNA through the demethylation of m6A, leading to the differentiation of bone mesenchymal stem cells to adipocytes rather than osteoblasts (Shen et al., 2018). FTO also plays an intrinsic role in osteoblasts by enhancing the stability of mRNAs of proteins that can protect cells from genotoxic damage via Hspa1a-NF-κB signaling (Zhang et al., 2019). Altogether, these findings provide new perspectives on the pivotal role of m6A in regulating age-related bone diseases such as osteoporosis.

7 | RNA MODIFICATIONS IN AGING-RELATED FERTILITY DECLINE

Age-related fertility decline is inevitable and irreversible, especially for female reproductive potential. Several demographic and epidemiological studies have long recognized that female fertility declines with age, most notably the decline in ovarian function (Leridon, 2004; Menken et al., 1986; Nelson et al., 2013). The mechanisms involved in the process of ovarian aging have gained increased attention and focus. Herein, we highlight the importance of RNA modification in ovarian aging.

All m6A modifications of the granulosa cells of aged human ovaries were measured in order to investigate the relationship between ovarian aging and m6A modification. It was found the level of m6A modifications was significantly increased and the expression level of FTO was downregulated. m6A sequencing showed that increased m6A in the 3′UTR of FOS mRNAs resulted in reinforcing the stability of FOS mRNAs (Jiang et al., 2021). Another study also concurrently found that the expression of FTO decreased and the content of m6A increased with aging in human follicular fluid, granulosa cells, and mouse ovary (Sun, Zhang, et al., 2021). Besides, the chemotherapy drug, cyclophosphamide, could increase the m6A level and significantly inhibit the expression levels of RNA demethylase FTO in a time- and concentration-dependent manner, which is further associated with premature ovarian aging (Huang et al., 2019). More research exploring the precise mechanism of RNA modifications in ovarian aging would give insight into possible strategies to postpone ovarian aging.

8 | CONCLUSION AND PERSPECTIVES

In conclusion, the field of epitranscriptomics has emerged rapidly in recent years and RNA modifications have been emerging as a new focus and novel therapeutical targets against aging-related diseases. In this review, we have summarized RNA epitranscriptomic regulation and the mechanisms involved in aging-related diseases. We found that RNA modification is involved in many diseases that are aging-related, and plays an essential role in impacting mRNA stability, translation, and control of protein levels of key genes that are involved in pertinent disease-associated pathways (Table 1).

TABLE 1 The regulation and roles of RNA modifications in aging-related diseases

Category of diseases	Pathogenic phenotype	RNA modification	Gene expression alterations	Molecular consequences of altered RNA modification/pathogenic relevance	References
Alzheimer's disease (AD)	AD	m6A	Decreased METTL3 expression	Many AD-related transcripts exhibit decreased m6A modification, which is correlated with reduced protein levels.	(Shafik et al., 2021)
	AD	m6A	Decreased METTL3 expression	METTL3 depletion resulted in elevated levels of m6A-modified CCND2	(Zhao et al., 2021)
	AD	m6A	Decreased METTL3 expression and increased RBM15B expression	Significant correlation with the expression level of insoluble Tau protein in the postmortem of human AD	(Huang et al., 2020)
	Diabetes and obesity-associated AD	m6A	Increased FTO expression	Promoting the activation of mTOR by increasing the mRNA level of TSC1	(Li et al., 2018)
	AD	Multiple RNA modifications	Altered modification on small RNAs, including tsRNA, rsRNAs, ysRNAs, and other unannotated RNAs	Not specified	(Zhang, Trebak, et al., 2020)
	AD	A-to-I editing	Aberrant expression of ADAR1 and ADARB1	Editing levels of 35 target sites within 22 genes were significantly altered in AD patients' brain tissues	(Khermesh et al., 2016)
Amyotrophic lateral sclerosis (ALS)	ALS	A-to-I editing	Decreased ADAR2 expression	Failure of A-to-I transition at GluA2 Q/R locus; reduced glutamate receptor GRIA2 editing in the motor neurons	(Hideyama et al., 2012; Kwak et al., 2008; Maas et al., 2006)
Atherosclerosis	Atherogenesis	m6A	Increased METTL3 expression	Stabilization of NLRP1 mRNA and degradation of KLF4 mRNA	(Chien et al., 2021)
	Atherosclerosis development	m6A	Increased METTL14 expression	Promoting FOXO1 translation	(Jian et al., 2020)
Atherosclerosis	The proliferation and invasion of ASVEC	m6A	Increased METTL14 expression	Promoting the maturation of miR-19a	(Zhang et al., 2020)
	Atherosclerotic carotid plaques	A-to-I editing	Increased ADAR1 expression	Enhancing the stability of Cathepsin S (CTSS)	(Stellos et al., 2016)
	Atherosclerosis	A-to-I editing	Not specified	Stabilizing the atherosclerosis-associated NEAT1 lncRNA expression	(Vlachogiannis et al., 2021)
Cardiac Hypertrophy	Cardiac hypertrophy	m6A	Increased METTL3 expression	Stabilizing a subpopulation of mRNAs driving cardiac hypertrophy	(Dorn et al., 2019; Kmietczyk et al., 2019)
		m6A	Increased FTO expression	Hypertrophic response to leptin	(Gan et al., 2013)
		m6A	Blockage of METTL3 function by cardiac-hypertrophy-associated piRNA (CHAPIR)	CHAPIR–PIWIL4 complexes block METTL3 from catalyzing m6A modification on Parp10 mRNAs, which upregulates PARP10 expression and promotes NFATC4-dependent pathological hypertrophy	(Gao et al., 2020)
		m6A	Decreased miR-133a expression	IGF2BP2 promotes the localization of m6A-modified miR-133a in AGO2-RISC complex and enhances the function of miR-133a	(Qian et al., 2021)

(Continues)

TABLE 1 (Continued)

Category of diseases	Pathogenic phenotype	RNA modification	Gene expression alterations	Molecular consequences of altered RNA modification/pathogenic relevance	References
Heart Failure (HF)	Cardiac dysfunction	A-to-I editing	Decreased ADAR1 expression	Resulting a global reduction of miRNAs, especially miR-199a-5p, which activates UPR in cardiomyocytes	(El Azzouzi et al., 2020)
	HF	m6A	Not specified	Regulating RNA translation efficiency	(Berulava et al., 2020)
Stroke	Stroke	m6A	Decreased FTO expression and increased expression of YTHDF1 and YTHDF3	Altering the m6A level of 147 transcripts that are involved in inflammation, apoptosis, and transcriptional regulation	(Chokkalla et al., 2019)
	Brain infarct volume	m6A	Increased YTHDC1 expression	Facilitating the degradation of PTEN mRNA	(Zhang, Wang, et al., 2020)
Cataract	Cataract	m6A	Increased ALKBH5 expression	Decreasing the m6A modifications of circRNAs	(Li, Yu, et al., 2020)
	Proliferation and apoptosis of LECs	m6A	Increased METTL3 expression	Stabilizing the ICAM-1 mRNA	(Yang et al., 2020)
Cataract	High myopia	m6A	Increased METTL14 expression and decreased expression of ALKBH5, METTL3, FTO, YTHDF1, and YTHDF2	Differentially methylated genes were enriched in the pathways regulating the formation of extracellular matrix.	(Wen et al., 2021)
	Cataract	pseudouridine	Decreased DKC1 expression	Defective pseudouridination of small nucleolar ribonucleoproteins	(Balogh et al., 2020)
Osteoporosis	Bone formation	m6A	Decreased METTL3 expression	Enhancing the cellular stability of RUNX2	(Yan et al., 2020)
	Osteogenic and adipogenic differentiation of MSCs	m6A	Decreased METTL3 expression	Reduced translation efficiency of Pth1r due to decreased METTL3 expression	(Wu et al., 2018)
	Osteoclast differentiation	m6A	Increased METTL3 expression	METTL3 deficiency promotes the stability and the expression of Atp6v0d2 mRNA and reduced the expression level of Vegfa and its splice variants	(Li, Cai, et al., 2020; Tian et al., 2019)
	osteoclast differentiation	m6A	Increased METTL3 expression and decreased ALKBH5 expression	Facilitating m6A modifications of MYD88-RNA and then inducing the activation of NF-κB	(Yu et al., 2020)
	Osteoblast activity	m6A	Increased miR-103-3p level and decreased METTL14 expression	Regulating the maturation process of miR-103-3p, which directly targets METTL14 to inhibit osteoblast activity	(Sun, Wang, et al., 2021)
	Maintenance of bone mass	m6A	Increased FTO expression	Demethylating and enhancing the stability of the mRNAs of Hspa1a and other genes that can protect osteoblasts from genotoxic damage	(Zhang et al., 2019)
	Osteoporosis	m6A	Increased FTO expression	Regulated the stability of Pparg mRNA	(Shen et al., 2018)
Fertility Decline	Ovarian aging	m6A	Decreased FTO expression	Increasing the stability of FOS mRNA	(Jiang et al., 2021; Sun, Zhang, et al., 2021)

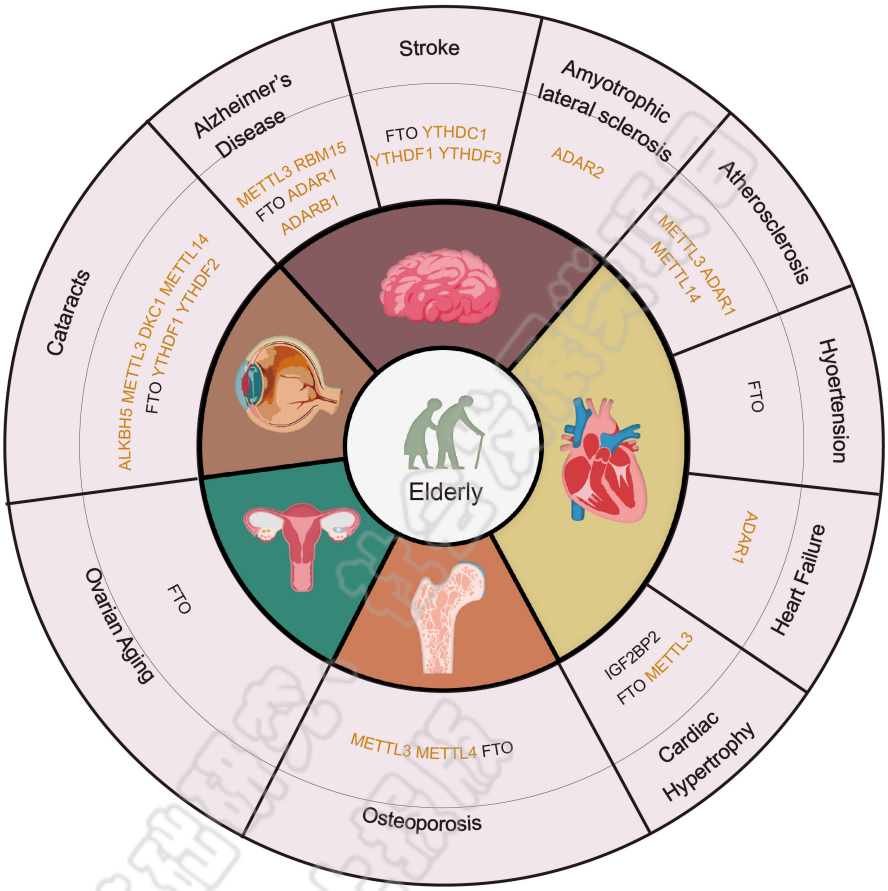

FIGURE 3 RNA modification genes associated with aging-related diseases

Collectively, we have summarized several studies that highlight the crucial role of RNA modification in aging-related diseases (Figure 3). Understanding their functions in the context of aging-related disease could provide newer perspectives that enrich the theoretical basis of aging-related disease. However, a few more points need to be further thoroughly analyzed. (1) The epigenetic mechanisms of aging-related diseases have predominantly focused on DNA methylation, histone modifications, and chromatin rearrangement, while the important biological functions of m6A modification have been ignored and require thorough future exploration. (2) Although m6A modification is increasingly being studied in other fields, there are still many modifying erasers/writers/readers that remain to be discovered. Their functions and potential therapeutic implications in aging-associated diseases have yet to be investigated. Moreover, few studies that have focused on m6A application and m6A-targeting drug therapy need to be further explored in-depth. (3) PD is another common progressive neurodegenerative disorder, which is characterized by rigidity, bradykinesia, tremor, and gait disturbances (Jankovic, 2008). In addition to DNA methylation and chromatin remodeling, a recent work identified m6A-modifying genes (including METTL3, METTL14, WTAP, FTO, ALKBH5, YTHDF1, YTHDF2, YTHDF3, HNRNPC, and ELAVL1) in a total of 1647 sporadic PD patients, among them were 214 rare variants in these 10 m6A-modification genes and 16 common variants in seven genes. Although an apparent association of 10 m6A-modification genes and sporadic PD in the Chinese cohort was not found, further functional studies are needed to explore the association between RNA modifications and PD, given the impact of RNA modification on brain development and other aging-related neurological disorders (Qin et al., 2020). There are very few studies on RNA modification related to macular degeneration and the regulation of gut microbes, which are areas worth exploring to gain more knowledge and advance the field of aging-associated RNA modifications. Taken together, further efforts are required to gain an in-depth insight into the role of RNA modifications in aging-related diseases and would provide new potential molecular targets for research and development of pharmacological and clinical therapies for many aging-related diseases.

AUTHOR CONTRIBUTION

Z.J., D.S., L.H., Y.G., and G.L. conceived the manuscript. Z.J., D.S., L.H., S.S., and L.Z. drafted the manuscript, made the figures, and summarized the Tables. HI.L., P.G., G.V., Y.G., and G.L. finalized the manuscript, figures, and Tables. L.H. and Y.G. significantly contributed to the manuscript revision.

ACKNOWLEDGEMENT

This work was supported by National Natural Science Foundation of China (81900287 to Z.J, and 82072788 to Y.G.) and Tianshan Youth Foundation of Xinjiang (2019Q066 to Z.J.).

CONFLICT OF INTEREST

The authors declare that they have no conflict of interest.

DATA AVAILABILITY STATEMENT

Data sharing is not applicable to this article as no new data were created or analyzed in this study.

ORCID

Guoping Li https://orcid.org/0000-0003-3874-0744

REFERENCES

Aas, P. A., Otterlei, M., Falnes, P. Ø., Vågbø, C. B., Skorpen, F., Akbari, M., Sundheim, O., Bjørås, M., Slupphaug, G., Seeberg, E., & Krokan, H. E. (2003). Human and bacterial oxidative demethylases repair alkylation damage in both RNA and DNA. *Nature*, *421*, 859–863. https://doi.org/10.1038/nature01363

Aizawa, H., Sawada, J., Hideyama, T., Yamashita, T., Katayama, T., Hasebe, N., Kimura, T., Yahara, O., & Kwak, S. (2010). TDP-43 pathology in sporadic ALS occurs in motor neurons lacking the RNA editing enzyme ADAR2. *Acta Neuropathologica*, *120*, 75–84. https://doi.org/10.1007/s00401-010-0678-x

Alexander, D., Lombardi, R., Rodriguez, G., Mitchell, M. M., & Marian, A. J. (2011). Metabolomic distinction and insights into the pathogenesis of human primary dilated cardiomyopathy. *European Journal of Clinical Investigation*, *41*, 527–538. https://doi.org/10.1111/j.1365-2362.2010.02441.x

Balogh, E., Chandler, J. C., Varga, M., Tahoun, M., Menyhárd, D. K., Schay, G., Goncalves, T., Hamar, R., Légrádi, R., Szekeres, Á., Gribouval, O., Kleta, R., Stanescu, H., Bockenhauer, D., Kerti, A., Williams, H., Kinsler, V., di, W. L., Curtis, D., … Tory, K. (2020). Pseudouridylation defect due to DKC1 and NOP10 mutations causes nephrotic syndrome with cataracts, hearing impairment, and enterocolitis. *Proceedings of the National Academy of Sciences of the United States of America*, *117*, 15137–15147. https://doi.org/10.1073/pnas.2002328117

Belanger, F., Stepinski, J., Darzynkiewicz, E., & Pelletier, J. (2010). Characterization of hMTr1, a human Cap1 2'-O-ribose methyltransferase. *The Journal of Biological Chemistry*, *285*, 33037–33044. https://doi.org/10.1074/jbc.M110.155283

Berulava, T., Buchholz, E., Elerdashvili, V., Pena, T., Islam, M. R., Lbik, D., Mohamed, B. A., Renner, A., Lewinski, D., Sacherer, M., Bohnsack, K. E., Bohnsack, M. T., Jain, G., Capece, V., Cleve, N., Burkhardt, S., Hasenfuss, G., Fischer, A., & Toischer, K. (2020). Changes in m6A RNA methylation contribute to heart failure progression by modulating translation. *European Journal of Heart Failure*, *22*, 54–66. https://doi.org/10.1002/ejhf.1672

Boccaletto, P., Stefaniak, F., Ray, A., Cappannini, A., Mukherjee, S., Purta, E., Kurkowska, M., Shirvanizadeh, N., Destefanis, E., Groza, P., Avşar, G., Romitelli, A., Pir, P., Dassi, E., Conticello, S. G., Aguilo, F., & Bujnicki, J. M. (2022). MODOMICS: A database of RNA modification pathways. 2021 update. *Nucleic Acids Research*, *50*, D231–D235. https://doi.org/10.1093/nar/gkab1083

Bohnsack, K. E., Hobartner, C., & Bohnsack, M. T. (2019). Eukaryotic 5-methylcytosine (m(5)C) RNA methyltransferases: Mechanisms, cellular functions, and links to disease. *Genes (Basel)*, *10*, 102. https://doi.org/10.3390/genes10020102

Brummer, A., Yang, Y., Chan, T. W., & Xiao, X. (2017). Structure-mediated modulation of mRNA abundance by A-to-I editing. *Nature Communications*, *8*, 1255. https://doi.org/10.1038/s41467-017-01459-7

Carlile, T. M., Rojas-Duran, M. F., Zinshteyn, B., Shin, H., Bartoli, K. M., & Gilbert, W. V. (2014). Pseudouridine profiling reveals regulated mRNA pseudouridylation in yeast and human cells. *Nature*, *515*, 143–146. https://doi.org/10.1038/nature13802

Chalk, A. M., Taylor, S., Heraud-Farlow, J. E., & Walkley, C. R. (2019). The majority of A-to-I RNA editing is not required for mammalian homeostasis. *Genome Biology*, *20*, 268. https://doi.org/10.1186/s13059-019-1873-2

Chatterjee, B., Shen, C. J., & Majumder, P. (2021). RNA modifications and RNA metabolism in neurological disease pathogenesis. *International Journal of Molecular Sciences*, *22*, 11870. https://doi.org/10.3390/ijms222111870

Chien, C. S., Li, J. Y. S., Chien, Y., Wang, M. L., Yarmishyn, A. A., Tsai, P. H., Juan, C. C., Nguyen, P., Cheng, H. M., Huo, T. I., Chiou, S. H., & Chien, S. (2021). METTL3-dependent N(6)-methyladenosine RNA modification mediates the atherogenic inflammatory cascades in vascular endothelium. *Proceedings of the National Academy of Sciences of the United States of America*, *118*, e2025070118. https://doi.org/10.1073/pnas.2025070118

Chokkalla, A. K., Mehta, S. L., Kim, T. H., Chelluboina, B., Kim, J., & Vemuganti, R. (2019). Transient focal ischemia significantly alters the m(6)a Epitranscriptomic tagging of RNAs in the brain. *Stroke*, *50*, 2912–2921. https://doi.org/10.1161/STROKEAHA.119.026433

Collaborators, G. B. D. S. (2021). Global, regional, and national burden of stroke and its risk factors, 1990-2019: A systematic analysis for the global burden of disease study 2019. *Lancet Neurology*, *20*, 795–820. https://doi.org/10.1016/S1474-4422(21)00252-0

Coughlan, T., & Dockery, F. (2014). Osteoporosis and fracture risk in older people. *Clinical Medicine (London, England)*, *14*, 187–191. https://doi.org/10.7861/clinmedicine.14-2-187

Cowling, V. H. (2009). Regulation of mRNA cap methylation. *The Biochemical Journal*, *425*, 295–302. https://doi.org/10.1042/BJ20091352

Cui, X., Liang, Z., Shen, L., Zhang, Q., Bao, S., Geng, Y., Zhang, B., Leo, V., Vardy, L. A., Lu, T., Gu, X., & Yu, H. (2017). 5-Methylcytosine RNA methylation in *Arabidopsis thaliana*. *Molecular Plant*, *10*, 1387–1399. https://doi.org/10.1016/j.molp.2017.09.013

Cummings, J. L., Morstorf, T., & Zhong, K. (2014). Alzheimer's disease drug-development pipeline: Few candidates, frequent failures. *Alzheimer's Research & Therapy*, *6*, 37. https://doi.org/10.1186/alzrt269

Dai, X., Wang, T., Gonzalez, G., & Wang, Y. (2018). Identification of YTH domain-containing proteins as the readers for N1-Methyladenosine in RNA. *Analytical Chemistry*, *90*, 6380–6384. https://doi.org/10.1021/acs.analchem.8b01703

de Crecy-Lagard, V., Boccaletto, P., Mangleburg, C. G., Sharma, P., Lowe, T. M., Leidel, S. A., & Bujnicki, J. M. (2019). Matching tRNA modifications in humans to their known and predicted enzymes. *Nucleic Acids Research*, *47*, 2143–2159. https://doi.org/10.1093/nar/gkz011

De Paolis, V., Lorefice, E., Orecchini, E., Carissimi, C., Laudadio, I., & Fulci, V. (2021). Epitranscriptomics: A new layer of microRNA regulation in cancer. *Cancers (Basel)*, *13*, 3372. https://doi.org/10.3390/cancers13133372

Decatur, W. A., & Fournier, M. J. (2002). rRNA modifications and ribosome function. *Trends in Biochemical Sciences*, *27*, 344–351. https://doi.org/10.1016/s0968-0004(02)02109-6

Delatte, B., Wang, F., Ngoc, L. V., Collignon, E., Bonvin, E., Deplus, R., Calonne, E., Hassabi, B., Putmans, P., Awe, S., Wetzel, C., Kreher, J., Soin, R., Creppe, C., Limbach, P. A., Gueydan, C., Kruys, V., Brehm, A., Minakhina, S., … Fuks, F. (2016). RNA biochemistry. Transcriptome-wide distribution and function of RNA hydroxymethylcytosine. *Science*, *351*, 282–285. https://doi.org/10.1126/science.aac5253

Dinescu, S., Ignat, S., Lazar, A., Constantin, C., Neagu, M., & Costache, M. (2019). Epitranscriptomic signatures in lncRNAs and their possible

roles in cancer. *Genes (Basel)*, *10*, 52. https://doi.org/10.3390/genes10010052

Dominissini, D., Moshitch-Moshkovitz, S., Schwartz, S., Salmon-Divon, M., Ungar, L., Osenberg, S., Cesarkas, K., Jacob-Hirsch, J., Amariglio, N., Kupiec, M., Sorek, R., & Rechavi, G. (2012). Topology of the human and mouse m6A RNA methylomes revealed by m6A-seq. *Nature*, *485*, 201–206. https://doi.org/10.1038/nature11112

Dominissini, D., Nachtergaele, S., Moshitch-Moshkovitz, S., Peer, E., Kol, N., Ben-Haim, M. S., Dai, Q., di Segni, A., Salmon-Divon, M., Clark, W. C., Zheng, G., Pan, T., Solomon, O., Eyal, E., Hershkovitz, V., Han, D., Doré, L. C., Amariglio, N., Rechavi, G., & He, C. (2016). The dynamic N(1)-methyladenosine methylome in eukaryotic messenger RNA. *Nature*, *530*, 441–446. https://doi.org/10.1038/nature16998

Dorn, L. E., Lasman, L., Chen, J., Xu, X., Hund, T. J., Medvedovic, M., Hanna, J. H., van Berlo, J. H., & Accornero, F. (2019). The N(6)-Methyladenosine mRNA methylase METTL3 controls cardiac homeostasis and hypertrophy. *Circulation*, *139*, 533–545. https://doi.org/10.1161/CIRCULATIONAHA.118.036146

Dubin, D. T., & Taylor, R. H. (1975). The methylation state of poly A-containing messenger RNA from cultured hamster cells. *Nucleic Acids Research*, *2*, 1653–1668. https://doi.org/10.1093/nar/2.10.1653

Dubois, V. D., & Bastawrous, A. (2017). N-acetylcarnosine (NAC) drops for age-related cataract. *Cochrane Database of Systematic Reviews*, *2*, CD009493. https://doi.org/10.1002/14651858.CD009493.pub2

Dunn, D. B. (1961). The occurrence of 1-methyladenine in ribonucleic acid. *Biochimica et Biophysica Acta*, *46*, 198–200. https://doi.org/10.1016/0006-3002(61)90668-0

Duque, G., Rivas, D., Li, W., Li, A., Henderson, J. E., Ferland, G., & Gaudreau, P. (2009). Age-related bone loss in the LOU/c rat model of healthy ageing. *Experimental Gerontology*, *44*, 183–189. https://doi.org/10.1016/j.exger.2008.10.004

El Azzouzi, H., et al. (2020). Cardiomyocyte specific deletion of ADAR1 causes severe cardiac dysfunction and increased lethality. *Frontiers in Cardiovascular Medicine*, *7*, 30. https://doi.org/10.3389/fcvm.2020.00030

Enroth, C., Poulsen, L. D., Iversen, S., Kirpekar, F., Albrechtsen, A., & Vinther, J. (2019). Detection of internal N7-methylguanosine (m7G) RNA modifications by mutational profiling sequencing. *Nucleic Acids Research*, *47*, e126. https://doi.org/10.1093/nar/gkz736

Eyler, D. E., Franco, M. K., Batool, Z., Wu, M. Z., Dubuke, M. L., Dobosz-Bartoszek, M., Jones, J. D., Polikanov, Y. S., Roy, B., & Koutmou, K. S. (2019). Pseudouridinylation of mRNA coding sequences alters translation. *Proceedings of the National Academy of Sciences of the United States of America*, *116*, 23068–23074. https://doi.org/10.1073/pnas.1821754116

Fernandez, I. S., Ng, C.L., Kelley, A.C., Wu, G., Yu, Y.T., & Ramakrishnan, V. (2013). Unusual base pairing during the decoding of a stop codon by the ribosome. *Nature*, *500*, 107–110. https://doi.org/10.1038/nature12302

Fleg, J. L., Aronow, W. S., & Frishman, W. H. (2011). Cardiovascular drug therapy in the elderly: Benefits and challenges. *Nature Reviews. Cardiology*, *8*, 13–28. https://doi.org/10.1038/nrcardio.2010.162

Frye, M., Jaffrey, S. R., Pan, T., Rechavi, G., & Suzuki, T. (2016). RNA modifications: What have we learned and where are we headed? *Nature Reviews. Genetics*, *17*, 365–372. https://doi.org/10.1038/nrg.2016.47

Gan, X. T., Zhao, G., Huang, C. X., Rowe, A. C., Purdham, D. M., & Karmazyn, M. (2013). Identification of fat mass and obesity associated (FTO) protein expression in cardiomyocytes: Regulation by leptin and its contribution to leptin-induced hypertrophy. *PLoS One*, *8*, e74235. https://doi.org/10.1371/journal.pone.0074235

Gao, X., Shin, Y. H., Li, M., Wang, F., Tong, Q., & Zhang, P. (2010). The fat mass and obesity associated gene FTO functions in the brain to regulate postnatal growth in mice. *PLoS One*, *5*, e14005. https://doi.org/10.1371/journal.pone.0014005

Gao, X. Q., Zhang, Y. H., Liu, F., Ponnusamy, M., Zhao, X. M., Zhou, L. Y., Zhai, M., Liu, C. Y., Li, X. M., Wang, M., Shan, C., Shan, P. P., Wang, Y., Dong, Y. H., Qian, L. L., Yu, T., Ju, J., Wang, T., Wang, K., … Wang, K. (2020). The piRNA CHAPIR regulates cardiac hypertrophy by controlling METTL3-dependent N(6)-methyladenosine methylation of Parp10 mRNA. *Nature Cell Biology*, *22*, 1319–1331. https://doi.org/10.1038/s41556-020-0576-y

Giles, T. D., Materson, B. J., Cohn, J. N., & Kostis, J. B. (2009). Definition and classification of hypertension: An update. *Journal of Clinical Hypertension (Greenwich, Conn.)*, *11*, 611–614. https://doi.org/10.1111/j.1751-7176.2009.00179.x

Gistera, A., & Hansson, G. K. (2017). The immunology of atherosclerosis. *Nature Reviews. Nephrology*, *13*, 368–380. https://doi.org/10.1038/nrneph.2017.51

Han, X., Guo, J., & Fan, Z. (2021). Interactions between m6A modification and miRNAs in malignant tumors. *Cell Death & Disease*, *12*, 598. https://doi.org/10.1038/s41419-021-03868-5

Harcourt, E. M., Kietrys, A. M., & Kool, E. T. (2017). Chemical and structural effects of base modifications in messenger RNA. *Nature*, *541*, 339–346. https://doi.org/10.1038/nature21351

Heidenreich, P. A., Albert, N. M., Allen, L. A., Bluemke, D. A., Butler, J., Fonarow, G. C., Ikonomidis, J. S., Khavjou, O., Konstam, M. A., Maddox, T. M., Nichol, G., Pham, M., Piña, I. L., & Trogdon, J. G. (2013). Forecasting the impact of heart failure in the United States: A policy statement from the American Heart Association. *Circulation. Heart Failure*, *6*, 606–619. https://doi.org/10.1161/HHF.0b013e318291329a

Heidenreich, P. A., Trogdon, J. G., Khavjou, O. A., Butler, J., Dracup, K., Ezekowitz, M. D., Finkelstein, E. A., Hong, Y., Johnston, S. C., Khera, A., Lloyd-Jones, D. M., Nelson, S. A., Nichol, G., Orenstein, D., Wilson, P. W. F., & Woo, Y. J. (2011). Forecasting the future of cardiovascular disease in the United States: A policy statement from the American Heart Association. *Circulation*, *123*, 933–944. https://doi.org/10.1161/CIR.0b013e31820a55f5

Helm, M., & Motorin, Y. (2017). Detecting RNA modifications in the epitranscriptome: Predict and validate. *Nature Reviews. Genetics*, *18*, 275–291. https://doi.org/10.1038/nrg.2016.169

Hideyama, T., & Kwak, S. (2011). When does ALS start? ADAR2-GluA2 hypothesis for the etiology of sporadic ALS. *Frontiers in Molecular Neuroscience*, *4*, 33. https://doi.org/10.3389/fnmol.2011.00033

Hideyama, T., Yamashita, T., Aizawa, H., Tsuji, S., Kakita, A., Takahashi, H., & Kwak, S. (2012). Profound downregulation of the RNA editing enzyme ADAR2 in ALS spinal motor neurons. *Neurobiology of Disease*, *45*, 1121–1128. https://doi.org/10.1016/j.nbd.2011.12.033

Hideyama, T., Yamashita, T., Suzuki, T., Tsuji, S., Higuchi, M., Seeburg, P. H., Takahashi, R., Misawa, H., & Kwak, S. (2010). Induced loss of ADAR2 engenders slow death of motor neurons from Q/R site-unedited GluR2. *The Journal of Neuroscience*, *30*, 11917–11925. https://doi.org/10.1523/JNEUROSCI.2021-10.2010

Hoernes, T. P., Clementi, N., Faserl, K., Glasner, H., Breuker, K., Lindner, H., Hüttenhofer, A., & Erlacher, M. D. (2016). Nucleotide modifications within bacterial messenger RNAs regulate their translation and are able to rewire the genetic code. *Nucleic Acids Research*, *44*, 852–862. https://doi.org/10.1093/nar/gkv1182

Holley, R. W., Apgar, J., Everett, G. A., Madison, J. T., Marquisee, M., Merrill, S. H., Penswick, J. R., & Zamir, A. (1965). Structure of a ribonucleic acid. *Science*, *147*, 1462–1465. https://doi.org/10.1126/science.147.3664.1462

Hu, L., Liu, S., Peng, Y., Ge, R., Su, R., Senevirathne, C., Harada, B. T., Dai, Q., Wei, J., Zhang, L., Hao, Z., Luo, L., Wang, H., Wang, Y., Luo, M., Chen, M., Chen, J., & He, C. (2022). M(6)a RNA modifications are measured at single-base resolution across the mammalian transcriptome. *Nature Biotechnology*. https://doi.org/10.1038/s41587-022-01243-z

Huang, B., Ding, C., Zou, Q., Wang, W., & Li, H. (2019). Cyclophosphamide regulates N6-Methyladenosine and m6A RNA enzyme levels in human granulosa cells and in ovaries of a premature ovarian aging mouse model. *Frontiers in Endocrinology (Lausanne)*, *10*, 415. https://doi.org/10.3389/fendo.2019.00415

Huang, H., Camats-Perna, J., Medeiros, R., Anggono, V., & Widagdo, J. (2020). Altered expression of the m6A methyltransferase METTL3 in Alzheimer's disease. *eNeuro*, *7*. https://doi.org/10.1523/ENEURO.0125-20.2020

Hussain, S., Sajini, A. A., Blanco, S., Dietmann, S., Lombard, P., Sugimoto, Y., Paramor, M., Gleeson, J. G., Odom, D. T., Ule, J., & Frye, M. (2013). NSun2-mediated cytosine-5 methylation of vault noncoding RNA determines its processing into regulatory small RNAs. *Cell Reports*, *4*, 255–261. https://doi.org/10.1016/j.celrep.2013.06.029

Jankovic, J. (2008). Parkinson's disease: Clinical features and diagnosis. *Journal of Neurology, Neurosurgery, and Psychiatry*, *79*, 368–376. https://doi.org/10.1136/jnnp.2007.131045

Jia, G., Fu, Y., Zhao, X., Dai, Q., Zheng, G., Yang, Y., Yi, C., Lindahl, T., Pan, T., Yang, Y. G., & He, C. (2011). N6-methyladenosine in nuclear RNA is a major substrate of the obesity-associated FTO. *Nature Chemical Biology*, *7*, 885–887. https://doi.org/10.1038/nchembio.687

Jian, D., Wang, Y., Jian, L., Tang, H., Rao, L., Chen, K., Jia, Z., Zhang, W., Liu, Y., Chen, X., Shen, X., Gao, C., Wang, S., & Li, M. (2020). METTL14 aggravates endothelial inflammation and atherosclerosis by increasing FOXO1 N6-methyladeosine modifications. *Theranostics*, *10*, 8939–8956. https://doi.org/10.7150/thno.45178

Jiang, Z. X., Wang, Y. N., Li, Z. Y., Dai, Z. H., He, Y., Chu, K., Gu, J. Y., Ji, Y. X., Sun, N. X., Yang, F., & Li, W. (2021). The m6A mRNA demethylase FTO in granulosa cells retards FOS-dependent ovarian aging. *Cell Death & Disease*, *12*, 744. https://doi.org/10.1038/s41419-021-04016-9

Juhling, F., Morl, M., Hartmann, R. K., Sprinzl, M., Stadler, P. F., & Putz, J. (2009). tRNAdb 2009: Compilation of tRNA sequences and tRNA genes. *Nucleic Acids Research*, *37*, D159–D162. https://doi.org/10.1093/nar/gkn772

Karijolich, J., & Yu, Y. T. (2011). Converting nonsense codons into sense codons by targeted pseudouridylation. *Nature*, *474*, 395–398. https://doi.org/10.1038/nature10165

Keller, L., Xu, W., Wang, H. X., Winblad, B., Fratiglioni, L., & Graff, C. (2011). The obesity related gene, FTO, interacts with APOE, and is associated with Alzheimer's disease risk: A prospective cohort study. *Journal of Alzheimer's Disease*, *23*, 461–469. https://doi.org/10.3233/JAD-2010-101068

Khermesh, K., D'Erchia, A. M., Barak, M., Annese, A., Wachtel, C., Levanon, E. Y., Picardi, E., & Eisenberg, E. (2016). Reduced levels of protein recoding by A-to-I RNA editing in Alzheimer's disease. *RNA*, *22*, 290–302. https://doi.org/10.1261/rna.054627.115

Khoddami, V., & Cairns, B. R. (2013). Identification of direct targets and modified bases of RNA cytosine methyltransferases. *Nature Biotechnology*, *31*, 458–464. https://doi.org/10.1038/nbt.2566

Kmietczyk, V., Riechert, E., Kalinski, L., Boileau, E., Malovrh, E., Malone, B., Gorska, A., Hofmann, C., Varma, E., Jürgensen, L., Kamuf-Schenk, V., Altmüller, J., Tappu, R., Busch, M., Most, P., Katus, H. A., Dieterich, C., & Völkers, M. (2019). M(6)A-mRNA methylation regulates cardiac gene expression and cellular growth. *Life Sci Alliance*, *2*, e201800233. https://doi.org/10.26508/lsa.201800233

Knuckles, P., & Buhler, M. (2018). Adenosine methylation as a molecular imprint defining the fate of RNA. *FEBS Letters*, *592*, 2845–2859. https://doi.org/10.1002/1873-3468.13107

Komal, S., Zhang, L. R., & Han, S. N. (2021). Potential regulatory role of epigenetic RNA methylation in cardiovascular diseases. *Biomedicine & Pharmacotherapy*, *137*, 111376. https://doi.org/10.1016/j.biopha.2021.111376

Kumar, S., & Mohapatra, T. (2021). Deciphering Epitranscriptome: Modification of mRNA bases provides a new perspective for post-transcriptional regulation of gene expression. *Frontiers in Cell and Developmental Biology*, *9*, 628415. https://doi.org/10.3389/fcell.2021.628415

Kumari, R., Ranjan, P., Suleiman, Z. G., Goswami, S. K., Li, J., Prasad, R., & Verma, S. K. (2021). mRNA modifications in cardiovascular biology and disease: With a focus on m6A modification. *Cardiovascular Research*, 1–13. https://doi.org/10.1093/cvr/cvab160

Kwak, S., Nishimoto, Y., & Yamashita, T. (2008). Newly identified ADAR-mediated A-to-I editing positions as a tool for ALS research. *RNA Biology*, *5*, 193–197. https://doi.org/10.4161/rna.6925

Lavi, U., Fernandez-Munoz, R., & Darnell, J. E., Jr. (1977). Content of N-6 methyl adenylic acid in heterogeneous nuclear and messenger RNA of HeLa cells. *Nucleic Acids Research*, *4*, 63–69. https://doi.org/10.1093/nar/4.1.63

Lee, R. C., Feinbaum, R. L., & Ambros, V. T. C. (1993). Elegans heterochronic gene lin-4 encodes small RNAs with antisense complementarity to lin-14. *Cell*, *75*, 843–854. https://doi.org/10.1016/0092-8674(93)90529-y

Leger, A., Amaral, P. P., Pandolfini, L., Capitanchik, C., Capraro, F., Miano, V., Migliori, V., Toolan-Kerr, P., Sideri, T., Enright, A. J., Tzelepis, K., van Werven, F. J., Luscombe, N. M., Barbieri, I., Ule, J., Fitzgerald, T., Birney, E., Leonardi, T., & Kouzarides, T. (2021). RNA modifications detection by comparative nanopore direct RNA sequencing. *Nature Communications*, *12*, 7198. https://doi.org/10.1038/s41467-021-27393-3

Leridon, H. (2004). Can assisted reproduction technology compensate for the natural decline in fertility with age? A model assessment. *Human Reproduction*, *19*, 1548–1553. https://doi.org/10.1093/humrep/deh304

Li, D., Cai, L., Meng, R., Feng, Z., & Xu, Q. (2020). METTL3 modulates osteoclast differentiation and function by controlling RNA stability and nuclear export. *International Journal of Molecular Sciences*, *21*, 1660. https://doi.org/10.3390/ijms21051660

Li, H., Ren, Y., Mao, K., Hua, F., Yang, Y., Wei, N., Yue, C., Li, D., & Zhang, H. (2018). FTO is involved in Alzheimer's disease by targeting TSC1-mTOR-tau signaling. *Biochemical and Biophysical Research Communications*, *498*, 234–239. https://doi.org/10.1016/j.bbrc.2018.02.201

Li, P., Yu, H., Zhang, G., Kang, L., Qin, B., Cao, Y., Luo, J., Chen, X., Wang, Y., Qin, M., Wu, J., Huang, Y., Zou, X., Guan, H., & Wang, Y. (2020). Identification and characterization of N6-Methyladenosine CircRNAs and methyltransferases in the lens epithelium cells from age-related cataract. *Investigative Ophthalmology & Visual Science*, *61*, 13. https://doi.org/10.1167/iovs.61.10.13

Li, X., Xiong, X., Wang, K., Wang, L., Shu, X., Ma, S., & Yi, C. (2016). Transcriptome-wide mapping reveals reversible and dynamic N(1)-methyladenosine methylome. *Nature Chemical Biology*, *12*, 311–316. https://doi.org/10.1038/nchembio.2040

Li, X., Xiong, X., Zhang, M., Wang, K., Chen, Y., Zhou, J., Mao, Y., Lv, J., Yi, D., Chen, X. W., Wang, C., Qian, S. B., & Yi, C. (2017). Base-resolution mapping reveals distinct m(1)a methylome in nuclear- and mitochondrial-encoded transcripts. *Molecular Cell*, *68*, 993–1005. https://doi.org/10.1016/j.molcel.2017.10.019

Li, Y., Yang, F., Gao, M., Gong, R., Jin, M., Liu, T., Sun, Y., Fu, Y., Huang, Q., Zhang, W., Liu, S., Yu, M., Yan, G., Feng, C., He, M., Zhang, L., Ding, F., Ma, W., Bi, Z., … Yang, L. (2019). miR-149-3p regulates the switch between Adipogenic and osteogenic differentiation of BMSCs by targeting FTO. *Molecular Therapy Nucleic Acids*, *17*, 590–600. https://doi.org/10.1016/j.omtn.2019.06.023

Linder, B., Grozhik, A. V., Olarerin-George, A. O., Meydan, C., Mason, C. E., & Jaffrey, S. R. (2015). Single-nucleotide-resolution mapping of m6A and m6Am throughout the transcriptome. *Nature Methods*, *12*, 767–772. https://doi.org/10.1038/nmeth.3453

Liu, F., Clark, W., Luo, G., Wang, X., Fu, Y., Wei, J., Wang, X., Hao, Z., Dai, Q., Zheng, G., Ma, H., Han, D., Evans, M., Klungland, A., Pan, T., & He, C. (2016). ALKBH1-mediated tRNA demethylation regulates translation. *Cell*, *167*, 816–828 e816. https://doi.org/10.1016/j.cell.2016.09.038

Liu, J., Yue, Y., Han, D., Wang, X., Fu, Y., Zhang, L., Jia, G., Yu, M., Lu, Z., Deng, X., Dai, Q., Chen, W., & He, C. (2014). A METTL3-METTL14 complex mediates mammalian nuclear RNA N6-adenosine methylation. *Nature Chemical Biology*, *10*, 93–95. https://doi.org/10.1038/nchembio.1432

Lopez-Otin, C., Blasco, M. A., Partridge, L., Serrano, M., & Kroemer, G. (2013). The hallmarks of aging. *Cell*, *153*, 1194–1217. https://doi.org/10.1016/j.cell.2013.05.039

Maas, S., Kawahara, Y., Tamburro, K. M., & Nishikura, K. (2006). A-to-I RNA editing and human disease. *RNA Biology*, *3*, 1–9. https://doi.org/10.4161/rna.3.1.2495

Marcadenti, A., Fuchs, F. D., Matte, U., Sperb, F., Moreira, L. B., & Fuchs, S. C. (2013). Effects of FTO RS9939906 and MC4R RS17782313 on obesity, type 2 diabetes mellitus and blood pressure in patients with hypertension. *Cardiovascular Diabetology*, *12*, 103. https://doi.org/10.1186/1475-2840-12-103

Mendel, M., Chen, K. M., Homolka, D., Gos, P., Pandey, R. R., McCarthy, A. A., & Pillai, R. S. (2018). Methylation of structured RNA by the m(6)a writer METTL16 is essential for mouse embryonic development. *Molecular Cell*, *71*, 986–1000 e1011. https://doi.org/10.1016/j.molcel.2018.08.004

Menken, J., Trussell, J., & Larsen, U. (1986). Age and infertility. *Science*, *233*, 1389–1394. https://doi.org/10.1126/science.3755843

Meyer, K. D. (2019). DART-seq: An antibody-free method for global m(6)a detection. *Nature Methods*, *16*, 1275–1280. https://doi.org/10.1038/s41592-019-0570-0

Meyer, K. D., Saletore, Y., Zumbo, P., Elemento, O., Mason, C. E., & Jaffrey, S. R. (2012). Comprehensive analysis of mRNA methylation reveals enrichment in 3' UTRs and near stop codons. *Cell*, *149*, 1635–1646. https://doi.org/10.1016/j.cell.2012.05.003

Mo, X. B., Lei, S. F., Zhang, Y. H., & Zhang, H. (2019a). Examination of the associations between m(6)A-associated single-nucleotide polymorphisms and blood pressure. *Hypertension Research*, *42*, 1582–1589. https://doi.org/10.1038/s41440-019-0277-8

Mo, X. B., Lei, S. F., Zhang, Y. H., & Zhang, H. (2019b). Integrative analysis identified IRF6 and NDST1 as potential causal genes for ischemic stroke. *Frontiers in Neurology*, *10*, 517. https://doi.org/10.3389/fneur.2019.00517

Molinie, B., Wang, J., Lim, K. S., Hillebrand, R., Lu, Z. X., van Wittenberghe, N., Howard, B. D., Daneshvar, K., Mullen, A. C., Dedon, P., Xing, Y., & Giallourakis, C. C. (2016). M(6)A-LAIC-seq reveals the census and complexity of the m(6)a epitranscriptome. *Nature Methods*, *13*, 692–698. https://doi.org/10.1038/nmeth.3898

Mortality, G. B. D., & Causes of Death, C. (2013). Global, regional, and national age-sex specific all-cause and cause-specific mortality for 240 causes of death, 1990–2013: A systematic analysis for the global burden of disease study. *Lancet*, *385*, 117–171. https://doi.org/10.1016/S0140-6736(14)61682-2

Mozaffarian, D., Benjamin, E. J., Go, A. S., Arnett, D. K., Blaha, M. J., Cushman, M., de Ferranti, S., Despres, J. P., Fullerton, H. J., Howard, V. J., Huffman, M. D., Judd, S. E., Kissela, B. M., Lackland, D. T., Lichtman, J. H., Lisabeth, L. D., Liu, S., Mackey, R. H., Matchar, D. B., … Turner, M. B. (2015). Heart disease and stroke statistics--2015 update: A report from the American Heart Association. *Circulation*, *131*, e29–e322. https://doi.org/10.1161/CIR.0000000000000152

Nelson, S. M., Telfer, E. E., & Anderson, R. A. (2013). The ageing ovary and uterus: New biological insights. *Human Reproduction Update*, *19*, 67–83. https://doi.org/10.1093/humupd/dms043

Nishikura, K. (2016). A-to-I editing of coding and non-coding RNAs by ADARs. *Nature Reviews. Molecular Cell Biology*, *17*, 83–96. https://doi.org/10.1038/nrm.2015.4

North, B. J., & Sinclair, D. A. (2012). The intersection between aging and cardiovascular disease. *Circulation Research*, *110*, 1097–1108. https://doi.org/10.1161/CIRCRESAHA.111.246876

Oskarsson, B., Gendron, T. F., & Staff, N. P. (2018). Amyotrophic lateral sclerosis: An update for 2018. *Mayo Clinic Proceedings*, *93*, 1617–1628. https://doi.org/10.1016/j.mayocp.2018.04.007

Porath, H. T., Knisbacher, B. A., Eisenberg, E., & Levanon, E. Y. (2017). Massive A-to-I RNA editing is common across the Metazoa and correlates with dsRNA abundance. *Genome Biology*, *18*, 185. https://doi.org/10.1186/s13059-017-1315-y

Qian, B., Wang, P., Zhang, D., & Wu, L. (2021). m6A modification promotes miR-133a repression during cardiac development and hypertrophy via IGF2BP2. *Cell Death Discovery*, *7*, 157. https://doi.org/10.1038/s41420-021-00552-7

Qin, L., Min, S., Shu, L., Pan, H., Zhong, J., Guo, J., Sun, Q., Yan, X., Chen, C., Tang, B., & Xu, Q. (2020). Genetic analysis of N6-methyladenosine modification genes in Parkinson's disease. *Neurobiology of Aging*, *93*, 143.e9–143.e13. https://doi.org/10.1016/j.neurobiolaging.2020.03.018

Reitz, C., Tosto, G., Mayeux, R., Luchsinger, J. A., & NIA-LOAD/NCRAD Family Study Group, Alzheimer's Disease Neuroimaging Initiative. (2012). Genetic variants in the fat and obesity associated (FTO) gene and risk of Alzheimer's disease. *PLoS One*, *7*, e50354. https://doi.org/10.1371/journal.pone.0050354

Roundtree, I. A., Evans, M. E., Pan, T., & He, C. (2017). Dynamic RNA modifications in gene expression regulation. *Cell*, *169*, 1187–1200. https://doi.org/10.1016/j.cell.2017.05.045

Safra, M., Sas-Chen, A., Nir, R., Winkler, R., Nachshon, A., Bar-Yaacov, D., Erlacher, M., Rossmanith, W., Stern-Ginossar, N., & Schwartz, S. (2017). The m1A landscape on cytosolic and mitochondrial mRNA at single-base resolution. *Nature*, *551*, 251–255. https://doi.org/10.1038/nature24456

Saul, D., & Kosinsky, R. L. (2021). Epigenetics of aging and aging-associated diseases. *International Journal of Molecular Sciences*, *22*, 401. https://doi.org/10.3390/ijms22010401

Schwartz, S., Bernstein, D. A., Mumbach, M. R., Jovanovic, M., Herbst, R. H., León-Ricardo, B. X., Engreitz, J. M., Guttman, M., Satija, R., Lander, E. S., Fink, G., & Regev, A. (2014). Transcriptome-wide mapping reveals widespread dynamic-regulated pseudouridylation of ncRNA and mRNA. *Cell*, *159*, 148–162. https://doi.org/10.1016/j.cell.2014.08.028

Shafik, A. M., Zhang, F., Guo, Z., Dai, Q., Pajdzik, K., Li, Y., Kang, Y., Yao, B., Wu, H., He, C., Allen, E. G., Duan, R., & Jin, P. (2021). N6-methyladenosine dynamics in neurodevelopment and aging, and its potential role in Alzheimer's disease. *Genome Biology*, *22*, 17. https://doi.org/10.1186/s13059-020-02249-z

Shen, G. S., Zhou, H. B., Zhang, H., Chen, B., Liu, Z. P., Yuan, Y., Zhou, X. Z., & Xu, Y. J. (2018). The GDF11-FTO-PPARgamma axis controls the shift of osteoporotic MSC fate to adipocyte and inhibits bone formation during osteoporosis. *Biochimica et Biophysica Acta - Molecular Basis of Disease*, *1864*, 3644–3654. https://doi.org/10.1016/j.bbadis.2018.09.015

Shen, L., Liang, Z., Wong, C. E., & Yu, H. (2019). Messenger RNA modifications in plants. *Trends in Plant Science*, *24*, 328–341. https://doi.org/10.1016/j.tplants.2019.01.005

Sommer, B., Kohler, M., Sprengel, R., & Seeburg, P. H. (1991). RNA editing in brain controls a determinant of ion flow in glutamate-gated channels. *Cell*, *67*, 11–19. https://doi.org/10.1016/0092-8674(91)90568-j

Song, T., Yang, Y., Wei, H., Xie, X., Lu, J., Zeng, Q., Peng, J., Zhou, Y., Jiang, S., & Peng, J. (2019). Zfp217 mediates m6A mRNA methylation to orchestrate transcriptional and post-transcriptional regulation to promote adipogenic differentiation. *Nucleic Acids Research*, *47*, 6130–6144. https://doi.org/10.1093/nar/gkz312

Soria Lopez, J. A., Gonzalez, H. M., & Leger, G. C. (2019). Alzheimer's disease. *Handbook of Clinical Neurology*, *167*, 231–255. https://doi.org/10.1016/B978-0-12-804766-8.00013-3

Squires, J. E., Patel, H. R., Nousch, M., Sibbritt, T., Humphreys, D. T., Parker, B. J., Suter, C. M., & Preiss, T. (2012). Widespread occurrence

of 5-methylcytosine in human coding and non-coding RNA. *Nucleic Acids Research*, *40*, 5023–5033. https://doi.org/10.1093/nar/gks144

Statello, L., Guo, C. J., Chen, L. L., & Huarte, M. (2021). Gene regulation by long non-coding RNAs and its biological functions. *Nature Reviews. Molecular Cell Biology*, *22*, 96–118. https://doi.org/10.1038/s41580-020-00315-9

Stellos, K., Gatsiou, A., Stamatelopoulos, K., Perisic Matic, L., John, D., Lunella, F. F., Jaé, N., Rossbach, O., Amrhein, C., Sigala, F., Boon, R. A., Fürtig, B., Manavski, Y., You, X., Uchida, S., Keller, T., Boeckel, J. N., Franco-Cereceda, A., Maegdefessel, L., … Dimmeler, S. (2016). Adenosine-to-inosine RNA editing controls cathepsin S expression in atherosclerosis by enabling HuR-mediated post-transcriptional regulation. *Nature Medicine*, *22*, 1140–1150. https://doi.org/10.1038/nm.4172

Sun, X., Zhang, Y., Hu, Y., An, J., Li, L., Wang, Y., & Zhang, X. (2021). Decreased expression of m(6)a demethylase FTO in ovarian aging. *Archives of Gynecology and Obstetrics*, *303*, 1363–1369. https://doi.org/10.1007/s00404-020-05895-7

Sun, Z., Wang, H., Wang, Y., Yuan, G., Yu, X., Jiang, H., Wu, Q., Yang, B., Hu, Z., Shi, F., Cao, X., Zhang, S., Guo, T., & Zhao, J. (2021). MiR-103-3p targets the m(6) a methyltransferase METTL14 to inhibit osteoblastic bone formation. *Aging Cell*, *20*, e13298. https://doi.org/10.1111/acel.13298

Suzuki, T. (2021). The expanding world of tRNA modifications and their disease relevance. *Nature Reviews. Molecular Cell Biology*, *22*, 375–392. https://doi.org/10.1038/s41580-021-00342-0

Tan, M. H., Li, Q., Shanmugam, R., Piskol, R., Kohler, J., Young, A. N., Liu, K. I., Zhang, R., Ramaswami, G., Ariyoshi, K., Gupte, A., Keegan, L. P., George, C. X., Ramu, A., Huang, N., Pollina, E. A., Leeman, D. S., Rustighi, A., Goh, Y. P. S., … Li, J. B. (2017). Dynamic landscape and regulation of RNA editing in mammals. *Nature*, *550*, 249–254. https://doi.org/10.1038/nature24041

Tian, C., Huang, Y., Li, Q., Feng, Z., & Xu, Q. (2019). Mettl3 regulates osteogenic differentiation and alternative splicing of Vegfa in bone marrow mesenchymal stem cells. *International Journal of Molecular Sciences*, *20*, 551. https://doi.org/10.3390/ijms20030551

Trotman, J. B., Giltmier, A. J., Mukherjee, C., & Schoenberg, D. R. (2017). RNA guanine-7 methyltransferase catalyzes the methylation of cytoplasmically recapped RNAs. *Nucleic Acids Research*, *45*, 10726–10739. https://doi.org/10.1093/nar/gkx801

Vlachogiannis, N. I., Sachse, M., Georgiopoulos, G., Zormpas, E., Bampatsias, D., Delialis, D., Bonini, F., Galyfos, G., Sigala, F., Stamatelopoulos, K., Gatsiou, A., & Stellos, K. (2021). Adenosine-to-inosine Alu RNA editing controls the stability of the pro-inflammatory long noncoding RNA NEAT1 in atherosclerotic cardiovascular disease. *Journal of Molecular and Cellular Cardiology*, *160*, 111–120. https://doi.org/10.1016/j.yjmcc.2021.07.005

Warda, A. S., Kretschmer, J., Hackert, P., Lenz, C., Urlaub, H., Höbartner, C., Sloan, K. E., & Bohnsack, M. T. (2017). Human METTL16 is a N(6)-methyladenosine (m(6)a) methyltransferase that targets pre-mRNAs and various non-coding RNAs. *EMBO Reports*, *18*, 2004–2014. https://doi.org/10.15252/embr.201744940

Watkins, N. J., & Bohnsack, M. T. (2012). The box C/D and H/ACA snoRNPs: Key players in the modification, processing and the dynamic folding of ribosomal RNA. *Wiley Interdiscip Rev RNA*, *3*, 397–414. https://doi.org/10.1002/wrna.117

Wen, J., Min, S., Shu, L., Pan, H., Zhong, J., Guo, J., Sun, Q., Yan, X., Chen, C., Tang, B., & Xu, Q. (2018). Zc3h13 regulates nuclear RNA m(6)a methylation and mouse embryonic stem cell self-renewal. *Mol Cell*, *69*, 1028–1038 e1026. https://doi.org/10.1016/j.molcel.2018.02.015

Wen, K., Zhang, Y., Li, Y., Wang, Q., & Sun, J. (2021). Comprehensive analysis of transcriptome-wide m(6)a methylome in the anterior capsule of the lens of high myopia patients. *Epigenetics*, *16*, 955–968. https://doi.org/10.1080/15592294.2020.1834917

White, R. R., Milholland, B., MacRae, S. L., Lin, M., Zheng, D., & Vijg, J. (2015). Comprehensive transcriptional landscape of aging mouse liver. *BMC Genomics*, *16*, 899. https://doi.org/10.1186/s12864-015-2061-8

Wu, S., Yang, M., Kim, P., & Zhou, X. (2021). ADeditome provides the genomic landscape of A-to-I RNA editing in Alzheimer's disease. *Briefings in Bioinformatics*, *22*, bbaa384. https://doi.org/10.1093/bib/bbaa384

Wu, Y., Xie, L., Wang, M., Xiong, Q., Guo, Y., Liang, Y., Li, J., Sheng, R., Deng, P., Wang, Y., Zheng, R., Jiang, Y., Ye, L., Chen, Q., Zhou, X., Lin, S., & Yuan, Q. (2018). Mettl3-mediated m(6)a RNA methylation regulates the fate of bone marrow mesenchymal stem cells and osteoporosis. *Nature Communications*, *9*, 4772. https://doi.org/10.1038/s41467-018-06898-4

Yan, G., Yuan, Y., He, M., Gong, R., Lei, H., Zhou, H., Wang, W., du, W., Ma, T., Liu, S., Xu, Z., Gao, M., Yu, M., Bian, Y., Pang, P., Li, X., Yu, S., Yang, F., Cai, B., & Yang, L. (2020). M(6)a methylation of precursor-miR-320/RUNX2 controls osteogenic potential of bone marrow-derived mesenchymal stem cells. *Molecular Therapy Nucleic Acids*, *19*, 421–436. https://doi.org/10.1016/j.omtn.2019.12.001

Yang, J., Liu, J., Zhao, S., & Tian, F. (2020). N(6)-Methyladenosine METTL3 modulates the proliferation and apoptosis of lens epithelial cells in diabetic cataract. *Molecular Therapy Nucleic Acids*, *20*, 111–116. https://doi.org/10.1016/j.omtn.2020.02.002

Yang, X., Pan, X., Zhao, X., Luo, J., Xu, M., Bai, D., Hu, Y., Liu, X., Yu, Q., & Gao, D. (2019). Autophagy and age-related eye diseases. *BioMed Research International*, *2019*, 5763658–5763612. https://doi.org/10.1155/2019/5763658

Yang, X., Yang, Y., Sun, B. F., Chen, Y. S., Xu, J. W., Lai, W. Y., Li, A., Wang, X., Bhattarai, D. P., Xiao, W., Sun, H. Y., Zhu, Q., Ma, H. L., Adhikari, S., Sun, M., Hao, Y. J., Zhang, B., Huang, C. M., Huang, N., … Yang, Y. G. (2017). 5-methylcytosine promotes mRNA export - NSUN2 as the methyltransferase and ALYREF as an m(5)C reader. *Cell Research*, *27*, 606–625. https://doi.org/10.1038/cr.2017.55

Yildirim, I., Kierzek, E., Kierzek, R., & Schatz, G. C. (2014). Interplay of LNA and 2'-O-methyl RNA in the structure and thermodynamics of RNA hybrid systems: A molecular dynamics study using the revised AMBER force field and comparison with experimental results. *The Journal of Physical Chemistry. B*, *118*, 14177–14187. https://doi.org/10.1021/jp506703g

Yu, J., Shen, L., Liu, Y., Ming, H., Zhu, X., Chu, M., & Lin, J. (2020). The m6A methyltransferase METTL3 cooperates with demethylase ALKBH5 to regulate osteogenic differentiation through NF-kappaB signaling. *Molecular and Cellular Biochemistry*, *463*, 203–210. https://doi.org/10.1007/s11010-019-03641-5

Yue, Y., Liu, J., Cui, X., Cao, J., Luo, G., Zhang, Z., Cheng, T., Gao, M., Shu, X., Ma, H., Wang, F., Wang, X., Shen, B., Wang, Y., Feng, X., He, C., & Liu, J. (2018). VIRMA mediates preferential m(6)a mRNA methylation in 3'UTR and near stop codon and associates with alternative polyadenylation. *Cell Discov*, *4*, 10. https://doi.org/10.1038/s41421-018-0019-0

Zhang, B. Y., Han, L., Tang, Y. F., Zhang, G. X., Fan, X. L., Zhang, J. J., Xue, Q., & Xu, Z. Y. (2020). METTL14 regulates M6A methylation-modified primary miR-19a to promote cardiovascular endothelial cell proliferation and invasion. *European Review for Medical and Pharmacological Sciences*, *24*, 7015–7023. https://doi.org/10.26355/eurrev_202006_21694

Zhang, Q., Riddle, R. C., Yang, Q., Rosen, C. R., Guttridge, D. C., Dirckx, N., Faugere, M. C., Farber, C. R., & Clemens, T. L. (2019). The RNA demethylase FTO is required for maintenance of bone mass and functions to protect osteoblasts from genotoxic damage. *Proceedings of the National Academy of Sciences of the United States of America*, *116*, 17980–17989. https://doi.org/10.1073/pnas.1905489116

Zhang, X., Cozen, A. E., Liu, Y., Chen, Q., & Lowe, T. M. (2016). Small RNA modifications: Integral to function and disease. *Trends in Molecular Medicine*, *22*, 1025–1034. https://doi.org/10.1016/j.molmed.2016.10.009

Zhang, X., Trebak, F., Souza, L. A. C., Shi, J., Zhou, T., Kehoe, P. G., Chen, Q., & Feng Earley, Y. (2020). Small RNA modifications in Alzheimer's disease. *Neurobiology of Disease*, *145*, 105058. https://doi.org/10.1016/j.nbd.2020.105058

Zhang, Y., Chen, W., Zheng, X., Guo, Y., Cao, J., Zhang, Y., Wen, S., Gao, W., & Wu, Y. (2021). Regulatory role and mechanism of m(6)a RNA modification in human metabolic diseases. *Mol Ther Oncolytics*, *22*, 52–63. https://doi.org/10.1016/j.omto.2021.05.003

Zhang, Z., Wang, Q., Zhao, X., Shao, L., Liu, G., Zheng, X., Xie, L., Zhang, Y., Sun, C., & Xu, R. (2020). YTHDC1 mitigates ischemic stroke by promoting Akt phosphorylation through destabilizing PTEN mRNA. *Cell Death & Disease*, *11*, 977. https://doi.org/10.1038/s41419-020-03186-2

Zhao, B. S., Roundtree, I. A., & He, C. (2017). Post-transcriptional gene regulation by mRNA modifications. *Nature Reviews. Molecular Cell Biology*, *18*, 31–42. https://doi.org/10.1038/nrm.2016.132

Zhao, F., Xu, Y., Gao, S., Qin, L., Austria, Q., Siedlak, S. L., Pajdzik, K., Dai, Q., He, C., Wang, W., O'Donnell, J. M., Tang, B., & Zhu, X. (2021). METTL3-dependent RNA m(6)a dysregulation contributes to neurodegeneration in Alzheimer's disease through aberrant cell cycle events. *Molecular Neurodegeneration*, *16*, 70. https://doi.org/10.1186/s13024-021-00484-x

Zhou, H., Kimsey, I. J., Nikolova, E. N., Sathyamoorthy, B., Grazioli, G., McSally, J., Bai, T., Wunderlich, C. H., Kreutz, C., Andricioaei, I., & al-Hashimi, H. M. (2016). M(1)a and m(1)G disrupt A-RNA structure through the intrinsic instability of Hoogsteen base pairs. *Nature Structural & Molecular Biology*, *23*, 803–810. https://doi.org/10.1038/nsmb.3270

Zhou, Z., Lv, J., Yu, H., Han, J., Yang, X., Feng, D., Wu, Q., Yuan, B., Lu, Q., & Yang, H. (2020). Mechanism of RNA modification N6-methyladenosine in human cancer. *Molecular Cancer*, *19*, 104. https://doi.org/10.1186/s12943-020-01216-3

How to cite this article: Jiapaer, Z., Su, D., Hua, L., Lehmann, H. I., Gokulnath, P., Vulugundam, G., Song, S., Zhang, L., Gong, Y., & Li, G. (2022). Regulation and roles of RNA modifications in aging-related diseases. *Aging Cell*, *00*, e13657. https://doi.org/10.1111/acel.13657